energies

Selected Papers from the 8th Annual Conference of Energy Economics and Management

Edited by
Leixun Yang, Xinye Zheng and Zhan-Ming Chen

Printed Edition of the Special Issue Published in *Energies*

www.mdpi.com/journal/energies

Selected Papers from the 8th Annual Conference of Energy Economics and Management

Selected Papers from the 8th Annual Conference of Energy Economics and Management

Special Issue Editors

Leixun Yang
Xinye Zheng
Zhan-Ming Chen

MDPI • Basel • Beijing • Wuhan • Barcelona • Belgrade

Special Issue Editors
Leixun Yang
National Natural Science Foundation
of China
China

Zhan-Ming Chen
Renmin University of China
China

Xinye Zheng
Renmin University of China
China

Editorial Office
MDPI
St. Alban-Anlage 66
4052 Basel, Switzerland

This is a reprint of articles from the Special Issue published online in the open access journal *Energies* (ISSN 1996-1073) from 2017 to 2019 (available at: https://www.mdpi.com/journal/energies/special_issues/cseem)

For citation purposes, cite each article independently as indicated on the article page online and as indicated below:

LastName, A.A.; LastName, B.B.; LastName, C.C. Article Title. *Journal Name* **Year**, *Article Number*, Page Range.

ISBN 978-3-03921-457-0 (Pbk)
ISBN 978-3-03921-458-7 (PDF)

Contents

About the Special Issue Editors

Liexun Yang received his Doctorate in Management Science from Xi'an Jiaotong University in 2001. He is Vice Director-General of the Department of Management Sciences of National Natural Science Foundation of China (NSFC). He was Visiting Scholar at the Kennedy School of Government at Harvard University in 2004 and Visiting Professor of the College of Management at National Sun Yat-sen University (NSYSU, Taiwan, China). He has published 4 monographs and over 50 journal papers about technology project management, information management, research policy, and other related areas. His current research interests include public policy, project evaluation and selection, and research policy.

Xinye Zheng received his Doctorate in Economics from Georgia State University in 2006. He is Professor and Dean of the School of Applied Economics, Renmin University of China. He is also Director of the Energy and Resource Strategy Research Center of the National Development and Strategy Research Institute of Renmin University of China, and Vice President of the Economic Research Institute of the "Belt and Road" of Renmin University of China. He was selected for the Cultural Masters ("four batches") talent program organized by Central Propaganda Department and "New Century Excellent Talents Support Program" organized by the Ministry of Education. His research fields include energy economics, industrial organization, and public economics. He has published more than 60 papers, an English monograph and 8 books in Chinese. He has provided decision-making consulting services for many departments of Chinese government and also wrote columns for news media such as China Energy News and China Business News, and been widely interviewed, covering CCTV news broadcasts, focus interviews, CCTV English channels, NHK Japan, to name but a few.

Zhan-Ming Chen received his Doctorate from College of Engineering, Peking University, in 2011 and BS/BEc from the Department of Mechanics and Engineering Science/China Center for Economics Research, Peking University, in 2006. He is now Associate Professor and Assistant Dean of the School of Applied Economics, Renmin University of China. Dr. Chen's current research focuses on energy economics and policy. He has published over 70 peer-reviewed papers with an h-index of 29 and over 2800 citations.

Preface to "Selected Papers from the 8th Annual Conference of Energy Economics and Management"

This volume is a collection of eight papers selected from the 8th Annual Conference of Energy Economics and Management held in Beijing, China on 22–24 September 2017. With over 500 participants, the conference was one of the leading conferences in China for presenting novel and fundamental advances in energy economics and management. The purpose of this conference is for scientists, scholars, engineers, and graduate students from universities and research institutes to present ongoing research activities in order to exchange research ideas in the area of energy economics and management. Selected papers cover different aspects of the broad spectrum of energy economics and management at both macro- and microlevels, including building energy efficiency, industrial energy demand, public policy to promote new energy technology, power system control technology, emission reduction policies in energy-intensive industries, emission measurements of cities, energy price movement, and the impact of new energy vehicles.

Leixun Yang, Xinye Zheng, Zhan-Ming Chen
Special Issue Editors

energies

MDPI

Article

Coal Supply Chains: A Whole-Process-Based Measurement of Carbon Emissions in a Mining City of China

Guangfang Luo [1,2], Jianjun Zhang [1,3,*], Yongheng Rao [1], Xiaolei Zhu [1] and Yiqiang Guo [3,4]

1 School of Land Science and Technology, China University of Geosciences, Beijing 100083, China; luoyi630@163.com (G.L.); yonghengrao@126.com (Y.R.); zhuxiaolei_cugb@163.com (X.Z.)
2 China Three Gorges Corporation Chongqing Branch, Chongqing 401147, China
3 Key Laboratory of Land Consolidation and Rehabilitation, Ministry of Land and Resources, Beijing 100083, China; guoyiqiang2002@126.com
4 Land Consolidation and Rehabilitation Center, Ministry of Land and Resources, Beijing 100035, China
* Correspondence: zhangjianjun_bj@126.com

Received: 10 October 2017; Accepted: 9 November 2017; Published: 13 November 2017

Abstract: The purpose of the study is to understand the carbon emissions in the coal supply chains of a mining city. The paper employed a conceptual methodology for the estimation of carbon emissions in the four processes of coal mining, selection and washing, transportation and consumption. The results show that the total carbon emission of the coal supply chain in Wu'an is up to 3.51×10^{10} kg and is mainly sourced from the coal mining and consumption, respectively accounting for 13.10% and 84.62%, which indicates that deep coal processing plays a more critical determinant in coal production and consumption. Among the pillar industries, the carbon emissions from the steel industry accounts for 85.41% of the total in the coal consumption process, which indicates that the structure of carbon emissions is dependent on the local industrial structure. Additionally, the carbon directly from CO_2 accounts for 89.46%. Our study is not only to be able to supply references for the formulation strategy of a low carbon city, but also to provide a new approach to urban development patterns with a new view for coal resource management.

Keywords: coal supply chain; carbon emission; whole process; mining city; China

1. Introduction

Over the recent decades, global carbon emissions have been experiencing a rapid increase owing to continued incredible economic growth and soaring carbon-intensive fossil-fuel consumption [1–3]. Such a significant increment of carbon emissions may induce climate change, sea level rise, and global temperature increases and shoreline erosion, which bring environmental impacts [4,5]. The IPCC (Intergovernmental Panel on Climate Change) affirms that greenhouse gases (GHG), in particular carbon emissions, from human activities has been the dominant reason for the observed global warming since the mid-20th century [6]. As one manifestation generated by industrialization, the loss of coal reserves has become one cause of man-made environmental liabilities [7], and its production concerns the mitigation of climate change [8]. Currently, coal provides about 30% of global primary energy needs, and remains a key primary energy resource globally [9,10], which consequently creates a big source of greenhouse gas emissions [11]. Environmentally, the country inventories of greenhouse gas emission sources and sinks are requested and commenced with the carbon emission of fossil fuels [12,13]. Crossing the national scale, like the US and Australia [14,15], to the local scale, like the Northwest of the UK [16], Beijing [17], etc., the calculation of carbon emissions generated by the consumption of fossil fuels has been treated as a key governmental task and is the concern of international scientific communities [18].

As a commodity, coal is experiencing the whole process from its production to consumption. The process in this cycle requires inputs and produces outputs, which include both materials and energy, and it transforms and dissipates energy in different ways [19]. To generate energy, the operation phase is extended to the mining and transportation of coal (upstream processes) as well as waste disposal and the recovery of land (downstream processes) [20]. However, at the same time, the various unfavorable environmental effects are simultaneously produced [21], including carbon emissions and their induced disasters [22]. Responding to the whole process of coal exploration and utilization, the carbon footprint is traced and measured by coal supply chains from mining, selection and washing, transportation, distribution and consumption [23,24], especially in the process of power generation [25,26]. Besides, the research into carbon emissions from energy consumption lists is gradually transited to the side view of product consumption [27–29], and the relevant method for carbon emissions is adopted to estimate the emission coefficient of each stage in the coal-extracted and -fired process [30,31]. Clearly, the carbon emissions associated with the coal industry completely follow the whole process from production to consumption [32].

The measure method, material balance method and discharge coefficient method are the three major adopted ways to estimate the carbon emissions from coal and other energy sources [33]. In general, there are two methods to calculate the coal bed methane emissions in the coal mining procedure: one is the IPCC guidelines for national greenhouse gas inventories, which combines the coal bed methane with the coal production [34], and the other is the measure method, including the gas concentration–depth relationship method, mine gas emission method and analogy method [35]. Accordingly, the model analysis method becomes the most effective method due to the complexity of research that carbon emission sources are related to all aspects of human production and living [36–39]. Provably, the framework of carbon emissions in coal power generation, which is composed of coal mining, coal transporting, coal combustion and waste disposal, has been modeled and examined [40].

As reported, it can be argued that the perspectives and objects of these researchers are mainly focused on a single aspect, such as coal-fired electricity or the steel industry chain rather than all industrial sectors which use coal as the main energy power [20,41–44]. Currently, many countries are involved in this research field, including China [45]. In the process of industrialization and urbanization in China, coal consumption accounts for 70% of energy consumption [46], and a characteristic significance exists in that it concentrates on the electricity, steel, cement and chemical industries. Moreover, in the foreseeable future, the coal will remain the dominating fuel and there is a great potential that its demand will be set to increase [47]. Therefore, understanding the carbon flows within the human–environment nexus will help to promote human well-being while protecting the earth's living systems [48]; besides, the carbon emissions in coal supply chains is of great importance for climate change mitigation and associated policy-making in developing countries. Based on these research gaps and possible contributions to urban sustainability, we choose Wu'an, a typical Chinese mining city, as a study case, and attempt to (1) establish the link of carbon emissions and coal supply chains; (2) measure and quantify the carbon emission in coal supply chains from coal mining, selection and washing, transportation, and consumption; and (3) create an understanding of land use changes in mitigating carbon emissions in the process of coal transportation. Our study, which regards the four main coal consumption sectors as a whole object in the coal consumption link, can improve the accuracy and rationality of the coal supply chain system.

2. Materials and Methods

2.1. General Situation of the Study Area

Wu'an, a mining city, belonging to the Hebei Province of China, lies at the eastern foot of the Taihang Mountains, and is located at 113°45′–114°22′ E, 36°28′–37°02′ N (Figure 1), which has a surface area of 1819 km^2. Wu'an is rich in mineral resources, such as coal, iron, cobalt, aluminum. The total coal reserve is up to 2.3 × 10^9 t, pig iron is as high as 1.61 × 10^7 t, crude steel is 1.66 × 10^7 t, and

cement is 1.85×10^7 t. The rapid industrial development increases the demand for coal resources and results in environmental deterioration.

Figure 1. Location of Wu'an in the Hebei Province of China.

2.2. Data Sources

The data in this study is categorized into three types. The first type is statistical data, including the consumption of coal, cement, electric power, steel, fertilizer production in various industries for the estimation of carbon emissions and local meteorological data for the correction of carbon density. The second type is raster data, including multi-phase remote sensing images, which are used to extract land use types for estimating the underlying indirect carbon emissions from coal transportation. Another type is retrieved from the IPCC guideline for national GHG inventories, including carbon emission coefficients, low calorific values, carbon coefficients of fossil energy, etc. [34].

2.3. Research Methods

2.3.1. Trace of Coal Supply Chains

In a mining city, the whole process of coal production and utilization is actually tied to a supply chain, which in our study is composed of the complete activities, including coal mining, coal selection and washing, coal transportation and finally delivered users or enterprises to finish the final consumption of coal products according to the consumer requirements. The electricity, steel, cement and chemical industries were selected as the four main coal consumers in Wu'an according to a local industrial structure and field investigation. Accordingly, the illustration of carbon emission accounts and sources in the coal supply chains of Wu'an mainly follow the whole process from coal production to consumption (Figure 2). The estimate of CO_2, N_2O and CH_4 emissions is involved in the process. Thus, our study is to make it clear that where the greenhouse gases come from, what role the whole process of coal production and utilization plays and which process is the determinant for carbon emissions in a mining city.

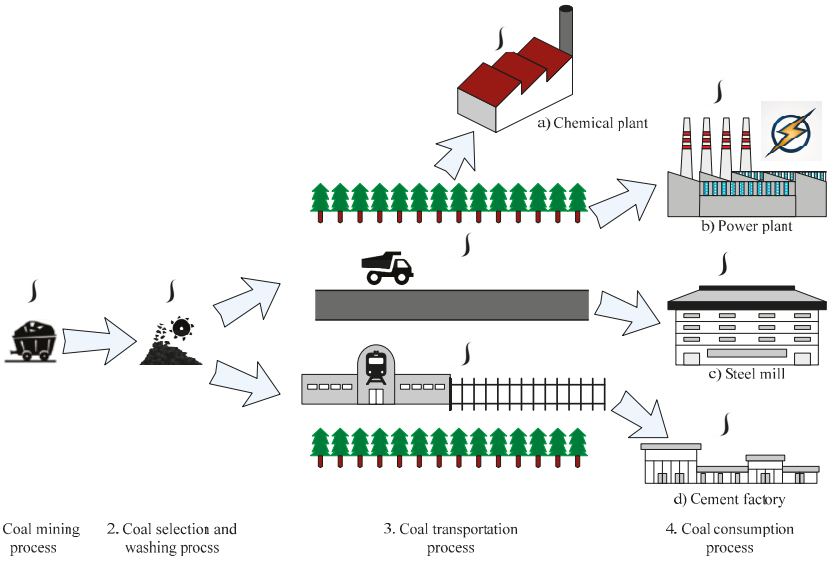

Figure 2. Coal supply chains in Wu'an.

The exploitation method, transportation path, and consumption type are the important sectors that affect carbon emissions in the complete coal supply chain. In the process of coal mining and selection and washing, the main carbon sources are from coal, electricity and energy consumption, and also include coalbed methane released in the mining process [45]. The carbon emissions in the coal transportation process mainly come from energy consumption and carbon sequestration by vegetation loss, as the construction of transport networks used by coal transportation has caused damage to the surrounding vegetation. In the coal consumption section, the carbon resources are mainly from fossil energy consumption, power consumption and chemical reaction to raw material production.

As shown in Figure 2, there are four main carbon-emitting processes in the coal supply chain of Wu'an: coal mining, coal selection and washing, coal transportation, and coal consumption. The carbon emissions in the coal supply chain are measured and summed by the carbon emissions of these four processes (Equation (1)).

$$E_{tc} = E_m + E_{sw} + E_t + E_c \quad (1)$$

where E_{tc} is the total carbon emissions in coal supply chains, E_m is the carbon emissions in the mining process, E_{sw} is the carbon emissions in the coal selection and washing process, E_t is the carbon emissions in the coal transportation process, and E_c is the carbon emissions in the coal consumption process.

2.3.2. Inventory of Carbon Emissions in Coal Supply Chains

Carbon Emissions in the Coal Mining Process

The carbon in the coal mining process is emitted from a coalbed carbon leak, energy consumption and motive power for machinery. The total carbon emissions in this process are calculated by Equation (2).

$$E_m = E_{cl} + E_{ec} + E_{ep} \quad (2)$$

where E_m is the total carbon emissions in mining process, E_{cl} is the coalbed carbon leak in this process, E_{ec} is the carbon emissions caused by energy consumption, E_{ep} is the carbon emissions caused by electricity consumption which provides motive power for running machinery.

(1) Coalbed carbon leaks in the coal mining process

According to the IPCC guideline for national greenhouse gas inventories [34], the coalbed methane emissions in the coal mining process is calculated by the Equation (3).

$$E_{cl} = P_c \times EF_j \times TF_j \times GWP_j \quad (3)$$

where E_{cl} is the energy consumed in the extraction of coal in the mining process, P_c is the amount of coal production, EF_j is the emission factor of greenhouse gas j (Table 1), TF_j is the transfer factor of greenhouse gas j under 20 °C and standard atmospheric pressure, GWP_j is the ratio of the greenhouse effect of a unit weight of greenhouse gas j emission (Table 2), named global warming potential of greenhouse gas j emission. The GWP value is used in the Kyoto Protocol of the United Nations Framework Convention on Climate Change as a metric for weighing the climatic effect of the emission of different GHGs.

Table 1. The factors influencing carbon emissions in coal production.

Mining Type	Mining Depth (m)	Emission Factors (m^3/t)
Underground coal mine	<200	10
	<400	18
	>400	25
Open strip mines	<25	0.3
	<50	1.2
	>50	2

Table 2. GWP values of greenhouse gases *.

GHG	GWP Default Values (g CO_2 Equivalent/g GHG)
CO_2	1
CH_4	23
N_2O	296

* The data was retrieved from the Third Assessment Report of the Intergovernmental Panel On climate Change [6].

(2) Carbon emissions caused by energy consumption

Underground mining is the main approach in Wu'an. The extraction of coal resources generally depends on energy consumption, including direct energy consumption such as the burning of fossil fuels for boilers [49] and the indirect electricity consumption for mining equipment [30]. They are estimated by Equations (4) and (5).

$$DE_{ec} = c_{ffi} \times NHV_i \times cc_i \times or_i \times r_c \quad (4)$$

where DE_{ec} is the direct carbon emission caused by energy consumption in the coal mining process, c_{ffi} is the amount of combusted fossil fuel i, NHV_i is the net heating value of combusted fossil fuel i, cc_i is the carbon content of combusted fossil fuel i, or_i is the oxidation ratio of fossil fuel i, r_c is the conversion ratio between CO_2 and C (44/12). This paper extracts the parameters from the "2006 IPCC Guidelines for National Greenhouse Gas Inventories" [34,50] (Table 3).

$$IE_{ec} = C_e \times P_c \times L_i \quad (5)$$

where IE_{ec} is the indirect carbon emission caused by energy consumption in coal mining process, C_e is the electricity consumption, P_c is the coal equivalent consumption for 1 kWh power, L_i is the emission coefficient of greenhouse gases. The emission coefficient of CO_2 is 840.1914 g CO_2/kWh, and that of N_2O is 0.053352 g CO_2/kWh [30].

Table 3. Net heating values and carbon contents of combusted fossil fuels.

Type	Lower Calorific Value (kJ/kg kJ/m^3)	Carbon Content (kg/GJ)
Raw coal	20,908	25.8
Coke	28,435	29.2
Washed coal	26,344	26.2
Crude oil	41,816	20
Gasoline	43,070	18.9
Kerosene	43,070	19.6
Diesel fuel	42,652	20.2
Natural gas	38,931	15.3

Carbon Emissions in the Coal Selection and Washing Process

Coal spontaneous combustion to a certain degree happens in the process of coal selection and washing [31], besides, electricity consumption also drives the equipment operations in that process, which both induce carbon emissions [43]. Similarly, the carbon is sourced from the two sources of direct and indirect emissions. The Equations (4) and (5) are similarly referenced for the calculation.

Carbon Emissions in the Coal Transportation Process

Mining and land use activities within the transport network are associated with energy consumption and carbon emissions. The sources are mainly from the combustion of fossil fuels for driving transport vehicles and the reduction of carbon sequestration capacity caused by vegetation loss along transportation lines, respectively regarded as direct and indirect carbon emissions.

(1) Direct carbon emissions in the coal transportation process

The calculation of direct carbon emissions is based on the coal transport modes and their corresponding consumption of fossil fuels for driving vehicles. The main means of coal transportation are railway and road in Wu'an and diesel fuels are combusted in the process of railway transport, while the road transport generally uses medium-duty trucks, which also provide the momentum by diesel fuels. The direct carbon emissions in coal transportation are calculated by Equation (6).

$$DE_{ct} = \sum_{i=1}^{n} P_c \times p_i \times l_i \times fc_i \times NHV_i \times cc_i \times or_i \quad (6)$$

where DE_{ct} is the direct carbon emission in the coal transportation process, P_c is the amount of coal production, p_i is the proportion of the transport capacity of mode i to the total, l_i is the average transport length of mode i, fc_i is the fuel consumption of mode i, NHV_i is the net heating value of diesel fuels consumed by mode i, cc_i is the carbon content of diesel fuels consumed by mode i, and or_i is the oxidation ratio of diesel fuels consumed by mode i.

According to the local survey, the ratio of transport volumes by railway and road is 1:3. The transport lengths of railways and roads are 164.78 km and 386.22 km, respectively, which were extracted from the transport network maps. The NHV of diesel fuels is 42,652 kJ/kg (Table 3). The fuel consumption of a diesel locomotive is 24.6 kg/(10^4 t·km) [30]. In general, the fuel consumption of road transport trucks is around 500–700 kg/(10^4 t·km) [51], and the value in this study is 650 kg/(10^4 t·km) according to local transport and vehicle conditions. The carbon content of diesel fuels is 20.2 kg/GJ (Table 3). The oxidation ratio is assumed as 100% (default value).

(2) Indirect carbon emissions in the coal transportation process

The carbon emissions caused by ground vegetation destruction has a profound impact on carbon fluxes [52]. The carbon sequestration capacity of vegetation is lost owing to the land use conversion within coal transport networks [53]. Clearly, land use change is a massive source of carbon emissions and a significant contributor to carbon emissions [54–56]. In Wu'an, long-term coal transportation accelerates the conversion of vegetative cover to bare land, which results in reducing the original vegetation carbon sequestration capacity. Thus, the calculation of carbon sequestration reduction relies on the land transfer matrix, followed by the steps [57]: (1) classify land use types by remote sensing images; (2) extract the transport networks from land use maps; (3) treat railway and road as the center and select 1000 m as the buffer distance acting on the surrounding land types to obtain the land transfer matrix (Figures 3 and 4). The loss of carbon sequestration by land use change along coal transport lines is measured by Equation (7).

$$L_{cs} = \Delta A_{i-j} \times k = \left(A_i - A_j\right) \times k \tag{7}$$

L_{cs} is the loss of carbon sequestration in coal transportation process, ΔA_{i-j} is the total area of land use type i that is converted to all other land use types j, k is the carbon density of corresponding land type. For cropland subjected to a cycle of planting to harvest within one year, the substantial carbon accumulation by vegetative cover is ignored. Additionally, water bodies play an insignificant role in carbon sequestration, so this part is also ignored. Thus, the carbon densities of forest and pasture are substantially needed, which are determined by the local context (temperature, precipitation, light intensity, etc.) and reported literatures [58–60].

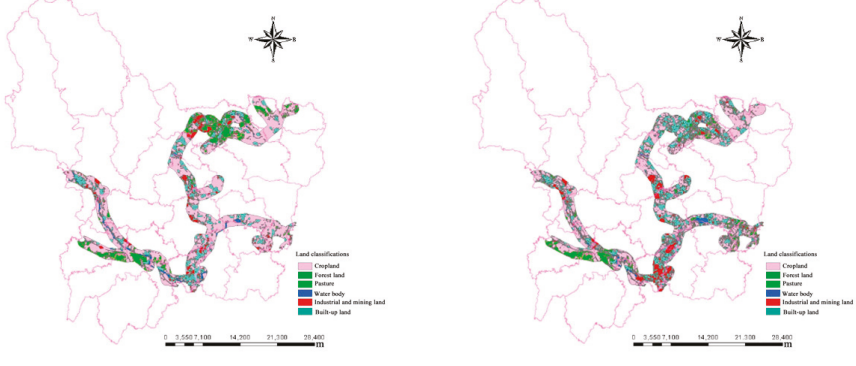

(**a**) 2010 (**b**) 2014

Figure 3. Land use within buffer zones along the railways of Wu'an in (**a**) 2010 and (**b**) 2014.

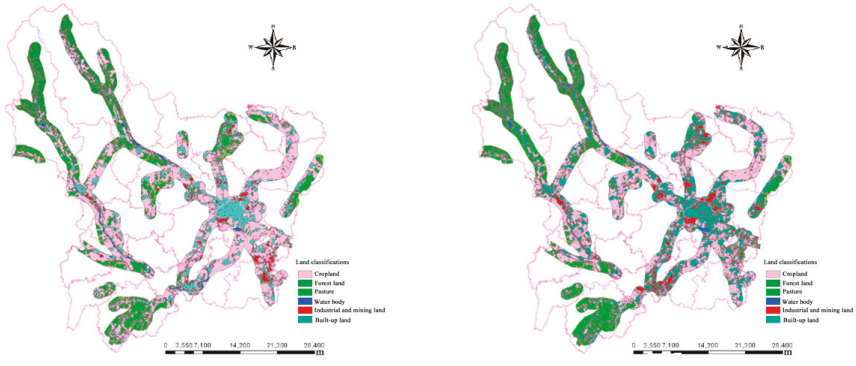

(**a**) 2010 (**b**) 2014

Figure 4. Land use within buffer zones along the roads of Wu'an in (**a**) 2010 and (**b**) 2014.

Carbon Emissions in the Coal Consumption Process

According to the Wu'an context, the electricity, steel, cement and chemical industries were selected as the coal consumption objects for further study. To avoid double counting, the carbon emissions caused by power consumption in these non-electricity industries will no longer be calculated separately, and the electricity industry is treated as a separate object. The calculation of carbon emissions in different industries are delineated as follows:

(1) Electricity industry

The electricity industry is currently the major driver of coal demand in China. The carbon emission is sourced from the two aspects of coal combustion for power generation and residue disposal. In our study, the estimate of carbon emissions similarly follows Equations (4) and (5).

(2) Steel industry

According to a variety of carbon sources in the steel industry, the carbon emissions come from the combustion of fossil fuels, chemical reactions in the production process, and electricity consumption for driving production. The estimate of the first carbon source is calculated by Equation (4), and raw coal, cleaned coal, coke, diesel fuel and gasoline are involved in the process. The estimate of the third carbon source is included in the calculation of the electricity industry, so this part is ignored. The estimate of the second carbon source is estimated by the reduction reaction for generating carbon dioxide. In general, 70% of consumed coal is used for coking, and 75% of coke is for combustion, and the rest (25%) is regarded as the reducing agent. The reduction reaction [43] and carbon emissions follow Equations (8) and (9)

$$C + Fe_xO_y = CO + Fe,\ CO + Fe_xO_y = Fe + CO_2 \tag{8}$$

$$E_{si} = M_{ra} \times EF \tag{9}$$

where E_{si} is the carbon emission by the reduction reaction in steel production process, M_{ra} is the mass of reducing agent (25% of coke consumption), and EF is the emission factor (here it is 3.1 [12]).

(3) Cement industry

The carbon emissions in the cement industry are sourced from the decomposition of limestone, the combustion of fossil fuels, and electricity consumption for driving production. The estimate of the first carbon source is calculated by Equation (10) [61], and the estimate of the second carbon source is

estimated by Equation (4) (raw coal and diesel fuel involved), and the last source is estimated in the electricity industry.

$$E_{ci} = P_{cm} \times p_{ck} \times p_l \times r_c \quad (10)$$

E_{ci} is the carbon emission by the decomposition of limestone in cement industry, P_{cm} is the production of cement, p_{ck} is the proportion of clinker in limestone (here it is 61%), p_l is the proportion of lime in the clinker (here it is 68% [61]), and r_c is the conversion ratio between CO_2 and lime (44/56).

(4) Chemical industry

In our study, the carbon emissions in the chemical industry are sourced from the consumption of fertilizers and electricity consumption for driving production. Similarly, the estimate of electricity consumption is involved in the electricity industry, and the use of fertilizers generates carbon in the steps of production and transportation, expressed by Equation (11).

$$E_{chi} = C_f \times k_f \quad (11)$$

E_{chi} is the carbon emission caused by the consumption of fertilizers in the chemical industry, C_f is the consumption of fertilizers, and k_f is the summed coefficient of carbon emissions in the steps of production and transportation (here it is 857.54 g/kg [62]).

2.3.3. Analysis and Interpretation

To cater for the research objectives, we employed the comparative analysis method and the statistical analysis method to recognize the critical devotion(s) to carbon emissions in the coal supply chains. This study conducted three layers for comparative and statistical analyses of separate process types, industrial types and greenhouse gas types. The results are mainly characterized by the structure of carbon emissions in these layers, and the possible causes and effects are analyzed to link the coal supply chain.

3. Results and Analysis

3.1. Calculation of Carbon Emissions in Coal Supply Chains

3.1.1. Carbon Emissions in the Coal Mining Process

According to the carbon sources in coal mining, the carbon emissions were calculated from coalbed carbon leaks and energy consumption.

(1) By coalbed carbon leak

The coal mining process generally leaks CH_4 and CO_2. In 2014, the production of coal in Wu'an was 9.44 million tons, and the mining depth was more than 400 m. According to the Equation (3), the emissions of CH_4 and CO_2 are estimated as follows:

CH_4: $9.44 \times 10^6 \times 25 \times 0.67 = 1.58 \times 10^8$ kg $CH_4 = 1.58 \times 10^8 \times 23$ kg $CO_2 = 3.64 \times 10^9$ kg CO_2
CO_2: $9.44 \times 10^6 \times 25 \times 0.8 = 1.89 \times 10^8$ kg CO_2
Total: $3.64 \times 10^9 + 1.89 \times 10^8 = 3.83 \times 10^9$ kg CO_2

(2) By energy consumption

As analyzed above, the energy consumption in the coal mining process mainly comes from two sources: coal consumption for heating boilers in the mining area and electricity consumption for the mining equipment [45]. The two categories of carbon emissions are calculated by Equations (4) and (5).

- Coal consumption for heating boilers:

  CO_2: $27.2 \times 9.44 \times 10^6 \times 20{,}908 \times 25.8 \times 10^{-6} \times 44/12 = 5.08 \times 10^8$ kg CO_2

- Electricity consumption for mining equipment:

  CO_2: $33.7 \times 9.44 \times 10^6 \times 840.1914 \times 10^{-3} = 2.67 \times 10^8$ kg CO_2

  N_2O: $33.7 \times 9.44 \times 10^6 \times 0.053352 \times 10^{-3} = 1.70 \times 10^4$ kg $N_2O = 1.70 \times 10^4 \times 296$ kg $CO_2 = 5.03 \times 10^6$ kg CO_2

  Total: $2.67 \times 10^8 + 5.03 \times 10^6 = 2.72 \times 10^8$ kg CO_2
- Total:

  CO_2: $5.08 \times 10^8 + 2.72 \times 10^8 = 7.80 \times 10^8$ kg CO_2

(3) Total carbon emissions in the coal mining process

The total carbon emission in coal mining process is summed by the emissions caused by coalbed carbon leaks and energy consumption.

CO_2: $3.83 \times 10^9 + 7.80 \times 10^8 = 4.61 \times 10^9$ kg CO_2

3.1.2. Carbon Emissions in the Coal Selection and Washing Process

In coal selection and washing, the source of carbon emissions is from electricity consumption by equipment and spontaneous coal combustion. It is estimated that, at the present stage in China, the energy consumption per ton of raw coal for the selection and washing processes is approximately 3 kWh, and the spontaneous loss rate is approximately 1%. Therefore, the carbon emissions in this process include:

- By coal combustion:

  CO_2: $9.44 \times 10^9 \times 1\% \times 20{,}908 \times 25.8 \times 10^{-6} \times 44/12 = 1.87 \times 10^8$ kg CO_2
- By electricity consumption:

  CO_2: $9.44 \times 10^6 \times 3 \times 840.1914 \times 10^{-3} = 2.38 \times 10^7$ kg CO_2

  N_2O: $9.44 \times 10^6 \times 3 \times 0.053352 \times 10^{-3} = 1.51 \times 10^3$ kg $CO_2 = 1.51 \times 10^3 \times 296$ kg $CO_2 = 4.50 \times 10^5$ kg CO_2

  Total: $2.38 \times 10^7 + 4.50 \times 10^5 = 2.43 \times 10^7$ kg CO_2
- Total carbon emission in coal selection and washing process:

  CO_2: $1.87 \times 10^8 + 2.43 \times 10^7 = 2.11 \times 10^8$ kg CO_2

3.1.3. Carbon Emissions in Coal Transportation Process

(1) Direct carbon emissions in coal transportation

- By railway transport:

  CO_2: $944 \times 25\% \times 24.6 \times 164.78 \times 42{,}652 \times 20.2 \times 10^{-6} \times 44/12 = 3.02 \times 10^6$ kg CO_2
- By road transport:

  CO_2: $944 \times 75\% \times 650 \times 386.22 \times 42{,}652 \times 20.2 \times 10^{-6} \times 44/12 = 5.61 \times 10^8$ kg CO_2
- Total:

  CO_2: $3.02 \times 10^6 + 5.61 \times 10^8 = 5.64 \times 10^8$ kg CO_2

(2) Indirect carbon emissions in coal transportation

As mentioned above, the 1000 m buffer zones were made along transport lines, and the transfer matrix of land use within buffer zones was extracted through the geographic information system (GIS) (Table 4). It is clear that, before and after intensified mining activities, a lot of cropland, forest, pasture and water bodies are encroached on by industrial and mining land as well as associated built-up land.

Table 4. Railway/road buffer transfer matrix of land use.

Land Use Type	Built-Up Land (ha)	Industrial and Mining Land (ha)
Cropland	6.12/8.00	0.63/0.61
Forest	0/0.09	0/0
Pasture	2.26/3.32	1.09/0.91
Water body	0.54/0.99	0.06/0.12
Built-up land	20.16/37.77	3.19/3.03

According to the Equation (7), the carbon emissions by the reduction of vegetative cover are:

- By forest:

  CO_2: $0.09 \times 73.24 \times 10^3 \times 44/12 = 2.42 \times 10^4$ kg CO_2
- By pasture:

  CO_2: $(2.26 + 1.09 + 3.32 + 0.91) \times 6.20 \times 10^3 \times 44/12 = 1.72 \times 10^5$ kg CO_2
- Total:

  CO_2: $2.42 \times 10^4 + 1.72 \times 10^5 = 1.96 \times 10^5$ kg CO_2

(3) Total carbon emissions in the coal transportation process

The total carbon emissions in the coal transportation process are summed by direct and indirect carbon emissions.

CO_2: $5.64 \times 10^8 + 1.96 \times 10^5 = 5.64 \times 10^8$ kg CO_2

3.1.4. Carbon Emissions in the Coal Consumption Process

(1) Electricity industry

The electricity consumption of Wu'an in 2014 was $346{,}028 \times 10^4$ kWh. Therefore, the carbon emissions of the electricity industry are measured by:

CO_2: $346{,}028 \times 10^4 \times 840.1914 \times 10^{-3} = 2.91 \times 10^9$ kg CO_2

N_2O: $346{,}028 \times 10^4 \times 0.053352 \times 10^{-3} = 1.85 \times 10^5$ kg $N_2O = 1.85 \times 10^5 \times 296$ kg $CO_2 = 5.48 \times 10^7$ kg CO_2

Total: $2.91 \times 10^9 + 5.48 \times 10^7 = 2.96 \times 10^9$ kg CO_2

(2) Steel industry

- By the combustion of fossil fuels:

  a. Raw coal:

     CO_2: $41.70 \times 10^7 \times 20{,}908 \times 25.8 \times 10^{-6} \times 44/12 = 8.25 \times 10^8$ kg CO_2

  b. Cleaned coal:

     CO_2: $233.26 \times 10^7 \times 26{,}344 \times 26.209 \times 10^{-6} \times 44/12 = 5.90 \times 10^9$ kg CO_2

  c. Coke:

     CO_2: $610.19 \times 10^7 \times 28{,}435 \times 29.2 \times 10^{-6} \times 75\% \times 44/12 = 1.39 \times 10^{10}$ kg CO_2

  d. Diesel fuel:

     CO_2: $1.08 \times 10^7 \times 42{,}652 \times 20.2 \times 10^{-6} \times 44/12 = 3.41 \times 10^7$ kg CO_2

  e. Gasoline:

     CO_2: $0.00476 \times 10^7 \times 43{,}070 \times 18.9 \times 10^{-6} \times 44/12 = 1.42 \times 10^5$ kg CO_2

     Total: $8.25 \times 10^8 + 5.90 \times 10^9 + 1.39 \times 10^{10} + 3.41 \times 10^7 + 1.42 \times 10^5 = 2.07 \times 10^{10}$ kg CO_2

- By chemical reaction

  CO_2: $610.19 \times 10^7 \times 25\% \times 3.1 = 4.73 \times 10^9$ kg CO_2
- Total carbon emissions in the steel industry (electricity consumption not included)

  CO_2: $2.07 \times 10^{10} + 4.73 \times 10^9 = 2.54 \times 10^{10}$ kg CO_2

(3) Cement industry

- By the combustion of fossil fuels

  a. Raw coal:

  CO_2: $17.04 \times 10^7 \times 20{,}908 \times 25.8 \times 10^{-6} \times 44/12 = 3.37 \times 10^8$ kg CO_2

  b. Diesel fuel:

  CO_2: $0.0179 \times 10^7 \times 42{,}652 \times 20.2 \times 10^{-6} \times 44/12 = 5.65 \times 10^5$ kg CO_2

  Total: $3.37 \times 10^8 + 5.65 \times 10^5 = 3.38 \times 10^8$ kg CO_2
- By the decomposition of limestone

  CO_2: $313.10 \times 10^7 \times 68\% \times 61\% \times 44/56 = 1.02 \times 10^9$ kg CO_2
- Total carbon emissions in the cement industry (electricity consumption not included)

  CO_2: $3.38 \times 10^8 + 1.02 \times 10^9 = 1.36 \times 10^9$ kg CO_2

(4) Chemical industry

The consumption of fertilizers in Wu'an in 2014 was 1.84×10^4 t. Therefore, the carbon emissions of the chemical industry are measured by:

CO_2: $1.84 \times 10^7 \times 836.08 \times 10^{-3} = 1.54 \times 10^7$ kg CO_2

(5) Total carbon emissions in the coal consumption process

CO_2: $2.96 \times 10^9 + 2.54 \times 10^{10} + 1.36 \times 10^9 + 1.54 \times 10^7 = 2.97 \times 10^{10}$ kg CO_2

3.2. Inventory of Carbon Emissions in Coal Supply Chains

According to the measurement model of carbon emissions in coal supply chains, the carbon emissions in different processes can be calculated and compared by using the normalized CO_2 equivalents, and thereby the total and subtotal carbon emissions are obtained (Table 5).

Table 5. Carbon emissions in the coal supply chains of Wu'an.

Process			GHG Type	GHG Emission (kg)	CO_2 Equivalent (kg)	Subtotal (kg)	Subtotal' (kg)	Total (kg)
Mining	Coalbed carbon leak		CO_2 CH_4	1.89×10^8 1.58×10^8	1.89×10^8 3.64×10^9	3.83×10^9	4.61×10^9	3.51×10^{10}
	Energy consumption		CO_2 N_2O	7.75×10^8 1.70×10^4	7.75×10^8 5.03×10^6	7.80×10^8		
Selecting and washing	Coal combustion		CO_2	1.87×10^8	1.87×10^8	1.87×10^8	2.11×10^8	
	Electricity consumption		CO_2 N_2O	2.38×10^7 1.51×10^3	2.38×10^7 4.50×10^5	2.43×10^7		
Transportation	Direct emission		CO_2	5.64×10^8	5.64×10^8	5.64×10^8	5.64×10^8	
	Indirect emission		CO_2	1.96×10^5	1.96×10^5	1.96×10^5		
Consumption	Electricity industry		CO_2 N_2O	2.91×10^9 1.85×10^5	2.91×10^9 5.48×10^7	2.96×10^9	2.97×10^{10}	
	Steel industry	Combustion of fossil fuels Chemical reaction	CO_2 CO_2	2.07×10^{10} 4.73×10^9	2.07×10^{10} 4.73×10^9	2.54×10^{10}		
	Cement industry	Combustion of fossil fuels Decomposition of limestone	CO_2 CO_2	3.38×10^8 1.02×10^9	3.38×10^8 1.02×10^9	1.36×10^9		
	Chemical industry		CO_2	1.54×10^7	1.54×10^7	1.54×10^7		

3.3. Analysis and Interpretation

3.3.1. Analysis by Different Processes

Based on the streamlined assessment methodology above, it can be concluded that the total carbon emissions of the coal supply chains in Wu'an is up to 3.51×10^{10} kg. Clearly, the carbon emissions in the coal supply chains are mainly sourced from coal mining and consumption, respectively accounting for 13.10% and 84.62% of the total (Table 6). That is to say, the end consumption of coal resources is the greatest contributor to the carbon emissions of a mining city, which can be the entry point to mitigate the negative effects. Besides, it was found that deep coal processing accelerates the conversion and release of carbon contained in coal resources.

Table 6. Structure of carbon emissions in different processes.

Processes	Carbon Emission (10^{10} kg)	Proportion (%)
Mining	0.46	13.10
Selecting and washing	0.02	0.57
Transportation	0.06	1.71
Consumption	2.97	84.62
Total	3.51	100

3.3.2. Analysis by Different Industrial Types

Among the industries, the carbon emissions from the steel industry accounts for 85.41% of the total in the coal consumption process, which indicates that the local pillar industry plays a critical role in carbon emissions, see Table 7. Due to the support of the electricity industry for all production operations, coal-fired power also plays a critical role in carbon emissions, and it may even last in Wu'an for the long term. The structure of carbon emissions in different industries is characterized by industrial and economic structures. If the carbon emissions from the electricity consumption in non-consumption processes is categorized as the inventory of the "electricity industry", the total carbon emissions in this industry can reach 3.26×10^9 kg CO_2 (mining process—2.72×10^8 kg, selecting and washing process—2.43×10^7 kg and consumption process—2.96×10^9 kg) accounting for 10.85% (with an increase of about 1%). Even in that case, the steel industry is still the biggest source among the pillar industries in Wu'an, accounting for near 85%. Even so, the carbon emission generated by the steel industry is sourced by the combustion of fossil fuels in the production, rather than the steel itself. Clearly, the industrial structure in a mining city basically determines the structure of carbon emissions.

Table 7. Structure of carbon emissions in different industry types.

Industrial Types	Carbon Emission (10^{10} kg)	Proportion (%)
Electricity industry	0.296	9.95
Steel industry	2.540	85.41
Cement industry	0.136	4.57
Chemical industry	0.002	0.07
Total	2.974	100

3.3.3. Analysis by Different Greenhouse Gas Types

In Wu'an, the coal supply chain generally generates three main types of greenhouse gases, including CH_4, N_2O and CO_2. The carbon from CO_2 accounts for 89.46% of the total, and the equivalent CO_2 converted from CH_4 is also an important source for carbon emissions (Table 8). The majority of these emissions results from direct coal combustion. Clearly, the direct carbon emissions are sourced from carbon-related greenhouse gases.

Table 8. Structure of emitted greenhouse gases in the coal supply chains.

Greenhouse Gases	Equivalent Carbon Emission (10^{10} kg)	Proportion (%)
CO_2	3.14	89.46
N_2O	0.01	0.28
CH_4	0.36	10.26
Total	3.51	100

4. Conclusions and Discussion

4.1. Main Achievements

In China, the emergence and development of mining cities mainly depends on coal supply chains, which furnish the energy and economic momentum. Therefore, to achieve a low carbon economy in coal supply chains is the emphasis of sustainable development in mining cities. This study employed a conceptual methodology for the estimation of the whole process-based carbon emissions in a Chinese mining city. The coal supply chain was established from the four processes of coal mining, selection and washing, transportation and consumption. Furthermore, a more comprehensive coal consumption system was established, and the coal consumers in our study were extended to the steel, cement and chemical industries, rather than the simply calculation of coal-fired power plants. The research results show that the end consumption of coal resources is the greatest contributor to the carbon emission of Wu'an, and the local pillar industry plays a critical role.

Human requirements and activities determine land use [63,64], while land use is one of the impact factors of key underlying carbon emissions in coal transportation. Especially in our study, land use change and its impacts on carbon sequestration from coal transportation were considered in the measurement. The analysis of the impact of transport networks on carbon sequestration capacity is the difficulty of the research, but it is also the breakthrough and innovation which relies on the correct interpretation of remote sensing images. We attempted to employ the land use transfer matrix within transport network buffers through remote sensing (RS) and geographic information system (GIS) platforms. Energy consumption is considered an important step to support regional carbon emission mitigation policies. For the coal supply chain, the biggest carbon emissions contributor to a mining city, understanding the carbon flows in the supply chain becomes a precondition for the mitigation of greenhouse gas emissions and for providing systematic regulation and management by the government conveniently.

4.2. Limitations and Uncertainties

The research on the carbon emissions in the coal supply chain is mainly sourced from the whole coal-extracted and -fired process, which determines the carbon emission system of a mining city. As reported, city carbon emissions mainly can be divided into the four types of direct emissions, responsible emissions, indirect emissions and logistic emissions [65]. Based on the comparative analysis, it was found that the coal supply chain also has the same four types of carbon emissions. Direct emissions are represented as carbon emissions caused by local coal production and consumption. Indirect emissions are the consumption of other products that are introduced into the supply chain. At the same time, the coal production not only provides their own energy needs, but a part is delivered to the surrounding towns for energy support, which is regarded as responsible emissions. Moreover, there is also the logistics emission mainly reflected in the transit of coal freight services. Our study adopts a relatively independent objective perspective to study the carbon emissions of a coal supply chain that strips the responsible emissions and logistic emissions, and regards the direct emissions and indirect emissions as the study objects from the entire range independently. This is an innovation point of the article but also the limitation in a sense, a further study needs to pay close attention to the two types of carbon emissions.

After our field investigation in the coal-related industries, it was found that the power supply for most of the large- and medium-scale industries is mostly sourced from themselves (self-generating electricity). In order to know the entirety of carbon emissions in each process of coal supply chains, this paper basically followed the original way of power generation in these industries. Thus, the understanding of carbon emissions in the consumption process deserves further debate. However, the analysis in Section 3.3.2 indicates that the structure of carbon emissions in our study is dependent on the local industrial structure. In addition, as the data cannot be acquired, the coefficients in coal mining and processing were estimated according to the relevant literatures. This may result in a certain deviation in the calculation. Therefore, a further study needs to conduct investigations into the actual production process of urban industries and local factors of the study area to improve the accuracy and precision.

4.3. Implications for Environmental Management

With growing concerns over anthropogenic climate change, an appropriate understanding of the carbon emission characteristics of coal supply chains from an environmental perspective is required. Our study provided the results of carbon emissions in coal supply chains, from coal mining, selection and washing, transportation to consumption, analyzed the carbon resources of each section and sought reduction directions, which provides a basis for evaluating the clean production and consumption of coal resources in a mining city.

In addition, China is the largest coal producer and consumer in the world and also the biggest carbon emission country, caused by coal production and consumption. The coal field focused on production is not only the main energy manufacturing unit, but also the energy consumption unit. Coal production, processing and utilization generates a lot of GHGs that place a severe burden on the environment, and the coal utilization problems of low efficiency and serious environmental destruction become a great challenge for the coal industry and even the whole society. Environmentally, future mineral extraction should be targeted at mineral production efficiency, and the coal supply chain should be focused on unit GDP energy consumption and energy efficiency. Local government also has to pay attention to the ecological damage and restoration of mineral extractions [66]. The accurate calculation of carbon emissions in the each process of coal supply chains is an important indicator for understanding the effect of coal-fired industries on global warming. Therefore, our study is not only able to supply references for the formulation strategy of a low carbon city, but also to provide a new approach to urban development patterns with a new view for coal resource management.

Acknowledgments: This article is supported by National Natural Science Foundation of China (Grant Nos.: 41571507, 41101531) and the Fundamental Research Funds for the Central Universities the China. Also, authors gratefully acknowledge the colleagues and friends in the Land Resources Bureau of Wu'an for providing the basic data and relevant information.

Author Contributions: Guangfang Luo analyzed the data and wrote the manuscript. Jianjun Zhang designed the research framework and wrote the manuscript. Yongheng Rao, Xiaolei Zhu and Yiqiang Guo collected and analyzed the data.

Conflicts of Interest: All the authors declare no competing financial interests.

References

1. Sheinbaum, C.; Ruíz, B.J.; Ozawa, L.; Nebra, S.A.; De Oliveira, S., Jr.; Bazzo, E. Energy consumption and related CO_2 emissions in five latin american countries: Changes from 1990 to 2006 and perspectives. *Energy* **2011**, *36*, 3629–3638. [CrossRef]
2. Chen, Z.M.; Chen, G.Q.; Chen, B. Embodied carbon dioxide emission by the globalized economy: A systems ecological input-output simulation. *J. Environ. Inform.* **2013**, *21*, 35–44. [CrossRef]
3. Zhou, Y.; Li, Y.P.; Huang, G.H. Planning sustainable electric-power system with carbon emission abatement through cdm under uncertainty. *Appl. Energy* **2015**, *140*, 350–364. [CrossRef]

4. Eissa, A.E.; Zaki, M.M. The impact of global climatic changes on the aquatic environment. *Procedia Environ. Sci.* **2011**, *4*, 251–259. [CrossRef]
5. Ghommem, M.; Hajj, M.R.; Puri, I.K. Influence of natural and anthropogenic carbon dioxide sequestration on global warming. *Ecol. Model.* **2012**, *235–236*, 1–7. [CrossRef]
6. Intergovernmental Panel on Climate Change (IPCC). *Climate Change 2001: The Scientific Basis. Third Assessment Report of the Intergovernmental Panel Onclimate Change*; Cambridge University Press: Cambridge, UK, 2001.
7. Cardoso, A. Behind the life cycle of coal: Socio-environmental liabilities of coal mining in Cesar, Colombia. *Ecol. Econ.* **2015**, *120*, 71–82. [CrossRef]
8. Ou, Y.; Zhai, H.; Rubin, E.S. Life cycle water use of coal- and natural-gas-fired power plants with and without carbon capture and storage. *Int. J. Greenh. Gas Control* **2016**, *44*, 249–261. [CrossRef]
9. Goto, K.; Yogo, K.; Higashii, T. A review of efficiency penalty in a coal-fired power plant with post-combustion CO_2 capture. *Appl. Energy* **2013**, *111*, 710–720. [CrossRef]
10. Dai, C.; Cai, X.H.; Cai, Y.P.; Huang, G.H. A simulation-based fuzzy possibilistic programming model for coal blending management with consideration of human health risk under uncertainty. *Appl. Energy* **2014**, *133*, 1–13. [CrossRef]
11. Sharifzadeh, M.; Bumb, P.; Shah, N. Carbon capture from pulverized coal power plant (pcpp): Solvent performance comparison at an industrial scale. *Appl. Energy* **2016**, *163*, 423–435. [CrossRef]
12. Intergovernmental Panel on Climate Change (IPCC). *Climate change 2007: Impacts, Adaptation and Vulnerability*; Contribution of Working Group II to the Fourth Assessment Report of the Intergovernmental Panel on Climate Change; IPCC: Geneva, Switzerland, 2007.
13. Zhao, Y.; Yuan, S.; Yun, W.; Guan, W.; Liu, H. Monitoring-assessing-prewarning system for agricultural land resources security. *Trans. Chin. Soc. Agric. Eng.* **2007**, *23*, 77–81.
14. Zhu, S. Good practices in australia for greenhouse gas inventory development. *Adv. Clim. Chang. Res.* **2011**, *7*, 204–209.
15. US DOE. *Carbon Dioxide Emissions From the Generation of Electric Power in the United States*; Department of Energy and Environmental Protection Agency: Washington, DC, USA, 2000.
16. Carney, S.; Shackley, S. The greenhouse gas regional inventory project (grip): Designing and employing a regional greenhouse gas measurement tool for stakeholder use. *Energy Policy* **2009**, *37*, 4293–4302. [CrossRef]
17. Xing, F.F.; Ouyang, Z.Y.; Wang, X.K.; Duan, X.N.; Zheng, H.; Miao, H. Inventory of final energy-carbon consumption and its structure in beijing; Abstracts of Ecosummit 2007—Ecological Complexity and Sustainability—Challenges & Opportunities for Century's Ecology. *Huanjing Kexue* **2007**, *28*, 1918–1923. [PubMed]
18. Benetto, E.; Rousseaux, P.; Blondin, J. Life cycle assessment of coal by-products based electric power production scenarios. *Fuel* **2004**, *83*, 957–970. [CrossRef]
19. Branco, D.A.C.; Moura, M.C.P.; Szklo, A.; Schaeffer, R. Emissions reduction potential from CO_2 capture: A life-cycle assessment of a brazilian coal-fired power plant. *Energy Policy* **2013**, *61*, 1221–1235. [CrossRef]
20. Odeh, N.A.; Cockerill, T.T. Life cycle analysis of uk coal fired power plants. *Energy Convers. Manag.* **2008**, *49*, 212–220. [CrossRef]
21. Stanek, W.; Czarnowska, L.; Pikoń, K.; Bogacka, M. Thermo-ecological cost of hard coal with inclusion of the whole life cycle chain. *Energy* **2015**, *92*, 341–348. [CrossRef]
22. Díaz, E.; Fernández, J.; Ordóñez, S.; Canto, N.; González, A. Carbon and ecological footprints as tools for evaluating the environmental impact of coal mine ventilation air. *Ecol. Indic.* **2012**, *18*, 126–130. [CrossRef]
23. Nease, J.; Ii, T.A.A. Comparative life cycle analyses of bulk-scale coal-fueled solid oxide fuel cell power plants. *Appl. Energy* **2015**, *150*, 161–175. [CrossRef]
24. Qin, Z.; Zhai, G.; Wu, X.; Yu, Y.; Zhang, Z. Carbon footprint evaluation of coal-to-methanol chain with the hierarchical attribution management and life cycle assessment. *Energy Convers. Manag.* **2016**, *124*, 168–179. [CrossRef]
25. Restrepo, Á.; Bazzo, E.; Miyake, R. A life cycle assessment of the brazilian coal used for electric power generation. *J. Clean. Prod.* **2014**, *92*, 179–186. [CrossRef]
26. Andrić, I.; Jamali-Zghal, N.; Santarelli, M.; Lacarrière, B.; Corre, O.L. Environmental performance assessment of retrofitting existing coal fired power plants to co-firing with biomass: Carbon footprint and emergy approach. *J. Clean. Prod.* **2015**, *103*, 13–27. [CrossRef]

27. Peters, G.P. From production-based to consumption-based national emission inventories. *Ecol. Econ.* **2008**, *65*, 13–23. [CrossRef]
28. Gavrilova, O.; Vilu, R. Production-based and consumption-based national greenhouse gas inventories: An implication for estonia. *Ecol. Econ.* **2012**, *75*, 161–173. [CrossRef]
29. Mózner, Z.V. A consumption-based approach to carbon emission accounting—Sectoral differences and environmental benefits. *J. Clean. Prod.* **2013**, *42*, 83–95. [CrossRef]
30. Xia, D.; Ren, Y.; Shi, L. Measurement of life-cycle carbon equivalent emissions of coal-energy chain. *Stat. Res.* **2010**, *8*, 13.
31. Xiao, B.; Zhang, A.L.; Chen, G.F. Life cycle inventory of clean coal-fired power generation in China. *Clean Coal Technol.* **2005**, *11*, 1–4.
32. Troy, S.; Schreiber, A.; Zapp, P. Life cycle assessment of membrane-based carbon capture and storage. *Clean Technol. Environ. Policy* **2016**, *18*, 1641–1654. [CrossRef]
33. Zhang, D. *A Study on Estimation Method of Carbon Emission in Industry Branch*; Beijing Forestry University: Beijing, China, 2005.
34. Lubetsky, J.; Steiner, B.A.; Lanza, R. *2006 Intergovernmental Panel on Climate Change (IPCC) Guidelines for National Greenhouse Gas Inventories*; IPCC: Geneva, Switzerland, 2006.
35. Jiang, G.Q. *Research on the Process and Measurement of Electric-Coalsupply Chain Carbon Emissions*; Beijing Jiaotong University: Beijing, China, 2013.
36. Du, Q.; Chen, Q.; Yang, R. Forecast carbon emissions of provinces in China based on logistic model. *Resour. Environ. Yangtze Basin* **2013**, *22*, 143–151.
37. Hamilton, L.D.; Goldstein, G.A.; Lee, J.; Marcuse, W.; Morris, S.C.; Manne, A.S.; Wene, C.O. *Markal-Macro: An Overview*; Brookhaven National Lab.: Upton, NY, USA, 1992.
38. Qiu, S.M.; Gu, P.L.; Hao, H. Study on increase and control of carbon dioxide emission from energy consumption. *J. China Coal Soc.* **2002**, *27*, 412–416.
39. Wang, X.N.; Gu, K.P. Present condition of estimate method of carbon emission in China. *Environ. Sci. Manag.* **2006**, *31*, 78–80.
40. Bin, Y.E.; Qiang, L.U.; Ji, L.I.; Chang, K. Coal power ghg emission intensity model and its application. *J. Harbin Univ. Sci. Technol.* **2011**, *5*, 27.
41. Weisser, D. A guide to life-cycle greenhouse gas (ghg) emissions from electric supply technologies. *Energy* **2007**, *32*, 1543–1559. [CrossRef]
42. Pehnt, M.; Henkel, J. Life cycle assessment of carbon dioxide capture and storage from lignite power plants. *Int. J. Greenh. Gas Control* **2009**, *3*, 49–66. [CrossRef]
43. Hou, Y.; Liang, C.; Tian, X.; Pan, D. Study on chinese steel industry carbon footprint analysis and emission reduction countermeasures. *Ecol. Econ.* **2012**, *12*, 22.
44. Hondo, H. Life cycle ghg emission analysis of power generation systems: Japanese case. *Energy* **2014**, *30*, 2042–2056. [CrossRef]
45. Yu, S.; Wei, Y.M.; Guo, H.; Ding, L. Carbon emission coefficient measurement of the coal-to-power energy chain in China. *Appl. Energy* **2014**, *114*, 290–300. [CrossRef]
46. Review, B.P.S.; June, W.E. *Bp Statistical Review of World Energy June 2011*; Bp España: London, UK, 2011.
47. You, C.F.; Xu, X.C. Coal combustion and its pollution control in China. *Energy* **2010**, *35*, 4467–4472. [CrossRef]
48. Liu, Z.; Feng, K.; Hubacek, K.; Liang, S.; Anadon, L.D.; Zhang, C.; Guan, D. Four system boundaries for carbon accounts. *Ecol. Model.* **2015**, *318*, 118–125. [CrossRef]
49. Geng, Y. *Quantification and Characteristics of Provincial-Level Carbon Emission from Energy Consumption in China*; China University of Geosciences: Wuhan, China, 2011.
50. Zhao, R. *A Study on Carbon Cycle and Land Control in Urban System*; Nanjing University Press: Nanjing, China, 2012.
51. Xia, D. *The Research on Life Cycle Carbon Emissions Measurement of Electric Power Generation Side Based on the Scenario Analysis Method*; Chongqing University: Chongqing, China, 2010.
52. Ge, Q.S.; Dai, J.H.; He, F.N.; Yuan, P.; Wang, M.M. Land use changes and their relations with carbon cycles over the past 300 a in China. *Sci. China Earth Sci.* **2008**, *51*, 871–884. [CrossRef]
53. Zhang, Y.; Yan, J.; Liu, L.; Bai, W.; Li, S.; Zheng, D. Impact of qinghai-xizang highway on land use and landscape pattern change: From golmud to tanggulashan pass. *Acta Geogr. Sin.* **2002**, *57*, 253–266.

54. Watson, R.T. *Land Use, Land-Use Change, and Forestry : A Special Report of the IPCC*; Cambridge University: Cambridge, UK, 2000.
55. Canadell, J.G.; Le Quéré, C.; Raupach, M.R.; Field, C.B.; Buitenhuis, E.T.; Ciais, P.; Conway, T.J.; Gillett, N.P.; Houghton, R.A.; Marland, G. Contributions to accelerating atmospheric CO_2 growth from economic activity, carbon intensity, and efficiency of natural sinks. *Proc. Natl. Acad. Sci. USA* **2007**, *104*, 18866–18870. [CrossRef] [PubMed]
56. Gullison, R.E.; Frumhoff, P.C.; Canadell, J.G.; Field, C.B.; Nepstad, D.C.; Hayhoe, K.; Avissar, R.; Curran, L.M.; Friedlingstein, P.; Jones, C.D. Tropical forests and climate policy: New science underscores the value of a climate policy initiative to reduce emissions from tropical deforestation. *Environment* **2007**, *316*, 985.
57. Lv, M. *Impact Studies of Tourism Development on Land Use Pattern in Jilin Changbai Mountain National Nature Reserve*; Northeast Normal University: Changchun, China, 2010.
58. Kerang, L.I.; Wang, S.; Cao, M. Vegetation and soil carbon storage in China. *Sci. China Ser.* **2004**, *47*, 49–57.
59. Fang, J.; Liu, G.; Xu, S. Soil carbon pool in China and its global significance. *J. Environ. Sci.* **1996**, *23*, 249–254.
60. Fang, J.; Chen, A.; Peng, C.; Zhao, S.; Ci, L. Changes in forest biomass carbon storage in China between 1949 and 1998. *Science* **2001**, *292*, 2320–2322. [CrossRef] [PubMed]
61. Tong, H.F.; Cui, Y.S.; Wei-Shuang, Q.U.; Liu, Y. System dynamic scenarios analysis of CO_2 emissions of China's cement industry. *China Soft Sci.* **2010**, *3*, 40–50.
62. West, T.O.; Marland, G. A synthesis of carbon sequestration, carbon emissions, and net carbon flux in agriculture: Comparing tillage practices in the United States. *Agric. Ecosyst. Environ.* **2002**, *91*, 217–232. [CrossRef]
63. Bacon, P.J.; Cain, J.D.; Howard, D.C. Belief network models of land manager decisions and land use change. *J. Environ. Manag.* **2002**, *65*, 1–23. [CrossRef]
64. Mohamed, A.A.; Sharifi, M.A.; Keulen, H.V. An integrated agro-economic and agro-ecological methodology for land use planning and policy analysis. *Int. J. Appl. Earth Obs. Geoinform.* **2000**, *2*, 87–103. [CrossRef]
65. Lebel, L.; Garden, P.; Banaticla, M.R.N.; Lasco, R.D.; Contreras, A.; Mitra, A.P.; Sharma, C.; Nguyen, H.T.; Ooi, G.L.; Sari, A. Management into the development strategies of urbanizing regions in asia: Implications of urban function, form, and role. *J. Ind. Ecol.* **2007**, *11*, 61–81. [CrossRef]
66. Zhang, J.; Fu, M.; Tao, J.; Huang, Y.; Hassani, F.P.; Bai, Z. Response of ecological storage and conservation to land use transformation: A case study of a mining town in China. *Ecol. Model.* **2010**, *221*, 1427–1439. [CrossRef]

energies

MDPI

Article

Research on CO_2 Emission Reduction Mechanism of China's Iron and Steel Industry under Various Emission Reduction Policies

Ye Duan [1], Nan Li [1], Hailin Mu [1,*] and Shusen Gui [2]

[1] Key Laboratory of Ocean Energy Utilization and Energy Conservation of Ministry of Education, Dalian University of Technology, Dalian 116024, China; dy200872083@mail.dlut.edu.cn (Y.D.); nanli.energy@dlut.edu.cn (N.L.)

[2] Faculty of Management and Economics, Dalian University of Technology, Dalian 116024, China; dutgss@hotmail.com

* Correspondence: mhldut@126.com; Tel.: +86-411-8470-8095

Received: 11 October 2017; Accepted: 22 November 2017; Published: 1 December 2017

Abstract: In this paper, a two-stage dynamic game model of China's iron and steel industry is constructed. Carbon tax levy, product subsidy, carbon capture and sequestration (CCS) and other factors are included in the emission reduction mechanism. The effects of emissions reduction and the economic impact of China's overall steel industry (and that of its six main regions) are investigated for the first time under different scenarios. As new findings, we report the following: (1) Not all factors declined. The overall social welfare, consumer surplus, output and emissions decrease with a gradual increase in the reduction target, whereas the carbon tax value, unit value of product subsidies and total subsidies show a rising trend; (2) A combination of multiple emissions reduction policies is more effective than a single policy. With the implementation of a combined policy, regional output polarization has eased; (3) Steel output does not exceed 950 million tons, far below the current peak. These results will help the industry to formulate reasonable emissions reduction and output targets. In short, in effort to eliminate industry poverty and to alleviate overcapacity, the industry should not only adopt the various coordinated reduction policies, but also fully consider regional differences and reduction needs.

Keywords: emission reduction mechanism research; China's iron and steel industry; a two-stage dynamic game; inter-regional product yield selection

1. Introduction

China has established the world's most complete iron and steel industry chain system, which provides most the iron and steel materials for the national economy [1]. In 2011, the output was 850 million tons and in 2015 it equaled 1.02 billion tons, after reaching a historical peak of 1.046 billion tons in 2014. The domestic market share of steel is over 99%, effectively satisfying national economic and social development.

Even so, the iron and steel industry faces non-neglected problems, especially the overcapacity. In 2015, China's steel production capacity reached 1.13 billion tons, far exceeding its 1.02 billion tons of actual production. Steel production capacity has gradually shifted from regional, structural surplus to absolute excess. The concentration degree has ceased to rise, and the first 10 iron and steel enterprises' concentration degree fell from 49% in 2010 to 34% of 2015. Although energy consumption and pollutant emissions of per ton steel are decreasing year over year, these changes cannot offset the increase in energy consumption and total pollutants caused by the excessive steel output. In particular, in the Beijing-Tianjin-Hebei region and the Yangtze River delta, the environmental carrying capacity has

reached its limit. A large area of haze has spurred significant environmental pressure and negative public opinion, forcing the government to enact more stringent industry policies and environmental protection measures in the iron and steel industry.

Therefore, the prediction of a reasonable production interval and calculation of the emissions level can provide data and reference support for eliminating excess capacity and formulating CO_2 emissions reduction targets. This is one of the starting points and importance of this paper.

In addition, in the future, sole dependence on technology innovation will no longer fulfill CO_2 emissions reduction targets, and this will also increase enterprises' investment. Therefore reasonable carbon tax policies and government subsidies are imperative. In addition, to better control emissions reduction, carbon capture and sequestration (CCS) represents another way to reduce CO_2 on a large-scale. Over the next 15 to 30 years, China's steel industry CCS demonstration projects will be planned and put into production, so large-scale investment in CCS projects also concerns to the enterprise and government. Therefore, reasonable reduction technologies and system policies can provide a foundation for the subsequent development of regional emissions reduction policies and economic impact assessment, hence the second aim of this paper.

The remainder of this paper is organized as follows: Section 2 provides a literature review focusing on the carbon tax levy system and production subsidies mechanism research. Section 3 introduces the two-stage game theory modeling, policy assumptions and data sources. In Section 4, based on accounting data and statistical analysis, we present and discuss our results in detail. Section 5 provides conclusions and policy recommendations for China's iron and steel industry.

2. Literature Review

Many economic scholars have studied CO_2 reduction policies, including carbon tax, carbon trading, and carbon sink. Most carbon tax levy systems and production subsidies have focused on the general equilibrium model. By setting different tax rate and output subsidy return conditions, the emissions reduction effect and impact on the economy have been analyzed using the CGE model (computable general equilibrium model, typically composed of a set of equations to describe supply, demand and market relationships). Other academic models have been employed as well.

In the field of CO_2 reduction, Jorgenson et al. [2,3] used the CGE model in pioneering research. Manne et al. [4] introduced a carbon tax module via the MERGE model, in which they calculated and analyzed the differences in cutting emissions costs in different regions of the world. Jorgenson and Wilcoxen [5] predicted the effect of the energy tax by using a CGE model. Zhang [6] used the CGE model to examine the economic implications of carbon abatement for the Chinese economy in the first systematic and comprehensive attempt. Later Zhai and Li [7], Xie et al. [8,9] conducted the similar study using the CGE model as well.

Since the beginning of the 21st century, the CGE model has been improved and developed. This model has been applied to many countries, sectors and more policy scenarios. For example, Kemferthe and Welsch [10] analyzed the economic effects of government carbon tax policy using a dynamic CGE model to discuss different elasticities and tax-returning mechanisms between energy and capital, energy and labor. Wendner [11] used a general equilibrium model to analyze the carbon tax impact on the Austrian economy. Van Heerden et al. [12] found that the environment tax can be given back to the industrial sector by reducing labor and capital taxes directly using a CGE model. Abrell [13] analyzed the use of market-based emissions regulation instruments to address CO_2 emissions in transportation. Benavides et al. [14] examined the economy-wide implications of a carbon tax applied in the Chilean electricity generation sector via both an energy sectorial model and a dynamic stochastic general equilibrium model. Yahoo and Othman [15] evaluated the economy-wide impacts of implementing two different types of CO_2 emissions abatement policies in Malaysia using market-based (i.e., carbon tax) and command-and-control mechanism (i.e., sectoral emissions standards). These papers were directed at a particular country or sector, with a specific tax

or subsidy value. By calculating the results using CGE models, researchers can gauge the economic and environmental response.

Using the input-output table published by the Chinese Statistical Department, scholars have analyzed the impact in China of imposing an energy tax and subsidy on the economy, energy, environment and production sectors. This research has been extended to provinces and sectors.

Liang et al. [16] examined how to reduce carbon tax on the export of energy-intensive industry international competitiveness by a CGE model. They suggested offering a tax break on energy-intensive, labor-intensive export industries, and implementing a carbon tax return for other industries Yang et al. [17] used a CGE model to quantitatively simulate the impact of energy tax scenarios. They found that an energy tax can help to minimize the CO_2 and SO_2 emissions, with increasing marginal emissions reduction costs. Wu et al. [18] developed the China regional dynamic general equilibrium model and analyzed the marginal cost curve between various provinces and cities from 2007 to 2020, then discussed carbon emissions trading and carbon tax policy choices. Xu and Zhang [19] applied a multi-sectoral dynamic CGE model to analyze the impacts of a carbon tax on China's economy and carbon intensity at the rate of 40 yuan/t without tax relief as a baseline scenario. They also compared the change trends of carbon intensity and the proportion of non-fossil energy in primary energy consumption from the perspective of achieving the emissions reduction targets in 2020 and 2030. Chen et al. [20] established an energy CGE model for Guangdong Province, and simulated the energy-saving and emissions reduction effects from the enactment of an energy tax or carbon tax at various tax rates, they also analyzed the mitigation effects on an economic system given various tax refund plans. Ling et al. [21] built a multi-sectoral dynamic CGE model with a coal resource tax module, to study the general impacts of such reform policy on the Chinese economy and environment. However, due to specific parameter values and assumptions, along with the rapid development of China's economy, these studies' results do not necessarily correspond to the actual situation. Moreover, the social accounting matrix (SAM) requirement is higher and this data is not published every year.

There have also been many papers on environmental regulations using game theoretic approaches. Scholars have applied game theory to the study of carbon tax levy and subsidy mechanism. Extant literatures have focused primarily on constructing a two-stage game model to establish the relationship between the government and enterprise, and between different enterprises. In particular, scholars have studied the optimal level of emissions and the optimal output of subsidy mechanisms.

Much of the early research on environmental regulations using game theoretic approach focused on permits, standards and technological innovation. Montero [22] and Bruneau [23] compared the incentives to invest in environmental research and development (R&D) offered by four policy instruments—emissions standards, performance standards, tradeable permits, and auctioned permits-and found the relationship between abatement, innovation, and the production process itself to be critical to a sound understanding of these incentives. Then product differentiation, countervailing incentives and other market-based instruments were incorporated into the theory, such as by Requate [24,25], Puller [26] and Poyago-Theotoky [27,28].

In subsequent studies, scholars have applied the game theory approach to environmental regulations and reduction mechanisms. Youssef et al. [29], Ouchida and Goto [30], and Moner-Colonques and Rubio [31] looked into the society economic levels under different environmental policies. Demailly and Quirion [32] quantified the impact of the European Emission Trading Scheme on two dimensions of competitiveness, production and profitability, for the iron and steel industry. Under a mixed market structure, Cato [33] proposed an emissions reduction mechanism based on a subsidy reduction, and demonstrated that the mechanism could achieve an optimal social result. Eyland and Zaccour [34] looked at the optimization of two different governments and their respective firms. Parametric values inside the set [0, 1) were used to represent the possible extents of the border tax adjustment (BTA) depending on both countries' respective environmental policies allowing countries to have different carbon policies. To examine the applicability of the "Pigouvian tax" in China's present low-carbon

economy, Ouchida and Goto [35] concluded that social welfare under a time-consistent emissions tax (emissions subsidy) policy was always welfare-enhancing rather than laissez-faire. McDonald and Poyago-Theotoky [36] found a counterintuitive positive relationship between R&D input spillovers and emissions taxes and a U-shaped relationship between the optimal emissions tax and R&D spillover in the d'Aspremont and Jacquemin (AJ henceforth) model. Lambertini et al. [37] explored the relationship between competition and innovation when R&D investment attempts to reduce pollutant emissions. They have uncovered an inverted U-shaped relationship between "green" innovation and competition. It can be said that the application of game theory abroad has been more mature and systematic.

In China, there is also much research on environmental regulations from a game theory approach. Li et al. [38] proposed a two-stage dynamic game model comprising two sub-games involving a government-firm and firm-firm relationship. They also investigated the second-best emissions tax and its revenues refunding scheme based on an output subsidy with exogenous abatement target. Li et al. [39] constructed a two-stage dynamic game model based on two representative iron and steel firms (eastern and western) to examine the effects of a uniform or discriminated emissions tax levied by the central government on abatement costs, social economic welfare and the firms' competitiveness. Zhang [40] built a three-stage game model between the government and enterprises to analyze the feasibility and mode selection of carbon tax policy. In the process of supply chain low-carbonization, a three-stage game model was constructed by Li et al. [41] between the government and enterprises by considering carbon tax as one regulation mode. Qiao et al. [42] made the first attempt to use non-cooperation game theory to study airlines' carbon tax strategies in the EU. Xu et al. [43] studied joint production and pricing problem in a manufacturing firm with multiple products under cap-and-trade and carbon tax regulations, and compared the effects of the two regulations on the total carbon emissions. However, because China has not yet implemented an emissions trading mechanism, carbon tax mechanism, or other emissions reduction policies, research can only establish models and make scenario assumptions.

Extant literature shows that the research on reduction mechanism is comparatively developed. Firstly, the CGE model and game theory can provide policy references for emissions reduction. Nevertheless, the CGE model used to study tax reduction mechanisms generally focuses on the specific tax rate and output subsidy, to identify the corresponding reduction. Game theory seeks to assess the optimal emissions level and output subsidy mechanism; therefore, this method is more suitable for the government to observe the economic and environmental changes between countries and regions when formulating a certain emissions reduction policy.

Secondly, we found that research has traditionally focused on national-level and overall sectors (e.g., industry, service industry, agriculture), whereas research on the provincial level and a single industry department is limited. Yet the steel industry is a foundational component of the China's national economy and one of the industrial sectors with the greatest CO_2 emissions, which undertakes important emissions reduction tasks to control the nation's greenhouse gases.

Thirdly, the literature highlights models, but empirical analysis is lacking. The basic parameters of empirical analysis (especially based on enterprises) are usually derived from existing data from developed countries. In developing countries like China, there are significant regional differences and regional economic development imbalances; thus, some areas' parameters and data, including those of the iron industry, need to be supplemented.

In addition, with the continuous development of China's economy and the world's constant attention to environmental problems, the pressure around emissions reduction will only continue to increase. A separate carbon tax or product subsidy policy would not meet the country's economic development and emissions reduction level needs. Projects such as CCS, carbon sinks and other significant CO_2 emissions reductions methods will likely be incorporated into the entire reduction system. Therefore, game theory warrants attention in this respect.

In conclusion, a reasonable reduction policy is the primary focus of this paper. The paper organizes energy, environment and economic data from the six main areas' of the iron and steel industry

in China. Combined with the corresponding long-term plan issued by the government, we consider and integrate the carbon tax, production subsidies, CCS, and external loss of CO_2 into the emissions reduction mechanism to build a two-stage dynamic game model. Then, based on different periods of the steel industry's carbon emissions with decreased demand, we discuss the six main areas' market game behavior under different reduction targets, and investigate the differential effects of emissions reduction scenarios and their economic impacts on the iron and steel industry.

3. Methods

3.1. Notations and Explanations

According to the regional division of China, China is divided into six regions: North China (i.e., Beijing, Tianjin, Hebei, Shanxi, and Inner Mongolia), Northeast China (i.e., Liaoning, Jilin, and Heilongjiang), East China (i.e., Shanghai, Jiangsu, Zhejiang, Anhui, Fujian, Jiangxi, and Shandong), South Central China (i.e., Henan, Hubei, Hunan, Guangdong, Guangxi, and Hainan), Southwest China (i.e., Chongqing, Sichuan, Guizhou, Yunnan, and Tibet), Northwest China (i.e., Shanxi, Gansu, Qinghai, Ningxia, and Xinjiang). In this paper, regions are presented by subscripts: 1 represents North China, 2 represents Northeast China, and so on.

The main research focus of this paper includes the government and the above six regions, the regional steel industry data is regarded as a steel enterprise entity). The government emissions reduction policy is a double game problem. Firstly, there is a decomposition game between the government and regional enterprises: government stipulates the emissions reduction target for a certain period, after which the regional enterprises should determine their respective reduction ranges according to their own cost curves. Secondly, there is a game of product output between the six regions, and the different targets of the regional enterprises will affect their respective output levels and market competitiveness.

Therefore, the resultant game order is as follows: in the first stage, the government set corresponding reduction targets and reduction policies (e.g., carbon tax, product subsidies, CCS, independent or mixed); in the second stage, on the premise of guaranteeing profit maximization, the regional enterprises choose their respective reduction targets and output levels simultaneously. Based on this idea, this paper adopts the inverse method to solve the two-stage game problem. The notations used in this paper and their explanations are presented in Table 1.

Table 1. Notations and explanations used in this paper.

Notations	Explanations
Q	Steel production
P	The price of steel
α	The constant of the market inverse demand curve
β	The primary coefficient of the market inverse demand curve
q_i	Steel production of region i
e	The national CO_2 emission intensity of per ton steel in 2010
$e_{2015,i}$	The region i CO_2 emission intensity of per ton steel in 2015
e_i	The region i CO_2 emission intensity of per ton steel at some stage
r_i	The decline range of CO_2 emission intensity of per ton steel in region i at some stage
R	The decline target of national CO_2 emission intensity of per ton steel at some stage
MAC	Marginal abatement cost curve in iron and steel industry
a_i	The primary coefficient of steel industry's MAC in region i
b_i	The quadratic coefficient of steel industry's MAC in region i
C_i	The cost function of steel industry in region i
$C_{0,i}$	The production cost of steel industry in region i
T	The total carbon tax
t	The unit value of carbon tax
W	Social welfare function

Table 1. *Cont.*

Notations	Explanations
CS	Consumer surplus
PS	Producer surplus
θ	The external loss parameter of CO_2
η	The production subsidies
m	The CO_2 emission reduced by CCS demonstration project
A	The primary coefficient of CCS demonstration project cost curve
B	The constant of CCS demonstration project cost curve
π_i	The profit function of steel industry in region i
E	The total CO_2 emissions in iron and steel industry
S	The total subsidy
M	The total cost of CCS demonstration project

It is assumed that each regional enterprise produces homogeneous products and compete for production in the product market. There is no regional variability and the prices of steel are the same. The market reverse demand curve of the enterprise is $P(Q)$. This paper describes the relationship between product price and demand using a linear combination, and $P'(Q) < 0$, where P indicates price, Q is total output, and $Q = \sum_{i=1}^{6} q_i$. At the same time, the paper assumes that in the future equilibrium market, production and consumption are equal. The production cost of the enterprise is different, while the marginal emissions reduction cost is incorporated into the cost function, namely $C_i(r_i, q_i)$, where $e_i = e_{2015,i}(1 - r_i)$. It is assumed that the cost function satisfies $\lim_{r_i=1} C_i(r_i, q_i) = +\infty$, $\partial C_i/\partial q_i > 0$, $\partial^2 C_i/\partial {q_i}^2 > 0$, $\partial C_i/\partial r_i > 0$, $\partial^2 C_i/\partial {r_i}^2 > 0$. $D(E)$ represents an external macro loss to the environment caused by CO_2 emissions, $D(E) = \theta(E) = \theta \sum_{i=1}^{6} e_i q_i$. In addition, because the CCS cost curve is still in the valuation stage, and is directly related to the amount of CO_2 trapped in the transport storage, the curve approximation is proposed to synthesize the linear relation, $M = am + b$.

3.2. Modeling

3.2.1. Scenario Analysis

In this section, we discuss three scenarios due to policy uncertainties:

Case 1: Only carbon tax scenario

At present, carbon taxes are likely to be the only policy tool for reducing emissions targets, due to policy and technological constraints.

Case 2: Mixed scenario, Carbon tax and subsidy

With the gradual increase in emission reduction targets, carbon tax reduction will seriously compress producers' profit, so subsidies based on product output may increase producers' enthusiasm and ability to produce. This paper assumes that subsidies are derived from carbon taxes. More specifically the carbon tax levy will be partially or entirely returned to the producer in the form of subsidies.

Case 3: Mixed scenario, Carbon tax, subsidy, and CCS

As emissions reduction targets continue to grow, carbon tax and subsidies may not fulfill the criteria for reducing emissions. At the same time, with advancing technology and increasing tax pressure, CCS will be employed over the mid- and long-term as a means of large-scale CO_2 emission reduction. A mix of reduction policies will help achieve the CO_2 emissions reduction target more easily.

This paper assumes that the subsidy comes from carbon tax, and CCS demonstration project is funded through government investment.

3.2.2. Two-Stage Dynamic Game Model

In the second phase of the game, the government sets emissions reduction targets and reduction policies. Regional enterprises choose their own production and reduction targets, and the profit function under different cases are as follows:

$$\pi_{case1,i} = P(Q)q_i - C_i q_i - T_i = (\alpha - \beta Q)q_i - q_i(C_{0,i} + \int_0^{r_i} MAC_i(r)\,dr) - te_i q_i \quad (1)$$

$$\pi_{case2,i} = P(Q)q_i - C_i q_i - T_i + S_i = (\alpha - \beta Q)q_i - q_i(C_{0,i} + \int_0^{r_i} MAC_i(r)\,dr) - te_i q_i + \eta q_i \quad (2)$$

$$\pi_{case3,i} = P(Q)q_i - C_i q_i - T_i + S_i = (\alpha - \beta Q)q_i - q_i(C_{0,i} + \int_0^{r_i} MAC_i(r)\,dr) - te_i q_i + \eta q_i \quad (3)$$

where the marginal cost of reducing emissions is $MAC = a_i e_{2015,i} r_i + b_i (e_{2015,i} r_i)^2$, and the region's steel industry carbon tax is calculated as $T_i = te_i q_i = te_{2015,i}(1 - r_i)q_i$.

In the case of certain carbon tax and subsidy values, CO_2 reduction and production yield is maximized in each region, namely $Max\ \pi_i$.

In this paper, due to the consideration of a various reduction policies, the social welfare function is extended to include consumer surplus, producer surplus, carbon tax levy, product subsidies, CCS investment, macro-environmental emissions losses, and so on. The specific forms are as follows:

$$\begin{aligned} W_{Case1} &= CS + PS + T - D(E) = \int_0^Q P(q)dq - P(Q)Q + \sum_{i=1}^{6} \pi_{case1,i} + \sum_{1}^{6} T_i - \theta E \\ &= \int_0^Q (\alpha - \beta q)dq - (\alpha - \beta \sum_{i=1}^{6} q_i) \sum_{i=1}^{6} q_i + \sum_{i=1}^{6} \pi_{case1,i} + \sum_{i=1}^{6} te_{2015,i}(1 - r_i)q_i - \theta \sum_{i=1}^{6} e_{2015,i}(1 - r_i)q_i \end{aligned} \quad (4)$$

$$\begin{aligned} W_{Case2} &= CS + PS + T - S - D(E) = \int_0^Q P(q)dq - P(Q)Q + \sum_{i=1}^{6} \pi_{case2,i} + \sum_{1}^{6} T_i - \eta Q - \theta E \\ &= \int_0^Q (\alpha - \beta q)dq - (\alpha - \beta \sum_{i=1}^{6} q_i) \sum_{i=1}^{6} q_i + \sum_{i=1}^{6} \pi_{case2,i} + \sum_{i=1}^{6} te_{2015,i}(1 - r_i)q_i - \eta \sum_{i=1}^{6} q_i - \theta \sum_{i=1}^{6} e_{2015,i}(1 - r_i)q_i \end{aligned} \quad (5)$$

$$\begin{aligned} W_{Case3} &= CS + PS + T - S - D(E) - M = \int_0^Q P(q)dq - P(Q)Q + \sum_{i=1}^{6} \pi_{case3,i} + \sum_{1}^{6} T_i - \eta Q - \theta E - (Am + B) \\ &= \int_0^Q (\alpha - \beta q)dq - (\alpha - \beta \sum_{i=1}^{6} q_i) \sum_{i=1}^{6} q_i + \sum_{i=1}^{6} \pi_{case3,i} + \sum_{i=1}^{6} te_{2015,i}(1 - r_i)q_i - \eta \sum_{i=1}^{6} q_i - \theta \sum_{i=1}^{6} e_{2015,i}(1 - r_i)q_i - (Am + B) \end{aligned} \quad (6)$$

In the first stage of the game, based on the achievement of emissions reduction targets and the response of regional enterprises to the government's emissions reduction policies, the government should formulate corresponding policies to maximize social welfare. The government's policy can be expressed as follows:

Case 1:

$$Max\ W$$
$$s.t. \begin{cases} \dfrac{\sum_{i=1}^{6} e_{2015,i}(1 - r_i)q_i}{\sum_{i=1}^{6} q_i} = e(1 - R) \\ r_i > 0 \\ e_i > 0 \\ q_i > 0 \\ t \geq 0 \\ i = 1, 2, 3, 4, 5, 6 \end{cases} \quad (7)$$

Case 2:

$$Max\ W \quad s.t. \begin{cases} \dfrac{\sum_{i=1}^{6} e_{2015,i}(1-r_i)q_i}{\sum_{i=1}^{6} q_i} = e(1-R) \\ r_i > 0 \\ e_i > 0 \\ q_i > 0 \\ t \geq 0 \\ \eta \geq 0 \\ 0 \leq \dfrac{\eta \sum_{i=1}^{6} q_i}{\sum_{i=1}^{6} te_{2015,i}(1-r_i)q_i} \leq 1 \\ i = 1,2,3,4,5,6 \end{cases} \tag{8}$$

Case 3:

$$Max\ W \quad s.t. \begin{cases} \dfrac{\sum_{i=1}^{6} e_{2015,i}(1-r_i)q_i - m}{\sum_{i=1}^{6} q_i} = e(1-R) \\ r_i > 0 \\ e_i > 0 \\ q_i > 0 \\ t \geq 0 \\ \eta \geq 0 \\ 0 \leq \dfrac{\eta \sum_{i=1}^{6} q_i}{\sum_{i=1}^{6} te_{2015,i}(1-r_i)q_i} \leq 1 \\ 1 \times 10^6 \leq m \leq 2 \times 10^6 \\ i = 1,2,3,4,5,6 \end{cases} \tag{9}$$

3.2.3. Policy Assumptions

To compare the effects of emissions reduction under different policies, this paper constructs a selection model of the steel industry in six regions in China. Current research is lacking in this area, and the target of emissions reduction and other policy planning is less and more ambiguous in China than in other countries. Therefore, according to relevant policies and planning, the paper assumes three reasonable policy scenarios. Each focuses on the decomposition of the intensity target of CO_2 emissions reduction in the steel industry under different policies, the influence of regional steel industry output and the change in social welfare. The main assumptions are as follows:

1. Carbon tax scenario in 2020

In this scenario, we assume that by 2020, the steel industry's CO_2 intensity will fall by at least 15% compared to in 2010. Given that technological innovation alone will not be sufficient for high carbon-intensity reduction, the carbon tax will be a necessary policy tool. The solution for this scenario is similar to that of Case 1. Then, we calculate the corresponding results of social welfare and investigate scenarios in which the intensity of CO_2 emissions dropped from 15 to 20%.

2. Carbon tax and product subsidy scenario in 2025

In this scenario, we assume that by 2025, the CO_2 intensity of the steel industry will fall by at least 20% compared to that in 2010. Again, because technological innovation alone will not be sufficient for high carbon-intensity reduction, the carbon tax will be a necessary policy tool. However the carbon tax

levy has greatly increased the industry's investment, and product subsides to producers can reduce the tax burden on producers while also meeting emissions demands. Thus, carbon tax and subsidy will comprise a dual method in 2025. The solution in this scenario corresponds to that of Case 2. Then, we calculate the social welfare results, and investigate scenarios in which the intensity of CO_2 emissions dropped by 20–25%.

3. Carbon tax, product subsidy, and CCS demonstration project coexistence scenario in 2030

In contrast to 2010, we assume that the steel industry's CO_2 intensity will fall by at least 25% by 2030. Again, because technological innovation alone will not be sufficient for high carbon-intensity reduction, the carbon tax and product subsidies will be necessary policy tools. With the improving CCS technology, large-scale CCS demonstration projects will be able to be applied to the steel industry. As a result, carbon tax, product subsidy, and CCS demonstration projects (i.e., 1–2 million ton CO_2 level) will be considered in 2030. The solution to this scenario corresponds to that of case 3. Then, we calculate the corresponding social welfare results, and investigate scenarios in which the intensity of CO_2 emissions dropped by 25–30%.

3.3. Parameters and Data Sources

In this paper, the CO_2 MAC (marginal abatement cost) results were derived from the CO_2 shadow price calculations in 2005–2015. According to [44–46], in the directional distance model the economic output is considered as desirable output, while CO_2 emissions is the undesirable output. An area's production possibility is defined as: $P(x) = \{(y, b) : x\ can\ produce\ (y, b)\}$. According to Färe's [47] description of the directional distance function, we introduce the direction vector $g = (g_y, g_b)$. The output-based distance function can be defined as follows:

$$D(x, y, b; g_y, g_b) = \max\{\beta : (y + \beta g_y, b - \beta g_b) \in P(x)\} \tag{10}$$

According to the method of nonparameter linear programming, the objective function is calculated as follows:

$$\begin{aligned} & D_k(x_k, y_k, b_k; g_y, g_b) = \max \beta_k \\ & s.t. \quad \sum_{j=1}^{n} \lambda_j x_j \leq x_k, \\ & \quad \sum_{j=1}^{n} \lambda_j y_j \geq y_k + \beta_k g_y, \\ & \quad \sum_{j=1}^{n} \lambda_j b_j = b_k - \beta_k g_b, \\ & \quad \lambda_j \geq 0, j = 1, 2, \ldots n \end{aligned} \tag{11}$$

According to Lee [48], the undesirable output shadow price calculation formula can be written as:

$$q = p \times \frac{\partial D(x, y^*, b^*)/\partial b^*}{\partial D(x, y^*, b^*)/\partial y^*} \times \frac{\sigma_b}{\sigma_y} \tag{12}$$

Then, according to the six regions' respective shadow price, the MACs of each region were fitted. The main parameters of each region are shown in Table 2.

The external macroscopic loss parameters of CO_2 emissions refer to Giorgio Guenno and Silvia Tiezzi [49], converted into 14.55 yuan per ton of CO_2.

In 2030, we assume that the steel industry will plan to build 1-2 million ton demonstration projects funded by the government. The cost curve refers to [50–53], and the linear curve is $M = 204.96m + 11.53 \times 10^6$, $m \in [1 \times 10^6, 2 \times 10^6]$ ton. The unit is RMB.

Provincial steel production data, economic data, and employee data were collected from the China Statistical Yearbook [54–65], China's Industrial Statistics Yearbook [66–77], and the China Steel Industry yearbook from 2005 to 2016 [78–89]. Energy consumption data came from the China Energy Statistics

Yearbook [90–101] and each province's Statistical Yearbook from 2005 to 2016. Economic data were calculated at the 2010 year price. In addition, CO_2 emissions in industrial production (IPPU CO_2) are included in this paper which also produce large amounts of CO_2. Therefore, CO_2 emissions accounting, emissions intensity and descent amplitude are based on energy consumption + IPPU CO_2 emissions.

Table 2. The result of parameter fitting in formula.

Notations	Value	Unit
α	15,668.39	Yuan
β	1.117×10^{-5}	
e	2.79	t CO_2/t
θ	14.55	Yuan/t CO_2
m	$[1 \times 10^6, 2 \times 10^6]$	t
A	204.96	
B	1.153×10^7	Yuan

Due to data availability, the steel industry's relevant energy consumption and economic data were derived from the ferrous metal smelting and calendering processing industry in the Statistical Yearbook. The CO_2 accounting of fossil energy consumption and IPPU refer to IPCC2006 [102] and Duan et al. [103].

4. Results and Discussions

4.1. The Results of Parameter Fitting

The production cost takes into account the current trend of steel development in China, based on average production costs of 2010–2015. The descent amplitude of different regions is controlled at 5–30%. The parameter fitting conditions are shown in Tables 2 and 3.

Table 3. The result of parameter fitting in different regions.

Notations	Unit		i = 1	i = 2	i = 3	i = 4	i = 5	i = 6
$e_{2015,i}$	t CO_2/t		2.34	3.53	2.81	2.85	3.40	4.49
a_i			954.57	886.60	2847.60	325.81	78.91	178.12
b_i			702.15	567.70	9983.42	832.07	91.47	251.25
$C_{0,i}$	Yuan	2020	3660.25	5469.57	3734.81	3910.43	5246.81	4759.35
		2025	3108.44	4646.29	2986.07	3326.32	4724.05	4520.52
		2030	2799.50	3944.25	2685.82	2997.62	4008.86	3844.57

4.2. Empirical Analysis

In the second stage of the game, the regional emissions and intensity of the steel industry are determined by its first-order conditions:

$$\begin{aligned} \partial \pi_i / \partial q_i &= 0 \\ \partial \pi_i / \partial r_i &= 0 \end{aligned} \tag{13}$$

The relationship between steel production, the descending amplitude and t, η of each region is obtained by solving the simultaneous equations. The equilibrium yield and emissions reduction of the second stage in different situations can be determined by t, η.

Then we put the equilibrium output and emission reduction determined by t, η into the first stage to get the expression formula of social economic welfare (W). In the first stage of the game, the government maximizes the level of social economic welfare determined by t, η. Finally, we get W and other corresponding conclusions.

4.2.1. 2020 Scenario

In 2020, the carbon tax will be the only emissions reduction policy. With the gradual rise of in reduction targets, the carbon tax value and its total scale have increased gradually. In particular, the carbon tax value has risen rapidly from 65.88 yuan/t to 114.69 yuan/t, and the total carbon tax levy rose 61.84%.

Total output, overall social welfare function, consumer surplus, producer surplus and emissions loss have all shown a downward trend, the total output remained at around 0.835-0.846 million tons. Compared with 1.123 billion tons in 2015, output will have dropped by more than 20%, suggesting that in terms of satisfying social welfare functions, the demand for China's steel industry market will also decrease significantly by 2020. This is in line with the current economic situation and the development of the steel industry. With the gradual rise in reduction targets, the total output, social welfare function, consumer surplus, producer surplus, and emissions losses are projected to fall by 1.22%, 0.37%, 2.43%, 1.17% and 7.03% respectively.

For the sub-regions, to reach the 15–20% target, the selection of emissions intensity and production yield are taken between regions. Emissions reduction efforts have increased in line with more ambitious reduction goals, but there are notable inter-regional differences. In the southwest and northwest regions, the intensity of emissions reduction is more than 20% in most cases. With an overall reduction target of 20%, the reduction in southwest China is the largest, at 25.81%. The reduction range is comparatively smaller in East China, North China and other places (approximately 6–10%) due to differences in production costs and emissions intensity. With the gradual increase in emissions reduction targets, except for in North China (0.44%), steel outputs in the rest regions of China are declining. The Northeast region has fallen especially significantly, by more than 8%. The results are shown in Tables 4 and 5 and Figures 1–3.

Table 4. The result of overall iron and steel industry in 2020 scenario.

Emission Reduction Target	15%	16%	17%	18%	19%	20%
Carbon tax value (Yuan)	65.88	74.75	84.06	93.83	104.03	114.69
Production (100 million tons)	8.4584	8.4394	8.4194	8.3987	8.3773	8.3552
Rate of change, production (with 15% as the base)	-	−0.23%	−0.46%	−0.71%	−0.96%	−1.22%
Rate of change, social welfare (with 15% as the base)	-	−0.06%	−0.13%	−0.20%	−0.29%	−0.37%
Rate of change, producer surplus (with 15% as the base)	-	−0.22%	−0.44%	−0.68%	−0.92%	−1.17%

Table 5. The result of regions' iron and steel industry in 2020 scenario.

Emission Reduction Target		15%	16%	17%	18%	19%	20%
Production (100 million tons)	North China	2.1579	2.1598	2.1617	2.1636	2.1655	2.1674
	Northeast China	0.4705	0.4636	0.4564	0.4488	0.4409	0.4327
	East China	2.0304	2.0289	2.0273	2.0255	2.0235	2.0213
	South Central China	1.9103	1.9096	1.9088	1.9080	1.9072	1.9063
	Southwest China	0.8197	0.8174	0.8151	0.8128	0.8106	0.8084
	Northwest China	1.0700	1.0602	1.0501	1.0399	1.0296	1.0192
Rate of change, production (with 15% as the base)	North China	-	0.09%	0.18%	0.27%	0.35%	0.44%
	Northeast China	-	−1.46%	−2.99%	−4.60%	−6.28%	−8.04%
	East China	-	−0.07%	−0.15%	−0.24%	−0.34%	−0.44%
	South Central China	-	−0.04%	−0.08%	−0.12%	−0.16%	−0.21%
	Southwest China	-	−0.28%	−0.56%	−0.84%	−1.11%	−1.39%
	Northwest China	-	−0.92%	−1.86%	−2.81%	−3.78%	−4.75%
The decline range of emission intensity (with data in 2015 as the base)	North China	6.23%	6.99%	7.77%	8.56%	9.38%	10.22%
	Northeast China	6.48%	7.24%	8.02%	8.82%	9.63%	10.46%
	East China	6.84%	7.49%	8.15%	8.80%	9.45%	10.11%
	South Central China	11.16%	12.17%	13.17%	14.17%	15.17%	16.17%
	Southwest China	19.41%	20.72%	22.01%	23.29%	24.55%	25.81%
	Northwest China	17.53%	19.03%	20.52%	22.00%	23.48%	24.95%

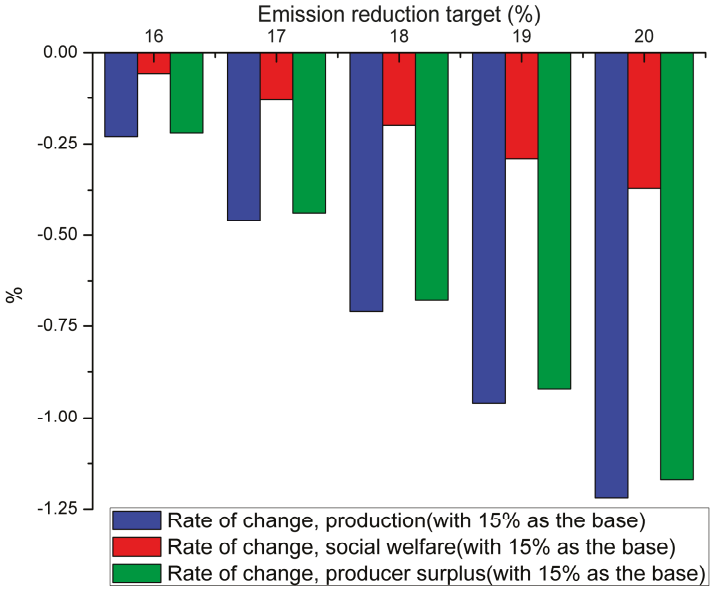

Figure 1. The change rate of total output, social welfare function, producer surplus with different reduction targets in 2020 scenario.

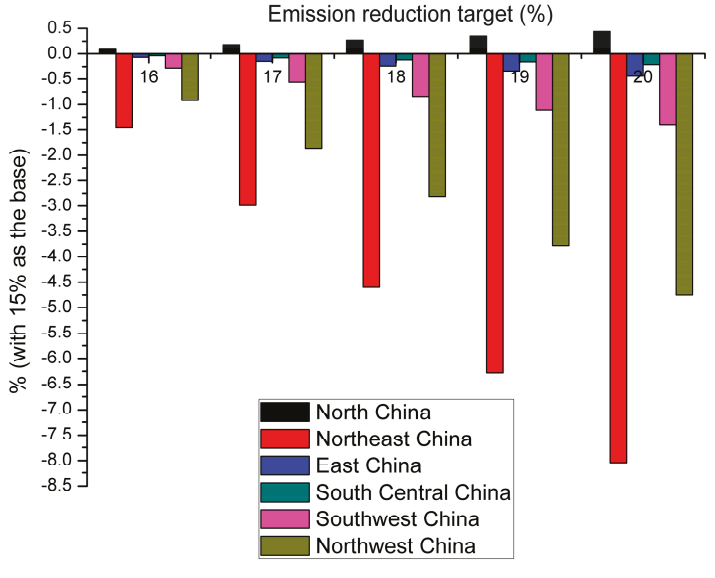

Figure 2. The change rate of regions' steel yield with different reduction targets in 2020 scenario.

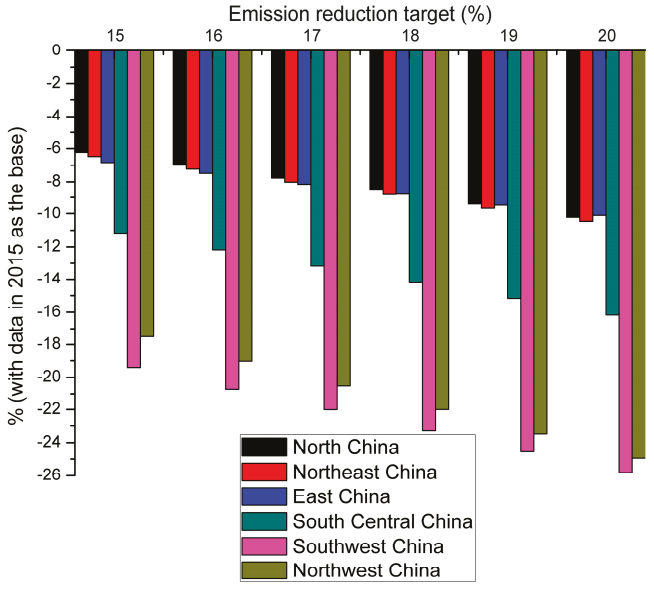

Figure 3. The regions' decline range of emission intensity with different reduction targets in 2020 scenario.

4.2.2. 2025 Scenario

In 2025, emissions reduction policies should include carbon taxes and product subsidies. With the gradual increase in reduction targets, carbon tax and the total scale of carbon tax, unit subsidy value and total subsidies will increase as well. The carbon tax value will have risen from 114.64 yuan/t to 178.04 yuan/t, and the levy of the total carbon tax also rises 45.19%. The unit subsidy value will have risen from 289 yuan/t to 421 yuan/t, and the total subsidy rises 45.28%. However, the carbon tax is not fully subsidized to steel companies, a very small surplus remains.

Total production will remain at around 900 million tons, although the pressure to reduce emissions will continue to rise to a 20–25% range compared with a modest increase in output in 2020. In this scenario, and with the gradual rise in reduction targets, total output, total social welfare, consumer surplus, producer surplus, and emissions losses should fall by 0.27%, 0.22%, 0.54%, 0.46%, and 6.51% respectively, and a slower rate of decline in 2020. Even when the target of reducing emissions increases, the producer surplus does the same, this suggests that although the target is more ambitious, CO_2 emissions tax subsidies for the enterprise can increase producers' enthusiasm for production, and help to increase total output and other corresponding indicators.

For the sub-region to reach the 20–25% target, emissions intensity and production yield are taken between regions. Emissions reduction efforts have increased in line with more ambitious reduction goals, but there are again notable inter-regional differences. In Southwest and Northwest China, the intensity of emissions reduction will have exceeded 25% in most cases. With an overall drop target of 25%, the reduction in Northwest China is the largest, at 32.6%. Relatively speaking, the reduction is smaller in East China, North China and other places, only 10–15%. It is slightly higher in South Central China, at 16–21%. In terms of output, the difference in production costs and the intensity of emissions reduction, combined with carbon tax and return subsidies, render significant changes in yield. The output in North China, East China, South Central China and Southwest China show a rising trend, whereas declines Northeast and Northwest China by approximately 4%. The results are shown in Tables 6 and 7 and Figures 4–6.

Table 6. The result of overall iron and steel industry in 2025 scenario.

Emission Reduction Target	20%	21%	22%	23%	24%	25%
Carbon tax value (Yuan)	114.64	126.34	138.52	151.18	164.43	178.04
Unit value of subsidy (Yuan)	289.00	314.50	340.50	367.00	394.00	421.00
Production (100 million tons)	9.0203	9.0160	9.0114	9.0065	9.0013	8.9985
Rate of change, production (with 20% as the base)	-	−0.05%	−0.10%	−0.15%	−0.21%	−0.27%
Rate of change, social welfare (with 20% as the base)	-	−0.03%	−0.07%	−0.12%	−0.17%	−0.22%
Rate of change, producer surplus (with 20% as the base)	-	0.10%	0.20%	0.29%	0.38%	0.46%

Table 7. The result of regions' iron and steel industry in 2025 scenario.

Emission Reduction Target		20%	21%	22%	23%	24%	25%
Production (100 million tons)	North China	2.2551	2.2603	2.2656	2.2709	2.2763	2.2816
	Northeast China	0.7635	0.7577	0.7516	0.7452	0.7384	0.7313
	East China	2.2818	2.2825	2.2831	2.2836	2.2838	2.2838
	South Central China	2.0230	2.0253	2.0276	2.0299	2.0322	2.0344
	Southwest China	0.8701	0.8711	0.8722	0.8734	0.8747	0.8762
	Northwest China	0.8268	0.8191	0.8113	0.8036	0.7959	0.7884
Rate of change, production (with 20% as the base)	North China	-	0.23%	0.47%	0.70%	0.94%	1.17%
	Northeast China	-	−0.76%	−1.56%	−2.40%	−3.29%	−4.21%
	East China	-	0.03%	0.06%	0.08%	0.09%	0.09%
	South Central China	-	0.11%	0.23%	0.34%	0.45%	0.57%
	Southwest China	-	0.11%	0.24%	0.38%	0.53%	0.70%
	Northwest China	-	−0.94%	−1.88%	−2.81%	−3.74%	−4.65%
The decline range of emission intensity (with data in 2015 as the base)	North China	0.1021	0.1111	0.1202	0.1295	0.1390	0.1485
	Northeast China	0.1046	0.1134	0.1224	0.1314	0.1407	0.1499
	East China	0.1010	0.1079	0.1148	0.1216	0.1285	0.1354
	South Central China	0.1616	0.1721	0.1825	0.1929	0.2034	0.2138
	Southwest China	0.2581	0.2713	0.2843	0.2974	0.3104	0.3232
	Northwest China	0.2494	0.2649	0.2802	0.2955	0.3109	0.3260

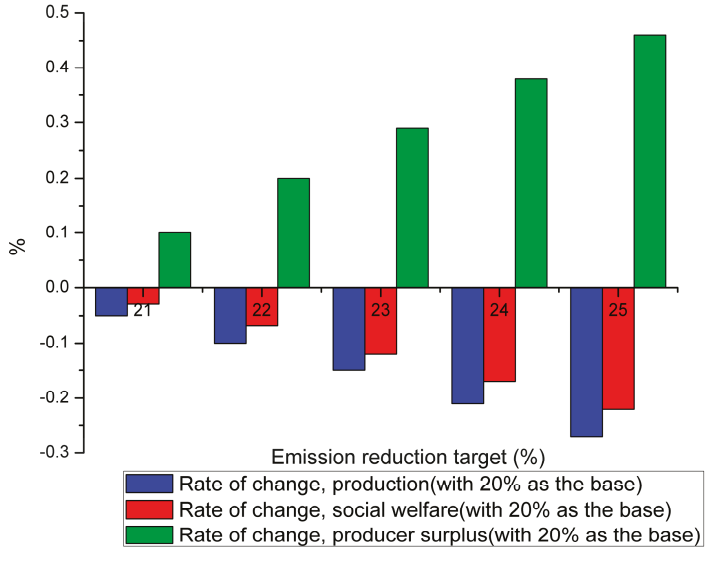

Figure 4. The change rate of total output, social welfare function, producer surplus with different reduction targets in 2025 scenario.

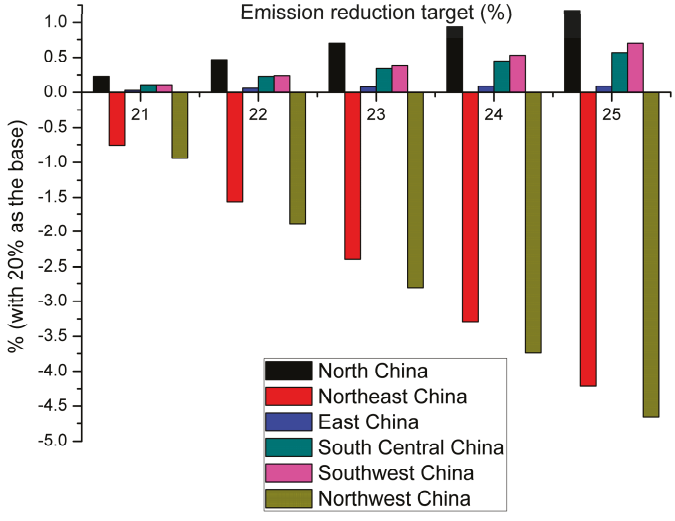

Figure 5. The change rate of regions' steel yield with different reduction targets in 2025 scenario.

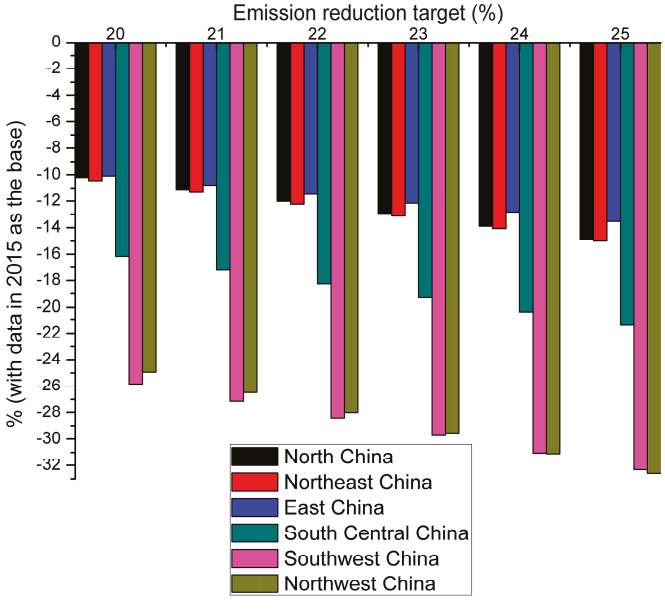

Figure 6. The regions' decline range of emission intensity with different reduction targets in 2025 scenario.

4.2.3. 2030 Scenario

In 2030, emissions reduction policies should include carbon taxes, product subsidies, and CCS demonstration projects. With the gradual increase in reduction targets, come increases in the carbon tax and its total scale, unit subsidy value and total subsidies. The carbon tax value is projected to rise from 192.29 yuan/t to 266.17 yuan/t, and the total carbon tax should increase 28.79%. The unit subsidy value will have risen from 455 yuan/t to 588 yuan/t, and the total subsidy rose 28.78%. However, the carbon tax is not fully subsidized to steel companies, there is still a very small surplus.

The CO_2 emissions from the CCS demonstration project also show an increase, with the target of 30% (M = 1.9 million tons) and a 44.24% increase in funding for CCS projects.

Total production should remain at around 935 million-938 million tons, although the pressure continues to increase to 25–30%, compared with a modest increase in production in 2020. In this scenario, with the gradual increase of reduction targets, total output, social welfare function, consumer surplus, producer surplus, and emissions losses are projected to fall by 0.35%, 0.46%, 0.69%, 0.06%, and 6.96% respectively, which also occurs alongside an increasing emissions reduction target. The producer surplus will increase as well. This shows that although the target is more ambitious, CO_2 emissions tax subsidies to enterprises and CCS can increase producers' enthusiasm for production, and help to increase total output and other corresponding indicators.

In order for sub-regions to reach the 25–30% target, emission intensity and production yield are taken between regions. Emissions reduction efforts have increased in line with more ambitious reduction goals, but there are again notable inter-regional differences. In Southwest and Northwest China, the intensity of emission reduction exceeds 33% in most cases. With an overall drop target of 30%, the reduction in the Northwest region is the largest, at 41.31%. By comparison, the emissions reduction in East China is the smallest (14–17%). The drop range in Northeast China, North China and other places is only 15–20%. It is slightly higher in South Central China at 22–27%. In terms of output, the difference in production costs and the intensity emissions reduction, combined with the carbon tax and return subsidies, affect yield changes. The output in North China, South Central China and Southwest China show a rising trend, whereas it is declining in Northeast, East and Northwest China. The Northeast region is projected to fall by more than 4%. The results are shown in Tables 8 and 9 and Figures 7–9.

Table 8. The result of overall iron and steel industry in 2030 scenario.

Emission Reduction Target	25%	26%	27%	28%	29%	30%
Carbon tax value (Yuan)	192.29	206.24	220.58	235.27	250.39	266.17
Unit value of subsidy (Yuan)	455.00	481.50	508.00	534.50	561.00	588.00
The CO_2 emission reduced by CCS demonstration project (million tons)	1.30	1.30	1.40	1.70	2.00	1.90
Production (100 million tons)	9.3831	9.3773	9.3710	9.3646	9.3577	9.3505
Rate of change, production (with 25% as the base)	-	−0.06%	−0.13%	−0.20%	−0.27%	−0.35%
Rate of change, social welfare (with 25% as the base)	-	−0.08%	−0.16%	−0.25%	−0.35%	−0.46%
Rate of change, producer surplus (with 25% as the base)	-	0.03%	0.05%	0.06%	0.06%	0.06%

Table 9. The result of regions' iron and steel industry in 2030 scenario.

Emission Reduction Target		25%	26%	27%	28%	29%	30%
Production (100 million tons)	North China	2.1759	2.1810	2.1860	2.1910	2.1959	2.2009
	Northeast China	0.9648	0.9574	0.9499	0.9420	0.9339	0.9254
	East China	2.1704	2.1699	2.1692	2.1683	2.1671	2.1656
	South Central China	1.9433	1.9455	1.9476	1.9496	1.9516	1.9525
	Southwest China	1.1304	1.1320	1.1338	1.1356	1.1376	1.1397
	Northwest China	0.9984	0.9914	0.9846	0.9780	0.9716	0.9654
Rate of change, production (with 25% as the base)	North China	-	0.23%	0.46%	0.69%	0.92%	1.15%
	Northeast China	-	−0.76%	−1.54%	−2.35%	−3.19%	−4.07%
	East China	-	−0.02%	−0.05%	−0.10%	−0.15%	−0.22%
	South Central China	-	0.11%	0.22%	0.32%	0.42%	0.52%
	Southwest China	-	0.15%	0.30%	0.46%	0.64%	0.83%
	Northwest China	-	−0.70%	−1.38%	−2.04%	−2.68%	−3.31%
The decline range of emission intensity (with data in 2015 as the base)	North China	0.1583	0.1676	0.1770	0.1865	0.1960	0.2058
	Northeast China	0.1594	0.1684	0.1775	0.1866	0.1957	0.2051
	East China	0.1423	0.1488	0.1554	0.1618	0.1683	0.1749
	South Central China	0.2242	0.2341	0.2439	0.2536	0.2634	0.2732
	Southwest China	0.3362	0.3484	0.3605	0.3726	0.3846	0.3967
	Northwest China	0.3413	0.3558	0.3702	0.3844	0.3987	0.4131

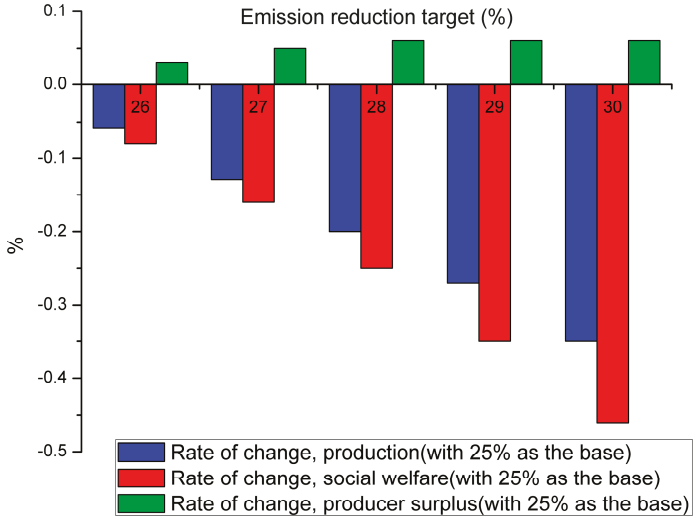

Figure 7. The change rate of total output, social welfare function, producer surplus with different reduction targets in 2030 scenario.

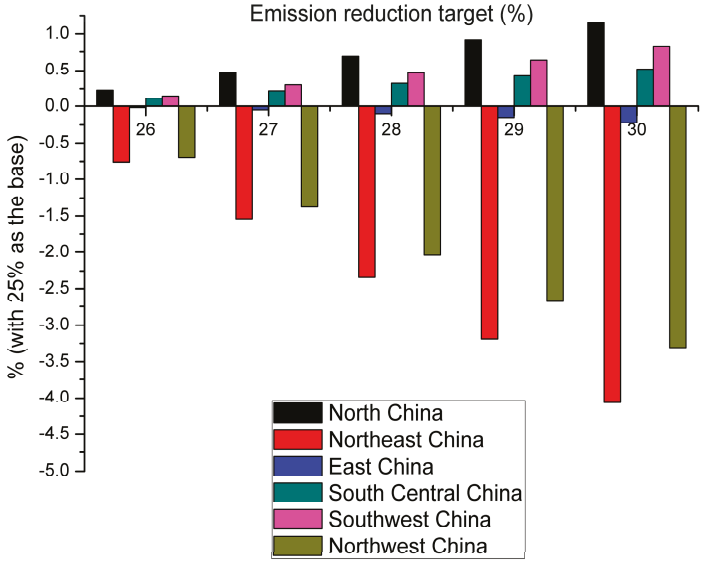

Figure 8. The change rate of regions' steel yield with different reduction targets in 2030 scenario.

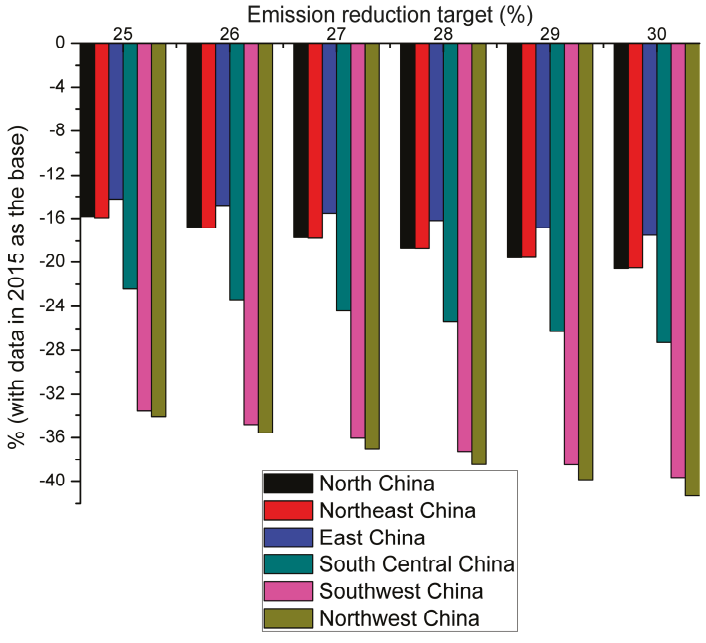

Figure 9. The regions' decline range of emission intensity with different reduction targets in 2030 scenario.

4.3. Discussion of Results

Current research on the future iron and steel industry emissions reduction targets is scarce, therefore, this paper does not discuss optimal emissions intensity. Only the aforementioned three scenarios were analyzed. Moreover, because of certain assumptions in the model, there were some gaps between the calculations and the actual results, but some trends and rules can still be found and identified.

On a national scale, with the gradual increase in reduction targets, the overall social welfare, consumer surplus, output and emission losses appear to be decreasing. The trend of carbon tax value, total carbon tax, unit value of output subsidies and total subsidies are rising. The change in producer surplus is irregular due to the comprehensive influence of production cost, production yield, carbon tax and subsidies.

Judging by the change range of the results, if only one emission reduction policy is considered, the overall social welfare, consumer surplus, output and loss are sharper than the results of multiple reduction policies. The adoption of a variety of reduction policies can compensate for the weakness associated with a single reduction in production costs, slow down the increase range in production costs, so as to reduce the overall range of changes. The total carbon tax and subsides are closely related to the unit value of carbon tax and the value of subsidy. Given the gradual increase in reduction targets, the change of total carbon tax and total subsidy range are significant.

For sub-region, which differ in production costs and emissions reduction costs, the optimal emissions range and output choices are related to the carbon tax value and subsides in different scenarios. Therefore, the result of each situation are quite different. According to the relevant national policy [1]: North and East China should focus on the mitigation of regional environmental pressure, relying on dominant enterprises. Through the reduction of restructuring, significantly reduce the excess steel capacity significantly and achieve regional reduction targets. The Midwest and Northeast old industrial base should rely on enterprises' regional comparative advantage, implement regional

integration, and reduce the number of entrepreneurs and excess steel production capacity. Steel output is be expected to peak in 2015–2020 intervals.

Our calculations show that, in three cases, output reduces by 150 to 200 million tons compared to that in 2015, with total output of about 900 million tons. After implementing of different carbon emissions reduction policies, production in North and East China should decrease about 1/3, South Central China production should remain in 180–200 million tons. The Northeast, Southwest, and Northwest region will increase but a much smaller rate compared to the reduction in North and East China. Although East and North China are still the main steel producing areas (about 50%), the output transition between the regions is from polarization to average. The polarization phenomenon appears to be easing, the regional maximum production ratio has declined from 10:1 to about 3:1. The results show a certain reference value in this calculation. Judging from the policy analysis aimed at "resolving excess capacity, prohibiting new capacity, production and consumption will enter the peak to the downward period" [1], the model and results have a certain reference value.

5. Conclusions

In light of the medium-and long-range plan promulgated by the government, a two-stage dynamic game model was constructed which incorporated the carbon tax, product subsidy, CCS, and other factors into the system of emission reduction mechanism. Then, we examined the resultant effects and economic impacts on six regions and China's overall steel industry. The model is the abstraction and assumption of a practical problem, so the calculation results may exist a little deviate from the actual situation, which makes the research result have some deviations. This paper emphasizes the change trends of corresponding indicators with increasing governmental pressure to reduce emissions. The main conclusions are as follows:

(I) Under a certain emissions reduction policy, with the gradual increase in reduction targets, the overall social welfare, consumer surplus, output and emissions losses are trending downward. The carbon tax unit value, total carbon tax, output subsidy unit value, and total subsidies demonstrate a rising trend.

(II) With the increasing target of reducing emissions, a variety of emissions reduction policies are more effective than a single reduction policy, which can slow down the indicators' decreasing range.

(III) For enterprises in the sub-regions, each region needs to choose its own reduction range and output. With the gradual increase in reduction targets, regional output has not shown a complete downward trend. Regional output has instead increased in some places likely duo to production function, carbon tax, subsidy and other comprehensive factors.

(IV) In the future, East and North China are expected to remain the primary producing areas, however, the proportion of production in the Northeast, Southwest and Northwest regions could rise. With the implementation of various emissions reduction policies, regional output polarization has eased.

Based on the above results and conclusions, when formulating emissions reduction targets and ancillary emissions reduction policies, the Chinese steel industry should use technological advances (i.e., lower production costs) along with several reasonable emissions reduction measures to achieve reduction targets into consideration. CCS can be implemented when the targets are too extreme and the CCS technology reaches a certain level. In future research, the impact of emissions reduction measures on the Chinese steel industry economy will be considered in the context of large-scale investment in CCS projects.

Secondly, China's steel industry is currently at overcapacity, that is, production capacity is far greater than the actual consumption. This paper's calculations show that when the market equilibrium is reached, the output and consumption of steel will be lower than they are at present.

Therefore, to alleviate the overcapacity contradiction and bring relief to the entire industry, China's steel industry needs to ban new steel production and push obsolete companies and

backward-producing enterprises out of the market as soon as possible. In the future, the government could levy more emission tax, reduce subsidies and conduct related policy research to address backward capacity, high-pollution emissions enterprises. These methods and impacts will be considered in subsequent research.

Thirdly, to improve the steel layout, the government should consider market demand, transportation, environment capacity and energy resources support conditions overall. Combined with solutions to address excess capacity and deepen regional layout reduction adjustments, the government should also encourage large-scale enterprises to reduce production capacity initiatively. Coastal areas' government should change their ideas. The blind relocation of steel enterprises from inland to coastal areas should be banned. And no longer layout the new coastal base. Based on the existing coastal base, the government should implement the "group development" to improve the quality and efficiency. Inland regions should take the regional market capacity and energy resources to support as the double bottom line, and withdraw non-competitive enterprises resolutely. Based on existing leading enterprises, the regional government should aim to integrate relief development, achieve a balance between regional steel productions and reduce polarization.

Acknowledgments: The authors gratefully acknowledge the financial support from the National Natural Science Foundation of China (71603039). This research has also been supported by China Postdoctoral Science Foundation (2015M571309) and Doctoral Startup Funds of Liaoning Province (201601049).

Author Contributions: Hailin Mu and Ye Duan had the original idea for the study, and conceived of and designed the methodology. Ye Duan drafted the manuscript, which was revised by Hailin Mu, Nan Li and Shusen Gui. All authors have read and approved the final manuscript.

Conflicts of Interest: The authors declare no conflict of interest.

References

1. Ministry of Industry and Information Technology of the People's Republic of China. Available online: http://www.miit.gov.cn/n1146285/n1146352/n3054355/n3057569/n3057573/c5353862/content.html (accessed on 14 November 2016).
2. Jorgenson, D.W.; Peter, J.W. Intertemporal General Equilibrium Modeling of U.S. Environmental Regulation. *J. Policy Model.* **1990**, *12*, 715–744. [CrossRef]
3. Jorgenson, D.W.; Peter, J.W. Reducing U.S. Carbon Dioxide Emissions: The Cost of Different Goals. *Adv. Econ. Energy Resour.* **1992**, *7*, 125–158.
4. Manne, A.S.; Mendelsohn, R.; Richels, R. MERGE: A model for evaluating regional and global effects of GHG reduction policies. *Energy Policy* **1995**, *23*, 17–34. [CrossRef]
5. Jorgenson, D.W.; Peter, J.W. Fundamental U.S. Tax Reform and Energy Markets. *Energy J.* **1997**, *18*, 1–30. [CrossRef]
6. Zhang, Z.X. Macroeconomic Effects of CO_2 Emission Limits: A Computable General Equilibrium Analysis for China. *J. Policy Model.* **1998**, *20*, 213–250. [CrossRef]
7. Fan, Z.; Li, S.T. Structural Change and Pollution Emission-perspective and policy impact analysis. *J. Quant. Tech. Econ.* **1998**, *8*, 8–14.
8. Jian, X.; Saltzman, S. Environmental Policy Analysis: An Environmental Computable General-Equilibrium Approach for Developing Countries. *J. Policy Model.* **2000**, *22*, 453–489.
9. Jian, X. An Environmentally Extended Social Accounting Matrix. *Environ. Resour. Econ.* **2000**, *16*, 391–406.
10. Kemfert, C.; Welsch, H. Energy capital labor Substitution and the economic effects of CO_2 abatement: Evidence for Germany. *J. Policy Model.* **2000**, *22*, 641–660. [CrossRef]
11. Wendner, R. An Applied Dynamic General Equilibrium Model of Environmental Tax Reforms and Pension Policy. *J. Policy Model.* **2001**, *23*, 25–50. [CrossRef]
12. Van Heeden, J.; Gerlagh, R.; Blignaut, J.; Horridge, M.; Hess, S.; Mabugu, R.; Mabugu, M. Searching for triple dividends in South Africa: Fighting CO_2 pollution and poverty while promoting growth. *Energy J.* **2006**, *27*, 113–141. [CrossRef]
13. Abrell, J. Regulating CO_2 emissions of transportation in Europe: A CGE analysis using market-based instruments. *Transp. Res. Part D* **2010**, *15*, 235–239. [CrossRef]

14. Benavides, C.; Gonzales, L.; Diaz, M.; Fuentes, R.; García, G.; Palma-Behnke, R.; Ravizza, C. The Impact of a Carbon Tax on the Chilean Electricity Generation Sector. *Energies* **2015**, *8*, 2674–2700. [CrossRef]
15. Yahoo, M.; Othman, J. Employing a CGE model in analysing the environmental and economy-wide impacts of CO_2 emission abatement policies in Malaysia. *Sci. Total Environ.* **2017**, *584–585*, 234–243. [CrossRef] [PubMed]
16. Liang, Q.M.; Fan, Y.; Wei, Y.M. Carbon taxation policy in China: How to protect energy and trade intensive sectors? *J. Policy Model.* **2007**, *29*, 311–333. [CrossRef]
17. Yang, L.; Mao, X.Q.; Liu, Q.; Liu, Z.Y. Impact Assessment for Energy Taxation Policy Based on A Computable General Equilibrium (CGE) Model. *China Popul. Resour. Environ.* **2009**, *19*, 24–29.
18. Wu, L.B.; Qian, H.Q.; Tang, W.Q. Selection Mechanism between Emission Trading and Carbon Tax based on Simulation of Dynamic Marginal Abatement Cost. *Econ. Res. J.* **2014**, *9*, 48–61.
19. Xu, S.C.; Zhang, W.W. Analysis of impacts of carbon taxes on China's economy and emissions reduction under different refunds: Based on dynamic CGE Model. *China Popul. Resour. Environ.* **2016**, *26*, 46–54.
20. Chen, W.; Zhou, J.F.; Li, S.Y.; Li, Y.C. Effects of an Energy Tax (Carbon Tax) on Energy Saving and Emission Reduction in Guangdong Province-Based on a CGE Model. *Sustainability* **2017**, 9. [CrossRef]
21. Ling, T.; Shi, J.R.; Yu, L.; Qin, B. Economic and environmental influences of coal resource tax in China: A dynamic computable general equilibrium approach. *Resour. Conserv. Recycl.* **2017**, *117*, 34–44.
22. Montero, J.P. Permits, Standards, and Technology Innovation. *J. Environ. Econ. Manag.* **2002**, *44*, 23–44. [CrossRef]
23. Bruneau, J.F. A Note on Permits, Standards, and Technology Innovation. *J. Environ. Econ. Manag.* **2004**, *48*, 1192–1199. [CrossRef]
24. Requate, T. Dynamic incentives by environmental policy instruments—A survey. *Ecol. Econ.* **2005**, *54*, 175–195. [CrossRef]
25. Requate, T. Timing and commitment of environmental policy, adoption of new technology, and repercussions on R & D. *Environ. Resour. Econ.* **2005**, *31*, 175–199.
26. Puller, S. The strategic use of innovation to influence regulatory standard. *J. Environ. Econ. Manag.* **2006**, *52*, 690–706. [CrossRef]
27. Poyago-Theotoky, J.; Teerasuwannajak, K. The Timing of Environmental Policy: A Note on the Role of Product Differentiation. *J. Regul. Econ.* **2002**, *21*, 305–316. [CrossRef]
28. Poyago-Theotoky, J.A. The organization of R & D and environmental policy. *J. Econ. Behav. Organ.* **2007**, *62*, 63–75.
29. Youssef, S.B.; Zaccour, G. Absorptive Capacity, R & D Spillovers, Emissions Taxes and R & D Subsidies. *Strateg. Behav. Environ.* **2014**, *4*, 41–58.
30. Ouchida, Y.; Goto, D. Cournot Duopoly and Environmental R & D under Regulator's Precommitment to an Emissions tax. *Appl. Econ. Lett.* **2016**, *23*, 324–331.
31. Moner-Colonques, R.; Rubio, S.J. The Strategic Use of Innovation to Influence Environmental Policy: Taxes versus Standards. *B.E. J. Econ. Anal. Policy* **2016**, *16*, 973–1000. [CrossRef]
32. Demailly, D.; Quirion, P. European Emission Trading Scheme and competitiveness: A case study on the iron and steel industry. *Energy Econ.* **2008**, *30*, 2009–2027. [CrossRef]
33. Cato, S. Environmental policy in a mixed market: Abatement subsidies and emissions taxes. *Environ. Econ. Policy Stud.* **2011**, *13*, 283–301. [CrossRef]
34. Eyland, T.; Zaccour, G. Strategic Effects of a Border Tax Adjustment. *Int. Game Theory Rev.* **2012**, *14*, 31–42. [CrossRef]
35. Ouchida, Y.; Goto, D. Do emission subsidies reduce emission? In the context of environmental R & D organization. *Econ. Model.* **2014**, *36*, 511–516.
36. McDonald, S.; Poyago-Theotoky, J. Green technology and optimal emissions taxation. *J. Public Econ. Theory* **2017**, *19*, 362–376. [CrossRef]
37. Lambertini, L.; Poyago-Theotoky, J.; Tampieri, A. Cournot Competition and "Green" Innovation: An Inverted-U Relationship. *Energy Econ.* **2017**, *68*, 116–123. [CrossRef]
38. Li, C.S.; Fan, Y.; Zhu, L. Emissions Tax and Its Revenue Refunding Scheme Design with Exogenous Abatement Target. *Syst. Eng.* **2012**, *30*, 82–86.
39. Li, C.S.; Fan, Y.; Zhu, L. The study of Carbon Dioxide Emission Intensity Abatement Mechanism of Iron and Steel Industry Based on Two-Stage Game Model. *Chin. J. Manag. Sci.* **2012**, *20*, 93–100. [CrossRef]

40. Yu, W.S.; Zhang, Z.Y. Feasibility and Mode Selection of Carbon Tax Policy in China based on Game Theory. *China Popul. Resour. Environ.* **2013**, *23*, 8–15.
41. Li, Y.; Zhao, D.Z.; Zhu, X.G. A Game Model for Government and Enterprise Behavior Based on a Carbon Tax. *Resour. Sci.* **2013**, *35*, 125–131.
42. Qiao, H.; Song, N.; Gao, H.W. Analysis on the strategies of European Union's airline carbon tax with Stackelberg game models. *Syst. Eng. Theory Pract.* **2014**, *34*, 158–167.
43. Xu, X.Y.; Xu, X.P.; He, P. Joint production and pricing decisions for multiple products with cap-and-trade and carbon tax regulations. *J. Clean. Prod.* **2016**, *112*, 4093–4106. [CrossRef]
44. Chen, S.Y. Industrial carbon dioxide shadow price: Parametric and nonparametric methods. *World Econ.* **2010**, *8*, 93–111.
45. Zhou, X.; Fan, L.W.; Zhou, P. Marginal CO_2 abatement costs: Findings from alternative shadow price estimates for Shanghai industrial sectors. *Energy Policy* **2015**, *77*, 109–117. [CrossRef]
46. Chen, D.H.; Pan, Y.C.; Wu, C.Y. Marginal abatement costs of CO_2 emission in China and its regional differences. *China Popul. Resour. Environ.* **2016**, *10*, 86–93.
47. Färe, R.; Grosskopf, S.; Pasurka, C.A., Jr. Environmental Production Functions and Environmental Directional Distance Functions. *Energy* **2007**, *32*, 1055–1066. [CrossRef]
48. Lee, J.D.; Park, J.B.; Kim, T.Y. Estimation of the shadow prices of pollutants with production/environment inefficiency taken into account: A nonparametric directional distance function approach. *J. Environ. Manag.* **2002**, *64*, 365–375. [CrossRef]
49. Guenno, G.; Tiezzi, S. *The Index of Sustainable Economics Welfare (ISEW) for Italy*; Nota Di Lavoro; Fondazione Eni Enrico Mattei: Milano, Italy, 1998.
50. Dahowski, R.T.; Li, X.; Davidson, C.L.; Wei, N.; Dooley, J.J.; Gentile, R.H. A Preliminary Cost Curve Assessment of Carbon Dioxide Capture and Storage Potential in China. *Energy Procedia* **2009**, *1*, 2849–2856. [CrossRef]
51. Liu, H.W.; Kelly, S.G. Preparing to ramp up large-scale CCS demonstrations: An engineering economic assessment of CO_2 pipeline transportation in China. *Int. J. Greenh. Gas Control* **2011**, *5*, 798–804. [CrossRef]
52. Wang, B.Q.; Li, H.Q.; Bao, W.J. A model of economy for overall process of CO_2 capture and saline storage. *CIESC J.* **2012**, *63*, 894–903.
53. Zhu, L.; Fan, Y. Modeling the Investment of Coal-fired Power Plant Retrofit with CCS and Subsidy Policy Assessment. *China Popul. Resour. Environ.* **2014**, *24*, 99–105.
54. National Bureau of Statistics of the People's Republic of China. *CSY, 2005. China Statistical Yearbook*; National Bureau of Statistics of the People's Republic of China: Beijing, China, 2005.
55. National Bureau of Statistics of the People's Republic of China. *CSY, 2006. China Statistical Yearbook*; National Bureau of Statistics of the People's Republic of China: Beijing, China, 2006.
56. National Bureau of Statistics of the People's Republic of China. *CSY, 2007. China Statistical Yearbook*; National Bureau of Statistics of the People's Republic of China: Beijing, China, 2007.
57. National Bureau of Statistics of the People's Republic of China. *CSY, 2008. China Statistical Yearbook*; National Bureau of Statistics of the People's Republic of China: Beijing, China, 2008.
58. National Bureau of Statistics of the People's Republic of China. *CSY, 2009. China Statistical Yearbook*; National Bureau of Statistics of the People's Republic of China: Beijing, China, 2009.
59. National Bureau of Statistics of the People's Republic of China. *CSY, 2010. China Statistical Yearbook*; National Bureau of Statistics of the People's Republic of China: Beijing, China, 2010.
60. National Bureau of Statistics of the People's Republic of China. *CSY, 2011. China Statistical Yearbook*; National Bureau of Statistics of the People's Republic of China: Beijing, China, 2011.
61. National Bureau of Statistics of the People's Republic of China. *CSY, 2012. China Statistical Yearbook*; National Bureau of Statistics of the People's Republic of China: Beijing, China, 2012.
62. National Bureau of Statistics of the People's Republic of China. *CSY, 2013. China Statistical Yearbook*; National Bureau of Statistics of the People's Republic of China: Beijing, China, 2013.
63. National Bureau of Statistics of the People's Republic of China. *CSY, 2014. China Statistical Yearbook*; National Bureau of Statistics of the People's Republic of China: Beijing, China, 2014.
64. National Bureau of Statistics of the People's Republic of China. *CSY, 2015. China Statistical Yearbook*; National Bureau of Statistics of the People's Republic of China: Beijing, China, 2015.

65. National Bureau of Statistics of the People's Republic of China. *CSY, 2016. China Statistical Yearbook*; National Bureau of Statistics of the People's Republic of China: Beijing, China, 2016.
66. National Bureau of Statistics of the People's Republic of China. *CIESY, 2005. China Industrial Economy Statistical Yearbook*; National Bureau of Statistics of the People's Republic of China: Beijing, China, 2005.
67. National Bureau of Statistics of the People's Republic of China. *CIESY, 2006. China Industrial Economy Statistical Yearbook*; National Bureau of Statistics of the People's Republic of China: Beijing, China, 2006.
68. National Bureau of Statistics of the People's Republic of China. *CIESY, 2007. China Industrial Economy Statistical Yearbook*; National Bureau of Statistics of the People's Republic of China: Beijing, China, 2007.
69. National Bureau of Statistics of the People's Republic of China. *CIESY, 2008. China Industrial Economy Statistical Yearbook*; National Bureau of Statistics of the People's Republic of China: Beijing, China, 2008.
70. National Bureau of Statistics of the People's Republic of China. *CIESY, 2009. China Industrial Economy Statistical Yearbook*; National Bureau of Statistics of the People's Republic of China: Beijing, China, 2009.
71. National Bureau of Statistics of the People's Republic of China. *CIESY, 2010. China Industrial Economy Statistical Yearbook*; National Bureau of Statistics of the People's Republic of China: Beijing, China, 2010.
72. National Bureau of Statistics of the People's Republic of China. *CIESY, 2011. China Industrial Economy Statistical Yearbook*; National Bureau of Statistics of the People's Republic of China: Beijing, China, 2011.
73. National Bureau of Statistics of the People's Republic of China. *CIESY, 2012. China Industrial Economy Statistical Yearbook*; National Bureau of Statistics of the People's Republic of China: Beijing, China, 2012.
74. National Bureau of Statistics of the People's Republic of China. *CIESY, 2013. China Industrial Economy Statistical Yearbook*; National Bureau of Statistics of the People's Republic of China: Beijing, China, 2013.
75. National Bureau of Statistics of the People's Republic of China. *CIESY, 2014. China Industrial Economy Statistical Yearbook*; National Bureau of Statistics of the People's Republic of China: Beijing, China, 2014.
76. National Bureau of Statistics of the People's Republic of China. *CIESY, 2015. China Industrial Economy Statistical Yearbook*; National Bureau of Statistics of the People's Republic of China: Beijing, China, 2015.
77. National Bureau of Statistics of the People's Republic of China. *CIESY, 2016. China Industrial Economy Statistical Yearbook*; National Bureau of Statistics of the People's Republic of China: Beijing, China, 2016.
78. The Editorial Board of China Steel Yearbook. *CSY, 2005. China Steel Yearbook*; The Editorial Board of China Steel Yearbook: Beijing, China, 2005.
79. The Editorial Board of China Steel Yearbook. *CSY, 2006. China Steel Yearbook*; The Editorial Board of China Steel Yearbook: Beijing, China, 2006.
80. The Editorial Board of China Steel Yearbook. *CSY, 2007. China Steel Yearbook*; The Editorial Board of China Steel Yearbook: Beijing, China, 2007.
81. The Editorial Board of China Steel Yearbook. *CSY, 2008. China Steel Yearbook*; The Editorial Board of China Steel Yearbook: Beijing, China, 2008.
82. The Editorial Board of China Steel Yearbook. *CSY, 2009. China Steel Yearbook*; The Editorial Board of China Steel Yearbook: Beijing, China, 2009.
83. The Editorial Board of China Steel Yearbook. *CSY, 2010. China Steel Yearbook*; The Editorial Board of China Steel Yearbook: Beijing, China, 2010.
84. The Editorial Board of China Steel Yearbook. *CSY, 2011. China Steel Yearbook*; The Editorial Board of China Steel Yearbook: Beijing, China, 2011.
85. The Editorial Board of China Steel Yearbook. *CSY, 2012. China Steel Yearbook*; The Editorial Board of China Steel Yearbook: Beijing, China, 2012.
86. The Editorial Board of China Steel Yearbook. *CSY, 2013. China Steel Yearbook*; The Editorial Board of China Steel Yearbook: Beijing, China, 2013.
87. The Editorial Board of China Steel Yearbook. *CSY, 2014. China Steel Yearbook*; The Editorial Board of China Steel Yearbook: Beijing, China, 2014.
88. The Editorial Board of China Steel Yearbook. *CSY, 2015. China Steel Yearbook*; The Editorial Board of China Steel Yearbook: Beijing, China, 2015.
89. The Editorial Board of China Steel Yearbook. *CSY, 2016. China Steel Yearbook*; The Editorial Board of China Steel Yearbook: Beijing, China, 2016.
90. National Bureau of Statistics of the People's Republic of China. *CESY, 2005. China Energy Statistical Yearbook*; National Bureau of Statistics of the People's Republic of China: Beijing, China, 2005.

91. National Bureau of Statistics of the People's Republic of China. *CESY, 2006. China Energy Statistical Yearbook*; National Bureau of Statistics of the People's Republic of China: Beijing, China, 2006.
92. National Bureau of Statistics of the People's Republic of China. *CESY, 2007. China Energy Statistical Yearbook*; National Bureau of Statistics of the People's Republic of China: Beijing, China, 2007.
93. National Bureau of Statistics of the People's Republic of China. *CESY, 2008. China Energy Statistical Yearbook*; National Bureau of Statistics of the People's Republic of China: Beijing, China, 2008.
94. National Bureau of Statistics of the People's Republic of China. *CESY, 2009. China Energy Statistical Yearbook*; National Bureau of Statistics of the People's Republic of China: Beijing, China, 2009.
95. National Bureau of Statistics of the People's Republic of China. *CESY, 2010. China Energy Statistical Yearbook*; National Bureau of Statistics of the People's Republic of China: Beijing, China, 2010.
96. National Bureau of Statistics of the People's Republic of China. *CESY, 2011. China Energy Statistical Yearbook*; National Bureau of Statistics of the People's Republic of China: Beijing, China, 2011.
97. National Bureau of Statistics of the People's Republic of China. *CESY, 2012. China Energy Statistical Yearbook*; National Bureau of Statistics of the People's Republic of China: Beijing, China, 2012.
98. National Bureau of Statistics of the People's Republic of China. *CESY, 2013. China Energy Statistical Yearbook*; National Bureau of Statistics of the People's Republic of China: Beijing, China, 2013.
99. National Bureau of Statistics of the People's Republic of China. *CESY, 2014. China Energy Statistical Yearbook*; National Bureau of Statistics of the People's Republic of China: Beijing, China, 2014.
100. National Bureau of Statistics of the People's Republic of China. *CESY, 2015. China Energy Statistical Yearbook*; National Bureau of Statistics of the People's Republic of China: Beijing, China, 2015.
101. National Bureau of Statistics of the People's Republic of China. *CESY, 2016. China Energy Statistical Yearbook*; National Bureau of Statistics of the People's Republic of China: Beijing, China, 2016.
102. Intergovernmental Panel on Climate Change (IPCC). *IPCC Guidelines for National Greenhouse Gas Inventories*; United Kingdom Meteorological Office: Bracknell, UK, 2006.
103. Duan, Y.; Mu, H.L.; Li, N. Analysis of the Relationship between China's IPPU CO_2 Emissions and the Industrial Economic Growth. *Sustainability* **2016**, *8*, 426. [CrossRef]

energies

MDPI

Article

Wide Area Coordinated Control of Multi-FACTS Devices to Damp Power System Oscillations

Shiyun Xu [1,2,*], Ying Yang [3,*], Kaixiang Peng [4], Linlin Li [4], Tasawar Hayat [2,5] and Ahmed Alsaedi [2]

1 China Electric Power Research Institute, Beijing 100192, China
2 Nonlinear Analysis and Applied Mathematics (NAAM) Research Group, Faculty of Science, King Abdulaziz University, Jeddah 21589, Saudi Arabia; tahaksag@yahoo.com (T.H.); aalsaedi@kau.edu.sa (A.A.)
3 College of Engineering, Peking University of China, Beijing 100871, China
4 Key Laboratory of Knowledge Automation for Industrial Processes of Ministry of Education, School of Automation and Electrical Engineering, University of Science and Technology Beijing, Beijing 100083, China; kaixiang@ustb.edu.cn (K.P.); linlin.li@uni-due.de (L.L.)
5 Department of Mathematics, Quaid-i-Azam University, 45320 Islamabad, Pakistan
* Correspondence: xushiyun@foxmail.com (S.X.); yy@mech.pku.edu.cn (Y.Y.)

Received: 3 November 2017; Accepted: 5 December 2017; Published: 14 December 2017

Abstract: Aiming at damping the inter-area oscillations of power systems, the present study proposes a wide-area decentralized coordinated control framework, where the upper-level controller is designed to coordinate the lower-level multiple FACTS devices. Based on the polytopic differential inclusion method, the derived controller adopts a decentralized structure and it is guaranteed to be robust to meet the demand of operation under multiple operating conditions. Since time delay of wide area signal transmission is inevitable, in what follows, the quantum evolution algorithm (QEA) method is introduced to find an optimal solution of the time-delay coordinated controller. In this regard, the stability of the system with a prescribed time delay is guaranteed and the system damping ratio is increased. Effectiveness and applicability of the proposed controller design methods have been demonstrated through numerical simulations.

Keywords: wide-area measurement system; FACTS devices; coordinated control; time delay; damping controllers; robustness

1. Introduction

With the rapid development of power systems, in recent years, the complexity of system structure and operating modes has been greatly increased [1] and the continuous and increasing demand of electrical energy consumption has greatly influenced the power system performance. In the operation of power systems, the insufficient damping of electromechanical oscillations is known to be a major constraint [2]. Such oscillations can be distinguished into two types, local oscillations that occur when generators in the same area oscillate with respect to each other and inter-area oscillations occurring among machines in different areas. If no adequate damping is available, the oscillations may cause operational limitations of power transmission capacity, or bring about the system separation, which in some cases may lead to blackouts [3–5].

Flexible AC Transmission System (FACTS) devices, including static var compensator (SVC), thyristor controlled series compensator (TCSC), static synchronous compensator (STATCOM) and so on, possess the rapid and reliable regulation property [6]. Since the construction of modern power grid demands the improvement of power flow distribution, system stability and transmission capacity in a flexible and reliable way, FACTS devices have been put into practical application and achieved satisfying control effects either act by modulating the reactive power or the active power or both [7].

FACTS controllers are located in the network where the controllability and observability of the inter-area oscillations are better. Generally speaking, FACTS devices exist in the power system are individually designed and installed for different targets due to local control and lack of coordination. Accordingly, a coordinated action among various FACTS devices is needed for the damping of inter-area oscillations and how to coordinately control the multi-FACTS devices to achieve greater effectiveness and at the same time, avoid adverse interaction that may occur between FACTS controllers have become an important research topic. Combined with modern control theory, the multi-FACTS coordinated control (MFCC) aiming at different control objectives has gained rich achievements over the past years [8,9]. In order to further improve system stability with the help of global information from wide-area measurement systems (WAMS) [10], more recently, the study of wide-area coordinated control is gradually increasing. However, it is noted that the study of MFCC based on WAMS is comparatively less, among which, reference [11] designs a controller that coordinates multiple robust FACTS damping controllers based on a BMI sequential approach. It indicates that MFCC can remarkably enhance system stability and at the same time, eliminate the negative interaction among devices and they also demonstrate the necessity of coordination.

Among the existing literature of MFCC, the control strategies are normally designed over a single dynamic model obtained from the linearization of system equations around one of the specific equilibria. Since system parameter matrices will change along with the variation of operating conditions, the derived control strategy should be guaranteed for each operating condition simultaneously, which leads to the complicatedness of calculation process. In this regard, how to meet the demand of operation under multiple cases is an important issue to be solved. On the other hand, time delays caused by the usage of communication networks to transfer the remote signal in the data transferring process is inevitable in WAMS, which will degrade the system performance or may even cause instability of the closed-loop system [12,13]. As a consequence, in a coordinated control strategy, it is of great significance to minimize the effect of time-delay [14]. Common methods of designing controllers to deal with the delay impact include equivalent treatment of time delay, robust control based on Linear Matrix Inequality (LMI) [15,16] and so on. However, for such robust coordinated controllers, the effect of time delay has seldom been taken into account in the previous literatures.

Based on the above considerations, the present study proposes a wide-area decentralized coordinated control framework for multiple FACTS devices. Aiming at realizing different control objectives, the upper-level coordinated controller is designed as both a robust dynamic output feedback controller and a time-delay output feedback controller. The polytopic differential inclusion method is introduced such that the derived dynamic output feedback controller is robust to various operating conditions. Moreover, the system damping ratio has been taken into account in the controller design strategy such that the system is capable to be operated under strong damping modes. In order to design the time-delay MFCC such that the stability of the system with a prescribed time delay is guaranteed, the sufficient condition of time-delay stability criterion proposed in [17] can be utilized. However, since the unknown objective parameters are coupled in the matrix inequalities, they cannot be solved by the LMI control toolbox in Matlab (R2016a, MathWorks, Natick, MA, USA). Aimed at deriving the controller parameter matrix, the quantum evolution algorithm (QEA) method is introduced to find an optimal solution. In this regard, the stability of the system with a prescribed time delay is guaranteed and the system damping ratio is increased. Validity and applicability of the proposed coordinated control algorithms are demonstrated in a two-area four-generator system. Simulation results demonstrate that the under robust coordinated control, the controlled power system successfully runs in strong damping modes in four different operating conditions and the algorithm exhibits good control effect in a wide range of time-delay.

2. Problem Formulation

In order to make preparation for the MFCC design, this section presents the MFCC framework based on WAMS. In the proposed framework, as is shown in Figure 1, a coordinated controller receives

the WAMS information and carries out calculation based on the state and output variable measured by WAMS data platform. The control instruction is then derived to be assigned to each FACTS device.

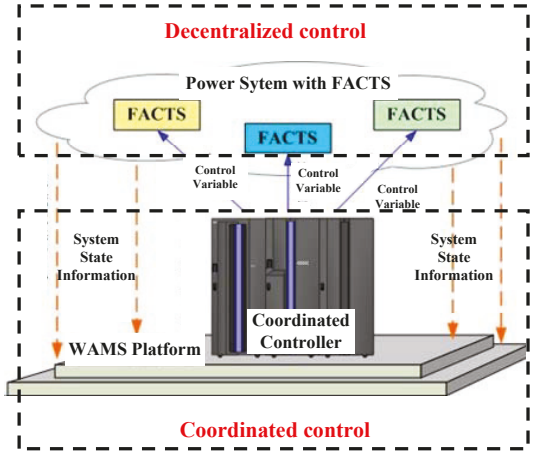

Figure 1. Coordinated control among FACTS devices based on WAMS.

By allocating the derived control signal as auxiliary input variables, the coordinated control among FACTS devices is then realized. For each FACTS device, the coordinated control variable u is received as a part of the controller input signal. It will be transmitted to the controller together with the local variable. Compared with local control, the wide-area coordination scheme is able to achieve global control through coordination control in a better way but it requires the entire system information, which may to some extent, influence the speed and accuracy of control.

In what follows, we give a brief description of some aspects involved in the power system model used in this work. For the sake of simplicity, the dynamic devices considered in this study mainly include generators and FACTS devices.

2.1. Generator Model

The generator is represented as a dynamic model equipped with a rapid excitation, whose model is described as:

$$\begin{aligned}
\dot{\delta}_i &= \omega_0(\omega_i - 1) \\
\dot{\omega}_i &= \tfrac{1}{2H_i}[P_{m_i} - E'_{d_i} I_{d_i} - E'_{q_i} I_{q_i} - D_i(\omega_i - 1)] \\
\dot{E}'_{q_i} &= \tfrac{1}{T'_{d0_i}}[E'_{fd_i} - (x_{d_i} - x'_{d_i}) I_{d_i} - E'_{q_i}] \\
\dot{E}'_{fd_i} &= \tfrac{1}{T_A}[-E_{fd_i} + K_A(V_{\mathrm{ref}i} - V_{\mathrm{t}})]
\end{aligned} \tag{1}$$

for $i = 1, 2, \ldots, n$, where n is the number of synchronous generators. Referred to the generator i, δ_i is the rotor angle, ω_i is the rotor speed with respect to a synchronous reference, E'_{q_i} is the quadrature-axis transient voltage, E_{fd_i} is the field voltage, V_{t} is the terminal bus voltage magnitude. The definitions of the electrical quantities in Equation (1) can be found in [18].

2.2. TCSC Model

TCSC is a device constituted by a series capacitor bank with fixed value and a Thyristor-Controlled Reactor (TCR) [19]. It is installed directly in the transmission system and its equivalent reactance can be varied by adjusting the fire angle of the thyristors. In order to guarantee the additional damping supply to the inter-area oscillations of interest, a supplementary controller is required. TCSC is usually

represented by a first order linear model in small signal stability studies [20], which is also adopted in the present study. The block diagram of the adopted TCSC with a supplementary controller is given in Figure 2.

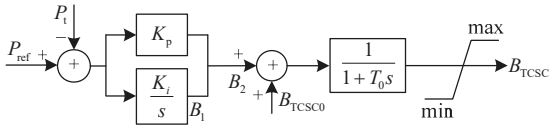

Figure 2. Dynamic model of TCSC.

The dynamic model based on Figure 2 can be written as:

$$\begin{cases} \dot{B}_1 = K_i(P_{\text{ref}} - P_t) \\ B_2 = B_1 + K_p(P_{\text{ref}} - P_t) \\ \dot{B}_{\text{TCSC}} = (B_2 + B_{\text{TCSC0}})/T_0 \end{cases} \tag{2}$$

where B_{TCSC} is the deviation of the equivalent TCSC reactance with respect to the nominal value, B_{TCSC0} is the reference for the desired reactance deviation (from its nominal value) in steady state, B_2 is the stabilizing signal from the proposed supplementary controller, B_1 is an intermediate variable and T_0 is the device time constant. K_p and K_i are the gains of the PI control loop; P_{ref} and P_t are the active power reference and the active power of the TCSC control line, respectively.

2.3. SVC Model

SVC is one of the most widely applied FACTS devices which can maintain voltage stability and at the same time, improve the system damping. In this study, the control block of SVC mathematical formulation is shown in Figure 3.

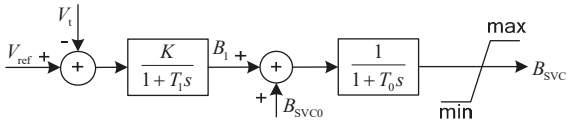

Figure 3. Dynamic model of SVC.

whose dynamical model is described as:

$$\begin{cases} \dot{B}_1 = \frac{1}{T_1}[-B_1 + K(V_{\text{ref}} - V_t)] \\ \dot{B}_{\text{SVC}} = \frac{1}{T_0}[B_1 - B_{\text{SVC}}] \end{cases} \tag{3}$$

where B_{SVC} is the equivalent susceptance output of SVC, B_{SVC0} is the steady-state susceptance of SVC, B_1 is an intermediate variable and K is the gain of controller measurement. T_1 and T_0 are time constants, V_{ref} is the reference voltage and V_t is the measurement voltage of the SVC control point.

By integrating Equations (1)–(3), we derive the power system model composed by multiple generators and FACTS devices. After linearization around an equilibrium point, the state-space power system model can be represented by a linear time invariant (LTI) model given by a set of linear equations:

$$\begin{cases} \dot{x} = Ax + Bu \\ y = Cx \end{cases} \tag{4}$$

where x is the n-dimensional state vector, u is the p-dimensional system control input vector and y is the q-dimensional system output vector. A, B, C are given system parameter matrices with appropriate dimensions.

Aiming at realizing different control objectives, in this study, the upper-level wide-area coordinated controller is firstly designed as a robust dynamic output feedback controller. By further taking the time-delay into account, a time-delay output feedback controller is then proposed.

3. Main Results

During the practical operation of power systems, the state matrix A in Equation (4) may vary along with the changing of operating modes. In order to ensure the controller robustness to the variation of operating conditions, in this section, the wide-area MFCC adopts the dynamic output feedback control strategy for better dynamic characteristics, which is given as:

$$\begin{cases} \dot{x}_C = A_C x_C + B_C y \\ u = C_C x_C \end{cases} \tag{5}$$

where x_C is the n-dimensional state vector of controller and A_C, B_C, C_C are parameter matrices to be determined. Combining with the system dynamical Equation (4), the closed-loop controlled system is derived as:

$$\dot{\widetilde{x}} = \widetilde{A}\widetilde{x} \tag{6}$$

where:

$$\widetilde{x} = \begin{bmatrix} x \\ x_C \end{bmatrix}, \widetilde{A} = \begin{bmatrix} A & BC_C \\ B_C C & A_C \end{bmatrix} \tag{7}$$

3.1. Robust MFCC Design

Based on the Lyapunov method [21], the problem of stabilizing system Equation (4) by the output feedback controller Equation (5) can be solved if and only if there exist matrices A_C, B_C, C_C and $\widetilde{P} > 0$ for system Equation (6) such that the following matrix inequality holds:

$$\widetilde{A}^T \widetilde{P} + \widetilde{P}\widetilde{A} < 0 \tag{8}$$

In system Equations (6) and (7), the parameter matrix $\widetilde{A}$ varies along with the variation of operating conditions. If system stability under different operating conditions is satisfied simultaneously, matrix inequality Equation (8) should be guaranteed for each operating condition, which leads to the complicatedness of calculation process. In order to solve the above-mentioned problem, the robust damping controller design method proposed in [22] treats the operating condition variation as uncertainties of nominal systems and the polytopic modeling method is introduced aiming at satisfying the robustness requirements.

Here, a polytopic model is composed by a series of p typical operating points. More specifically, under the ith operating condition, parameter matrices of system Equation (6) are presented as A_i, $i = 1, \cdots, p$, which forms vertices of the polytope. The parameter matrices of state equations under the above p operating conditions compose a set:

$$\Phi = \{A_1, A_2, \cdots, A_m\} \tag{9}$$

Construct a polytope Ω whose vertices are composed by elements of set Φ:

$$\Omega = \left\{ \sum_{i=1}^{m} s_i A_i, A_i \in \Phi, \sum_{i=1}^{m} s_i = 1, s_i \in R, s_i \geq 0 \right\} \tag{10}$$

Then for each vertex system, the closed-loop control system with a dynamic output feedback controller can be written as:

$$\dot{\widetilde{x}} = \widetilde{A}_i\widetilde{x},\ \widetilde{A}_i = \begin{bmatrix} A_i & BC_C \\ B_C C & A_C \end{bmatrix} \tag{11}$$

where variables are defined the same as in Equations (6) and (7). In this regard, Equation (8) can be interpreted as finding a positive definite matrix $\widetilde{P}$ and appropriate control parameter matrices A_C, B_C, C_C such that the following inequalities hold for $i = 1, \cdots, p$:

$$\widetilde{A}_i^T\widetilde{P} + \widetilde{P}\widetilde{A}_i < 0 \tag{12}$$

Based on the polytopic property, unknown matrices A_C, B_C, C_C that satisfy Equation (12) can simultaneously stabilize, not limited to the chosen p vertex systems but all of the linear models included in the polytope. In other words, calculation procedure can be greatly simplified by utilizing the polytopic model [22].

Remark 1. *Power systems are huge dimensional nonlinear dynamical systems and the system state-space matrices dimensions derived from linearization may leads to great difficulties in calculation. In practice, only several particular modes are useful for analysis, thus reducing the original systems into lower dimensional systems is commonly adopted as the first step to controller design and in this regard, critical system operating modes can be remained. In this study, the Hankel reduction method* [23] *is chosen for system reduction, which ensures that the errors of system Hankel singular value are in a relatively small range between the non-reduced and reduced systems.*

In practical situations, power systems may possibly be operated under weak damping modes. Generally speaking, if and only if the damping ratios of all operation modes are larger than the damping ratio threshold ζ_0 (which is practically chosen as 0.03 or 0.05), then the system is said to be operated under a strong damping mode. However, condition Equation (12) does not guarantee a global minimum damping ratio of the system. Accordingly, stability criterion based on damping ratio can be realized by the pole placing method given in Theorem 1 [24].

Theorem 1. *For a given minimum damping ratio $\zeta_{\min}$ of closed-loop system Equations (6) and (7), if and only if there exists a positive definite matrix $\widetilde{P}$ such that the following matrix inequality holds*

$$\begin{bmatrix} \sin\sigma(\widetilde{A}^T\widetilde{P} + \widetilde{P}\widetilde{A}) & \cos\sigma(\widetilde{A}^T\widetilde{P} - \widetilde{P}\widetilde{A}) \\ * & \sin\sigma(\widetilde{A}^T\widetilde{P} + \widetilde{P}\widetilde{A}) \end{bmatrix} < 0 \tag{13}$$

where $\sigma = \arccos\zeta_0$, then system Equations (6) and (7) is said to be asymptotically stable and meanwhile, $\zeta_{\min} \geq \zeta_0$ is guaranteed.

Remark 2. *Due to the long distances among the generators and FACTS devices, it is desirable to implement a decentralized structure for damping controllers* [25]. *On the other hand, in matrix inequality Equation (13), the parameter matrix $\widetilde{A}$ that includes unknown controller parameter matrix variables A_C, B_C, C_C is coupled with the unknown matrix variable $\widetilde{P}$. Accordingly, Equation (13) turns out to be nonlinear and can only be solved by iteration, which leads to calculation time consumption and low efficiency. In this regard, reference* [26] *proposes a decoupling method of decentralized coordinated controller design, which transforms Equation (13) into an LMI that is conveniently solvable through Matlab LMI control toolbox.*

In this study, the above-mentioned method is extended to the design of a robust MFCC algorithm for multiple operating modes, which is carried out in the next theorem. Choose p typical operating points and carry out Hankel order reduction, then we derive the state matrix parameters A_{i}, B and C of the closed-loop control system Equation (11) for $i = 1, \cdots, p$.

Theorem 2. *If there exist a positive symmetric matrix $Y > 0$, symmetric matrices P, X and matrices L, F, S such that LMIs Equations (14) and (15) holds for $i = 1, \cdots, p$*

$$\begin{bmatrix} \sin\sigma(A_iY + YA_i^T + BL + L^TB^T) & \cos\sigma(YA_i^T - A_iY + L^TB^T - BL) \\ * & \sin\sigma(A_iY + YA_i^T + BL + L^TB^T) \end{bmatrix} < 0 \tag{14}$$

$$\begin{bmatrix} P & P \\ P & X \end{bmatrix} > 0, \quad \begin{bmatrix} \Theta_{11} & \Theta_{12} & \Theta_{13} & \Theta_{14} \\ * & \Theta_{22} & \Theta_{14}^T & \Theta_{24} \\ * & * & \Theta_{11} & \Theta_{12} \\ * & * & * & \Theta_{22} \end{bmatrix} < 0 \tag{15}$$

where $\Theta_{11} = \sin\sigma(PW_i + W_i^TP)$, $\Theta_{12} = \sin\sigma(PA_i + W_i^TX + C^TF^T + S)$, $\Theta_{13} = \cos\sigma(W_i^TP - PW_i)$, $\Theta_{14} = \cos\sigma(-PA_i + W_i^TX + C^TF^T + S)$, $\Theta_{22} = \sin\sigma(XA_i + W_i^TX + FC + C^TF^T)$, $\Theta_{24} = \cos\sigma(-XA_i + A_i^TX - FC + C^TF^T)$, *with* $W_i = A_i + BC_C$, *then the close-loop system with coordinated controller is said to be asymptotically stable under operating modes* $i = 1, \cdots, p$ *and the MFCC parameter variables can be obtained by* $A_C = U^{-1}S^TP^{-T}P$, $B_C = (P - X)^{-1}F$, $C_C = LY^{-1}$.

Proof. Set A_C, B_C, C_C as diagonal matrices, then the controller added to each generator is related to its own input and output. Define diagonal matrices

$$\widetilde{P} = \begin{bmatrix} X & U \\ U^T & X_c \end{bmatrix}, \ \widetilde{P}^{-1} = \begin{bmatrix} Y & V \\ V^T & Y_c \end{bmatrix} \tag{16}$$

and matrix variables $M = VA_C^TU^T$, $P = Y^{-1}$, $F = UB_C$, $S = Y^{-1}M$, $L = C_CV^T$. In combination with Equation (13), Equation (15) is equivalent to the following LMIs

$$AY + YA^T + BL + L^TB^T < 0 \tag{17}$$

$$\begin{bmatrix} PA + PBC_C + A^TP + C_C^TB_CP & PA + A^TX + C_C^TB^TX + C^TF^T + S \\ * & A^TX + XA + FC + C^TF^T \end{bmatrix} < 0 \tag{18}$$

where * denotes the symmetric part of the matrix, thus completes the proof. □

3.2. Time-Delay MFCC Design

As is previously mentioned, time delay degrades the dynamic performance and even violates the stability of a control system. However, the wide-area robust coordinated control algorithm proposed in the previous subsection has not taken the influence of time-delay into consideration. If the time-delay is relatively large, the controller may no longer stabilize the system. Moreover, during the design procedure of a wide-area measurement based controller, it is of great importance to estimate the maximum allowed time delay τ_0 that will not cause the loss of system stability. Aiming at eliminating the time-delay effect, in what follows, the time-delay MFCC will be designed as a dynamic and static output feedback controller, respectively.

A. Dynamic output feedback controller design

Suppose there is a constant time delay τ existing in the system output feedback of the output dynamic feedback controller Equation (5), namely, the controller is given by

$$\begin{cases} \dot{x}_C(t) = A_Cx_C(t) + B_Cy(t - \tau) \\ u(t) = C_Cx_C(t) \end{cases} \tag{19}$$

The closed-loop system that includes the power system with FACTS devices, the time-delay MFCC given in Equation (19), and the wide-area signal transmission time delay τ is shown as in Figure 4.

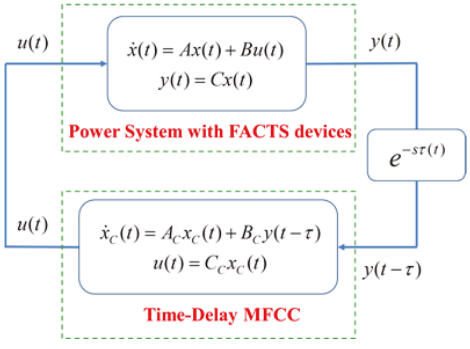

Figure 4. Closed-loop time-delay system under dynamic output feedback control.

By combining with the system equation, the closed-loop power system with time-delay is in the following form

$$\dot{\widetilde{x}}(t) = A_0\widetilde{x}(t) + A_\tau\widetilde{x}(t-\tau) \tag{20}$$

where $\widetilde{x}$ is the same as in Equation (7) and the parameter matrices

$$A_0 = \begin{bmatrix} A & BC_C \\ A_C & 0 \end{bmatrix}, A_\tau = \begin{bmatrix} 0 & 0 \\ B_C C & 0 \end{bmatrix} \tag{21}$$

The following theorem can be used to determine the time-delay margin τ_0.

Theorem 3. *For the time-delay system Equation (20), if there exist positive definite matrices P, Q, V and a matrix W such that the following LMI holds*

$$\begin{bmatrix} (A_0+A_\tau)^T P + P(A_0+A_\tau) + W^T A_\tau + A_\tau^T W + Q & -W^T A_\tau & A_0^T A_\tau^T V & 0 \\ * & -Q & A_\tau^T A_\tau^T V & 0 \\ * & * & -V & 0 \\ * & * & * & -V \end{bmatrix} < -\tau_0 \begin{bmatrix} 0 & 0 & 0 & (W+P) \\ * & 0 & 0 & 0 \\ * & * & 0 & 0 \\ * & * & * & 0 \end{bmatrix} \tag{22}$$

then for all $\tau < \tau_0$, system (17) is asymptotically stable.

The proof of Theorem 3 can be found in [15]. By solving Equation (22) through the LMI control toolbox, the time-delay margin τ_0 can be conveniently derived.

B. Static output feedback controller considering time-varying delay

In order to eliminate the time delay effect, the MFCC designed in this part adopts a static output feedback control structure, where the system output variable y is the controller input. Then the output feedback coordinated controller considering time delay is given as

$$u(t) = Ky(t - \tau(t)) \tag{23}$$

where K is the coefficient matrix of controller, $\tau(t)$ is a time-varying delay, which is a continuous function of time and satisfies

$$0 \le \tau(t) \le \alpha, \left|\dot{\tau}(t)\right| \le \beta \le 1 \tag{24}$$

where α and β are upper bounds of time delay and its rate, respectively. For a constant time delay, $\beta = 0$, $\tau(t) = \tau = \alpha$.

The closed-loop system that includes the power system with FACTS devices, the time-delay MFCC given in Equation (24), and the time-varying wide-area signal transmission delay $\tau(t)$ is shown as in Figure 5. State equations of the closed-loop power system model with time-delay can be described by

$$\dot{x}(t) = Ax(t) + A_d x(t - \tau(t)) \tag{25}$$

where $A_d = BKC$ and the main task of designing a time-delay coordinated controller is to find a suitable K that stabilizes system Equation (25).

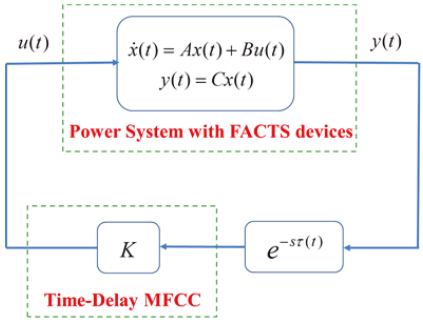

Figure 5. Closed-loop time-delay system under static output feedback control.

In order to guarantee the stability of time-delay system Equation (25), many methods have been proposed based on the Lyapunov theory. Among these methods, the free-weighting matrices method proposed in [27] has less conservativeness and the main idea is recalled briefly in the following theorems.

Theorem 4. *If there exist matrices* $P = P^T > 0$, $Q = Q^T > 0$, $Z = Z^T > 0$, $X = \begin{bmatrix} X_{11} & X_{12} \\ * & X_{22} \end{bmatrix} \geq 0$, *and any matrices* N_1 *and* N_2 *with appropriate dimensions such that the following matrix inequalities hold*

$$\begin{bmatrix} PA + A^T P + N_1 + N_1^T + Q + \alpha X_{11} & PA_d - N_1 + N_2^T + \alpha X_{12} & \alpha A^T Z \\ * & -N_2 - N_2^T - (1-\beta)Q + \alpha X_{22} & \alpha A_d^T Z \\ * & * & -\alpha Z \end{bmatrix} < 0 \tag{26}$$

$$\begin{bmatrix} X_{11} & X_{12} & N_2 \\ * & X_{22} & N_1 \\ * & * & Z \end{bmatrix} \geq 0 \tag{27}$$

then the system Equation (25) with time-varying delay is said to be asymptotically stable.

For a time-invariant delay system, set $X_{12} = 0$, $X_{22} = 0$ and $T = 0$ in Theorem 4, then we yield the following Corollary 1.

Corollary 1. *If there exist matrices* $P = P^T > 0$, $Q = Q^T > 0$, $Z = Z^T > 0$, $X \geq 0$, *and any matrix* N *with appropriate dimension such that the following matrix inequalities hold*

$$\begin{bmatrix} PA + A^T P + N + N^T + Q + \tau X & PA_d - N & \tau A^T Z \\ * & -Q & \tau A_d^T Z \\ * & * & -\tau Z \end{bmatrix} < 0 \tag{28}$$

$$\begin{bmatrix} X & N \\ * & Z \end{bmatrix} \geq 0 \tag{29}$$

then the system Equation (25) with a constant time delay is said to be asymptotically stable.

Remark 3. *Theorem 4 and Corollary 1 present sufficient conditions to determine the stability of closed-loop systems with time-varying and constant time delay, respectively. However, since the unknown parameters are coupled in nonlinear matrix Equations (26) and (28), they cannot be solved by the LMI control toolbox in Matlab (R2016a, MathWorks, Natick, MA, USA). In fact, Corollary 1 only provides a sufficient condition of stability of Equation (6) for a given τ. In order to derive the controller parameter K, the QEA optimum algorithm is introduced in the following part.*

Based on the concept and principles of quantum computing such as a quantum bit and superposition of states, QEA has been widely applied to seek the appropriate controller coefficients in control systems (one can refer to [28] for more detailed information). QEA combines the features of the quantum computation and the evolutionary algorithms, which has unique advantages in deriving the optimal solution, that is, the small population scale, fast convergence and capability of global optimization and so on. The basic QEA optimization procedure is shown as in Figure 6.

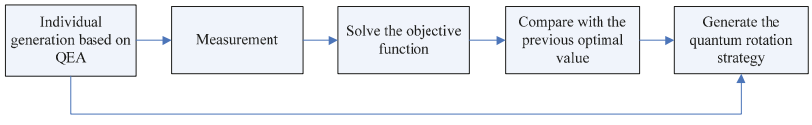

Figure 6. QEA optimization procedure.

After the iteration, the optimal value of the objective function can be derived within certain evolution algebra. Details of the algorithm and iterative parameter setting methods can be found in [20], where one only needs to set the range of *K* during application.

During the application of the QEA optimization, the constraint condition can be set as the existence of solution of Equations (26) and (27), such that the asymptotically stability of the obtained system is guaranteed. In what follows, for the sake of simplicity, the time-delay is chosen to be a constant number, and accordingly, the constraint condition can be set as the existence of solution of Equations (28) and (29) in Corollary 1. However, since multiple sets of feasible solutions may exist, therefore, by taking the practical demand of power systems into consideration, the objective function here is set to maximize the minimum system damping ratio. In this regard, the larger the minimum system damping ratio is, the more stable the system will be. At the same time, in order to make the control strategy reasonable, we set a minimum threshold of damping ratio (e.g., 7%). Once the threshold is exceeded, the optimization procedure will come to an end.

Before solving system damping ratio, the eigenvalue λ should be derived. The characteristic equation of time-delay system Equation (25) is

$$\det(\lambda I - A - A_d e^{-\tau\lambda}) = 0 \tag{30}$$

Equation (24) cannot be solved directly since it is a transcendental equation. To this end, in this study, the PDE discretization method is adopted for the approximation analysis. The delay differential equations of system Equation (25) can be converted to a set of Hyperbolic Partial Differential Equations (H-PDE) under the interconnected boundary conditions. As a consequence, the eigenvalues of the augmented matrix that obtained through fine discretization on PDE approximate to those of Equation (28). One can find more specific algorithm introduced in [29]. It should be noted that the number of Chebyshev discrete nodes needs to be set in this algorithm. Since we only focus on the

electromechanical modes, it would be precise enough by setting this number within the range of 20~30. In summary, the flow chart of time-delay MFCC design algorithm is shown in Figure 7.

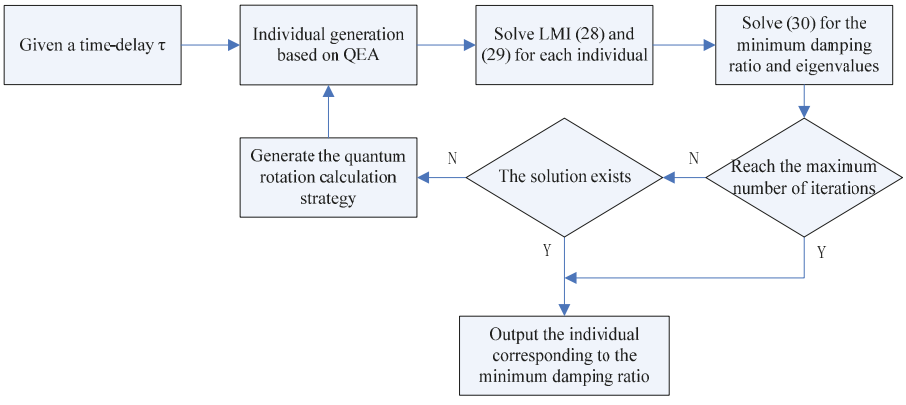

Figure 7. Flow chart of the controller design algorithm.

4. Numerical Simulations

In order to demonstrate the effectiveness of the two MFCC design algorithms proposed in the previous sections, consider the following two-area four-generator system shown as in Figure 8, where the system parameters are the same as in [18]. Since the voltage of Bus 7 is the lowest based on current system operation, an SVC is equipped to increase voltage and at the same time, a TCSC is equipped in the bus of inter-area system tie-line to remain the stability of power and damp inter-area oscillations.

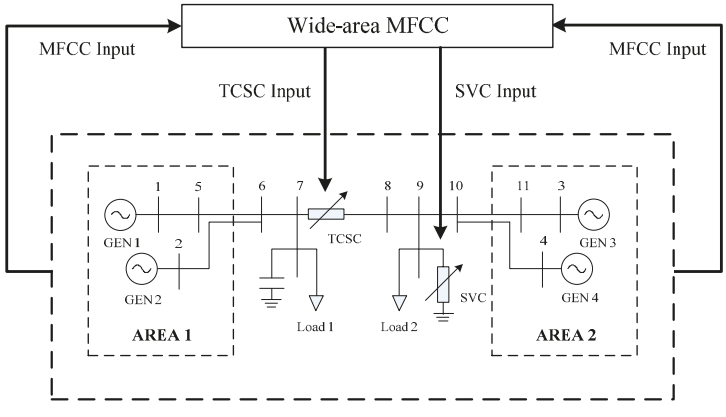

Figure 8. A four-machine, two area test system equipped with TCSC and SVC.

In virtue of the standard parameter tuning method for SISO controller design [30], the parameters of the SVC can be derived as $K = 100$, $T_1 = 0.05$, $T_0 = 0.01$; while the parameters of the TCSC can be derived as $K_P = 0.8$, $K_i = 10$, $T_0 = 0.01$. Characteristics under the above basic operation mode is derived as follows.

It is known from Table 1 that there is an inter-area oscillation mode of low damping in the system, thus in what follows, the proposed MFCC will be applied to improve the system damping and the effectiveness will be verified. Choose the velocity difference $\Delta\omega_1$ and $\Delta\omega_3$ of the most

relevant generators GEN1 and GEN3 for the system output, which is derived through the network communication system and carry out calculation.

Table 1. Modes Characteristics under the basic operation mode.

Modes	$-0.018 \pm j3.528$	$-0.728 \pm j6.324$	$-0.789 \pm j6.356$
Frequency/Hz	0.562	1.006	1.012
Damping Ratio	0.524%	11.443%	12.319%

Since system Equation (6) is a 24th-order dynamic model, it brings about great difficulties to the calculation of coordinated controllers. In order to speed up calculation, the Hankel reduction method introduced in Section 3.1 is applied to reduce the system into a 7th-order model. Comparison of the singular value before and after system reduction is shown in Figure 9. It can be observed from Figure 8 that the two curves almost perfectly in a wide range of frequencies.

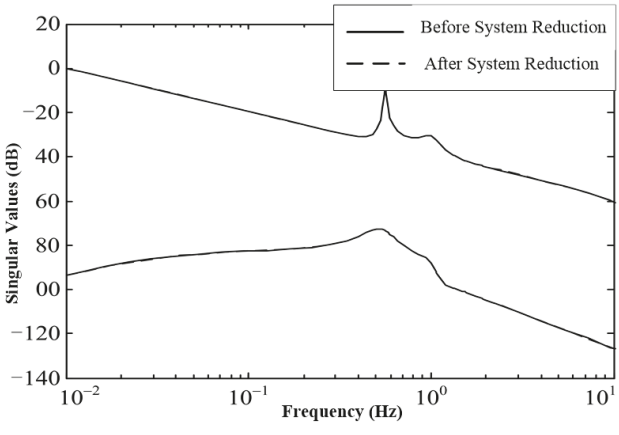

Figure 9. Comparison of Singular Values Before and After System Reduction.

In what follows, the effectiveness of the robust coordinated controller will be verified under three different operating conditions, built from variations of the load levels (shown as Load 1 and Load 2 in Figure 4) in both areas. The base case was also taken as a vertex system, the other two vertex systems are selected as increasing Load 1 by 100 MW while decreasing Load 2 by 100 MW, as well as decreasing Load 1 by 100 MW while increasing Load 2 by 100 MW, respectively. In this regard, the electromechanical modes under these three operating modes are given in Table 2.

Table 2. Modes Characteristics under three different cases.

	Description	Modes	Frequency/Hz	Damping Ratio
Case 1	Base Case	$-0.018 \pm j3.528$	0.562	0.524%
		$-0.728 \pm j6.324$	1.006	11.443%
		$-0.789 \pm j6.356$	1.012	12.319%
Case 2	Load 1: −100 MW Load 2: +100 MW	$-0.008 \pm j3.362$	0.535	0.231%
		$-0.728 \pm j6.291$	1.002	11.495%
		$-0.779 \pm j6.340$	1.009	12.194%
Case 3	Load 1: +100 MW Load 2: −100 MW	$-0.028 \pm j3.628$	0.578	0.7614%
		$-0.725 \pm j6.350$	1.011	11.339%
		$-0.795 \pm j6.364$	1.012	12.402%

It can be observed from Table 2 that, there exists weak damping of inter-area oscillation modes under the three operating modes. Set the damping ratio threshold as $\zeta_0 = 0.1$. The FACTS coordinated controller design algorithm in Theorem 2 is utilized to increase the system damping ratio, which guarantees that the minimum damping ratio is larger than 0.1. By solving Equations (14) and (15), the controller transfer function is derived as follows:

$$\begin{aligned}
H_{11}(s) &= \frac{-0.181 \times 10^3 (s + 2.543 \pm 6.240\mathrm{j})(s + 1.327 \pm 1.769\mathrm{j})(s + 0.042)(s + 0.856)}{(s + 3.165 \pm 6.160\mathrm{j})(s + 2.807 \pm 3.079\mathrm{j})(s + 1.55642 \pm 1.219\mathrm{j})(s - 0.017)} \\
H_{12}(s) &= \frac{-1.055 \times 10^3 (s + 2.240 \pm 6.772\mathrm{j})(s + 2.432 \pm 4.172\mathrm{j})(s + 0.320)(s + 0.025)}{(s + 3.165 \pm 6.160\mathrm{j})(s + 2.807 \pm 3.079\mathrm{j})(s + 1.55642 \pm 1.219\mathrm{j})(s - 0.017)} \\
H_{21}(s) &= \frac{0.135 \times 10^3 (s + 0.630 \pm 6.553\mathrm{j})(s + 1.626 \pm 2.041\mathrm{j})(s + 0.030)(s + 1.260)}{(s + 3.165 \pm 6.160\mathrm{j})(s + 2.807 \pm 3.079\mathrm{j})(s + 1.55642 \pm 1.219\mathrm{j})(s - 0.017)} \\
H_{22}(s) &= \frac{1.475 \times 10^3 (s + 1.700 \pm 7.307\mathrm{j})(s + 2.421 \pm 3.526\mathrm{j})(s + 0.015)(s + 0.409)}{(s + 3.165 \pm 6.160\mathrm{j})(s + 2.807 \pm 3.079\mathrm{j})(s + 1.55642 \pm 1.219\mathrm{j})(s - 0.017)}
\end{aligned} \tag{31}$$

where $H_{11}(s)$ and $H_{12}(s)$ are the transfer functions from the input value of the coordinated controller $\Delta\omega_1$ to the SVC and TCSC controller input, respectively; while $H_{21}(s)$ and $H_{22}(s)$ are the transfer function from the input value of the coordinated controller $\Delta\omega_3$ to the SVC and TCSC controller input, respectively.

Effectiveness of the control strategy is verified in the following operating conditions. The new electromechanical modes of the system under FACTS coordinated control are given in the following table and it can be observed from Table 3 that, the damping ratios under each electromechanical mode are larger than 10%, which satisfies the requirement of controller design.

Table 3. Characteristics of modes in three load cases with FACTS coordination.

	Description	Modes	Frequency/Hz	Damping Ratio
Case 1	Base Case	$-0.675 \pm \mathrm{j}3.482$	0.554	19.0319%
		$-0.715 \pm \mathrm{j}6.401$	1.018 7	11.0982%
		$-0.816 \pm \mathrm{j}6.241$	0.993 3	12.958%
Case 2	Load 1: −100 MW Load 2: +100 MW	$-0.699 \pm \mathrm{j}3.329$	0.529 9	20.5334%
		$-0.711 \pm \mathrm{j}6.371$	1.013 9	11.0872%
		$-0.809 \pm \mathrm{j}6.232$	0.991 8	12.8706%
Case 3	Load 1: +100 MW Load 2: −100 MW	$-0.633 \pm \mathrm{j}3.552$	0.565 3	17.5471%
		$-0.716 \pm \mathrm{j}6.420$	1.021 8	11.0898%
		$-0.817 \pm \mathrm{j}6.247$	0.994 2	12.9673%

Moreover, the time delay margin can be calculated by the LMI Equation (22) given in Theorem 3. In virtue of the LMI robust control toolbox of Matlab (R2016a, MathWorks, Natick, MA, USA), the minimum time delay margin under each operation conditions of the controller are derived as $\tau_0 \approx 350$ ms. The theoretical results can be verified through exerting a large perturbation on the system. Choose a three-phase short-cut fault at bus 8 at 1 s, which is cleared at 1.1 s. Figure 10 depicts the time variation of inter-area tie-line power oscillations for different time delays of 100 ms, 200 ms, 300 ms and 330 ms, respectively.

It can be observed from Figure 9 that, the designed MFCC is tolerant to time delay less than 350 ms under different operating modes, which satisfies the demand of WAMS signal transmission.

In what follows, the effectiveness of the time-delay coordinated controller will be demonstrated. Assume that signal transmission time delay through WAMS is about 200 ms and the range of parameters in the QEA is set as [10, 10]. The minimum damping ratio threshold value is chosen as 7%. By carrying out the time-delay MFCC algorithm in Section 3.2, we arrive at the final optimization result of controller parameter K.

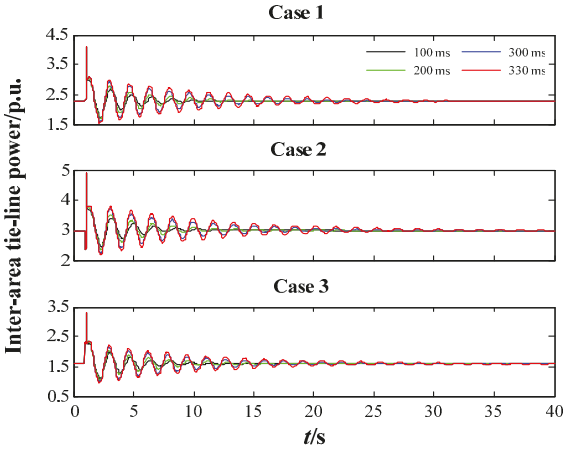

Figure 10. Power oscillation of the tie-line under different delay in three load cases.

In order to demonstrate the effectiveness of the derived controller, set the system disturbance as follows: increase the reference voltage of SVC by 0.01 p.u. at 1 s; and reduce it by 0.01 p.u. at 2 s. Figure 10 shows the curve of the inter-area tie-line power response, which compares the simulation results with and without coordinated control. It can be observed from Figure 11 that, since the minimum threshold of damping ratio is set, the system under coordinated control is able to be operated under strong damping mode with the controller K obtained by the algorithm proposed in this study. In consequence, considering the existence of signal transmission delay, the control performance of the MFCC is better than the individual control of FACTS without coordination.

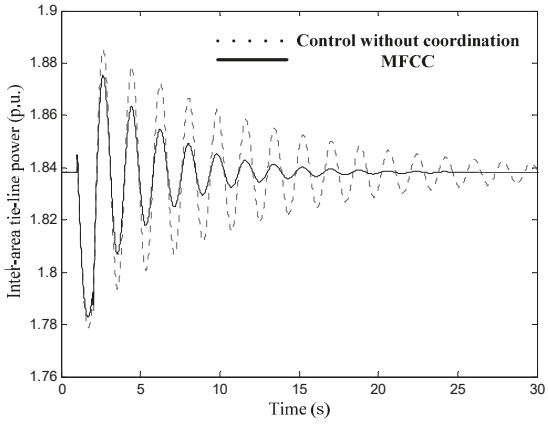

Figure 11. Power oscillation of the tie-line under 200 ms delay.

In order to determine the time-delay margin within which the coordinated controller can stabilize the system, Figure 11 depicts the curves of the minimum damping ratio of coordinated control system under different time delays, where the dashed horizontal line 0.0276 is the minimum damping ratio of system without coordinated control. It can be observed from Figure 12 that, since the MFCC algorithm is designed based on the time-delay of 200 ms, the minimum damping ratio reaches its maximum value under this time delay, which is about 0.07. Define the damping ratio above 0.03 as strong damping ratio, then for time delay less than 570 ms, the system will be operated under strong damping modes.

If the time delay is less than 600 ms, coordinated control can make the system damping better than that of control without coordination. It indicates that the algorithm proposed in this part has a relatively large delay margin, which guarantees that the system can be stabilized by the designed controller within the margin, that is, it demands less for the WAMS signal delay estimate.

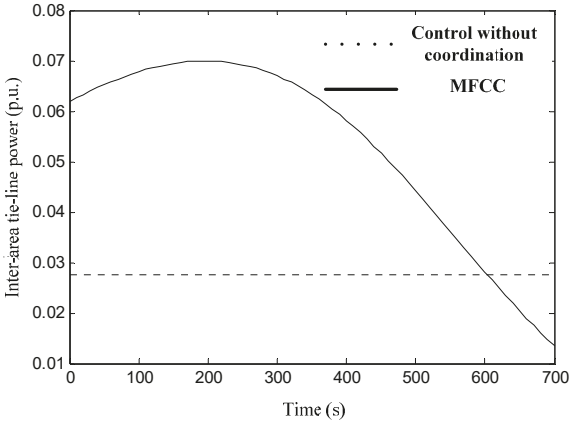

Figure 12. Ratio of power system under different delays.

5. Conclusions

The present study proposes a wide-area decentralized coordinated control framework for power systems with multiple FACTS devices, where the upper-level coordinated controller is designed as both a robust dynamic output feedback controller and a time-delay output feedback controller. The polytopic differential inclusion method is introduced during the dynamic output feedback controller design procedure and the derived controller is capable to be operated under strong damping modes and also remain robust to various operating conditions. The time-delay MFCC is designed in virtue of the output feedback signals from WAMS. In order to find an optimal solution, the quantum evolution algorithm (QEA) method is introduced. In this regard, the stability of the system with a prescribed time delay is guaranteed and the system damping ratio is increased. Validity and applicability of the proposed coordinated control algorithms are demonstrated in a two-area four-generator system. Simulation results demonstrate that the under robust coordinated control, the controlled power system successfully runs in strong damping modes in four different operating conditions and the algorithm exhibits good control effect in a wide range of time-delay.

Acknowledgments: We thank Liuqiang Huang for discussions and general support. This research has been supported by the key project of smart grid technology and equipment of national key research and development plan of china (2016YFB0900600) as well as the National Natural Science Foundation of China (71403285 and 71403017).

Author Contributions: S.X. and Y.Y. proposed the coordinated control strategy and the main theories; K.P. and L.L. helped with the optimization algorithm and performed numerical simulations; T.H. and A.A. contributed materials and analysis tools; S.X. wrote the paper.

Conflicts of Interest: The authors declare no conflicts of interest.

References

1. Klein, M.; Rogers, G.; Kundur, P. A fundamental study of inter-area oscillations in power systems. *IEEE Trans. Power Syst.* **1991**, *6*, 914–921. [CrossRef]
2. Kamwa, I.; Grondin, G.; Hebert, Y. Wide-area measurement based stabilizing control of large power systems—A decentralized/hierarchical approach. *IEEE Trans. Power Syst.* **2001**, *16*, 136–153. [CrossRef]

3. Paserba, J. *Analysis and Control of Power System Oscillations*; CIGRE Special Publication 38.01.07, Technical Brochure III; International Council on Large Electric Systems (CIGRE): Paris, France, 1996.
4. Tedesco, F.; Casavola, A. Fault-tolerant distributed load/frequency supervisory strategies for networked multi-area microgrids. *Int. J. Robust Nonlinear Control* **2014**, *24*, 1380–1402. [CrossRef]
5. Magdy, E.; Sallam, A.; McCalley, J.; Fouad, A.A. Damping controller design for power system oscillation. *IEEE Trans. Power Syst.* **1996**, *11*, 767–773.
6. De Oliveira, R.V.; Kuiava, R.; Ramos, R.A.; Bretas, N.G. Automatic tuning method for the design of supplementary damping controllers for flexible alternating current transmission system devices. *IET Gener. Transm. Distrib.* **2009**, *3*, 919–929. [CrossRef]
7. Simfukwe, D.D.; Pal, B.C.; Jabr, R.A.; Martins, N. Robust and low-order design of flexible AC transmission systems and power system stabilisers for oscillation damping. *IET Gener. Transm. Distrib.* **2012**, *6*, 445–452. [CrossRef]
8. Sanchez-Gasca, J.J. Coordinated control of two FACTS devices for damping interarea oscillations. *IEEE Trans. Power Syst.* **1998**, *13*, 428–434. [CrossRef]
9. Noroozian, L.; Angquist, L.; Ghandhari, M.; Andersson, G. Improving power system dynamics by series-connected FACTS devices. *IEEE Trans. Power Deliv.* **1997**, *12*, 1635–1641. [CrossRef]
10. Phadke, A.G. Synchronized phasor measurements in power system. *IEEE Comput. Appl. Power* **1993**, *6*, 10–15. [CrossRef]
11. Deng, J.; Li, C.; Zhang, X.-P. Coordinated Design of Multiple Robust FACTS Damping Controllers: A BMI-Based Sequential Approach with Multi-Model Systems. *IEEE Trans. Power Syst.* **2015**, *30*, 3150–3159. [CrossRef]
12. Leon, A.E.; Solsona, J.A. Power Oscillation Damping Improvement by Adding Multiple Wind Farms to Wide-Area Coordinating Controls. *IEEE Trans. Power Syst.* **2014**, *29*, 1356–1364. [CrossRef]
13. Jiang, L.; Yao, W.; Wu, Q.H.; Wen, J.Y.; Cheng, S.J. Delay-dependent stability for load frequency control with constant and time-varying delays. *IEEE Trans. Power Syst.* **2012**, *27*, 932–941. [CrossRef]
14. Wei, Y.; Jiang, L.; Wen, J.; Wu, Q.H.; Cheng, S. Wide-area damping controller of FACTS devices for inter-area oscillations considering communication time delays. *IEEE Trans. Power Syst.* **2014**, *29*, 318–329.
15. Boyd, S.; El Ghaoui, L.; Feron, E.; Balakrishnan, V. *Linear Matrix Inequalities in System and Control Theory*; Society for Industrial and Applied Mathematics (SIAM): Philadelphia, PA, USA, 1994.
16. Gahinet, P.; Nemirovski, A. *LMI Control Toolbox for Use with MATLAB*; Mathworks Inc.: Natick, MD, USA, 1995.
17. Wu, M.; He, Y. *Robust Control of Time-Delay System*; Science Press: Beijing, China, 2007.
18. Anderson, P.M.; Fouad, A.A. *Power System Control and Stability*; IEEE Press: Piscataway, NJ, USA, 1994.
19. Hingorani, N.G.; Gyugyi, L. *Understanding FACTS: Concepts and Technology of Flexible AC Transmission Systems*; IEEE Press: New York, NY, USA, 2000.
20. Del Rosso, D.; Canizares, C.A.; Dona, V.M. A study of TCSC controller design for power system stability improvement. *IEEE Trans. Power Syst.* **2003**, *18*, 1487–1496. [CrossRef]
21. Zhou, K.; Doyle, J.C.; Golver, K. *Robust and Optimal Control*; Prentice Hall: Upper Saddle River, NJ, USA, 1995.
22. Pal, B.C.; Coonick, A.H.; Jaimoukha, I.M.; El-Zobaidi, H. A linear matrix inequality approach to robust damping control design in power systems with superconducting magnetic energy storage device. *IEEE Trans. Power Syst.* **2000**, *15*, 356–362. [CrossRef]
23. Kung, S.; Lin, D.W. Optimal Hankel-norm model reductions: Multivariable systems. *IEEE Trans. Autom. Control* **1981**, *26*, 832–852. [CrossRef]
24. Chiali, M.; Bretas, P.G. H_∞ design with pole placement constraints: An LMI approach. *IEEE Trans. Autom. Control* **1996**, *41*, 358–367. [CrossRef]
25. Xu, S.Y.; Sun, H.D.; Li, B.Q.; Bu, G.Q. Wide-Area Robust Decentralized Coordinated Control of HVDC Power System Based on Polytopic System Theory. *Math. Probl. Eng.* **2015**, *2015*, 510216. [CrossRef]
26. Oliveira, M.C.; Geromel, J.C.; Bernussou, J. Design of dynamic output feedback decentralized controllers via a separation procedure. *Int. J. Control* **2000**, *73*, 371–381. [CrossRef]
27. Wu, M.; He, Y.; She, J.H.; Liu, G.P. Delay-dependent criteria for robust stability of time-varying delay systems. *Automatica* **2004**, *40*, 1435–1439. [CrossRef]

28. Han, K.; Kim, H. Quantum-inspired evolutionary algorithm for a class of combinatorial optimization. *IEEE Trans. Evol. Comput.* **2002**, *6*, 580–593. [CrossRef]
29. Bellen, A.; Maset, S. Numerical solution of constant coefficient linear delay differential equations as abstract Cauchy problems. *Numer. Math.* **2000**, *84*, 351–374. [CrossRef]
30. Astrom, K.J.; Wittenmark, B. *Computer-Controlled Systems-Theory and Design*, 3rd ed.; Tsinghua University Press: Beijing, China, 2002; pp. 100–110.

energies

MDPI

Article

Does Dynamic Efficiency of Public Policy Promote Export Prformance? Evidence from Bioenergy Technology Sector

Bongsuk Sung [1] and Woo-Yong Song [2,*]

[1] Department of International Business Management, Woosong University, 171, Dongdaejeon-ro, Dong-gu, Daejeon 34518, Korea; bsssung@wsu.ac.kr

[2] Department of Management and Accounting, Habat National University, Duckmyoung-Dong 125 Dongseo-Daero Yuseong-Gu, Daejeon 34518, Korea

* Correspondence: wysong@hanbat.ac.kr, Tel.:+82-42-821-1336; Fax: +82-42-821-1597

Received: 27 October 2017; Accepted: 5 December 2017; Published: 14 December 2017

Abstract: This study examines how the dynamic efficiency of public policy influences the export performance of bioenergy technologies in the short and long run using panel data over the 1995–2012 period for 16 countries that are members of the OECD. Various dynamic panel framework tests to check data characteristics are performed. The study found evidence of co-movement among the series, and set up the panel vector error correction mechanism to evaluate the short- and long-run Granger-causality between the following variables: dynamic efficiency of public policy, export, and environmental policy stringency. This study highlighted positive effects of the dynamic efficiency of public policy and environmental policy efforts on exports in both the short and long run. This study proposes policy considerations based on its results.

Keywords: bioenergy technology; dynamic efficiency of public policy; export performance; panel data approach

1. Introduction

To date, numerous studies have addressed the role of public policy in the promotion of renewable energy technologies (RETs). In the literature, two research fields have emerged—an experimental setting for discussions on policy efficiency, and empirical research on the relationship between government policy and export. Studies on the measurement of the efficiency of government policy in the RET sector have tried to define efficiency; discuss various policy input and output factors for particular policy measures; and evaluate the efficiency of a number of public policies in terms of cost reduction, price reduction of power, power capacity enhancement, and electricity generation, among others, which are triggered by policy inputs. These studies are conducted through comparative analyses (e.g., [1–3]), estimations (e.g., [4,5]), and descriptive analyses [6]. Nonetheless, research on the dynamic efficiency of public policy remains at a conceptual level [7]. In other words, the literature does not provide quantitative indicators of the dynamic efficiency of RET policies. Empirical studies (e.g., [8,9]) have shown that government policy positively affects the export performance of bioenergy technologies. However, most RETs are at an immature phase in terms of industrial development, and need continuous innovation [10]. Moreover, public support is one of main forces of innovation in the biofuels sector [11–13]. Consequently, the investigation of mechanisms, from public policy to increased exports through innovation creation, remains a challenge.

There are different rationales for supporting RETs—including bioenergy technologies—in which long-term cost reduction has been central to RET policies of each country examined [14]. Despite such policy efforts, many RETs, as immature technologies [10], are poised for further and perhaps

significant cost reduction and performance improvement [15]. This implies that successes in the RET sector, such as market penetration and larger market shares, mainly depend on creating the potential for technological innovation and diffusion through reduced costs [16]. In the works by Del Río [3] and Del Río and Bleda [17], the ability of policy instruments to induce a continuous incentive for technological improvement and cost reduction of existing RETs—the dynamic efficiency of a RET policy—is very important for the promotion of exports and industrial growth. Dynamic efficiency is a synergy that promotes industries' or firms' performance. Efficiency that constantly boosts the ability to innovate is considered dynamic [18], implying continuous innovative efficiency [19,20], which, in turn, implies using the lowest amount of inputs in producing any given outputs [21]. Empirical results show that there is no systematic relationship between the level of policy input to support industrial activities (e.g., R&D expenditure) and public policy outcomes (e.g., market performance) [22,23], while others indicate that the dynamic efficiency of public policy is more important than the amount of policy input for promoting industrial performance and growth [24].

Nonetheless, there is no study that empirically investigates the relevance of the dynamic efficiency (or continuous innovative efficiency) of public policy instruments in promoting the export performance in the bioenergy technologies sector. After a review of the extant literature, this study aims to address this gap by empirically testing the role of the dynamic efficiency of public policy on the export performance of bioenergy technologies using panel data.

For an empirical contribution in line with the extant literature, the current study considers four relevant aspects that may strongly influence the direction and robustness of empirical results vis-à-vis the relationship between the dynamic efficiency of policy and exports. First, this study uses export performance, instead of export competitiveness indexes, in line with studies such as Jha [8], Sung [9], Costantini and Crespi [25], and Sung and Song [26] that show that export performance is significantly affected by public policy. Second, although there are studies on the dynamic efficiency of public policy, they remain at a conceptual level [7]. Thus, this study evaluates the changes in the dynamic efficiency of public policy for supporting the bioenergy technology sector using the Malmquist productivity growth index analysis (MPGI) proposed by Färe et al. [27]. It incorporates these changes into the model, which coincides with the dynamic panel approach adopted in the current study. Third, this study includes environmental policy in the model to control for potential omitted variables that may influence the relationship between the dynamic efficiency of public policy and the export flow dynamics of bioenergy technologies. Environmental policy positively influences technological innovation [12,13,28] that triggers higher efficiency in the production process—productivity growth [29]—through various complementarity mechanisms [25,28,30,31]. This then leads to the promotion of export specialization and the enhancement of comparative advantages for manufacturing goods [32] like bioenergy technologies, as well as components that are regarded as environment-related products and technologies. Fourth, since most panel data are heterogeneous and non-stationary co-integrated, and improvements in export performance tend to become evident after an enhancement of the dynamic efficiency of public policy, this study takes a dynamic approach. In this respect, Hirshleifer et al. [20] found that there is a time lag between dynamic efficiency and firm performance; there are dynamic effects in export performance, dynamic efficiency, and environmental policy (implying that inputs in period t are, to some extent, invested in promoting output in period $t + 1$), as well as in their interactions [9,33]. When employing a dynamic panel approach, notably, it is important to account for possible structural breaks and cross-sectional dependency that influence the applicability of tests for the presence of stationarity and cointegration. Moreover, the choice of the empirical model that can be set up to test for the Granger-causality of the short- and/or long-run relationships among the variables to be examined depends on the results of the panel unit-root and cointegration tests. Specifically, a panel vector autoregression (VAR) model is needed to test the short-run linear causality (only in presence of panel unit-roots), while a panel vector error correction model (VECM) is suitable to evaluate the short- and long-run directions of causality among variables (with evidence of panel unit-roots and cointegration). In addition, sample size and

data characteristics (e.g., cross-sectional dependence, heteroscedasticity, simultaneity, etc.) should be taken into account in the estimation of the empirical model.

This study starts by contextualizing the relationship between the dynamic efficiency of public policy for and exports of bioenergy technologies based on the extant literature. Then, the model, data, and empirical methodology employed are presented, followed by the description of the empirical results and their interpretation. Finally, the main findings are summarized, and the implications and limitations of the study are outlined.

2. Conceptual Framework: Dynamic Efficiency of Public Policy and Exports

In open economies, government policy promotes the export performance of bioenergy technologies (e.g., [8,9]); wind; solar; and several aggregated RETs (e.g., [25,26,28,31,32]), which leads to growth of the RET industry [5,34] and, generally, the economy [35]. This growth provides the rationale for government policy to promote the technological development of firms directly, as it boosts their R&D activities, further increases their market shares, and ultimately reduces the prices of their products [36]. In relation to immature technologies like RETs, public policies act on both the demand and the supply sides to spur innovation [11–13]. By empirically demonstrating that both demand-pull and technology-push policies are valid supports for stimulating innovation, Costantini et al. [13] confirmed that these two types of public policies are important in the biofuels sector. This is because every government considers supporting innovation in the RET sector continuously as a major policy initiative toward achieving environmentally sound and sustainable development by addressing aspects of energy security, environmental protection, and economic growth [37]. Government policy, as one of the strongest extrinsic political forces, proactively facilitates various innovation activities to create both local and export markets for RETs [28] for helping firms in the industry to become isomorphic with the government's expectations. The positive effects of innovation on export performance become mostly evident in extant empirical studies (e.g., [38,39]) using heterogeneous firm trade theory [40].

The aforementioned points indicate that the influences of public policies on export performance must be explored by simultaneously taking into account policy inputs (demand-pull and technology-push supports) and policy output (innovation). Therefore, the study aims to explore the relevance of dynamic efficiency (or continuous innovative efficiency) of public policy in improving the export performance of the bioenergy technologies sector, instead of tackling policy inputs and outputs separately. According to Johnstone et al. [11], Johnstone et al. [12], and Costantini et al. [13], in the RET sector, innovation (policy output) measured by the number of patent application is triggered by government policy (policy inputs) when the government constantly provides incentives for technological improvements. This means that the steady implementation of innovation-friendly policy—either dynamic [3,17] or continuously innovative efficiency [19,20]—is important for promoting growth in the RET sector.

Firms try to increase their profits through innovation [41]. However, innovation stakeholders, including firms, may not be able to utilize the full innovation potential without public intervention [42], which is especially relevant for immature technologies, like RETs, which face large systemic barriers in innovation creation [43]. Furthermore, renewable energy entrepreneurs often tend to pursue short-term, individually oriented strategies instead of strategies that are more oriented toward the build-up of innovation systems [44]. In this context, inefficiency in public policy may change the risk-return relationship in the RETs investment, and consequently affect investors' behaviors [45]. Additionally, such changes in the risk-return relationship can shrink the industry's investment environment, leading manufacturers to disrupt the smooth functioning of various activities, thus decreasing productivity in the RETs sector [46]. However, the dynamic efficiency of public policy plays a crucial role in continuously pushing firms to change their methods of innovation, pull the manufacturers in order to adjust innovation methods, and exercise full innovation potential to meet the markets' needs. Hence, dynamic efficiency can be defined as a tool that can encourage entrepreneurial alertness to valuable knowledge, thereby enabling firms to discover and increase awareness of the phenomenon [47].

This indicates that the degree of dynamic efficiency of public policy is closely related to the extent of encouraging entrepreneurship. One of the ways in which this relationship manifests is by strengthening the linkages between stakeholders, where, for example, a policy calls for "special and innovative mechanisms for fostering the academia-research-industry partnership." For other examples, see Abhyankar [48] (p. 15), and Cumming and Li [49] (pp. 346–349).

Entrepreneurship, encouraged by such collaboration through the steady implementation of innovation-friendly policy, is regarded as a productive factor in that it provides a systemic coordinating function facilitating the allocation of resources to their highly valued uses [50,51]. This makes a pivotal contribution toward enhancing a firm's ability to succeed in an ever-changing and increasingly competitive global marketplace. Furthermore, from the perspective of economics and policy science, the dynamic efficiency of public policy closely relates to continuous policy-driven cost reductions through innovation, leading to the achievement of economies of scale and higher competitiveness. This suggests that an enhancement in the dynamic efficiency of public policy—innovation influence of public policy [52]—can play a key role in increasing the international competitiveness of RETs.

3. The Model

The model to test the effect of dynamic efficiency of public policy on the export performance is expressed as follows:

$$EX_{it} = \alpha_{1j} + \sum_{p=1}^{n} \beta_{i1p} EX_{it-p} + \sum_{p=1}^{n} \beta_{i2p} DE_{it-p} + \sum_{p=1}^{n} \beta_{i3p} EPS_{it-p} + \eta_{it} + \varepsilon_{it} \quad (1)$$

where, $i = 1, \ldots, N$ is the country; $t = 1, \ldots, T$ is the time period; η_{it} is the country-specific effect; and ε_{it} is the error term. *EX* is the natural logarithm of export performance. *DE* is the dynamic efficiency that represents changes in the dynamic efficiency of public policies to support the bioenergy technologies sector; it was measured using the MPGI analysis proposed by Färe et al. [27], and calculated using data envelopment analysis (DEA) under the assumption of variable returns to scale. DEA is a non-parametric method used because of its transparency, ability to handle multiple inputs, conditions that do not require specific assumptions about a specific functional form of production function [53], and appropriateness—considering the objective of the study. According to Färe et al. [27], Barros and Alvese [54], and Price and Weyman-Jones [55], the productivity growth between t and $t+1$ in Figure 1 can be measured in terms of the change from the input-output bundle $z(t)$ to the input-output bundle $z(t+1)$.

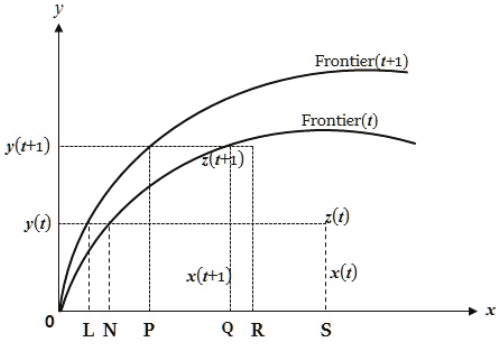

Figure 1. Malmquist Productivity Growth Index. (Source: [54]).

The production frontier represents the efficient levels of policy output (y) that can be produced from a given level of policy input (x). When the public policy of a country is efficient in period t,

it produces the maximum output attainable along the frontier. Each country on input-output bundle $z(t)$ in period t is not efficient as they use more than the minimum amount of policy input to produce a given level of policy output. To make the production efficient, the input-output bundle $z(t)$ needs to be reduced by the horizontal distance ratio ($= ON/OS$). The frontier can shift over time. The input-output bundle $z(t+1)$ should be multiplied by the horizontal distance ratio ($= OR/OQ$) to achieve comparable efficiency. Since the frontier has shifted, the bundle $z(t+1)$ is inefficient in period $t+1$. To make the bundle $z(t+1)$ efficient in period $t+1$, it should be reduced by the horizontal distance ratio ($= OP/OQ$). The relative movement of a production observation over time may occur because countries are catching up with their own frontier or because the frontier shifts upwards over time. The $MPGI$ is the ratio of the two distances in periods t and $t+1$. To break down the index in catching up (MC) and shifting up (MF) effects, $MPGI$ is rescaled by multiplying the top and bottom by OR/OQ: $\frac{OR \cdot ON}{OQ \cdot OS} = \left[\frac{OP \cdot ON}{OQ \cdot OS}\right] \cdot \frac{OR}{OP} = MC \cdot MF$.

A variety of policy instruments to promote the RET industry have been implemented in many countries. The development path of policy support for RETs has been similar in all European countries [56]. The first wave of policies that started in the late 1970s and early 1980s focused on public R&D and investment incentives, along with voluntary programs and obligations. A second wave of policies in the 1990s mainly concentrated on feed-in tariffs and tax incentives. The following decade, instead, was characterized by the implementation of quota systems based on renewable energy certificates. China has introduced many policy instruments to support the RET industry since the early 1980s. In this context, feed-in tariffs, financial subsidies like public R&D and investment incentives, and other forms of technological support emerged as favorable policy instruments [57]. The US has also employed many policy instruments since 1978. The main policies included investment subsidies like R&D and tax incentives, and generation incentives like feed-in tariffs and quota systems [58]. The policy instruments for technology diffusion are often classified by scholars into two broad categories: market-pull (also referred to as demand-pull) and supply-push (also referred to as technology-push) approaches [59]. The stimulus for new RETs through technology-push policy measures mainly comes from R&D investments, most commonly made by the government. As for market-pull measures, feed-in tariffs are the most common and effective policy measure currently being implemented (or revised) in both developed and developing countries. Thus, overall, public R&D expenditures and feed-in tariffs are considered as the most important and prominent drivers in spurring RETs innovation and diffusion [60]. This study uses two policy input factors—technology-push and demand-pull policy instruments [3,17,60]—and one output factor—innovation outcome [11–13,20,25], which are directly related to bioenergy technologies. Public R&D expenditure is taken as a proxy for the technology-push policy [5,9,11,28]. Extant literature, such as Johnstone et al. [11], uses a dummy variable to capture the effect of the implementation of a feed-in tariff. The dummy variable is not continuous and suitable as a policy input factor. The contribution of bioenergy to the total energy supply is taken as a proxy for a directed feed-in tariff, owing to the lack of a reference database. This represents the demand-pull policy [9]. It follows from the logic that a feed-in tariff positively affects the percentage of renewable energy in the grid (contribution of bioenergy to the total energy supply and the feed-in tariff, constituting a composite variable, are highly correlated at 0.7 [8]). The number of patent applications is taken as a proxy for the innovation outcome [11,13,61]. The number of patent applications of bioenergy technologies and the contribution of bioenergy to total energy supply are measured in terms of flow. The public R&D expenditure of bioenergy technologies is measured in terms of stock. The R&D stock of each country i at the time t ($RADS_{it}$) is computed from public R&D expenditures through the perpetual inventory model—$RADS_{it} = (1-\delta)RADS_{i,t-1} + RAD_{i,t-x}$—where δ (the depreciation rate) is set at 10% and x (the time lag) is set at five years [9]. Based on the review of previous studies, such as Söderholm and Klaassen [16], Bosetti et al. [61], Kobos et al. [62], Popp et al. [63], and Bointner [64], the current study assumes a five-year time lag and a depreciation rate of 10% for the R&D stock estimation. We measure the initial value of the stock by dividing the average of the first four observations of R&D expenditure

in bioenergy technologies by the sum of the R&D depreciation rate of 10% and an estimate of the R&D growth rate of each country during the period, for the years for which the R&D expenditure data are available in each country up to 2012. In calculating the dynamic efficiency, this study uses each country *i*'s patent applications in year *t*, and the contribution of bioenergy to the total energy supply in year *t*. Each country *i*'s R&D stock in fiscal year ending in year $t-2$ is used based on the approach by Popp [65], Johnstone et al. [11], and Hirshleifer et al. [20]. As the dynamic efficiency, MPGI, is often zero, we used *DE* as the natural log of one plus MPGI in the model. It is based on a study that uses the natural log of one plus a firm's innovative efficiency that is measured as the ratio of its patents and scaled by its R&D capital [20]. *EPS* is the natural logarithm of a composite index of environmental policy stringency (EPS) in the energy sector developed by the OECD [66]. The ESP indicator includes a market- and non-market-based component [67]. The former groups market-based policy instruments that assign an explicit price to the externalities, while the latter clusters command-and-control instruments. Following Costantini and Crespi [25], Costantini and Mazzanti [28], and Groba [31,32], the current study uses both broad (general) and sector-specific proxies for environmental policy stringency to control the nexus between environmental policy and export. However, in analyzing specific sectors (as in this study), using a broad proxy may not capture the true relationships [31]. Therefore, we used the environmental policy stringency based on policies in the energy sector.

4. Data and Methodology

The data used in this study consist of annual measures for each country over the 18-year period from 1995 to 2012 for 16 OECD countries (for the countries, see Table 1). Data on bioenergy technology exports were obtained from the Personal Computer Trade Analysis System (PC-TAS) database released by the International Trade Centre based on the topologies of bioenergy technologies and components proposed by Jha [8] using the Harmonized Commodity Description and Coding System 1996. The public R&D expenditures of bioenergy technologies are obtained from the freely available database of the International Energy Agency's Energy Technology Research and Development section. The contribution of bioenergy to the total energy supply for each country is calculated from data obtained from the IEA's Renewable and Waste Energy Supply Database and the US Energy Information Administration's International Energy Statistics. The patent counts were generated for the International Patent Classification codes for bioenergy using the OECD Patent Statistical Database. The codes include C10L 5/42 (solid fuels based on materials of non-mineral origin or vegetables), F02B 43/08 (engines operating on gaseous fuels obtained from solid fuel—wood), C10L 1/4C (liquid carbonaceous fuel—organic compounds), and B01J 4/16C (anion exchange—use of materials, cellulose, or wood). Only patent applications deposited at the European Patent Office were included, following Johnstone et al. [11]. Exports and R&D stock are calculated at 2009 prices and international purchasing power parity levels.

In a panel context, a test for determining the relationship among the variables considered is conducted. In estimating the panel, it is important to check for the possibility of a structural break or cross-sectional dependence. First, the Jarque-Bera [68] test for normality, the cumulative sum of recursive residuals (CUSUM), and the cumulative sum of recursive residuals of squares (CUSUMQ) tests for structural breaks [69] in each individual time series are performed. Second, to detect the presence of cross-sectional dependence, the study employs the Lagrange Multiplier (LM) tests of Breusch and Pagan [70]. It is suitable when $\mathrm{T(time)} > N(\text{number of cross} - \text{section})$ (as is the case in this study). Third, panel unit-root tests to investigate the order of integration of the series in the panel data are performed. A number of panel unit-root tests are proposed in the literature (e.g., [71–73]). The alternative that can be applied in a test for stationarity in panel data depends on whether the panels allow for both structural breaks and cross-sectional dependence or either one of them. Fourth, if the panel unit-root exists, this study conducts panel cointegration tests based on the methodologies by Pedroni [74], Banerjee and Carrioni-i-Silvestre [75], or Westerlund [76] to confirm

a long-term relationship among the variables, while taking explicitly into account the results of the Jarque-Bera [68] test, CUSUM and CUSUMQ tests, and LM tests of Breusch and Pagan [70]. Finally, the study sets an empirical model based on the results of the panel unit-root and cointegration tests, whereupon the short- and/or long-run estimations are performed while accounting for sample size and panel data characteristics (e.g., cross-sectional dependence, heteroscedasticity, simultaneity).

5. Empirical Analysis

5.1. Testing Panel Frameworks

We performed the Jarque-Bera's [68] test for normality. The test results in Table 1 show that these series do not deviate substantially from the normal distribution, except for the dynamic efficiency variables of Canada and Denmark, and the environmental policy stringency variable of Japan.

Table 1. Descriptive Statistics (Variables in Natural Logarithm).

Country	Variable	Mean	SD	MIN	MAX	Skewness	Kurtosis	J-B
Australia	*EX*	6.330	0.476	5.730	7.153	0.326	1.596	1.679
	DE	0.464	0.435	0.000	1.160	0.230	1.591	1.556
	EPS	0.345	0.621	−0.780	1.313	−0.269	2.295	0.557
Austria	*EX*	5.990	0.903	4.362	7.020	−0.429	1.956	1.294
	DE	0.437	0.508	0.000	1.479	0.774	2.312	2.037
	EPS	0.898	0.204	0.617	1.202	0.023	1.619	1.351
Canada	*EX*	6.501	0.624	5.110	7.284	−0.775	2.828	1.727
	DE	0.453	0.515	0.000	2.037	1.675	6.207	15.240 ***
	EPS	0.422	0.738	−0.780	1.349	−0.103	1.524	1.572
Denmark	*EX*	5.625	0.850	4.273	7.311	0.123	2.216	0.478
	DE	0.828	0.283	0.529	1.655	1.502	5.319	10.230 ***
	EPS	1.031	0.247	0.682	1.404	0.169	1.889	0.954
Finland	*EX*	4.832	0.604	4.078	5.862	0.470	1.632	1.953
	DE	0.470	0.515	0.000	1.699	0.775	2.749	1.750
	EPS	0.831	0.337	0.303	1.246	−0.236	1.482	1.789
France	*EX*	7.713	0.575	6.524	8.410	−0.476	2.294	0.995
	DE	0.725	0.359	0.000	1.350	−0.407	3.315	0.541
	EPS	0.740	0.442	0.136	1.308	−0.012	1.333	1.969
Germany	*EX*	8.530	0.695	7.259	9.386	−0.595	2.230	1.423
	DE	0.811	0.187	0.457	1.104	−0.367	2.199	0.835
	EPS	0.914	0.189	0.617	1.144	−0.326	1.520	1.852
Italy	*EX*	7.527	0.444	6.833	8.129	0.026	1.430	1.748
	DE	0.654	0.492	0.000	2.009	0.980	4.564	4.460
	EPS	0.657	0.304	0.303	1.044	0.166	1.204	2.361
Japan	*EX*	8.440	0.380	7.588	8.907	−0.863	2.958	2.115
	DE	0.529	0.411	0.000	1.127	−0.036	1.901	0.858
	EPS	0.555	0.258	0.287	1.252	1.592	4.924	9.808 ***
The Netherlands	*EX*	7.468	1.055	4.909	8.176	−1.090	3.642	3.661
	DE	0.706	0.468	0.000	1.544	−0.099	2.160	0.527
	EPS	0.813	0.395	0.206	1.419	0.434	1.577	1.439
Norway	*EX*	4.807	1.103	2.276	6.392	−0.914	3.177	2.392
	DE	0.575	0.511	0.000	1.676	0.434	2.297	0.884
	EPS	0.542	0.445	0.020	1.181	0.245	1.583	1.592
Spain	*EX*	6.140	0.822	4.434	7.369	−0.243	2.347	0.469
	DE	0.543	0.401	0.000	1.081	−0.435	1.562	2.002
	EPS	0.847	0.218	0.446	1.098	−0.573	2.169	1.421
Sweden	*EX*	5.993	0.650	4.529	6.797	−0.738	2.587	1.665
	DE	0.729	0.566	0.000	2.282	1.108	4.334	4.742
	EPS	0.802	0.411	0.040	1.206	−0.968	2.352	2.952

Table 1. *Cont.*

Country	Variable	Mean	SD	MIN	MAX	Skewness	Kurtosis	J-B
Switzerland	*EX*	6.413	0.387	5.566	6.992	−0.878	3.323	2.261
	DE	0.780	0.458	0.000	1.452	−0.089	2.150	0.532
	EPS	0.833	0.223	0.523	1.203	0.720	2.056	2.103
The United Kingdom	*EX*	7.492	0.436	6.438	8.052	−1.126	3.808	4.062
	DE	0.689	0.496	0.000	1.718	0.648	3.197	1.218
	EPS	0.475	0.559	−0.207	1.285	−0.013	1.492	1.610
The Unites States of America	*EX*	8.529	0.642	7.354	9.497	−0.016	1.950	0.781
	DE	0.778	0.203	0.445	1.193	0.231	2.639	0.243
	EPS	0.485	0.410	0.048	1.152	0.434	1.415	2.314

Notes: *** denotes significance at the 1% level. The Jarque-Bera statistic is used to determine whether the data come from a normal distribution. The null hypothesis is normality. J-B denotes the Jarque-Bera statistic.

The study also performs CUSUM and CUSMUSQ tests to detect whether systematic changes in long-term coefficients of regression occur, and whether deviations from the short-term constancy of regression coefficients are randomized and occasional. Apart from the CUSUM test results of Finland and Italy and the CUSUMQ test results of Canada, the Netherlands, and Spain, the results of the tests also suggest that almost all the series are stable over the observation period (for the full results, refer to Figure S1 in the supplementary material available online).

The LM tests of Breusch and Pagan [70] based on the fixed-effects model are conducted to detect the presence of cross-sectional dependence. In the pooled cross-section time series context, the assumptions of the model's error process (independently and identically distributed) may be violated in several ways [77]. The error process may be homoskedastic within cross-sectional units, but its variance may differ across units—a condition known as groupwise heteroscedasticity. A modified Wald statistic for groupwise heteroscedasticity in the residuals of a fixed-effects regression model is calculated, following Greene [78] (p. 598). The results of LM tests revealed that cross-sectional dependence exists (Breusch-Pagan LM test of independence = 312.669, $p = 0.000$). The modified Wald test result showed that there is no homoscedasticity within cross-sectional units (modified Wald test for groupwise heteroscedasticity = 844.007, $p = 0.000$).

Table 2. Results of Panel Unit-root Tests.

Variables		*EX*	Δ*EX*	*DE*	Δ*DE*	*EPS*	Δ*EPS*
Pesaran CADF	(A)	0.522	−3.636 ***	0.695	−4.224 ***	−2.081 *	−2.194 **
test z (t-bar) stat.	(B)	−1.169	−4.319 ***	−0.292	−2.673 ***	−2.304	−4.202 ***

Notes: The individual intercept and time trend are included in (A) and the individual intercept in (B). The lag lengths for the panel test are based on those employed in the univariate ADF test. The normalized z-test statistic is calculated by using the t-bar statistics. ***, **, and * denote significance at 1%, 5%, and 10%, respectively.

Having established that the series display cross-sectional correlation, we conduct Pesaran's [73] panel unit-root test that allows for the presence of cross-sectional dependence. The results of Pesaran's [73] test that include an intercept, as well as those with an intercept and a linear trend for *EX*, *DE*, and *EPS*, as presented in Table 2, indicate that the hypothesis of the series containing a unit root is confirmed, and that the first difference of the three variables is stationary.

The results of panel unit-root tests suggest that there can be co-movement among variables. Hence, the current study implements Westerlund's [76] heterogeneous panel cointegration tests, which allow for cross-sectional dependence.

Table 3 shows the results of Westerlund's [76] panel cointegration tests that include an intercept, as well as those with an intercept and a linear trend. The results demonstrate that, overall, there is at least some evidence of co-movement among the variables for bioenergy technologies, showing significance in both cases, with the constant (statistic G_t, G_α, P_t, and P_α) and with the constant and the trend (statistic G_t and P_t).

Table 3. Results of Panel Cointegration Tests.

Statistics	With Trend			Without Trend		
	Value	***Z***	**Robust *p*-Value**	**Value**	***Z***	**Robust *p*-Value**
G_t	−3.004	−2.262	0.057	−2.796	−3.304	0.011
G_a	−7.136	3.545	0.198	−8.303	3.545	0.011
P_t	−10.829	−1.861	0.062	−11.519	−4.515	0.009
P_t	−6.446	2.392	0.268	−8.249	1.706	0.017

Notes: The lag and lead lengths are set to 1 and 0, respectively. To control for cross-sectional dependence, robust critical values are obtained through 5000 bootstrap replications.

5.2. Model Specification and Empirical Test

Presence of cointegration indicates that the Engle and Granger [79] approach can be used to estimate an error correction model. Hence, this study performs dynamic panel causality tests based on the vector error correction model (VECM) to evaluate the short- and long-run directions of causality between the examined variables. Granger causality is not a relationship between causes and effects, but a method for testing the predictability of a series. It is defined in terms of predictive ability [80] based on the following premises: (i) a cause occurs before its effect, and (ii) knowledge of a cause improves the prediction of its effect [79]. The Granger causality model used in this study is based on the panel VECM. It can be expressed as follows:

$$\Delta EX_{it} = \sum_{p=1}^{n-1} \beta_{11p} \Delta EX_{it-p} + \sum_{p=1}^{n-1} \beta_{12p} \Delta DE_{it-p} + \sum_{p=1}^{n-1} \beta_{13p} \Delta EPS_{it-p} + \gamma_{1i} ECT_{it-1} + \Delta\varepsilon_{1it} \quad (2)$$

$$\Delta DE_{it} = \sum_{p=1}^{n-1} \beta_{21p} \Delta EX_{it-p} + \sum_{p=1}^{n-1} \beta_{22p} \Delta DE_{it-p} + \sum_{p=1}^{n-1} \beta_{23p} \Delta EPS_{it-p} + \gamma_{2i} ECT_{it-1} + \Delta\varepsilon_{2it} \quad (3)$$

$$\Delta EPS_{it} = \sum_{p=1}^{n-1} \beta_{31p} \Delta EX_{it-p} + \sum_{p=1}^{n-1} \beta_{32p} \Delta DE_{it-p} + \sum_{p=1}^{n-1} \beta_{33p} \Delta EPS_{it-p} + \gamma_{3i} ECT_{it-1} + \Delta\varepsilon_{3it} \quad (4)$$

where Δ is the first difference operator; EX is the natural logarithm of exports; DE is the natural logarithm of one plus MPGI, which represents the dynamic efficiency of public policy of bioenergy; EPS is the natural logarithm of environmental policy stringency based on energy sector; ECT_{it-1} is the error correction term lagged by one period coming from the lagged residuals derived from the long-run cointegrated relationship; b_{ij} are the short-run adjustment coefficients; and ε_{it} are error terms.

This study uses a single estimator proposed by Kao and Chiang [81], called dynamic ordinary lease squares (DOLS), to estimate the long-term equilibrium coefficients. The DOLS estimator is fully parametric, computationally convenient, and more precise than other single equation estimators in estimating the long-run relationship. By including the past and future values of the differenced I(1) regressors, it corrects the serial correlation in the error and the endogeneity of regressors that are normally present in the long-run relationship between the variables. In this way, it produces an unbiased estimate of the long-run parameters. Considering these points, we used the DOLS to estimate long-run coefficients in a cointegrated panel regression. However, to estimate the long- and short-run parameters of the panel VECM, Pesaran et al.'s [82] pooled mean group [PMG] estimator is used. The PMG requires reparameterization into the error correction form; it combines both pooling and averaging in its estimation procedure. It is considered an intermediated estimator that can allow the evaluation of two different Granger causality relationships—a short-run causality that tests the significance of coefficients related to the lagged difference between the variables in question (heterogeneous short-run dynamics) and a long-run causality related to the coefficient of the error correction term in the panel VECM (identical long-run dynamics). Despite these advantages of the DOLS and PMG estimators, they cannot allow for cross-sectional dependence. Hence, cross-sectional

dependence is another challenge that must be addressed for producing accurate and efficient parameter estimates. According to Roodman [83] and Sarafidis et al. [84], cross-sectional dependence among errors can be eliminated by including time dummies or cross-sectionally demeaning the data. We created year-dummy control variables to prevent cross-individual correlation [83,84].

The DOLS results in Table 4 show that *DE* and *EPS* have positive effects on *EX* at the 1% significant level. This means that a 1% increase in the dynamic efficiency of public policy and a 1% increase in the environmental policy stringency will increase the export by 0.939% and 0.426% in the long run, respectively.

Table 4. Panel DOLS Long-run Estimates (Panel with Time Dummies).

Estimators	**Variables**	
	DE	***EPS***
Coefficients	0.939 (8.18) [0.115]	0.426 (2.870) [0.148]

Notes: The results are those of model tests, wherein EX is the dependent variable. Numbers in parentheses are *t*-statistics. Numbers in square brackets represent standard errors.

Since the variables are cointegrated, the PMG estimator is used to perform Granger-causality tests for the *DE* export nexus in the sector of bioenergy technologies. However, in the VECM Equations (2)–(4), differencing introduces a simultaneity problem because the lagged endogenous variables on the right-hand side correlate with the new differenced error term.

In addition, the genuine errors across industries are heteroscedastic. This leads us to use instrumental variables (IV) [85] or the generalized method of moments (GMM) [86] to efficiently estimate coefficients. However, with these techniques, under certain conditions, the variance of the estimates may increase asymptotically and generate considerable bias. This occurs if the sample is finite (as in this study) [87]. When $T(time) \to \infty$, the least squares dummy variable (LSDV) estimator is consistent, and it is biased at a negligible degree [88]. However, when T is smaller than 30, Judson and Owen [89] showed that the LSDV estimator has a bias of up to 20% of the time value coefficient of interest.

When T is smaller than 30 (as in this study), a bias-corrected LSDV (LSDVC) estimator outperforms IV, GMM, and LSDV estimation techniques for the balanced [89] and unbalanced panels [90] in terms of bias and root mean squared error of the short- and long-term coefficient estimates, regardless of the initiating estimator. An important advantage of using the LSDVC estimator is that its performance is independent of the ratio of the fixed effects' variance to the error term's variance. Moreover, the LSDVC can be the most accurate estimator in the absence of endogenous independent variables and second order serial correlation.

Thus, Equations (2)–(4) are estimated using LSDVC. The equations include the error correction term and one-period lagged dependent and independent variables. The results from the two estimators—Ander Hsiao (AH) and Arellano Bond (AB)—in Table 5 are similar in terms of estimated parameters and corresponding *p*-values. However, the LSDVC estimation initiated by the AB estimator (part II of Table 5) exhibits smaller *p*-values compared to the one that initially uses AH (part I of Table 5), since the former estimator is more efficient [91].

The panel vector error correction results (Panel A and B in part II of Table 5) show that, in the short run, *DE* and *EPS* in period $t-1$ positively influence *EX* in period t at the 1% significance level. However, there is no short-run path-dependent process between *EPS* and *DE*, or from *EX* to *DE* and *EPS*. This study also highlights the presence of positive, significant (at the 1% level) short-run relationships between the contemporaneous and the one-period lagged *EX* and *EPS* in two out of three equations; additionally, the joint tests of *EX* and *EPS* (not reported for conciseness) show that the export performance is positively correlated with a country's environmental policy stringency.

Table 5. Panel Vector Error Correction Results of Dynamic Efficiency of Public Policy-export Nexus (Panel with Time Dummies).

Panel A: Bias-Corrected LSDVC Estimation							
Independent Variables		**(I) Initial (AH)**			**(II) Initial (AB)**		
		Dependent Variables			**Dependent Variables**		
		Δ*EX*	**Δ*DE***	**Δ*EPS***	**Δ*EX***	**Δ*DE***	**Δ*EPS***
ΔEX_{it-1}		0.190 (0.039) ***	0.007 (0.105)	0.010 (0.041)	0.191 (0.038) ***	0.105 (0.077)	0.008 (0.033)
ΔDE_{it-1}		0.086 (0.031) ***	0.101 (0.078)	−0.030 (0.029)	0.086 (0.031) ***	0.006 (0.103)	−0.024 (0.024)
ΔEPS_{it-1}		0.508 (0.063) ***	0.133 (0.158)	0.896 (0.109) ***	0.506 (0.062) ***	0.135 (0.154)	0.826 (0.052) ***
ECT_{it-1}		0.695 (0.038) ***	−0.004 (0.087)	−0.074 (0.033) **	0.694 (0.038) ***	0.001 (0.085)	−0.080 (0.026) ***
Panel B: Statistical Values for Panel Causality Tests							
Independent Variables		**Dependent Variable**			**Dependent Variable**		
		Δ*EX*	**Δ*DE***	**Δ*DE***	**Δ*EX***	**Δ*DE***	**Δ*DE***
Short run	ΔEX	-	0.000	0.070	-	0.000	0.060
	ΔDE	7.620 ***	-	1.080	7.680 ***	-	0.960
	ΔEPS	64.180 ***	0.710	-	64.180 ***	0.770	-
Long run	ECT	330.340 ***	0.000	4.860 *	331.830 ***	0.000	9.120 ***

Notes: The results are based on biased corrected LSDV estimations, which initially utilize Anderson Hsiao (AH) and Arellano Bond estimators, respectively. Bias is corrected up to the first order, 0 (1/T), and 500 replications are used in bootstrap procedure to find asymptotic variance-covariance matrix of estimators. Leg length is chosen as one based on BIC. ***, **, and * denote the 1%, 5%, and 10% significance levels, respectively. Standard errors are in parentheses.

The coefficient of *ECT*, wherein ΔEPS_{it} is the dependent variable (Equation (4)), is negative (−0.080) and significant, indicating that *EPS* could be a key adjustment factor as the system departs from the long-run equilibrium. However, the coefficients of *ECT* in Equations (2) and (3) are positive and insignificant (or significant), indicating that *EX* and *GDP* cannot be considered as adjustment factors for closing the gap with respect to the long-run relationship between the two variables.

6. Discussion

6.1. Summary and Policy Implications

The current study investigated the relationship between dynamic efficiency of public policy and export performance in the bioenergy technologies sector using panel data for 16 OECD countries over the 1995–2012 period. The study used the panel VECM as an empirical model to test causal relationships, while considering the results of various panel framework analyses to check the characteristics of the data. The parameter of long-term dynamic efficiency of public policy is calculated using the DOLS. The PMG estimator is used to estimate the long- and short-run parameters in the dynamic panel through the following Granger-causality tests: (1) LSDVC estimations were conducted to avoid autocorrelation and endogeneity problems in the model and to overcome the limit of the finite sample; (2) subsequently, based on the LSDVC estimation results, causality is determined by running Wald tests on the coefficients of the variables.

The main results of this study and their implications are as follows.

First, this study finds convincing evidence of a positive long-run relationship between the dynamic efficiency of public policy and export performance. Specifically, from the DOLS results, it emerges that a 1% increase in the dynamic efficiency of public policy will increase exports by 0.939% in the long run. This study also highlights a positive short-run linear causal relationship. These relationships suggest that governments should continue to focus on a reliable and flexible long-term dynamic efficiency of the bioenergy technology policy fostering exports, while building reliable and positive short-term dynamic efficiency of public export policies. Moreover, these policies should be harmonized with the long-term policy goals. Dynamic efficiency of public policy in the RET sector involves the extent to which public policy (policy input) can encourage firms to make more proactive efforts to foster innovation (policy output). This requires governments to provide continuous incentives and create favorable conditions for technological improvement or innovation [11–13]. It is important to note that public policy does not lead to an immediate knowledge increase [92]. Following the implementation of any energy policy, facilitating knowledge increases requires time; additionally, scientific capacity, as an important driver of innovation [11], is somewhat inelastic to knowledge increases to a certain extent [64]. Further, both uncertainty and/or inefficiency in public policies reduce private incentives to invest [45,93], thus compromising the smooth running of various entrepreneurial activities. They decrease productivity in the RET sector [46]. In this context, the steady and continuous provision and creation of incentives and favorable conditions for facilitating an increase in knowledge-based technological capacity in the long run becomes essential, in the sense that such stability and continuity may leverage complementary private investments [61,94] to develop and diffuse RETs [38]. This would contribute to the RET industry growth [5,34] by creating both local and export markets. Therefore, policymakers should make great efforts to monitor and evaluate the development and export specialization position of bioenergy technologies, and explicitly consider the monitoring and evaluation results in the implementation of public policies. Since the bioenergy technology sector is influenced by various policies not restricted to the energy, industrial, environmental, and competition fronts [95], such efforts need to be undertaken in all these domains.

Second, since the coefficient of the error correction term in Equation (4) using *EPS* as the dependent variable is negative and significant, this study finds evidence that environmental policy could be a key adjustment factor for closing the gap with respect to the long-run equilibrium between exports and the dynamic efficiency of public policy. In Equation (4), this study also shows that exports have a positive

effect on environmental policy stringency in the short run. Exports could deviate from the long-run equilibrium because of shocks in the short run; however, after the shock, they eventually converge to the equilibrium in subsequent periods. In such a framework, the long-run export dynamics are driven by both the changes in environmental policy and the stable nature of the long-run equilibrium. The adjustment factor, thus, reflects the speed of adjustment toward the equilibrium in case of deviation. Furthermore, based on the Granger representation theorem, a negative and significant adjustment coefficient implies a long-run relationship between the variables, which, in this study, it is confirmed for export performance, dynamic efficiency of public policy, and environmental policy stringency. The results also show that the short-run environmental policy plays an important role in promoting steady and stable export growth in the long run, by converging quickly to equilibrium with about 8% of the discrepancy corrected in each period. This suggests that it is possible for governments to achieve environmentally sound and sustainable development by enhancing export competitiveness, promoting the growth of the bioenergy technologies sector, and increasing environmental sustainability (e.g., greenhouse gas emissions' reduction) at the same time. Hence, wherever possible, policymakers should formulate and implement policy strategies related to the bioenergy technologies sector aiming to implement mechanisms able to build a positive relationship between export and environmental policy efforts, especially taking into account their path-dependent processes (i.e., a dynamic learning effect).

Third, this study shows that environmental policy stringency has a positive effect on export performance. As seen in the DOLS results, this also suggests that the environmental policy of the energy sector can drive the exports of bioenergy technologies in the long run. Specifically, stringent environmental policy may not necessarily be detrimental to industrial productivity if policymakers adequately take into account the dynamic dimension of the Porter and Van der Linde hypothesis [96]. According to Porter and Van der Linde [29], increasing the number of stringent environmental policies will lead to innovations that would reduce inefficiencies, thus eventually reducing costs. This implies that due emphasis should be placed on the role played by environmental regulations in the energy sector in order to promote the export performance of bioenergy technologies. Governments remain the most important and strongest stakeholders that can influence industries to improve their environmental performance by using both market- and non-market-based instruments. According to Botta and Kózluk [66], who developed the composite index of environmental policy stringency (EPS) adopted in this study, market-based policies include instruments that can be used for punishing environmentally harmful activities (e.g., taxes on pollutants), while non-market measures aim to reward environmentally-friendly activities (e.g., incentives). In this context, this study's finding suggests that governments need to develop and implement environmental policy measures to promote various activities based on an understanding of the voluntary, eco-friendly, and innovative initiatives independently undertaken by firms and industries themselves.

Fourth, this study shows that there is no short-run bidirectional causal relationship between dynamic efficiency of public policy and environmental policy stringency. The study also highlights that there is no casual linear relationship running from exports to the dynamic efficiency of public policy and to the environmental policy stringency. These findings do not necessarily imply that a growth in exports cannot contribute to an increase in the dynamic efficiency of public policy and promote environmental policy efforts at all, but rather that, due to various factors, such contribution has not been significant. In reality, there are many relevant factors, such as public sector functioning, social conditions, and politics, which may affect the dynamic efficiency of public policy [57] and environmental policy efforts. In such a context, the findings of this study suggest that, at least in the short run, policymakers should make great efforts to understand the interaction between these relevant factors and the dynamic efficiency of public policy and environmental policy efforts by conducting various qualitative and quantitative studies.

6.2. Limitations and Future Research

Although this study contributes to an understanding of the importance of maintaining a consistent innovation-friendly policy—maintaining policy dynamic efficiency—for promoting exports of bioenergy technologies, it has several limitations. First, this study does not control for the variable related to policy strategies (e.g., industry-specific export promotion [97]) that is a relevant factor, and likely to affect the extant of exports. Hence, future research should consider it. Second, this study focuses on the role of the dynamic efficiency of public policy in ways that only consider output in terms of economic aspects in the promotion of exports of bioenergy technologies. However, according to Shen et al. [37], policies to promote the renewable energy technology sector also have a non-economic goal of environmental protection, which requires the examination of undesirable factors in efficiency evaluation and the consideration of eco-innovations. This can be achieved by including the contribution of bioenergy policies toward sustainability by reducing the environmental burdens in the overall evaluation. Further research should address these issues. Third, despite their influence on the renewable energy technology sector, this study does not control for the presence of other renewable energy technology policies (e.g., voluntary programs, obligations, tradable certificates, tax credits, etc.) [11], as well as economic and social factors (e.g., social acceptance, energy price, FDI, and private innovation) [98–101]. Further research should account for these omitted variables.

Supplementary Materials: The following are available online at www.mdpi.com/1996-1073/10/12/1231/s1.

Acknowledgments: This paper is financially supported by the National Research Foundation of Korea Grant funded by the Korean Government (NRF-2016S1A5A2A03927419).

Author Contributions: Bongsuk Sung, and Woo-Yong Song designed the study. Bongsuk Sung analyzed the final simplified panel data model presented in this paper. Woo-Yong Song proposed some implications based on the results of this paper. All authors have read and approved the final manuscript.

Conflicts of Interest: The authors declare no conflict of interest.

References

1. Finon, D.; Perez, Y. The social efficiency of instruments of promotion of renewable energies: A transaction-cost perspective. *Ecol. Econ.* **2007**, *62*, 77–92. [CrossRef]
2. Hass, R.; Resch, G.; Panzer, C.; Busch, S.; Ragwitz, M.; Held, A. Efficiency and effectiveness of promotion systems for electricity generation from renewable energy sources—Lessons from EU countries. *Energy* **2011**, *36*, 2186–2193. [CrossRef]
3. Del Río, P. The dynamic efficiency of feed-in tariffs: The impact of different design elements. *Energy Policy* **2012**, *41*, 139–151. [CrossRef]
4. Held, F.; Haas, R.; Ragwitz, M. On the success of policy strategies for the promotion of electricity from renewable energy sources in the EU. *Energy Environ.* **2006**, *17*, 849–868. [CrossRef]
5. Lund, P.D. Effects of energy policies on industry expansion in renewable energy. *Renew. Energy* **2009**, *34*, 53–64. [CrossRef]
6. Bürer, M.J.; Wüsternhagen, R. Which renewable energy policy is a venture capitalist's best friend? Empirical evidence from a survey of international cleantech investors. *Energy Policy* **2009**, *37*, 4997–5006. [CrossRef]
7. Verbruggen, A.; Lauber, V. Assessing the performance of renewable electricity support instruments. *Energy Policy* **2012**, *45*, 635–644. [CrossRef]
8. Jha, V. *Trade Flows, Barriers and Market Drivers in Renewable Energy Supply Goods: The Need to Level the Playing Field*; ICTSD Trade and Environment Issue Paper 10; International Centre for Trade and Sustainable Development: Geneva, Switzerland, 2009.
9. Sung, B. Public policy supports and export performance of bioenergy technologies: A dynamic approach. *Renew. Sustain. Energy Rev.* **2015**, *24*, 477–495. [CrossRef]
10. Midttun, A.; Gautesen, K. Feed in or certificates, competition or complementarity? Combining a static efficiency and a dynamic innovation perspective on the greening of the energy industry. *Energy Policy* **2007**, *35*, 1419–1422. [CrossRef]

11. Johnstone, N.; Haščič, L.; Popp, D. Renewable energy policies and technological innovation: Evidence based on patent counts. *Environ. Resour. Econ.* **2010**, *45*, 133–155. [CrossRef]
12. Johnstone, N.; Haščič, L.; Poirier, J.; Hemar, M.; Michel, C. Environmental policy stringency and technological innovation: Evidence from survey data and patent counts. *Appl. Econ.* **2012**, *44*, 2157–2170. [CrossRef]
13. Costantini, V.; Crespi, F.; Martini, C.; Pennacchio, L. Demand-pull and technology-push public support for eco-innovation: The case of the biofuels sector. *Res. Policy* **2015**, *44*, 577–595. [CrossRef]
14. Zachmann, G.; Serwaah, A.; Peruzzi, M. *When and How to Support Renewables? Letting the Data Speak*; Working Paper 2014/01; Bruegel: Brussels, Belgium, 2014.
15. Arent, D.J.; Wise, A.; Gelman, R. The status and prospects of renewable energy for combating global warming. *Energy Econ.* **2011**, *33*, 584–593. [CrossRef]
16. Söderholm, D.; Klaassen, G. Wind power in Europe: A simultaneous innovation-diffusion model. *Environ. Resour. Econ.* **2007**, *36*, 163–190. [CrossRef]
17. Del Río, P.; Bleda, M. Theoretical Approaches to Dynamic Efficiency in Policy Contexts: The Case of Renewable Electricity. In *The Dynamics of Economic and Environmental Systems*; Costantini, V., Mazzanti, M., Eds.; Springer: Rotterdam, The Netherlands, 2013; pp. 45–60.
18. Organization for Economic Co-operation and Development (OECD). *Dynamic Efficiencies in Merger Analysis*; OECD: Paris, France, 2007.
19. Fu, X.; Yang, Q.G. Exploring the cross-country gap in patenting: A stochastic frontier approach. *Res. Policy* **2009**, *38*, 1303–1313. [CrossRef]
20. Hirshleifer, D.; Hsu, P.-H.; Li, D. Innovative efficiency and stock returns. *J. Financ. Econ.* **2013**, *107*, 632–654. [CrossRef]
21. Jayamaha, A.; Mula, J.M. Productivity and efficiency measurement technologies: Identifying the efficiency of techniques for financial institutions in developing countries. *J. Emerg. Trends Econ. Manag. Sci.* **2012**, *2*, 454–460.
22. Hall, B.H.; Oriani, R. Does the market value R&D investment by European firms? Evidence from a panel of manufacturing firms in France, Germany, and Italy. *Int. J. Ind. Organ.* **2006**, *24*, 971–993.
23. Duqi, A.; Torluccio, G. Can R&D expenditures affect firm market value? An empirical analysis of a panel of European listed firms. In *Bank Performance Risk and Firm Financing*; Molyneux, P., Ed.; Palgrave Macmillan: England, UK, 2011; pp. 215–241.
24. Conte, A.; Scheweizer, P.; Dierx, A.; Ilzkovitz, F. *An Analysis of the Efficiency of Public Spending and National Policies in the Error of R&D*; Occasional Paper 54; European Commission: Brussels, Belgium, 2009.
25. Costantini, V.; Crespi, F. Environmental regulation and the export dynamics of energy technologies. *Ecol. Econ.* **2008**, *66*, 447–460. [CrossRef]
26. Sung, B.; Song, W.-Y. Causality between public policies and exports of renewable energy technologies. *Energy Policy* **2013**, *55*, 95–104. [CrossRef]
27. Färe, R.; Grosskopt, S.; Norris, M.; Zhang, Z. Productivity growth, technical progress and efficiency change in industrialized countries. *Am. Econ. Rev.* **1994**, *84*, 66–83.
28. Costantini, V.; Mazzanti, M. On the green and innovative side of trade competitiveness? The impact of environmental policies and innovation on EU exports. *Res. Policy* **2012**, *41*, 132–153. [CrossRef]
29. Porter, M.E.; Van der Linde, C. Toward a new conception of the environment-competiveness relationship. *J. Econ. Perspect.* **1995**, *9*, 97–118. [CrossRef]
30. Albrizio, S.; Kozluk, T.; Zipperer, V. Environmental policies and productivity growth: Evidence across industries and firms. *J. Environ. Econ. Manag.* **2017**, *81*, 209–226. [CrossRef]
31. Groba, F. *Determinants of Trade with Solar Energy Technology Components: Evidence on the Porter Hypothesis?* Discussion Papers 1163; German Institute for Economic Research: Berlin, German, 2011.
32. Groba, F. Environmental Regulation, Solar Energy Technology Components and International Trade—An Empirical Analysis of Structure and Drives. Presented at the World Renewable Energy Congress, Linköping, Sweden, 8–13 May 2011; pp. 3670–3677.
33. Smith, P.C.; Street, A.A. Measuring the efficiency of public services: The limits of analysis. *J. R. Stat. Soc. Ser. A* **2005**, *168*, 401–417. [CrossRef]
34. International Energy Agency (IEA). *World Energy Outlook 2016*; OECD/IEA: Paris, France, 2016.
35. Kahia, M.; Kadria, M.; Ben Aissa, M.S.; Lanouar, C. Modeling the treatment effect of renewable energy policies on economic growth: Evaluation from MENA countries. *J. Clean. Prod.* **2017**, *149*, 845–855. [CrossRef]

36. Ru, P.; Zhi, Q.; Zhang, F.; Zhong, X.; Li, J.; Su, J. Behind the development of technology: The transition of innovation modes in China's wind turbine manufacturing industry. *Energy Policy* **2012**, *43*, 58–69. [CrossRef]
37. Shen, Y.-C.; Chou, C.J.; Lin, G.T.G. The portfolio of renewable energy sources for achieving the three E policy goal. *Energy* **2011**, *36*, 2589–2598. [CrossRef]
38. Bernard, A.B.; Jensen, J.B.; Redding, S.J.; Schott, P.K. Firms in international trade. *J. Econ. Perspect.* **2007**, *21*, 105–130. [CrossRef]
39. Costantini, J.; Melitz, M. The Dynamics of Firm-Level Adjustment to Trade Liberalization. In *The Organization of Firms in a Global Economy*; Helpman, E., Marin, D., Verdier, T., Eds.; Harvard University Press: Cambridge, MA, USA, 2007; pp. 15–36.
40. Melitz, M.J. The impact of trade on intra-industry reallocations and aggregate industry productivity. *Econometrica* **2003**, *71*, 1695–1725. [CrossRef]
41. Schumpeter, J. *Capitalism, Socialism and Democracy*; Harper: New York, NY, USA, 1942.
42. Leitner, K.H. *Innovations Management*; Lecture Notes; Vienna University of Technology: Vienna, Austria, 2005.
43. Kahouli-Brahmi, S. Testing for the presence of some features of increasing returns to adoption factors in energy system dynamics: An analysis via the learning curve approach. *Ecol. Econ.* **2009**, *68*, 1195–1212. [CrossRef]
44. Negro, S.O.; Alkemade, F.; Hekkert, M.P. Why does renewable energy diffuse so slowly? A review of innovation system problems. *Renew. Sustain. Energy Rev.* **2012**, *16*, 3836–3846. [CrossRef]
45. Zhang, D.; Cao, H.; Zou, D. Exuberance in China's renewable energy investment: Rationality, capital structure and implications with firm level evidence. *Energy Policy* **2016**, *95*, 468–478. [CrossRef]
46. Lin, B.; Yang, L. Efficiency effect of changing investment structure on China's power industry. *Renew. Sustain. Energy Rev.* **2014**, *39*, 403–411. [CrossRef]
47. Kirzner, I. *How Markets Work: Disequilibrium, Entrepreneurship and Discovery*; Hobart Paper No. 133; Institute of Economic Affairs: London, UK, 1997.
48. Abhyankar, R. The government of India's role in promoting innovation through policy initiatives for entrepreneurship development. *Technol. Innov. Manag. Rev.* **2014**, *4*, 11–17.
49. Cumming, D.; Li, D. Public policy, entrepreneurship, and venture capital in the United States. *J. Corp. Financ.* **2013**, *23*, 345–367. [CrossRef]
50. Lewin, P. Entrepreneurial opportunity as the potential to create value. *Rev. Aust. Econ.* **2005**, *28*, 1–15.
51. De Soto, J.H. *The Theory of Dynamic Efficiency*; Routledge: New York, NY, USA, 2009.
52. Nill, J.; Kemp, R. Evolutionary approaches for sustainable innovation policies: From niche to paradigm? *Res. Policy* **2009**, *38*, 668–680. [CrossRef]
53. Mihaiui, D.M.; Opeana, A.; Cristescu, M.P. Efficiency, effectiveness and performance of the public sector. *Rom. J. Econ. Forecast.* **2010**, *4*, 132–147.
54. Barros, C.P.; Alves, C. An empirical analysis of productivity growth in a Portuguese retail chain using Malmquist productivity index. *J. Retail. Consum. Sc.* **2004**, *11*, 269–278. [CrossRef]
55. Price, C.W.; Weyman-Jones, T. Malmquist indices of productivity change in the UK gas industry before and after privatisation. *Appl. Econ.* **1996**, *28*, 29–39. [CrossRef]
56. Nicolli, F.; Vona, F. Heterogeneous policies, heterogeneous technologies: The case of renewable energy. *Energy Econ.* **2016**, *56*, 190–204. [CrossRef]
57. He, Y.; Xu, Y.; Pang, Y.; Tian, H.; Wu, R. A regulatory policy to promote renewable energy consumption in China: Review and future evolutionary path. *Renew. Energy* **2016**, *89*, 695–705. [CrossRef]
58. Kilinc-Ata, N. The evaluation of renewable energy policies across EU countries and US states: An econometric approach. *Energy Sustain. Dev.* **2016**, *31*, 83–90. [CrossRef]
59. Hills, J.M.; Michalena, E. Renewable energy pioneers are threatened by EU policy reform. *Renew. Energy* **2017**, *108*, 26–36. [CrossRef]
60. Zachmann, G.; Serwaah-Panin, A.; Peruzzi, M. When and How to Support Renewables?—Letting the Data Speak. In *Green Energy and Efficiency. An Economic Perspective*; Ansuategi, A., Delgado, J., Galarraga, I., Eds.; Springer: Cham, Switzerland, 2015; pp. 291–332.
61. Bosetti, V.; Carraro, C.; Massetti, E.; Sgobbi, A.; Tavoni, M. Optimal energy investment and R&D strategies to stabilize atmospheric greenhouse gas concentrations. *Resour. Energy Econ.* **2009**, *31*, 123–137.
62. Kobos, P.H.; Erickson, J.D.; Drennen, T.E. Technological learning and renewable energy costs: Implications for US renewable energy policy. *Energy Policy* **2006**, *34*, 1645–1658. [CrossRef]

63. Popp, D.; Hascic, I.; Medhl, N. Technology and the diffusion of renewable energy. *Energy Econ.* **2011**, *33*, 648–662. [CrossRef]
64. Bointner, R. Innovation in the energy sector: Lessons learnt from R&D expenditures and patents in selected IEA countries. *Energy Policy* **2014**, *73*, 733–747.
65. Popp, D. Induced innovation and energy prices. *Am. Econ. Rev.* **2002**, *92*, 160–180. [CrossRef]
66. Botta, E.; Kózluk, T. *Measuring Environmental Policy Stringency in OECD Countries: A Composite Index Approach*; OECD Economics Department Working Paper No. 1177; OECD: Paris, France, 2014.
67. De serres, A.; Murtin, F.; Nicoletti, G. *A Framework for Assessing Green Growth Policies*; OECD Economic Department Working Paper; OECD: Paris, France, 2010.
68. Jarque, C.M.; Bera, A.K. A test for normality of observation and regression residual. *Int. Stat. Rev.* **1987**, *55*, 163–172. [CrossRef]
69. Brown, R.L.; Durbin, J.; Evans, J.M. Technologies for testing the constancy of regression relationships over time. *J. R. Stat. Soc. B* **1975**, *37*, 149–192.
70. Breusch, T.; Pagan, A. The LM Test and its application to model specification in econometrics. *Rev. Econ. Stud.* **1989**, *47*, 239–254. [CrossRef]
71. Breitung, J. The local power of some unit root tests for panel data. *Adv. Econom.* **2001**, *15*, 161–177.
72. Carrion-i-Silvestre, J.L.; Del Barrio-Castro, T.; Lópes-Bazo, E. Breaking the panels: An application to the GDP per capita. *Econom. J.* **2005**, *8*, 159–175. [CrossRef]
73. Pesaran, H.M. A simple panel unit root test in the presence of cross-section dependence. *J. Appl. Econ.* **2007**, *22*, 265–312. [CrossRef]
74. Pedroni, P. Panel cointegration: Asymptotic and finite sample properties of pooled time series tests with an application to the PPP hypothesis. *Econom. Theory* **2004**, *20*, 597–625. [CrossRef]
75. Banerjee, A.; Carrion-i-Silvestre, J.L. *Cointegration in Panel Data with Breaks and Cross-Section Dependence*; Working Paper No. 591; European Central Bank: Frankfurt am Main, Germany, 2006.
76. Westerlund, J. Testing for error correction in panel data. *Oxf. Bull. Econ. Stat.* **2007**, *69*, 709–748. [CrossRef]
77. Baum, C.F. Residual diagnostics for cross-section time series regression models. *Stata J.* **2001**, *1*, 101–104.
78. Greene, W. *Econometric Analysis*; Prentice-Hall: Upper Saddle River, NJ, USA, 2000.
79. Engle, R.; Granger, C.W.J. Cointegration and error correction: Representation, estimation, and testing. *Econometrica* **1987**, *55*, 251–276. [CrossRef]
80. Shmueli, G. To explain or to predict? *Stat. Sci.* **2010**, *25*, 289–310. [CrossRef]
81. Kao, C.; Chiang, M. On the estimation and inference of a cointegrated regression in panel data. *Adv. Econ.* **2000**, *15*, 179–222.
82. Pesaran, M.H.; Shin, Y.; Smith, R.P. Pooled mean group estimation of dynamic heterogeneous panels. *J. Am. Stat. Assoc.* **1999**, *94*, 621–634. [CrossRef]
83. Roodman, D. How to extabond 2: An introduction to difference and system GMM in stata. *Stata J.* **2009**, *9*, 86–136.
84. Sarafidis, V.; Yamagata, T.; Robertson, D. A test for cross section dependence for a linear dynamic panel model with regressors. *J. Econom.* **2009**, *148*, 149–161. [CrossRef]
85. Anderson, T.W.; Hsiao, C. Formulation and estimation of dynamic models using panel data. *J. Econom.* **1982**, *18*, 570–606. [CrossRef]
86. Arellano, M.; Bond, S. Some Tests of Specification for Panel Data: Monte Carlo Evidence and an Application to Employment Equations. *Rev. Econ. Stud.* **1991**, *58*, 277–297. [CrossRef]
87. Blundell, R.; Bond, S. Initial conditions and moment restrictions in dynamic panel data models. *J. Econ.* **1998**, *87*, 115–143. [CrossRef]
88. Nickell, S. Biases in dynamic models with fixed effects. *Econometrica* **1981**, *49*, 1417–1426. [CrossRef]
89. Judson, R.H.; Owen, A.L. Estimating dynamic panel data models: A guide for macroeconomists. *Econ. Lett.* **1999**, *65*, 9–15. [CrossRef]
90. Bruno, G. Approximating the bias of the LSDV estimator for dynamic unbalanced panel data models. *Econ. Lett.* **2005**, *87*, 361–366. [CrossRef]
91. Baltagi, H.B. *Econometric Analysis of Panel Data*, 3rd ed.; John Willey & Sons, Ltd.: Chichester, UK, 2005.
92. Popp, D. Innovation in climate policy models: Implementing lessons from the economics of R&D. *Energy Econ.* **2006**, *28*, 596–609.

93. Baccini, L.; Urpelainen, J. Legislative fractionalization and partisan shifts to the left increase the volatility of public R&D expenditures. *Energy Policy* **2012**, *46*, 49–57.
94. Grubb, M. Technology innovation and climate change policy: An overview of issues and options. *Keio Econ. Stud.* **2004**, *41*, 103–132.
95. Bauen, A.; Berndes, G.; Junginger, M.; Londo, M.; Vuille, F.; Ball, R.; Bole, T.; Chudziak, C.; Faaij, A.; Mozaffarian, H. *Bioenergy: A Sustainable and Reliable Energy Source. A Review of Status and Prospects*; International Energy Agency: Paris, France, 2009.
96. Ambec, S.; Cohen, M.A.; Elgie, S.; Lanoie, P. *The Porter Hypothesis at 20: Can Environmental Regulation Enhance Innovation and Competitiveness?* Discussion Paper No. 11-01; Resources for the Future: Washington, DC, USA, 2011.
97. Kanda, W.; Mejia-Dugand, S.; Hjelm, O. Governmental export promotion initiatives: Awareness, participation, and perceived effectiveness among Swedish environmental technology firms. *J. Clean. Prod.* **2015**, *98*, 222–228. [CrossRef]
98. Adams, P.W.; Hammond, G.P.; McManus, M.C.; Mezzullo, W.G. Barriers to and drivers for UK bioenergy development. *Renew. Sustain. Energy Rev.* **2011**, *15*, 1217–1227. [CrossRef]
99. Domac, J.; Richards, K.; Risovic, S. Socio-economic drivers in implementing bioenergy projects. *Biomass Bioenergy* **2005**, *28*, 97–106. [CrossRef]
100. Marques, A.C.; Fuinhas, J.A. Drivers promoting renewable energy: A dynamic panel approach. *Renew. Sustain. Energy Rev.* **2011**, *15*, 1601–1608. [CrossRef]
101. McKay, H. Environmental, economic, social and political drivers for increasing use of wood fuel as a renewable resource in Britain. *Biomass Bioenergy* **2006**, *30*, 308–315. [CrossRef]

energies

MDPI

Article

The Recurrence Interval Difference of Power Load in Heavy/Light Industries of China

Chi Zhang [1], Zhengning Pu [1,*] and Jiasha Fu [2,3,*]

[1] School of Economics and Management, Southeast University, Nanjing 211102, China; anhuizhc@outlook.com
[2] Research Institute of Economics and Management, Southwestern University of Finance and Economics, 55 Guanghuacun Street, Chengdu 610074, China
[3] Survey and Research Center for China Household Finance, Southwestern University of Finance and Economics, 55 Guanghuacun Street, Chengdu 610074, China
* Correspondence: puzhengning@seu.edu.cn (Z.P.); fujiasha@chfs.cn (J.F.); Tel.: +86-138-1398-0089 (Z.P.); +86-138-1167-2308 (J.F.)

Received: 25 October 2017; Accepted: 31 December 2017; Published: 3 January 2018

Abstract: The significant fluctuation of industrial electricity consumption has a high impact on power load, which makes the research on recurrence intervals between extreme events of theoretical and practical significance. The study uses a high-frequency data of heavy and light industries and employs recurrence interval analysis in different thresholds. We find that the reoccurrence interval of volatility can fit with the stretched exponential function and the probability density functions of recurrence intervals in various thresholds shows a scaling behavior. Then, the conditional probability density function and the multifractal detrended fluctuation analysis demonstrate the existence of short-range correlation, long-range correlation, and multifractal properties, respectively. We further construct a hazard function, introduce recurrence intervals into VaR calculation and establish a functional relationship between average recurrence interval and threshold. Following this result, we also shed light on policy discussion for multi-industrial electricity supply management.

Keywords: electricity fluctuation; recurrence interval analysis; risk estimation

1. Introduction

Over the past few decades, China has snowballed and surpassed Japan in 2010 to become the world's second-largest economy [1]. As for energy consumption, China's electricity consumption has also exceeded the United States in 2011 and ranked number one in the world [2]. In 2016, China's total electricity consumption was 5.92 trillion kWh with an annual growth rate of 5.0%. Figure 1 shows the proportion of electricity consumption of each industry in China. Compared to 2015, electricity consumption of the tertiary industry increased by 11.2% and continued to maintain a high growth rate, indicating that service consumption led the growth of China's economy. The electricity consumption of urban and rural household industry, secondary industry, and manufacturing industry increased by 10.8%, 2.9%, and 2.5%, respectively. For the four major energy-consuming sectors (Steel, Nonferrous Metals, Building Materials, Chemistry), the electricity consumption barely increased. Such non-increase is because it is apparently for equipment manufacturing, emerging technologies, and mass consumer goods industries, reflecting that the readjustment and upgrading of the industrial structure have a positive effect and the power consumption structure is continuously optimized. By the end of 2016, China's total power generation installed capacity was 1.65 billion kW with an annual increase of 8.2%, which further aggravated overcapacity in some areas. The non-fossil energy generation continued to increase, and the utilization of thermal power equipment further reduced to 4165 hours, which is the lowest since 1964. In summary, the overall electricity supply and demand in China was loose with a relative surplus in some areas [3]. Regarding price, the electricity price for industries is negotiated

in most times which varies in different regions. For example, we can see from Figure 2 that the price in developed areas such as Shanghai is higher than that in developing areas like Xinjiang (See http://www.askci.com/news/chanye/20161020/13442871189.shtml).

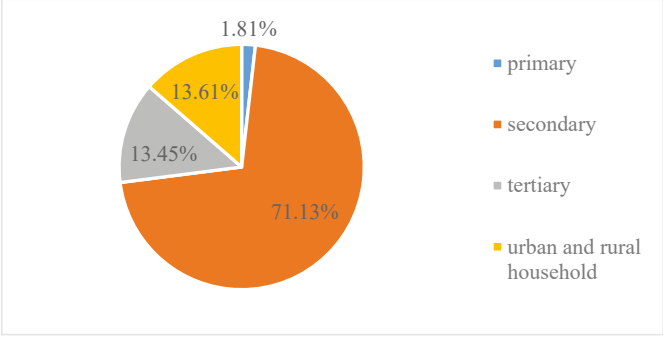

Figure 1. China's electricity consumption of each industry in 2016.

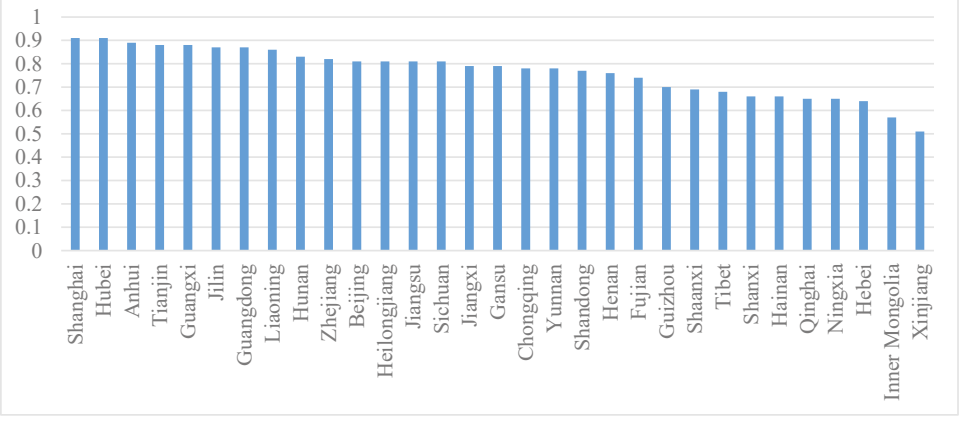

Figure 2. Price of industrial electricity in various provinces of China in late August 2016 (Unit: Yuan).

At the same time, the complexity of power consumption structure was also rising all over the country, which made regional electricity management a huge challenge both for public administrations and for power supply corporations. Therefore, since the year 2015, China has started a new round of electricity reform, which mainly included projects like power transmission, distribution price reform, energy market construction, electricity trading institution establishment and electricity supply reform. All of these projects require China's electricity supply companies to rebuild their organization structure and upgrade management plans to deal with more intense market competition. Accurately predicting the trend and change of regional/sector electricity consumption by energy consumption modeling can help electricity companies optimize their management strategies, reduce operation cost and prevent potential power supply risks, and can also help the nation save resources, avoid waste and reduce infrastructure over-investment.

As shown in Figure 1, China's energy consumption concentrated in the industrial sector. For enterprises belonging to different industry sectors (i.e., heavy industry or light industry), the power loads have quite a different magnitude. As is well known, people are more interested in large electricity fluctuations than small ones. For example, in a particular area, if the power load of light industry

enterprise reaches its peak, the power supply network in the area will not feel the pressure. However, if a heavy industry enterprise exceeds its peak power, this may pose an enormous risk of grid paralysis or even serious accidents, which would usually spread and cause an immeasurable damage and suffering to the society. Such differences require power supply companies to differentiate their load management strategies for different industries. Hence, analysis and comparison of heavy/light industrial electricity consumption patterns, especially the extreme electricity events will provide a theoretical foundation and practical guidance, which can help power supply companies avoid grave accidents, ensure the stability of power supply operation and keep power transfer equipment safe.

Due to the availability of real-time power load data, forecasting extreme events in electricity market becomes possible. In this paper, we use 15-min high-frequency electricity load data from two companies (one belongs to heavy industry, another belongs to light industry) for the city of Nanjing in China to study the recurrence pattern between fluctuations. The questions we tried to answer are as follows: How to describe the volatility behavior? If a massive volatility occurred, will it happen again or not? When will the next significant fluctuation occur? How to estimate the occurrence probability and the time interval between two extreme events?

Our study, therefore, contributes to the literature in the following perspectives. First, among plenty studies that have done in the electric field, research on the electricity consumption pattern between heavy and light industry is rare. So far as we know, this is the first paper to focus on the industrial difference of power load from a policy perspective. Second, as a major city with a fast-growing economy in China, Nanjing, the capital of Jiangsu province, has an urgent demand for energy especially electricity. Research on Nanjing can be a useful guide for other emerging first-tier cities in China. Most previous studies on Jiangsu area only use daily data [4–7] while here we use high-frequency data which can help to capture more specific properties. Finally, different from many studies using power law to model rare events in many fields [8–13] including electricity markets [14,15], we use the stretched exponential function to analyze the extreme events [16–18]. Unlike the power-law which displays a linear relationship in log-log plots, stretched exponential function has a significant curvature in log-log plots which can better describe the natural phenomena in nature and economy [19].

The rest of this paper is arranged as follows: Section 2 reviews current studies. Section 3 describes the method and presents basic statistics of the data set. Section 4 initials an empirical research, including distribution function, scaling properties, memory effect and risk estimation. Section 5 delivers management policy implications discussions for China's power supply company. Section 6 concludes.

2. Literature Review

Currently, plenty of models have been applied to forecast electricity load, and most of them can be classified into three categories: regression, data series analysis, and neural network.

Regression analysis considered power load as a dependent variable of other factors, such as weather or holidays [20], and tried to construct a function relationship between electricity load and other influence factors [21]. Such results were confirmed by the reality in some residential areas [22]. With technology evolving, a decomposition model was applied, and many vital factors were pinned in the evolution progress [23]. Also, GDP [24], income [24], seasonal variations [25], etc. were all confirmed to be relevant to electricity load forecast by regression analyses. In the 21st century, the emergence of smart technology could help researchers grab high-frequency data from a personal level and add human behavior into a regression model to improve the forecast accuracy [26,27]. Briefly, regression analysis aimed to describe the quantitative relationship between the observed variables in statistics, however, it could not capture the spatiotemporal variation and is sometimes restricted by the data volume.

Time series analysis considered that the electricity load pattern was a time series signal, which could be used to predict the future load with historical data [28]. With technology development, various time series models have been proposed [29]. Carmine et al. [30] applied time-series analysis model to the electricity consumption of public transportation in Sofia (Bulgaria) in 2011, 2012 and 2013 and

detected a periodic pattern, which could be used to improve electricity management. Dong et al. [31] proposed a hybrid model to predict residential load hour and day ahead with five different algorithms and the results improved prediction accuracy. Liang and Liang [32] proposed a mathematical hybrid method to analyze electricity demand in China and predicted the demand evolution in the next five years from 2016 to 2020. Though the predictable time spectrum of time series analyses varies from one hour to several years, the claim to the accuracy of historical data was very high. The algorithm might be complex and unstable in some cases. Additionally, when applying in short-term power load forecast, it was not sensitive to weather factors and not able to solve the inaccuracy problem caused by meteorological factors.

Artificial neural networks (ANNs) could estimate future loads with previous data without the presumption of the functional relationship between electricity load and other relative variables [29]. Compared with traditional methods, ANN was better at dealing with nonlinear relationships [33]. At present, the neural network was well applied in various fields including electric load forecasting [34–37]. Moreover, the integration of ANN and other methods has become a research hotspot. ANN was integrated with fuzzy logic [38], genetic algorithm [39], wavelet analysis [40,41], chaos theory [42], grey system [43], etc. However, ANN has its limitations: it is hard to avoid learning deficiency or over-fit phenomena, and the convergence speed is slow and easy to fall into local minima.

In this paper, we will use a different method: recurrence interval analysis (RIA), which belongs to time series analysis, to investigate the fluctuation characteristics of heavy/light industries. RIA has been widely used to analyze extreme events in many fields, for example, climate [44], earthquake activities [45,46], heartbeat monitoring [47,48] and financial volatility [49,50]. These events occur with a high magnitude and low probability. For a long time in the past, extreme events were assumed to be spontaneous, namely mutually uncorrelated. Nevertheless, researchers show that extreme events do not occur independently; contrarily, they gather and happen in a relatively short period. RIA focuses on the electricity fluctuation rather than the power load, which is good at depicting the volatility pattern and estimating the risk. Assuming occurrence probability of future events is constant and dependent on past events, RIA can estimate the probability of the events to happen again in the future. Here, Recurrence interval means the time interval between two consecutive events beyond (under) one certain threshold, which can be positive or negative. It is also powerful to characterize the fluctuation behaviors in different magnitudes [51] and sometimes even to construct a relationship among them.

3. Data Description

The data in this paper is extracted from the transformer of each corresponding area in 15-min frequency, and we chose two enterprises, which represented heavy and light industries, respectively. In the national economy, heavy and light industries refer to the sectors which provide capital and consumption goods, respectively. Heavy industry includes steel industry, metallurgical industry, machinery, energy (electricity, oil, coal, natural gas, etc.), chemistry and materials science. These industries provide technical equipment, power and raw materials for all branches of the national economy. Light industry mainly includes foodstuff, textile, leather, papermaking, daily chemical industry, culture, education and sporting goods industry. According to the data from National Bureau of Statistics of China, the finished goods of heavy and light industry were 2.608 and 1.341 trillion yuan in 2015, respectively (See http://data.stats.gov.cn/easyquery.htm?cn=C01&zb=A0E010D&sj=2015). In this paper, we select a steel/textile enterprise to represent the heavy/light industry. The sample period was from 1 January 2016 through 31 December 2016 and finally we ended up with 35,316 electricity load observations. The returns of time series are calculated by taking differences of the load as:

$$r(t) = l(t) - l(t - \Delta t) \tag{1}$$

where $l(t)$ is the electricity load (unit: kW) of the tth time and $\Delta t = 15$ because the data is 15-min frequent. Figure 3 shows the returns of heavy/light industries and Figure 4 is the frequency distribution of fluctuation. The statistics are summarized in Table 1.

Figures 3 and 4 and Table 1 show that the returns are not normally distributed. One has a sharp peak, and another has platy kurtosis. Though their average and standard deviation values have magnitude difference, the two industries also have common properties, like skewness. From Figure 3, it is clear that there are zero values in Figure 4b, which means in a specified period, the light industry enterprise was not in operation. When combining with Table 1, we can see that even a large company could not operate continually, which is the reason why the minimum values are both zero and why we used different values to describe fluctuation.

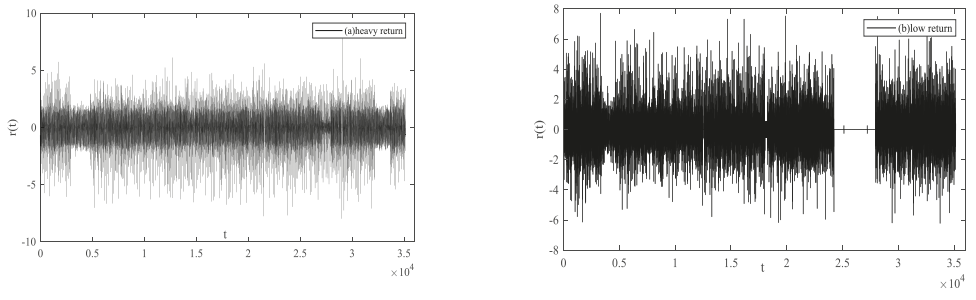

Figure 3. Returns of heavy/light industries. (**a**) Heavy return; (**b**) Low return.

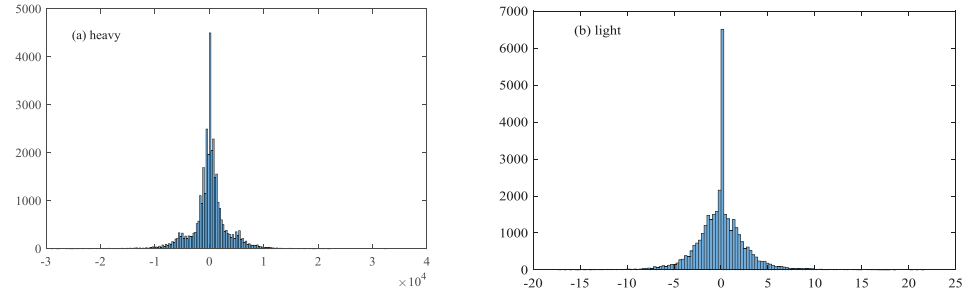

Figure 4. Frequency distribution of fluctuation. (**a**) Heavy; (**b**) Light.

Table 1. Statistics of the returns of heavy/light industries.

	Average	Maximum	Minimum	Std.	Skewness	Kurtosis	Nobs
Light	10.21	47.40	0	8.18	0.84	3.20	35,316
Heavy	1.54×10^4	3.70×10^4	0	8.70×10^3	0.61	1.91	35,316

The x-ray of Figure 5 is the value of threshold q, and y-ray is the number of extreme events of q; q measures the volatility of the normalized $r(t)$. Due to magnitude discrepancy of electricity consumption between heavy and light industries, we normalize the fluctuation for comparison purposes and the results are shown in Figure 5. It can be clearly seen that the number decreases with an increasing q, indicating that a larger fluctuation has less occurring probability, which is in accordance with reality. The slope is getting smaller when q increases for each curve, and there is an intersection point in the figure, indicating that small fluctuations more likely happen in heavy industry and larger volatilities more likely happen in light industry.

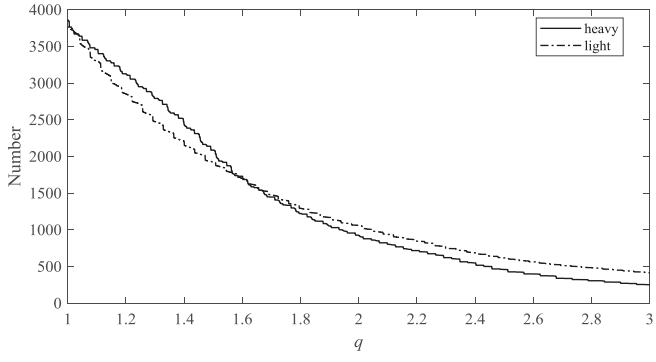

Figure 5. Number of extreme events of different threshold q.

4. Results

4.1. Probability Density Function

Consider τ as the recurrence interval when threshold is q, the overwhelming consensus is that the recurrence intervals of volatility are distributed as a stretched exponential.

$$f(x) = \alpha\overline{\tau}e^{-(\beta\overline{\tau}x)^{\gamma}} \tag{2}$$

In Equation (2), $\overline{\tau}$ is the mean recurrence interval that depends on the threshold q, where the probability distribution function of recurrence interval τ is $P_q(\tau)$, and α, β, γ are the parameters [16–18], where α and β are the coefficients related to the threshold q, while γ is the correlation exponent reflecting the long term memory of the recurrence intervals.

We normalize the returns of each series by dividing its standard deviation: $R(t) = \frac{r(t)}{[Er(t)^2 - E^2 r(t)]^{1/2}}$, where $[Er(t)^2 - E^2 r(t)]^{1/2}$ is the standard deviation of $r(t)$. For each threshold q, we can obtain a data set of recurrence interval τ, and then get the probability density function of τ. The q here is positive ($q > 0$) because our interest is the overload operation of the electrical system. The empirical parameters of the probability distribution function $P_q(\tau)$, calculated by maximum likelihood estimation are shown in Table 2.

Table 2. Estimates of the coefficients of stretched exponential functions.

Industry	q	α	β	γ
Heavy	1.0	0.031	0.090	0.684
	1.2	0.025	0.075	0.648
	1.4	0.018	0.058	0.587
	1.6	0.012	0.041	0.519
	1.8	0.008	0.029	0.448
Light	1.0	6.880	261.870	0.171
	1.2	5.072	193.056	0.170
	1.4	3.684	149.838	0.168
	1.6	2.542	115.224	0.165
	1.8	1.564	87.587	0.163

Note that the coefficients of the exponent γ of large enterprises are in the range between 0.448 and 0.684, while the corresponding exponents of the light enterprises are much smaller within the interval (0.163, 0.171). It is obvious that the long-term memory effect in the recurrence intervals of electricity usage in large enterprises dies out faster than that in light companies.

Figure 6 shows that first, for large fluctuations, $P_q(\tau)$ decays slowly, indicating that with q rises, recurrence intervals will be longer, in accordance with the fact that large fluctuations have more long intervals and less short intervals than small fluctuations. Second, when threshold q is fixed, $P_q(\tau)$ decreases with increasing recurrence interval τ. This implies that when the previous fluctuation occurred t units of time ago, if $\Delta t_1 < \Delta t_2$, the probability $P_q(\tau)$ of the next fluctuation to occur after Δt_1 is larger than Δt_2. The result suggests that if the enterprise suffers a huge electricity load rise, the enterprise should be aware that the probability that if another large load rise occurs within a shorter time interval it is likely to be larger with a longer time interval. Moreover, when recurrence interval is fixed, $P_q(\tau)$ increases with q. If an extreme event occurs, the probability that another extreme event occurs will be higher for a larger threshold q. Last, comparing Figure 6a,b, we can find for a same threshold q, $P_q(\tau)$ decreased faster along with τ for heavy enterprises than low enterprises, indicating that the probability of large fluctuations of heavy enterprise is less than light enterprise, which in accordance with the fact that heavy industry is less risk-taking to large volatility than light industry.

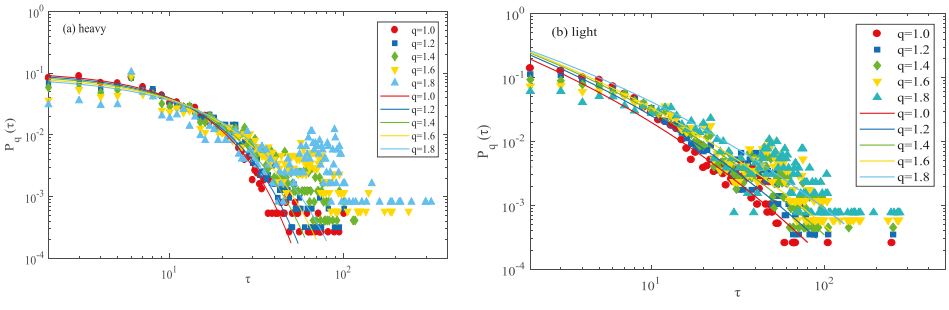

Figure 6. Empirical probability distribution of recurrence intervals with different thresholds. (**a**) Heavy; (**b**) Light.

From Figure 6, it can be seen that with q rising, recurrence intervals will be longer, in agreement with the fact that large fluctuations have more long intervals and less short intervals than small fluctuations, which means for large fluctuations, there is a higher probability that the time intervals between two consecutive events will increase.

Besides, by the observations in Table 2 and Figure 6, we find all the probability density function curves have similar shapes, which make us wonder whether there is a scaling behavior between these probability density functions? To examine that, we use Yamasaki et al.'s [52] method. Not only discovering the scaling behavior of events of different thresholds, but it can also efficiently solve the problem of insufficient data.

$$f_q(\tau/\overline{\tau}) = P_q(\tau)\overline{\tau} \tag{3}$$

where $\tau/\overline{\tau}$ is scaled recurrence interval and $P_q(\tau)\overline{\tau}$ is scaled PDFs. When threshold q changes, $\overline{\tau}$ changes and there is $(d\overline{\tau})/(dq) > 0$, indicating that with volatility increases, the mean time of recurrence interval increases, which is consistent with the fact. If $f_q(\tau/\overline{\tau})$ is independent to q, then there will be a unique function $f(x)$, for different threshold q.

$$f_q(x) = f(x) \tag{4}$$

Namely, the scaled probability distribution $f_q(\tau/\overline{\tau})$ will converge to the single curve $f(\tau/\overline{\tau})$ and recurrence intervals have a scaling behavior. To test that, we picture the scatter diagram of $f_q(\tau/\overline{\tau})$ as the function of $\tau/\overline{\tau}$ in Figure 7. It can be seen that for different thresholds q, $P_q(\tau)\overline{\tau}$ converge to one curve regardless of which enterprise it belongs, indicating that there exists a scaling behavior and we can deduce the behavior characteristics of large fluctuations by those of small fluctuations.

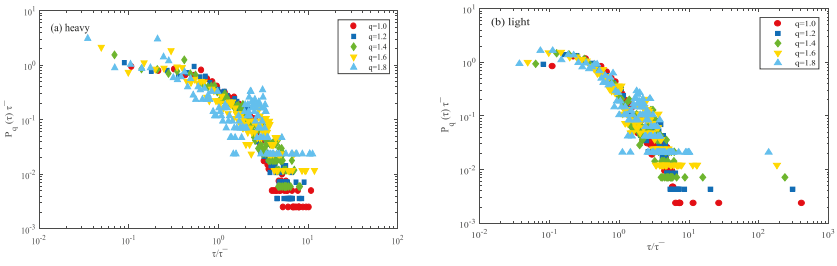

Figure 7. Scaled probability distributions of recurrence intervals with different thresholds. (**a**) Heavy; (**b**) Light.

4.2. Memory Effect

4.2.1. Short-Term Memory

Short-term memory means that small τ tends to follow small τ_0, and big τ tends to follow big τ_0. The conditional probability density functions $P_q(\tau|\tau_0)$ [52] can be used to reflect the occurrence probability of a recurrence interval τ immediately after the recurrence interval τ_0. If there is no short-term memory, $P_q(\tau|\tau_0)$ is independent of τ_0. However, due to the insufficiency of interval sample, it is impossible to calculate $P_q(\tau|\tau_0)$ for a single value τ_0. In order to obtain more data, we adopt a method based on the idea of coarse-graining [53–55] and calculate $P_q(\tau|\tau_0)$ for values of τ_0 in a certain interval instead of a single value τ_0. Specifically, for a given threshold q, all the recurrence intervals in the set T are sorted in an increasing order, and then we divide the set T into four non-overlapping subsets with the same size,

$$T = T_1 \cup T_2 \cup T_3 \cup T_4, T_i \cap T_j = \phi, i \neq j \tag{5}$$

where T_1 contains the smallest quarter while T_4 contains the largest. Then we estimate the conditional probability density functions:

$$P_q(\tau|T_i) = P_q(\tau|\tau_0 \in T_i) \tag{6}$$

If there is no short-term memory, we should find

$$P_q(\tau|T_i) = P_q(\tau|T_i), i \neq j \tag{7}$$

Figure 8 shows the results of $P_q(\tau|\tau_0)\overline{\tau}$ as a function of $\tau/\overline{\tau}$ for τ_0 in the smallest subset T_1 (filled symbols) and the largest subset T_4 (open symbols). Obviously, no matter for heavy or light enterprises, $P_q(\tau|T_i) \neq P_q(\tau|T_i)$. We also find that $P_q(\tau|\tau_0 \in T_1)$ is bigger than $P_q(\tau|\tau_0 \in T_4)$ for small $\tau/\overline{\tau}$, while for big $\tau/\overline{\tau}$, $P_q(\tau|\tau_0 \in T_1)$ is smaller than $P_q(\tau|\tau_0 \in T_4)$ in Figure 8a,b. There exists very short-term memory in the recurrence intervals.

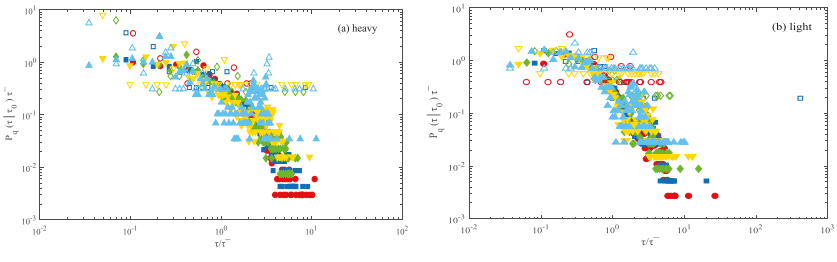

Figure 8. Conditional probability density functions $P_q(\tau|\tau_0)$ with $\tau_0 \in T_1$ (filled symbols) and $\tau_0 \in T_4$ (open symbols). (**a**) Heavy; (**b**) Light.

4.2.2. Long-Term Memory

Experience shows that scaling behavior and short-term memory is usually a foreshadowing of the long-term memory [56,57]. To figure out whether there exists long-term memory in electricity use of the high/light industries, we adopt the MF-DFA (multifractal detrended fluctuation analysis) method [56,58–60].

The conventional DFA method invented by Peng et al. (1994) [61], which is used to investigate the statistical self-affinity in time series analysis, but limited to scale the second order statistical moment of one-dimensional fractal time series by computing Hurst exponent.

In mathematics, a fractal is an abstract object used to describe and simulate naturally occurring objects. Artificially created fractals can exhibit similar patterns at increasingly small scales. So far several models applied in electricity market are proposed based on fractal theory [62–65]. With the study objects becoming increasingly diverse and complicated, fractal with a single exponent (the fractal dimension) is not capable of describing the dynamics in reality, like coastlines length, stock market time series, heartbeat dynamics, real-world scenes, etc. A continuous spectrum of exponents (singularity spectrum) is needed and then emerges the multifractal [66–69]. A multifractal system is a generalization of a fractal system and can be discovered in nature, which we can apply in a variety of practical situations such as electricity demand [70,71].

In 2002, Kantelhardt et al. [72] combined multifractal with DFA and put forward the MF-DFA, which can describe the multifractal characteristics of time sequence and computes the H(p) for all p-order statistical moments. As one practical method to test whether a non-stationary time series has multifractal characteristics, MF-DFA is widely applied in the financial markets [68], molecular biology [73], disaster prevention and control [69], power pricing analysis [74,75] and electricity market [71,76]. Assume the sample $X = \{x_k,\ k = 1,\ 2, \ldots, N\}$, the specific steps of this algorithm are as follows.

(1) Calculate the accumulated deviation N times of the original data and construct new time series:

$$Y = \left\{ y(i) = \sum_{k=1}^{i} (x_k - \overline{x}),\ k = 1, 2, \ldots, N \right\} \tag{8}$$

where $\overline{x}$ is the average of X.

(2) Divide new series Y into forward and backward direction, separately; the length of each unit is s, end up with $2N_s$ non-overlapping section with equal length, and $N_s = int(N/s)$, $int()$ is integer-valued function, which avoids information loss if N cannot be divisible by s.

(3) Use least square method for each new subinterval $v(v = 1,\ 2, \ldots, 2N_s)$ to curve-fitting, get first-order or multi-order local trend function $y_v(j)$. When $v = 1,\ 2, \ldots, N_s$, calculate residual sequence of subinterval v, when $v = N_s + 1, \ldots,\ 2\ N_s$,

$$Z_v(\mathrm{j}) = \frac{1}{s} \sum_{j=1}^{s} \{ Y[N - (v - N_s)s + i] - y_v(j) \} \tag{9}$$

(4) Calculate p-order volatility function of sequence

$$F^2(s, v) = \frac{1}{s} \sum_{j=1}^{s} {Z_v}^2(j), v = 1,\ 2, \ldots, 2\ N_s \tag{10}$$

$$F_p(\mathrm{s}) = \begin{cases} \left\{ \frac{1}{2N_s} \sum\limits_{v=1}^{2N_s} \left[F^2(s, v)^{p/2} \right] \right\}^{1/p}, p \neq 0 \\ \exp\left\{ \frac{1}{4N_s} \sum\limits_{v=1}^{2N_s} \left[F^2(s, v) \right] \right\}, p = 0 \end{cases} \tag{11}$$

when $p = 2$, it is standard DFA.

(5) Based on Equation (10), we know $F_p(s)$ is positively correlated with s, with log-log coordinate, we have

$$F_p(\mathrm{s}) \sim s^{h_p} \tag{12}$$

where h_p is Hurst exponent, for non-stationary time series, only when $0.5 < h_p < 1$, this series has a long-term correlation, indicating that the system has the fluctuation pattern in long-term evolution. When h_p is the function of p, $X(t)$ has multiple fractal characteristics.

In Figure 9, there are ten subfigures, and each subfigure has four sub-subfigures, which show the results of MF-DFA, respectively. It can be seen that the p-order Hurst exponent of each line is higher than 0.5 in a certain area, suggesting that long-term correlations and multifractal characteristics exist in the recurrence intervals. When $h_p < 0.5$; it means the volatility is of anti-continuity.

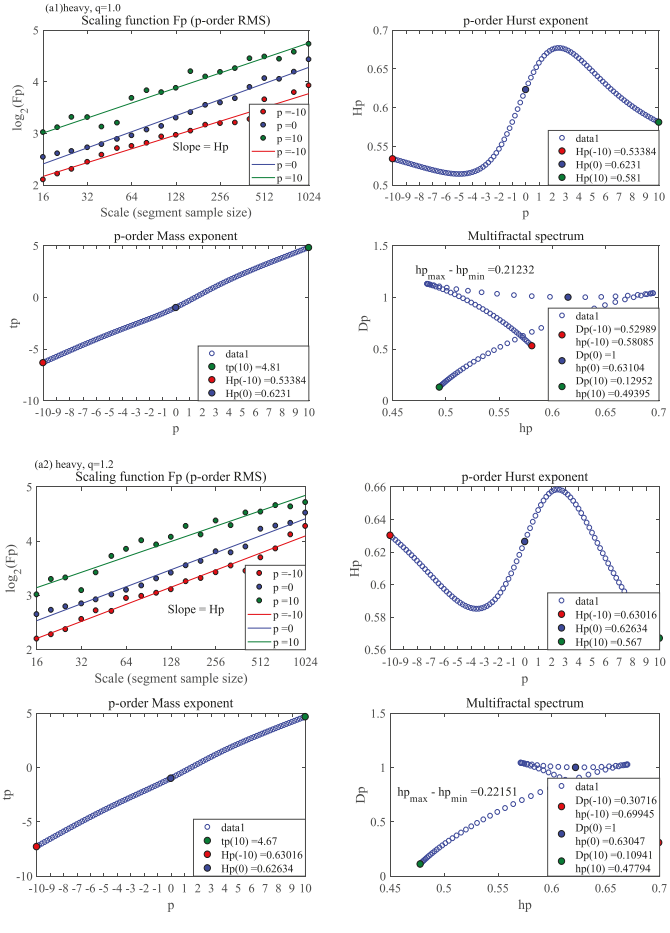

Figure 9. *Cont.*

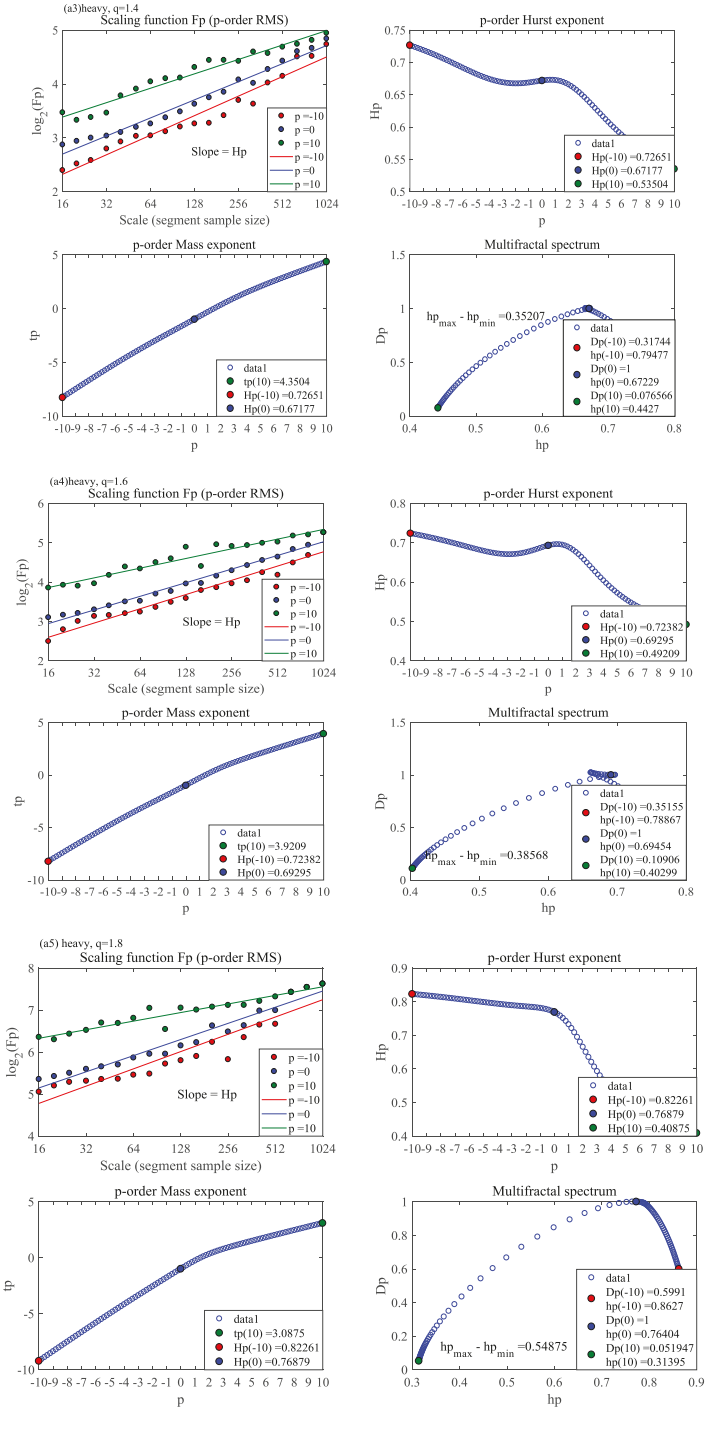

Figure 9. *Cont.*

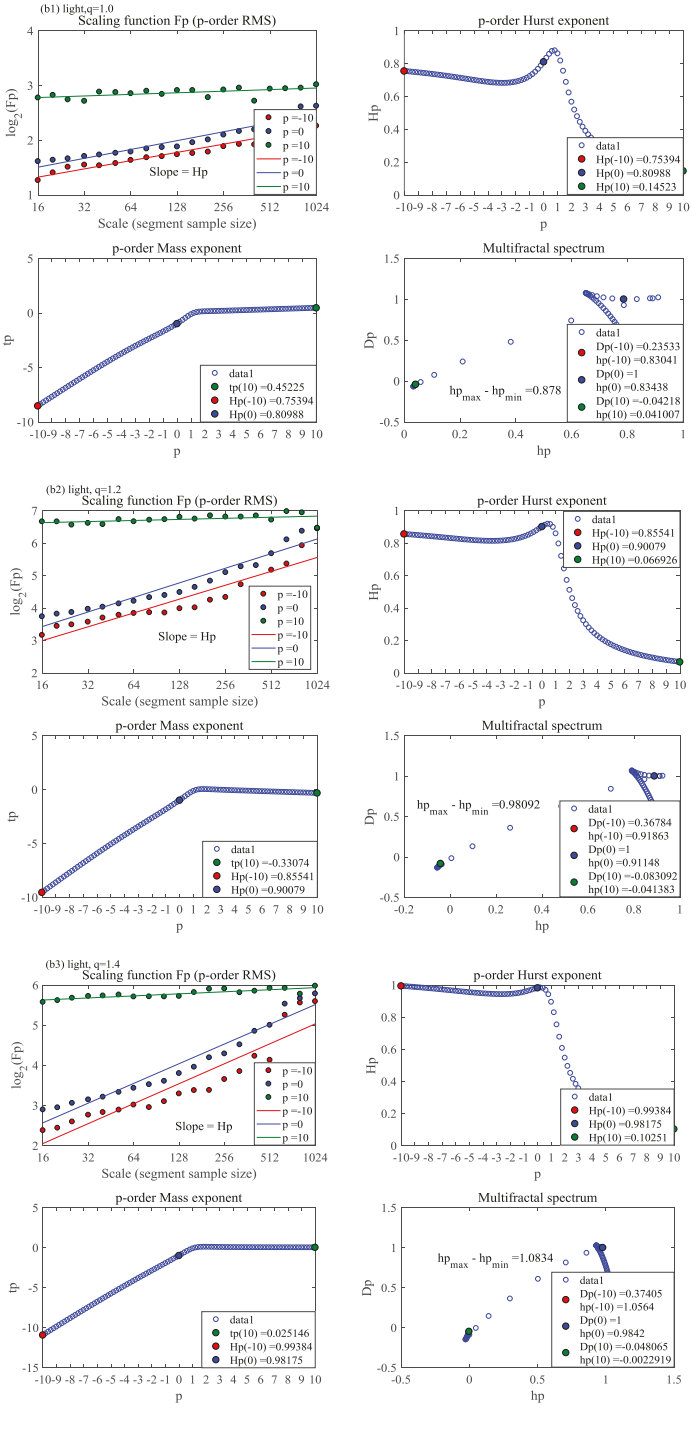

Figure 9. *Cont.*

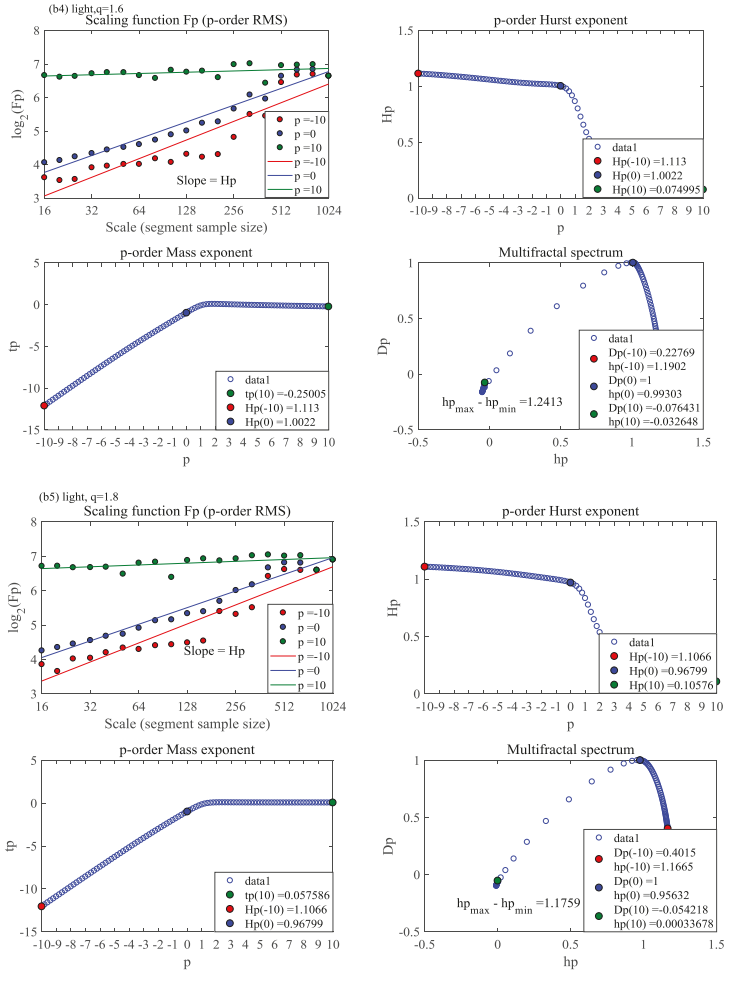

Figure 9. MF-DFA of heavy/light industry in different thresholds. (**a1**) Heavy, q = 1.0; (**a2**) Heavy, q = 1.2; (**a3**) Heavy, q = 1.4; (**a4**) Heavy, q = 1.6; (**a5**) Heavy, q = 1.8; (**b1**) Light, q = 1.0; (**b2**) Light, q = 1.2; (**b3**) Light, q = 1.4; (**b4**) Light, q = 1.6; (**b5**) Light, q = 1.8.

4.3. Risk Estimation

The hazard probability function $W_q(\Delta t|t)$ is an important method to estimate risk in recurrence interval analysis. Considering the fact that t units of time have passed since last large volatility is greater than q occurred, what fascinates us is the probability that the next large volatility greater than q will occur within Δt units of time. The hazard probability function is as follows:

$$W_q(\Delta t|t) = \frac{\int_t^{t+\Delta t} P_q(\tau)d\tau}{\int_t^{\infty} P_q(\tau)d\tau} \tag{13}$$

we can calculate the theoretical value of $P_q(\tau)$ with the parameters given in Table 2 if the distribution $P_q(\tau)$ fits with a stretched exponential index, and calculate the empirical value by rewriting $W_q(\Delta t|t)$ into:

$$W_q(\Delta t|t) = \frac{count(t < \tau_q \leq t + \Delta t)}{count(\tau_q > t)} \tag{14}$$

where "$count(\tau_q > t)$" is the number of recurrence intervals greater than t and "$count(t < \tau_q \leq t + \Delta t)$" is the number of recurrence intervals greater than t and less than $t + \Delta t$ for a given q.

Figure 10 is the hazard function; the symbols are empirical values and the curves are the theoretical values of $W_q(\Delta t = 15|t)$. We can observe that they are fitted very nicely and the discrepancy between empirical and theoretical curves decreases when t increases. Furthermore, $W_q(\Delta t = 15|t)$ decreases with increasing t, confirming that recurrence intervals exhibit clustering behaviors and long-term memory between volatilities and theoretical values will overestimate the risk in a short time period. For a given threshold q, we can calculate the recurrence probability of extreme events.

For risk estimation, value at risk (VaR) is widely applied. Here we use loss probability density function to define the risk at rising q: $\int_{-\infty}^{q} P(R)dR = P^*$, where $P(R)$ is the probability density function of normalized series $R(t)$, and P^* is the rise probability. The mean recurrence interval $\overline{\tau}_q$ is:

$$\overline{\tau}_q = \frac{1}{N_q} \sum_{i=1}^{\tau_q} \tau_{q,i} \tag{15}$$

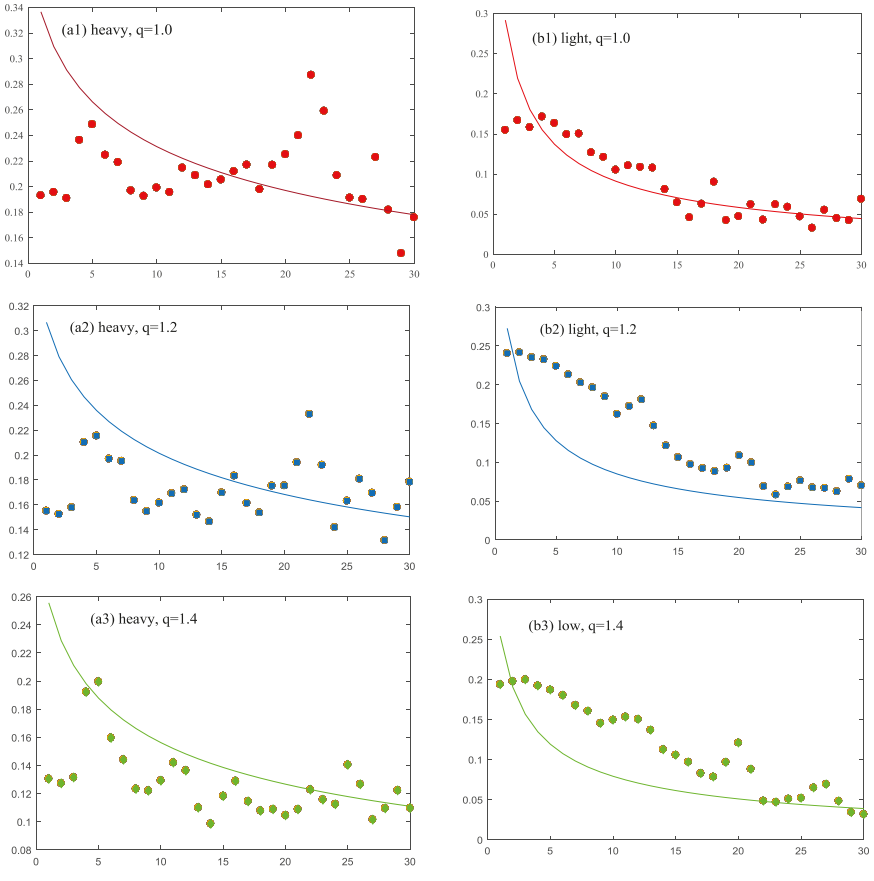

Figure 10. *Cont.*

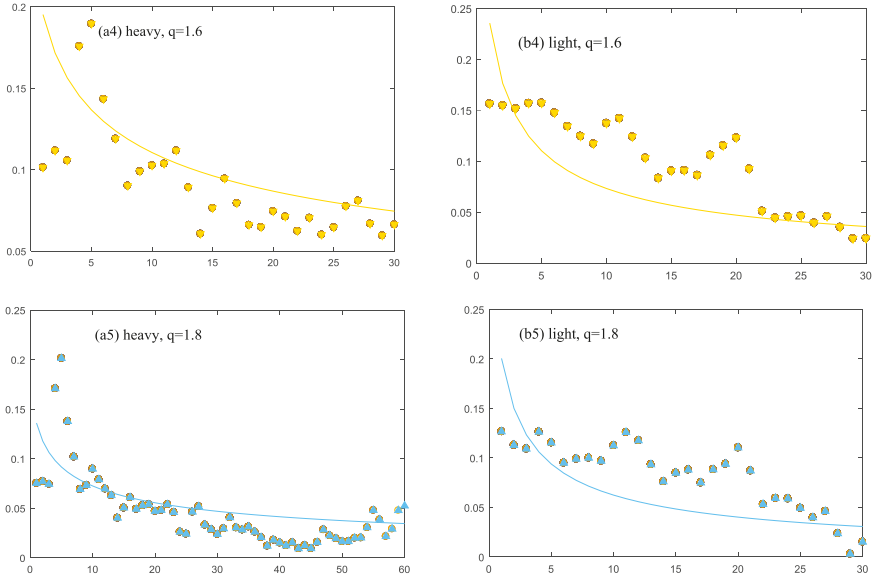

Figure 10. Theoretical (curves) and empirical (color symbols) value of $W_q(\Delta t = 15|t)$ (x-rays are t, y-rays are values of $W_q(\Delta t = 15|t)$).

N_q is the number of recurrence intervals below the threshold q, $\sum_{i=1}^{\tau_q} \tau_{q,i}$ is the total number of recurrence returns. Then the relation between mean recurrence interval and VaR can be expressed as:

$$1/\overline{\tau}_q = \int_{-\infty}^{q} P(R)dR = \frac{\text{number of } R(t) \text{ below } q}{\text{total number of } R(t)} \tag{16}$$

Equation (16) means that one$/\overline{\tau}_q$ defines the rise probability of q which is depicted in Figure 11. If one wants to know the risk level at 1% probability of rise they can find the q for $1/\overline{\tau}_q = 1\%$, which is the VaR one is looking for.

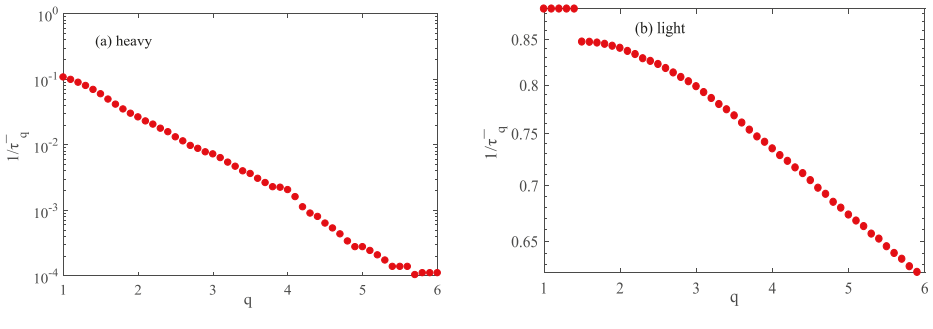

Figure 11. The reciprocal of mean recurrence interval one$/\overline{\tau}_q$ as a function of threshold q ($q = 1:6$). (**a**) Heavy; (**b**) Light.

5. Discussion

In the context of China's new round of power reform, according to the empirical analysis above, we propose several suggestions for power supply companies in various regions of China to promote future management.

Firstly, based on the analysis of probability density function and risk estimation, we can see that the power load of light industry is more likely to fluctuate than for heavy industry in China. Such fluctuation difference means that the power companies need more intensive and meticulous maintenance of the electricity load in the light industry, which is supported by all analyses including the risk analysis. However, since the power load consumed by the heavy industry is much higher than that of the light industry at the same time interval, the management of the heavy industry should be more biased towards safety checks of the pre-process and the normative constraint of the overall operation flow instead of increasing the times of maintenance of the electricity load.

Secondly, power enterprises can make load and customer management based on the analysis of load data. Power companies can increase the communication with their clients, plan the line redundancy, enlarge load redundancy of the existing heavy industry and eliminate the risk of equipment damage caused by capacity loads. Also, the electric power enterprise should incorporate the improvement of electricity utilization rate into management assessment, through the introduction of clean energy and distributed energy, and improve energy supply structure, to cope with the effects of the large power enterprises' sudden peak with least environment negative externalities.

Thirdly, existing power companies should pay more attention to the fluctuation characteristics of different industries to realize optimal management expenditure. As we demonstrated in Section 4, the enterprises of two distinct industries in this study have some similarities in fluctuation pattern, which makes it possible to use similar management strategies for maintaining related equipment. Moreover, the difference between the two enterprises' load peaks allows the power companies to design different maintenance teams to eliminate frequency to optimize the cost of management and maintenance.

Finally, an electric power company can make use of the correlation between small and large fluctuations, especially small fluctuations, and provide them as a value-added services to the existing large power customer to increase corporate earnings in this competitive market. For example, using the current fluctuation trends, the power enterprises can fully expect the changes of large fluctuations according to the characteristics of small fluctuations in the relevant industries. Based on pre-judgment, power companies can design different energy storage or line maintenance and support strategies, pack these strategies into different packages, and offer them to energy consumers in the form of value-added services. It can improve the efficiency of regional energy utilization, optimize local network and equipment management of electric circuitry, and also can bring extra income for the electric power company and improve the survivability of the electric power enterprises under the market reform.

6. Conclusions

The paper uses recurrence interval analysis to investigate the property of recurrence intervals of electricity fluctuations of heavy/low industries in China for different thresholds using 15-min high-frequency data, attempting to understand the behaviors of large volatilities in different industries.

First, we observe the distribution functions of recurrence and find the results that for different thresholds, the probability density function fits the stretched exponential function. We found that there is scaling behavior in the distributions for different thresholds after the recurrence intervals are scaled with the mean recurrence interval. Then we use conditional probability density function and MF-DFA to investigate the short-term, long-term memory and multi-fractural characteristics separately, indicating that the clusters of recurrence intervals of volatilities are not only caused by present conditions, but also long-term correlations. Later, we apply recurrence interval analysis to evaluate the risk of heavy/light industries, which provide relatively accurate estimates of hazard and

forge a link between loss possibility and VaR. Finally, we propose management suggestions to Chinese energy supply companies based on all previous analyses.

Of course, this paper still has deficiencies. For example, other forecasting methods could be used or more enterprises from heavy/light industry could be chosen to test the robustness of research results. These deficiencies could be perfected by subsequent researchers to help energy company administrators evaluate risk.

Acknowledgments: This research is supported by the China Social Science Fund (fund number 15AJL004, 15CJL048), the Fundamental Research Funds for the Central Universities (fund number 3214007103), the 111 Project (fund number B16040), and the Elementary Research Fund of Southeast University (fund number 2242017S10008).

Author Contributions: Chi Zhang conceived and designed the experiments; Zhengning Pu and Jiasha Fu performed the experiments; Chi Zhang and Jiasha Fu analyzed the data; Zhengning Pu contributed analysis tools; Chi Zhang wrote the paper.

Conflicts of Interest: The authors declare no conflict of interest.

References

1. Gong, L.; Zhang, S. The Inability of Japan to Adapt to China's Rise and China's Strategic Response. *Contemp. Int. Relat.* **2014**, *24*, 27–31.
2. Mingli, P. The Global Electricity Report in 2015. 2015. Available online: http://www.trqgy.cn/report/201512/25892.html (accessed on 29 December 2015).
3. China Electricity Council. Analysis and Prediction Report on National Electricity Demand and Supply in 2017. 2017. Available online: http://www.cec.org.cn/yaowenkuaidi/2017-01-25/164285.html (accessed on 25 Januray 2017).
4. Hou, X.Y.; Qiu, W.; Ping, J.U.; Zhao, J.Q.; Luo, J.Y.; Zhu, H. Study of the Optimization of Under-frequency Load Shedding in Jiangsu Power Grid. *Jiangsu Electr. Eng.* **2008**, *27*. [CrossRef]
5. Ning, A.N.; Zhou, S.X.; Zhu, L.Z.; Wang, Q.H.; Zong-Xiang, L.U.; Wei, H.U.; Wang, X.Y. Analysis of 2006 Jiangsu power grid voltage stability influenced by load characteristics. *Electr. Power* **2006**, *39*, 16–20.
6. Xia, L.I. Regression Forecasting of the Power Load in Jiangsu Province. *Value Eng.* **2014**, *3*, 64–65.
7. Yang, J.Y.; Zhou, Q.; Zhao, H.D.; Tan, J. Affection study on load and electricity consumption of Jiangsu power grid during Spring Festival. *Power Demand Side Manag.* **2015**, *17*. [CrossRef]
8. Bunde, A.; Eichner, J.F.; Havlin, S.; Kantelhardt, J.W. Return intervals of rare events in records with long-term persistence. *Phys. A Stat. Mech. Appl.* **2004**, *342*, 308–314. [CrossRef]
9. Matthews, J.O.; Hopcraft, K.I.; Jakeman, E.; Siviour, G.B. Accuracy analysis of measurements on a stable power-law distributed series of events. *J. Phys. A Gen. Phys.* **2006**, *39*, 45. [CrossRef]
10. Chow, J. *Power-Law Distributions In Events Involving Nuclear and Radiological Materials*; Massachusetts Institute of Technology: Cambridge, MA, USA, 2009.
11. Clauset, A.; Shalizi, C.R.; Newman, M.E.J. Power-Law Distributions in Empirical Data. *SIAM Rev.* **2009**, *51*, 661–703. [CrossRef]
12. Burioni, R.; Gradenigo, G.; Sarracino, A.; Vezzani, A.; Vulpiani, A. Rare events and scaling properties in field-induced anomalous dynamics. *J. Stat. Mech. Theory Exp.* **2013**, *2013*, 1267–1279. [CrossRef]
13. Gillespie, C.S. A complete data frame work for fitting power law distributions. *arXiv*. 2014. Available online: https://arxiv.org/abs/1408.1554 (accessed on 2 Januray 2018).
14. Sun, J.; Niu, D.; Li, C. Study on Chaos Characteristics of Electricity Price Based on Power-Law Distribution. *Lect. Notes Electr. Eng.* **2011**, *121*, 503–510.
15. Dologlou, E. Stability of a power law relation between characteristics of earthquakes and electric precursors. *Nat. Hazards Earth Syst. Sci.* **2012**, *12*, 1783–1787. [CrossRef]
16. Cardona, M.; Chamberlin, R.V.; Marx, W. The history of the stretched exponential function. *Ann. Phys.* **2010**, *16*, 842–845. [CrossRef]
17. Kisslinger, C. The stretched exponential function as an alternative model for aftershock decay rate. *J. Geophys. Res. Solid Earth* **1993**, *98*, 1913–1921. [CrossRef]

18. Lee, K.; Siegel, J.; Webb, S.; Leveque-Fort, S.; Cole, M.; Jones, R.; Dowling, K.; Lever, M.; French, P. Application of the stretched exponential function to fluorescence lifetime imaging. *Biophys. J.* **2001**, *81*, 1265–1274. [CrossRef]
19. Laherrère, J.; Sornette, D. Stretched exponential distributions in nature and economy: "Fat tails" with characteristic scales. *Eur. Phys. J. B Condens. Matter Complex Syst.* **1998**, *2*, 525–539. [CrossRef]
20. Hagan, M.T.; Behr, S.M. The time series approach to short term load forecasting. *IEEE Trans. Power Syst.* **1987**, *2*, 785–791. [CrossRef]
21. McSharry, P.E.; Bouwman, S.; Bloemhof, G. Probabilistic Forecasts of the Magnitude and Timing of Peak Electricity Demand. *IEEE Trans. Power Syst.* **2005**, *20*, 1166–1172. [CrossRef]
22. Fumo, N.; Rafe Biswas, M.A. Regression analysis for prediction of residential energy consumption. *Renew. Sustain. Energy Rev.* **2015**, *47*, 332–343. [CrossRef]
23. Pérez-García, J.; Moral-Carcedo, J. Analysis and long term forecasting of electricity demand trough a decomposition model: A case study for Spain. *Energy* **2016**, *97*, 127–143. [CrossRef]
24. Bianco, V.; Manca, O.; Nardini, S. Electricity consumption forecasting in Italy using linear regression models. *Energy* **2009**, *34*, 1413–1421. [CrossRef]
25. To, W.-M.; Lee, P.K.C.; Lai, T.-M. Modeling of Monthly Residential and Commercial Electricity Consumption Using Nonlinear Seasonal Models—The Case of Hong Kong. *Energies* **2017**, *10*, 885. [CrossRef]
26. Li, Y.; Guo, P.; Li, X. Short-Term Load Forecasting Based on the Analysis of User Electricity Behavior. *Algorithms* **2016**, *9*, 80. [CrossRef]
27. Quilumba, F.L.; Lee, W.-J.; Huang, H.; Wang, D.Y.; Szabados, R.L. Using Smart Meter Data to Improve the Accuracy of Intraday Load Forecasting Considering Customer Behavior Similarities. *IEEE Trans. Smart Grid* **2015**, *6*, 911–918. [CrossRef]
28. Nogales, F.J.; Contreras, J.; Conejo, A.J.; Espínola, R. Forecasting next-day electricity prices by time series models. *IEEE Trans. Power Syst.* **2002**, *17*, 342–348. [CrossRef]
29. Park, D.C.; El-Sharkawi, M.; Marks, R.; Atlas, L.; Damborg, M. Electric load forecasting using an artificial neural network. *IEEE Trans. Power Syst.* **1991**, *6*, 442–449. [CrossRef]
30. Tepedino, C.; Guarnaccia, C.; Iliev, S.; Popova, S.; Quartieri, J. A Forecasting Model Based on Time Series Analysis Applied to Electrical Energy Consumption. *Int. J. Math. Models Methods Appl. Sci.* **2015**, *9*, 432–445.
31. Dong, B.; Li, Z.; Rahman, S.M.M.; Vega, R. A hybrid model approach for forecasting future residential electricity consumption. *Energy Build.* **2016**, *117*, 341–351. [CrossRef]
32. Liang, J.; Liang, Y. Analysis and Modeling for China's Electricity Demand Forecasting Based on a New Mathematical Hybrid Method. *Information* **2017**, *8*, 33. [CrossRef]
33. Cerjan, M.; Matijas, M.; Delimar, M. Dynamic Hybrid Model for Short-Term Electricity Price Forecasting. *Energies* **2014**, *7*, 3304–3318. [CrossRef]
34. Kandananond, K. Forecasting Electricity Demand in Thailand with an Artificial Neural Network Approach. *Energies* **2011**, *4*, 1246–1257. [CrossRef]
35. Hippert, H.S.; Taylor, J.W. An evaluation of Bayesian techniques for controlling model complexity and selecting inputs in a neural network for short-term load forecasting. *Neural Netw.* **2010**, *23*, 386–395. [CrossRef] [PubMed]
36. Ekonomou, L.; Oikonomou, D.S. Application and comparison of several artificial neural networks for forecasting the Hellenic daily electricity demand load. In Proceedings of the 7th WSEAS International Conference on Artificial Intelligence, Knowledge Engineering and Databases, Cambridge, UK, 20–22 February 2008; pp. 67–71.
37. Suh, D.; Chang, S. An Energy and Water Resource Demand Estimation Model for Multi-Family Housing Complexes in Korea. *Energies* **2012**, *5*, 4497–4516. [CrossRef]
38. Chang, P.-C.; Fan, C.-Y.; Lin, J.-J. Monthly electricity demand forecasting based on a weighted evolving fuzzy neural network approach. *Int. J. Electr. Power Energy Syst.* **2011**, *33*, 17–27. [CrossRef]
39. Azadeh, A.; Ghaderi, S.; Tarverdian, S.; Saberi, M. Integration of artificial neural networks and genetic algorithm to predict electrical energy consumption. *Appl. Math. Comput.* **2007**, *186*, 1731–1741. [CrossRef]
40. Ulagammai, M.; Venkatesh, P.; Kannan, P.; Padhy, N.P. Application of bacterial foraging technique trained artificial and wavelet neural networks in load forecasting. *Neurocomputing* **2007**, *70*, 2659–2667. [CrossRef]
41. Bashir, Z.; El-Hawary, M. Applying wavelets to short-term load forecasting using PSO-based neural networks. *IEEE Trans. Power Syst.* **2009**, *24*, 20–27. [CrossRef]

42. Liao, G.-C.; Tsao, T.-P. Application of a fuzzy neural network combined with a chaos genetic algorithm and simulated annealing to short-term load forecasting. *IEEE Trans. Evolut. Comput.* **2006**, *10*, 330–340. [CrossRef]
43. Shi, C.K.; Yan, W.Q.; Zhang, X.H.; Zhang, B.; Fan, Y.H.; Tang, W. Heavy overload forecasting of distribution transformer during the spring festival based on BP network and grey model. *J. Electr. Power Sci. Technol.* **2016**, *31*. [CrossRef]
44. Forte, M.F.; Hanson, J.L.; Hagerman, G. North Atlantic Wind and Wave Climate: Observed Extremes, Hindcast Performance, and Extratropical Recurrence Intervals. In Proceedings of the 2012 Oceans, Hampton Roads, VA, USA, 14–19 October 2012.
45. Liu, C.; Dong, P.; Shi, Y. Recurrence interval of the 2008 Mw 7.9 Wenchuan earthquake inferred from geodynamic modelling stress buildup and release. *J. Geodyn.* **2017**, *110*, 1–11. [CrossRef]
46. Williams, R.T.; Goodwin, L.B.; Sharp, W.D.; Mozley, P.S. Reading a 400,000-year record of earthquake frequency for an intraplate fault. *Proc. Natl. Acad. Sci. USA* **2017**, *114*, 4893–4898. [CrossRef] [PubMed]
47. Bogachev, M.I.; Kireenkov, I.S.; Nifontov, E.M.; Bunde, A. Statistics of return intervals between long heartbeat intervals and their usability for online prediction of disorders. *New J. Phys.* **2009**, *11*, 063036. [CrossRef]
48. Huo, C.Y.; Lu, Y.; Huang, X.L.; Liu, H.X.; Ning, X.B. Multi-scale Recurrence Quantification Analysis of Heartbeat Interval Series in Healthy vs. Heart Failure Subjects. In Proceedings of the 2014 7th International Conference on Biomedical Engineering and Informatics (Bmei 2014), Dalian, China, 14–16 October 2014; pp. 347–352.
49. Xie, W.-J.; Jiang, Z.-Q.; Zhou, W.-X. Extreme value statistics and recurrence intervals of NYMEX energy futures volatility. *Econ. Model.* **2014**, *36*, 8–17. [CrossRef]
50. Suo, Y.-Y.; Wang, D.-H.; Li, S.-P. Risk estimation of CSI 300 index spot and futures in China from a new perspective. *Econ. Model.* **2015**, *49*, 344–353. [CrossRef]
51. Altmann, E.G.; Kantz, H. Recurrence time analysis, long-term correlations, and extreme events. *Phys. Rev. E* **2005**, *71 (5 Pt 2)*, 056106. [CrossRef] [PubMed]
52. Yamasaki, K.; Muchnik, L.; Havlin, S.; Bunde, A.; Stanley, H.E. Scaling and memory in volatility return intervals in financial markets. *Proc. Natl. Acad. Sci. USA* **2005**, *102*, 9424–9428. [CrossRef] [PubMed]
53. Müller-Plathe, F. Coarse-graining in polymer simulation: From the atomistic to the mesoscopic scale and back. *ChemPhysChem* **2002**, *3*, 754–769. [CrossRef]
54. Yamamoto, Y.; Hughson, R.L. Coarse-graining spectral analysis: New method for studying heart rate variability. *J. Appl. Physiol.* **1991**, *71*, 1143–1150. [CrossRef] [PubMed]
55. Izvekov, S.; Voth, G.A. A multiscale coarse-graining method for biomolecular systems. *J. Phys. Chem. B* **2005**, *109*, 2469–2473. [CrossRef] [PubMed]
56. Bunde, A.; Eichner, J.F.; Kantelhardt, J.W.; Havlin, S. Long-term memory: A natural mechanism for the clustering of extreme events and anomalous residual times in climate records. *Phys. Rev. Lett.* **2005**, *94*, 048701. [CrossRef] [PubMed]
57. Elder, J.; Serletis, A. Long memory in energy futures prices. *Rev. Financ. Econ.* **2008**, *17*, 146–155. [CrossRef]
58. Chen, Z.; Ivanov, P.; Hu, K.; Stanley, H.E. Effect of nonstationarities on detrended fluctuation analysis. *Phys. Rev. E* **2002**, *65 (4 Pt 1)*, 041107.
59. Hu, K.; Ivanov, P.C.; Chen, Z.; Carpena, P.; Stanley, H.E. Effect of trends on detrended fluctuation analysis. *Phys. Rev. E* **2001**, *64 (1 Pt 1)*, 011114. [CrossRef] [PubMed]
60. Lin, A.; Ma, H.; Shang, P. The scaling properties of stock markets based on modified multiscale multifractal detrended fluctuation analysis. *Phys. A Stat. Mech. Appl.* **2015**, *436*, 525–537.
61. Peng, C.K.; Buldyrev, S.V.; Havlin, S.; Simons, M.; Stanley, H.E.; Goldberger, A.L. Mosaic organization of DNA nucleotides. *Phys. Rev. E* **1994**, *49*, 1685–1689. [CrossRef]
62. Sun, K.; Chen, X.; Cao, Y.; Han, Z. Research on the Fractal Characteristics of Prices in Electricity Market. In Proceedings of the IET International Conference on Advances in Power System Control, Operation and Management, Hong Kong, China, 30 October–2 November 2006; p. 418.
63. Sun, K.; Han, Z.X. Fractal feature of prices in California electricity market. *Energy Eng.* **2006**, *5*, 1–3.
64. Boeing, G. Visual Analysis of Nonlinear Dynamical Systems: Chaos, Fractals, Self-Similarity and the Limits of Prediction. *Systems* **2016**, *4*, 37.
65. Jiang, A.; Gao, J. Fractal analysis of complex power load variations through adaptive multiscale filtering. In Proceedings of the International Conference on Behavioral, Economic and Socio-Cultural Computing, Cracow, Poland, 16–18 October 2017; pp. 1–5.

66. Sreenivasan, K.R. Fractals and Multifractals in Fluid Turbulence. *Annu. Rev. Fluid Mech.* **1991**, *23*, 539–604. [CrossRef]
67. Bogachev, M.I.; Eichner, J.F.; Bunde, A. Effect of nonlinear correlations on the statistics of return intervals in multifractal data sets. *Phys. Rev. Lett.* **2007**, *99*, 240601. [CrossRef] [PubMed]
68. Cao, G.; Cao, J.; Xu, L. Asymmetric multifractal scaling behavior in the Chinese stock market: Based on asymmetric MF-DFA. *Phys. A Stat. Mech. Appl.* **2013**, *392*, 797–807. [CrossRef]
69. de Benicio, R.B.; Stošić, T.; de Figueirêdo, P.H.; Stošić, B.D. Multifractal behavior of wild-land and forest fire time series in Brazil. *Phys. A Stat. Mech. Appl.* **2013**, *392*, 6367–6374. [CrossRef]
70. Liu, W.; Shang, J.; Zhou, W.; Wen, F.; Lin, Z. Evaluation of value-at-risk in electricity markets based on multifractal theory. *Autom. Electr. Power Syst.* **2013**, *37*, 48–54.
71. Gao, R.; Wang, F.; Liu, W. Competitive Electricity Price Characteristic Analysis Based On Multifractal Detrended Moving Average Analysis. In Proceedings of the 6th International Conference on Electrical and Control Engineering (ICECE2015) and The 4th International Conference on Materials Science and Manufacturing (ICMSM2015), Shanghai, China, 14–15 August 2015; pp. 129–134.
72. Jan, W.; Kantelhardt, S.A.Z.; Koscielny-Bundec, E.; Havlind, S.; Bunde, A.; Stanley, H.E. Multifractal detrended $uctuation analysis of nonstationary time series. *Phys. A Stat. Mech. Appl.* **2002**, *316*, 87–114.
73. Murguia, J.S.; Pérez-Terrazas, J.E.; Rosu, H.C. Multifractal properties of elementary cellular automata in a discrete wavelet approach of MF-DFA. *EPL Europhys. Lett.* **2009**, *87*, 28003. [CrossRef]
74. Cardella, E.; Ewing, B.T.; Williams, R.B. Price volatility and residential electricity decisions: Experimental evidence on the convergence of energy generating source. *Energy Econ.* **2017**, *62*, 428–437. [CrossRef]
75. Ciarreta, A.; Muniain, P.; Zarraga, A. Modeling and forecasting realized volatility in German-Austrian continuous intraday electricity prices. *J. Forecast.* **2017**, *36*, 680–690. [CrossRef]
76. Wang, F.; Liao, G.P.; Li, J.H.; Li, X.C.; Zhou, T.J. Multifractal detrended fluctuation analysis for clustering structures of electricity price periods. *Phys. A Stat. Mech. Appl.* **2013**, *392*, 5723–5734. [CrossRef]

energies

MDPI

Article

SWOT Analysis for the Promotion of Energy Efficiency in Rural Buildings: A Case Study of China

Lin Zhang [1], Shan Guo [2,3,*], Zezhou Wu [4], Ahmed Alsaedi [3] and Tasawar Hayat [3,5]

1 School of Management Engineering, Shandong Jianzhu University, 1000 Fengming Road, Licheng District, Jinan 250101, China; zhanglin2007@sdjzu.edu.cn
2 Department of Land Management, School of Public Administration and Policy, Renmin University of China, Beijing 100872, China
3 NAAM Group, Faculty of Science, King Abdulaziz University, 21589 Jeddah, Saudi Arabia; aalsaedi@kau.edu.sa (A.A.); tahaksag@yahoo.com (T.H.)
4 Department of Construction Management and Real Estate, Shenzhen University, Shenzhen 518060, China; wuzezhou@szu.edu.cn
5 Department of Mathematics, Quaid-i-Azam University, 45320 Islamabad, Pakistan
* Correspondence: shan.guo@ruc.edu.cn; Tel.: +86-188-1176-3368

Received: 14 March 2018; Accepted: 3 April 2018; Published: 5 April 2018

Abstract: Over half of China's total energy consumption is attributed to rural buildings. However, unlike the research into urban areas, few studies have explored the problems of building energy efficiency (BEE) in rural China. This study aims to establish an appropriate strategic plan for promoting rural BEE (RBEE) in China by conducting a strength-weakness-opportunity-threat (SWOT) analysis. Analysis data are obtained from multiple sources, including a comprehensive literature review, governmental reports, related regulations, and semi-structured interviews with a number of critical stakeholders. A matrix of the SWOT analysis is derived to reveal the drivers and barriers in the course of implementing RBEE. Five critical strategies are proposed. We also attempt to explore the internal and external conditions of RBEE in China, which can contribute to the customization and prioritization of policy recommendations for the Chinese government.

Keywords: SWOT analysis; building energy efficiency; rural area; strategic planning

1. Introduction

The improvements in rural residents' earnings and living conditions have remarkably increased the building energy consumption in rural China, which accounts for approximately 40% of the total energy consumption of the country [1]. Most rural buildings are characterized by poor thermal insulation performance, which can barely meet the basic living standards of rural residents. Since the Chinese government launched the so-called "New Countryside Initiative" in 2005, local governments have been focusing on the construction of rural infrastructure and new housing types to realize the targets of economic prosperity and built environment improvement. In this context, improving rural building energy efficiency (RBEE) has emerged as a crucial issue. The Chinese government has gradually recognized the importance of RBEE, which is considered a major opportunity for improving national building energy efficiency (BEE) [2]. In March 2017, the Ministry of Housing and Urban-Rural Development (MOHURD) launched the "13th Five-Year Plan for Building Energy Saving and Green Building Development". The objective is for the energy consumption of rural buildings to make a breakthrough in economically developed areas and for key development areas to adopt over 10% energy-saving measures [3].

Unlike urban BEE, RBEE is still in the initial stage of development. Furthermore, urban BEE has witnessed significant progress in the last two decades. The practices related to BEE are mostly

concentrated on the large-scale public, commercial, and urban residential buildings, with rural buildings receiving relatively little attention [4]. Moreover, rural buildings have not been included in the scope of mandatory criteria for BEE. Consequently, a significant gap in BEE exists between urban and rural regions.

Accelerating the promotion of RBEE has a potential strategic impact on reducing energy consumption and improving the living conditions of rural residents in the long run. The government plays an important role in implementing RBEE in the initial stage due to the externality and asymmetric information in the BEE market [5]. Therefore, strategic planning and the implementation of actions are urgently needed. Although the government has introduced ambitious energy efficiency targets in rural regions, the formulation of an applicable strategic plan remains unclear. The present study can contribute to the government's further understanding of the current situation and help in identifying the main problems and implementing effective measures [6]. Earlier studies have been conducted on RBEE, with the focus being the overview of the developments in RBEE [2,7], the assessment of RBEE [8], the critical factors to improve RBEE [9], and energy-saving optimization for the performance parameters of rural building shapes [4]. Research on the overview of the strengths, weaknesses, opportunities, and threats in RBEE is lacking. Thus, we aim to systematically express the status quo of RBEE and conduct a strength-weakness-opportunity-threat (SWOT) analysis of RBEE on the basis of a literature review, governmental reports, and semi-structured interviews. The established SWOT analysis strategic matrix on RBEE will enable the formulation of a strategic plan for government authorities.

2. RBEE in China

2.1. Characteristics of Rural Residential Buildings

Rural buildings are dramatically different from urban ones. Most rural buildings are traditional one-story or two-story stand-alone buildings with courtyards built on collective land for farmers [10], whereas urban buildings are commonly high-rise apartments [2]. For the longest time, farmers have constructed rural buildings by relying on their experiences, not on building construction codes. Therefore, the quality of the design and construction of rural buildings is lower than that of their urban counterparts. Research on building energy-saving technologies is mostly conducted for urban buildings. Energy conservation goals and mandatory standards also mainly target urban buildings.

Unlike urban housing, which has undergone rapid privatization, rural housing in China exhibits unique characteristics [11]. For example, in land ownership, rural residential lands are owned by village collectives, and an individual rural household can freely apply for one piece of residential land [10]. Therefore, current policies further entitle rural households with decision-making power in housing construction. Rural residents are wholly responsible for financing, constructing, managing, and maintaining their homes. Nevertheless, these houses cannot be traded in the market, and transfer is legally limited within villagers in the same household registration. All these characteristics imply that strategic planning for urban BEE cannot be replicated for RBEE.

Field investigation of real cases was conducted to clearly indicate the huge difference between urban and rural buildings. Two typical buildings in urban and rural Shandong, an eastern province of China, are illustrated in Figure 1. This traditional rural building was built in the countryside of Qufu, known as the hometown of Confucius, while high-rise housing was constructed in Jinan, the capital city of Shandong province. There are significant differences in terms of layout, building design style, cost, construction process, and, ultimately, levels of comfort and building energy efficiency.

(**a**) (**b**)

Figure 1. Different types of dwelling in the countryside and city. (**a**) a traditional village in Qufu, the hometown of Confucius in Shandong province; (**b**) the high-rise housing in Jinan, the capital of Shandong province, which was completed in 2015.

2.2. Current Situation of RBEE

With the development of rural regions in China, the energy consumption of rural buildings has gradually increased and accounted for a large proportion of the total. RBEE is not only a crucial issue of the New Socialist Countryside (NSC) and New Urbanization Initiative (NUI), but also an important field in energy efficiency and greenhouse gases that must not be overlooked. For instance, Wang, et al. [12] expressed that improving the living environment is an important indicator of the NSC. In March 2014, the "National New-Type Urbanization Plan (2014–2020)" was jointly launched by the Central Committee of the Communist Party of China and the State Council [13] to realize the sustainable development of rural energy. A series of studies have been conducted on energy consumption and greenhouse gas emissions at the global scale [14,15], which can significantly influence the development of the world economy; at the national scale [16], including China; at the urban scale [17–19], including Beijing and Macao; and at the building scale [20,21] with embodied energy consumption involved. However, rural regions have largely been neglected.

The data on energy consumption in rural buildings have been steadily expanding in recent years, as can be seen in a report on the development of Chinese building energy conservation in 2016 issued by the Science and Technology Development Promotion Center of the MOHURD. This report indicated that building energy consumption had increased from approximately 127 trillion ton coal equivalent to 161 trillion ton coal equivalent in the period of 2009–2013 [22] (Figure 2). The average annual growth reached 5.47%. In 2013, the energy consumption of rural buildings in China increased to approximately 20.3% of the total. An increase in residents' income can be expected to boost the amount of energy consumption.

Problems have also gradually emerged in rural buildings. Most rural buildings in China lack energy-saving measures due to the limited knowledge about energy-saving technologies and experiences. For example, in northern China, a majority of rural buildings feature few insulation measures, poor air tightness for the doors and windows, and inefficient heating devices. The rate of energy utilization in rural buildings is only approximately one-third of that in urban buildings because of the poor thermal performance of the rural building envelope. A significant amount of heat is lost, and thermal comfort is inferior. Villages have no unified planning. Buildings also lack reasonable orientation. For instance, the adverse east–west orientation of buildings is undesirable for acquiring substantial amounts of sunlight and ventilation, thermal insulation in winter, and ventilation in summer, and it leads to considerable energy loss. The Statistics of Survey from the Tsinghua

University and MOHURD in 2011 stated that the problems in RBEE include the absence of specialized planning, design, and construction, as well as necessary inspections and supervision of materials and the construction process, all of which lead to severe waste in land, materials, funds, and energy. Therefore, BEE should be promoted urgently in rural regions.

Figure 2. Amount of energy consumption in rural China in 2009–2013 (trillion ton).

3. Research Methodology

A SWOT analysis approach is used to study the strategic planning of enterprises or industries. This approach was initially adopted in business and marketing disciplines, and it has gradually been applied to various fields. For example, Ke, et al. [23] conducted a SWOT analysis for domestic private enterprises dealing with the development of infrastructure projects in China and concluded that the methodology is a useful tool for assessing continuous changes. SWOT analysis has been employed in renewable energy management [24–26], construction waste management [6], off-site construction [27], and building energy conservation [28]. Thus, SWOT analysis is a good approach for strategic planning research.

In the present study, SWOT analysis was employed to identify the factors that affect the promotion of RBEE. Weaknesses and threats could be overcome by following the principles of maximizing strengths and taking advantage of opportunities. A framework of the SWOT analysis (Figure 3) was proposed on the basis of the work in Reference [27]. In step 1, a generic framework was formulated to identify the RBEE factors. On the basis of the research of Shen, et al. [29], we classified the factors as those that affect RBEE's strengths and weaknesses (SW), including management ability, technological ability, financial ability, organization, and operations; and those that affect RBEE's opportunities and threats (OT), including social and political environments, economic environment, market opportunities, and competition mechanism.

In step 2, a list of strengths, weakness, opportunities, and threats of RBEE was derived from the literature review, governmental reports, and semi-structured interviews. The questions for the semi-structured interviews were modified and finalized after a brainstorming discussion among the researchers. The main research questions designed for the semi-structured interviews are presented in Table 1. Ten interviewees from Shandong Province, which comprised two officials in the government sector, two village leaders, two rural residents, one university researcher, one designer, one project manager, and one green building material supplier, were selected. All of the participants were stakeholders in RBEE with a relatively in-depth understanding of energy consumption in rural regions.

Semi-structured interviews were carried out in February 2017, and each interview session lasted for 30–40 min. Table 2 shows the profile of the interviewees.

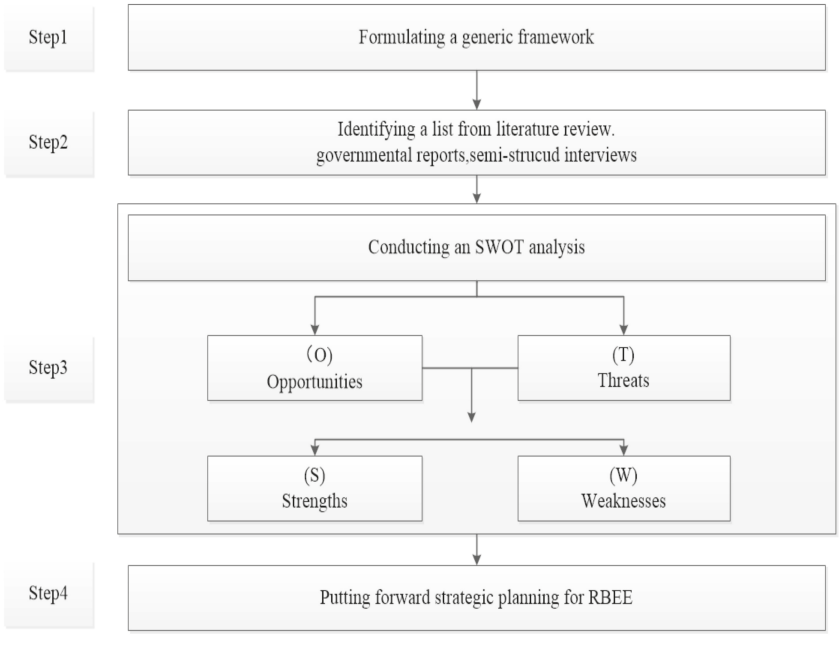

Figure 3. The basic flow of research [27].

Table 1. Main questions for semi-structured interviews.

Code	Question	Explanation
Q1	What are the opportunities for Rural Building Energy Efficiency (RBEE)?	What are the external prospects that can be taken advantage of for RBEE?
		What is the governmental guidance for promoting RBEE?
Q2	What are the threats to RBEE?	What are the external negative factors that restrict the development of RBEE?
Q3	What are the strengths of RBEE?	What are the benefits of promoting RBEE?
Q4	What are the weaknesses of RBEE?	What are the internal negative factors that restrict the development of RBEE?

Table 2. Profile of the interviewees.

N	Position	Company	Number
1	Project manager	Safety construction company in Changqing County in East China	1
2	Village leader	Zhou Village in Zhangqiu County	2
3	Rural resident	Zhou Village in Zhangqiu County	2
4	Researcher	Shandong Jianzhu University	1
5	Designer	Tong Yuan Design Company	1
6	Green building material supplier	Thermal insulation material company	1
7	Official	Department of Village and Town	1
8	Official	Department of Energy Conservation Science and Technology	1

The answers to the questions were abstracted to establish a list of SWOT analysis factors. On the basis of the literature review and governmental reports, the SWOT factors related to RBEE were initially identified. In step 3, six experts were invited to evaluate the reliability of the SWOT factors. In the evaluation, unsuitable factors, such as the number of migrants to cities, were removed, and important factors, such as low income of rural residents, were added. The final list of SWOT factors was finally attained after the evaluation. On the basis of the aforementioned analysis, we adopted a research method for integrating stakeholder analysis into the SWOT analysis. In step 4, five concrete strategic action plans were proposed for the government to promote RBEE.

4. SWOT Analysis of RBEE in Rural China

The SWOT analysis begins with "O + T" and ends with "S + W". The matrix of the SWOT analysis is established according to the literature review, governmental reports, and semi-structured interviews, as shown in Table 3, which sets forth the identified SWOT factors, types, and sources of origin [27]. The opportunities, threats, strengths, and weaknesses are discussed in detail to deepen the understanding of the current situation of RBEE in China.

Table 3. The matrix of strength-weakness-opportunity-threat (SWOT) analysis.

Analysis	SWOT	Type	Source
"O + T" Analysis	O1—top-to-bottom policy support	G	MOHURD, 13th Five-Year for Building Energy-Saving and Green Building Plan (2016–2020)
	O2—new socialist initiatives in the countryside	G, L	Yang, et al. [30], Proposal of the Central Committee of the Chinese Communist Party for the 11th Five-Year Plan for national economic and social development
	O3—appeals for enhancing RBEE	G, L	Wu, et al. [31], Development of Chinese BEE Report in 2016
	T1—lack of policies and standards	L, I	Sha and Wu [32]
	T2—unreasonable energy structure	L, I, G	Zhang, et al. [33], Guidance on Expanding BEE Pilot Project in 2009, official from the Department of Energy Conservation Science and Technology
	T3—lack of supervising mechanism	I, G	An official from the Department of Village and Town, 13th Five-Year Plan for Building Energy-Saving and Green Building Development
"S + W" Analysis	S1—significant energy efficiency potential	L, I, G	He, Yang, Ye, Mou and Zhou [1], Li, et al. [34], an official from the Department of Village and Town, notice of carrying out the green rural housing construction in 2013
	S2—abundant renewable energy resources	L, G	Zhang, et al. [35], Development of Chinese BEE Report in 2016
	S3—requirements for improving living comfort	L, I	Wu, Liu and Qin [31], rural resident, village leaders
	W1—poor building energy-saving consciousness	L, I	Ai, et al. [36], an official from the Department of Village and Town in Shandong Province
	W2—inadequate knowledge and information	L, I	Wimala, et al. [37], village leaders
	W3—low-income level of rural residents	L, I	Sha and Wu [32], village leaders

NOTE: Literature review (L); semi-structured interviews (I); governmental reports (G).

4.1. Opportunities

4.1.1. O1—Top-to-Bottom Policy Support

In the contexts of environmental degradation and energy crisis, "ecological civilization construction", especially in rural regions, is noted as a crucial topic in the report of the 19th National Congress of Communist Party in China. The BEE in rural regions has received considerable attention from governmental reports. Governmental reports related to RBEE are shown in Table 4. RBEE is expected to attain significant top-to-bottom policy support in the future.

Table 4. Governmental reports related to RBEE.

Year	Regulations	Issuers	Contents Regarding RBEE
2009	Accelerating the implementation of renewable energy building applications in rural areas	MOF, MOHURD	Renewable energy resources used in rural schools, rural residential buildings, village or town governmental offices, and health centers
2009	Guidance on Expanding BEE Pilot Project for Dangerous Rural Reconstruction	MOHURD	Focusing on energy-saving measures for building envelopes in walls, doors, roofs, and windows to improve the thermal comfort of rural residential buildings
2013	Green Building Action Plan	Office of the State Council	Promoting green rural housing construction, preparing technical guides for green buildings in villages or towns, freely providing technical services
2013	Notice of carrying out green rural housing construction	MOIIT, MOHURD	Exploring green rural housing construction method and technology; popularizing native green buildings; promoting green building materials to the countryside; demonstrating project of green rural housing
2015	Action Plan to Promote the Production and Application of Green Building Materials	MOIIT, MOHURD	Promoting green building materials to the countryside; preparing a green material product catalog for green rural housing
2017	13th Five-Year Plan for Building Energy-Saving and Green Building Development	MOHURD	Economically developed areas and key development areas should make a breakthrough in RBEE, and the proportion of energy-saving measures should be over 10%

Note: Ministry of Finance (MOF); Office of the State Council (OOSC); Ministry of Housing and Urban–Rural Development (MOHURD); Ministry of Industry and Information Technology (MOIIT).

4.1.2. O2—New Socialist Initiatives in the Countryside

Influenced by the long-term dual systems in China, the developments in urban and rural regions are unbalanced, and most rural residents remain relatively poor. In this context, new socialist initiatives in the countryside were introduced as part of the national strategic plan in the 1950s. However, such initiatives had not essentially played a significant role until the proposal of the Central Committee of the Chinese Communist Party on the 11th Five-Year Plan for National Economic and Social Development was issued.

In 2017, the central government proposed a national strategy called "Rural Revitalization", which aimed to construct an eco-friendly, livable, luxurious, and flourishing industrial countryside. The government is expected to attach high importance to the "problems of agricultural and rural areas" in the new era of socialism. The living environment will be markedly improved with the new socialist initiatives in the countryside. Driven by the construction of new socialist initiatives in the countryside at the national level, great opportunities for RBEE can be expected.

4.1.3. O3—Appeals for Enhancing RBEE

The "13th Five-Year Plan for National Economic and Social Development (2016–2020)" in China requires reducing the energy consumption per unit of gross domestic product (GDP) by 15% and the CO_2 emission per unit of GDP by 18%. Reducing the energy consumption in the construction industry is crucial to realize the macro goal. Furthermore, addressing the high energy consumption and low energy efficiency of rural buildings is an urgent appeal. With the development of urbanization and agricultural modernization, a growing number of rural residents are likely to pursue a high-quality

living environment. Echoed by the semi-structure interviews in the current work, enhancing RBEE is the best choice to realize the target of "beautiful countryside construction" at the national level.

4.2. Threats

4.2.1. T1—Lack of Policies and Standards

The legal environment is the major factor that affects the implementation of BEE [38]. Although the local government implemented the Energy Conservation Law in 2008, specific details related to buildings are lacking. Moreover, the existing standard system for BEE design remains imperfect. Most of the standards focus on urban buildings. Only one national standard exists for rural regions, that is, "The design standard for energy efficiency of rural residential buildings", which was launched in 2012 [8]. Several actions have been implemented in relation to RBEE, and they include "Promoting Renewable Energy in Rural Areas", "Dangerous Residential Reconstruction based on Energy-Saving Retrofitting", and "New Types of Green Construction Materials for the Countryside" [9]. Nevertheless, all these actions cover relatively limited rural regions. Most provinces and regions have yet to officially carry out energy efficiency actions [39]. The lack of policies and standards hinders the development of RBEE.

4.2.2. T2—Unreasonable Energy Structure

The energy structure in rural China is more unreasonable than that in the urban areas [40]. In rural households, traditional biomass is the dominant fuel, accounting for over 75% of the rural building energy use in 2005 [2]. With growing earnings of rural residents, they gradually switch from traditional biomass to commercial energy, especially coal. The energy structure in rural buildings remains dominated by coal and electricity. The proportions of electricity and coal are 41% and 44%, respectively, as depicted in Figure 4. Coal is used for terminal consumption in rural buildings, but it results in low energy efficiency and severe environmental pollution. Therefore, the unreasonable energy structure is a significant threat to the sustainable development of RBEE.

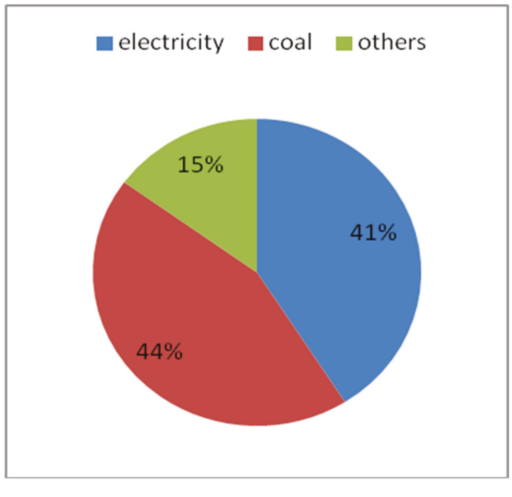

Figure 4. Energy structure in rural Chinese buildings in 2013 [22].

The findings of a survey by the Building Energy Efficiency Research Center of Tsinghua University (BEERCTU) in 2006–2007 revealed that the energy consumption in rural regions accounts for 37% of the total [41]. Nonrenewable energy, such as coal and electricity, and renewable energy, such as firewood and straw, contribute to 60% and 40% of the total, respectively. Ninety million tons of

standard coal are consumed annually for heating in northern rural areas [42]. Coal is the main fuel in the energy structure, and it puts great pressure on sustainable development and environmental protection. The unreasonable energy structure is thus an obvious threat to RBEE.

4.2.3. T3—Lack of Supervision Mechanism

The current rural market is chaotic. For example, scientific design standards and related supervisory systems are lacking, and rural residents randomly build their own housing. Without any supervision mechanism, rural residents do not voluntarily purchase new energy-efficient building materials [31]. Construction craftsmen, most of which have no professional training in construction and BEE technologies, are hired temporarily. Thus, rural buildings barely have energy-efficient measures. Although the amount of energy consumption for rural heating is 1.5–2 times that for urban heating, the survey of BEERCTU revealed that the indoor temperature in rural areas is significantly lower than that in urban areas [43]. The "Guidance on Improving the Living Environment in Rural Regions" issued by the General Office of the State Council of the People's Republic of China in 2014 required the strengthening of the quality and safety supervision of buildings and the improvement of the energy efficiency rate. Thus, the lack of supervision mechanisms is a major obstacle to the development of RBEE.

4.3. Strengths

4.3.1. S1—Significant Energy Efficiency Potential

Energy-saving measures are rarely adopted in housing development due to the absence of energy-saving technologies. Consequently, rural buildings present significant energy efficiency potential. For example, external walls are too thin, and they are mainly made of solid clay brick. This type of building material is inefficient for thermal insulation and energy conservation, which requires a large volume of clay, and results in damages to the ecological environment. Moreover, no insulation measures are adopted for external walls and roof. If the temperature rises by 14 degrees, the amount of energy consumption will increase by 1 degree [31]. All of these characteristics result in a considerable heating loss, high energy consumption, and an uncomfortable living environment. According to calculations, only 32% of heating energy is effectively used [1]. Li, Shan, Yang and Yang [34] concluded that when 30% and 50% of rural buildings were involved in energy-efficient retrofitting, the amounts of carbon dioxide emission decreased to 1.14 and 1.9 billion tons, which made up 2.2% and 3.8% of the total in 2008, respectively. Hence, if reasonable green technologies or measures are largely adopted in rural buildings, significant energy efficiency potential will be acquired.

4.3.2. S2—Abundant Renewable Energy Resources

As a result of the depletion of fossil energy resources and the increase of environmental pollution, the utilization of renewable energy has attracted considerable attention from around the world. Rural China is rich in renewable energy resources, including solar, geothermal, wind, and biomass energy. All of them are clean, pollution-free, and widely distributed [8]. Annually, the utilization of renewable energy resources in China is approximately 3 billion and 600 million tons standard coal, and in 2009, the total energy consumption reached 3 billion and 100 million tons [44]. Abundant renewable energy resources are available in China. For example, two-thirds of the country's territories can receive more than 2200 sunshine hours every year [45], and the same is especially true in vast rural areas. They are also naturally endowed with plenty of biomass resources, which serve as a rich source for biogas utilization. Biogas can be used for cooking and lighting for people's daily activities, and thus can greatly decrease indoor air pollution and reduce greenhouse gas emissions caused by the direct combustion of firewood and coal. In sum, abundant renewable energy resources represent a significant strength that favors the promotion of RBEE.

4.3.3. S3—Requirements for Improving Living Comfort

Wu, Liu and Qin [31] conducted a survey in northern China and found that the increase in rural residents' income also gradually enhances the demand for quality of life. Rural residents thus pursue high levels of comfort in terms of heating, cooking, etc. This condition is in accordance with our findings from the semi-structured interviews.

Approximately 95% of the rural residents surveyed hold strong demands for heating in winter [39]. An indoor temperature below 12 °C is difficult to bear. In addition, several rural residents have shifted their cooking mode from traditional firewood and straw, which is characterized by low energy efficiency and poor indoor environment, to convenient commercial energy resources. Rural residents also pursue large housing [2], with the average housing space increasing from 22.5 m^2 in 2001 to 28.2 m^2 in 2008 [31], thus implying a greater demand for energy consumption. In sum, the requirement for improving living comfort can enhance rural residents' willingness to consider RBEE.

4.4. Weaknesses

4.4.1. W1—Poor Energy Efficiency Awareness

Most rural buildings are built by rural residents themselves. Hence, the application of energy-saving technologies is limited. The resulting poor performance of thermal insulation then leads to uncontrollable energy losses. With the concepts of abundant resources and inexhaustible energy, rural residents seldom pay attention to the issue of energy efficiency. They primarily focus on the appearance and large size of living spaces for their homes. For example, when they accumulate funds to build their homes, they are inclined to focus on aesthetic qualities and neglect energy efficiency [36]. Owing to the social norms termed as the "bandwagon effect" in rural regions, other rural residents will behave in the same way. This behavior greatly restricts the popularization of energy efficiency in rural China. Obviously, poor energy efficiency awareness is an obstacle for RBEE.

4.4.2. W2—Inadequate Knowledge and Information

Rural buildings in China are generally built without the aid of professional design and construction practitioners. Most rural residents neglect the problems of energy efficiency because of their lack of relevant knowledge and information. Unlike urban residents, rural residents mostly have low education levels. Moreover, rural residents are unfamiliar with the benefits of BEE, leading to the difficult promotion of RBEE. Limited channels are available to receive information about BEE, with the main channels being TV broadcasts. From this top-to-bottom communication approach, a long period is required for rural residents to receive timely information about the government's technological support and economic subsidies. Inadequate knowledge and information is an obvious weakness that remarkably hinders the promotion of RBEE.

4.4.3. W3—Low Income of Rural Residents

Most rural residents in China are engaged in small-scale natural agriculture, which equates to a relatively low income. In the context of rapid urbanization, an increasing number of rural residents are moving to cities, with 16.4% of them aiming to work as construction workers and 21.1% of them securing positions in the service industry [46]. Although their income has gradually increased, rural residents significantly differ from urban residents. The income difference between rural and urban residents from 2012 to 2016 based on 2017 statistical data is shown in Figure 5. The increasing gap can be recognized starting in 2012. Currently, the income of some rural residents can only meet their basic living needs. Rural residents' own funds are utterly inadequate for BEE [32]. Such low income prevents rural residents from purchasing expensive energy-saving lamps and energy-efficient electric appliances or installing solar energy facilities. Therefore, the low income of rural residents is a weakness in RBEE promotion.

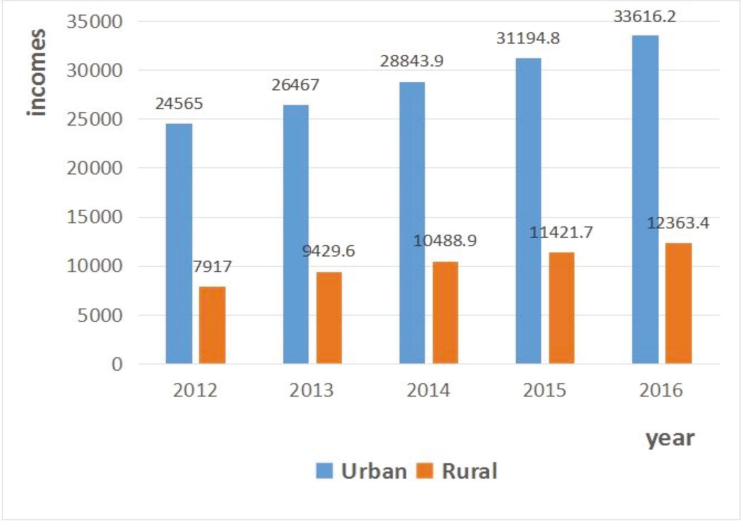

Figure 5. Incomes of urban and rural residents in 2012–2016.

5. Strategies for Promoting RBEE

A list of critical strategic plans for RBEE can be formulated according to the SWOT analysis matrix in Table 5. The principles behind the proposal of these strategies are modified from Yuan [6] and are described as "maximizing strengths and opportunities, transforming weaknesses to strengths, and neutralizing threats". The key strategies are comprehensively examined to underline the strategies and planning.

Table 5. Strategic planning based on the SWOT analysis matrix for RBEE.

Environment		Planning
External Environment	Opportunities (O)	1. Top-to-bottom policy support; 2. Construction of new socialist initiatives in the countryside; 3. Appeals for enhancing RBEE.
	Threats (T)	1. Lack of policies and standards; 2. Unreasonable energy structure; 3. Lack of supervision mechanism.
Internal Environment	Strengths (S)	1. Significant energy efficiency potential; 2. Abundant renewable energy resources; 3. Requirements for improving living comfort.
	Weaknesses (W)	1. Poor energy efficiency awareness; 2. Inadequate knowledge and information; 3. Low income of rural residents.
	SO strategies	S2: Establishing technology Research and Development (R&D) institutions in local regions; S3: Promoting demonstration projects of RBEE.
	WO strategies	S4: Carrying out RBEE training; S5: Providing economic subsidies to rural residents.
	ST strategies	S1: Formulating a carrot-and-stick policy governance mechanism; S3: Promoting demonstration projects of RBEE.
	WT strategies	S1: Formulating a carrot-and-stick policy governance mechanism; S5: Providing economic subsidies to rural residents.

5.1. Strategy 1—Formulating a Carrot-and-Stick Policy Governance Mechanism

A guidance policy plays a critical role in promoting RBEE. In the work of Wu and Yin [9], a questionnaire survey was distributed to experts in 17 BEE institutions, and policies were noted to have a more important role than technologies. According to different degrees of strictness of policies issued by the government, the three BEE policy instruments are voluntary scheme instrument, economic incentive instrument, and mandatory administration [47]. Only one standard code, the "Design Standard of BEE in Rural Regions", exists, but it is not mandatory. Stakeholders hardly comply with construction codes due to the lack of capital support and technical guidance in implemented standards. Thus, an appropriate governance mechanism should be established.

The "carrot-and-stick" strategies are among the best choices. A countryside-oriented policy governance mechanism is required to guarantee the implementation of technological and financing strategies. Mandatory administration and economic incentive instruments are equally critical. On the one hand, the government should establish a penalty system that forbids rural residents from using solid clay bricks. On the other hand, the government should formulate an economic incentive system that encompasses preferential policies in terms of governmental subsidies. This system should be interest-free to encourage rural residents to adopt inexpensive and practical green technologies or renewable energy sources.

5.2. Strategy 2—Establishing Technology R&D Institutions in Local Regions

Research on building energy-saving technologies has mainly focused on cities, and the energy conservation goals and mandatory standards issued by the government are mostly targeted at urban buildings. The construction specifications for rural buildings is remarkably different from those for urban ones due to different lifestyles and economic conditions. A reasonable technology is an effective channel to solve the problems in energy efficiency. Therefore, technology research, development, and promotion are vital. Materials and construction techniques in rural regions are remarkably distinct. Local governments should encourage local universities or institutions to establish R&D centers. The centers can be combined with enterprises and universities to establish a platform of "production, learning, and research" to work out low-cost and energy-efficient technological solutions, which suit local climate conditions and geographic characteristics. Developing and utilizing renewable energy resources in rural regions are also beneficial actions. In terms of climate and regional characteristics, thermal insulation technology and "Kang" can be promoted in the northern countryside, which can utilize solar energy for heating. In the southern countryside, eco-villages can be constructed through the development of passive housing technology and biogas pools for cooking and heating.

5.3. Strategy 3—Promoting Demonstration Projects of RBEE

The central government has launched a series of energy-efficient pilot programs for public and residential buildings in certain urban regions. The resulting experiences can be applied to RBEE. For example, the Beijing government launched the action initiative "Management Method of the Demonstration Project of Utilization of Innovative Wall Material for BEE in the Rural Residents" in 2007. By meeting stipulated conditions, rural residents could be awarded 20 thousand Chinese Yuan to subsidize the incremental cost of innovative wall materials. Although the scope of demonstration projects is limited to some developed rural regions, numerous rural residents will gradually know about the economic benefits and advantages of a healthy living environment through demonstration projects. These demonstration projects can be expanded to other regions. A prefabrication construction approach can be employed in the demonstration projects to speed up the development of high-quality structures and reduce energy consumption and carbon emissions [48]. Therefore, this approach shows great promise when implemented in rural buildings.

5.4. Strategy 4—Carrying out RBEE Training

Training is an effective approach to promote RBEE. Training can raise rural residents' awareness of RBEE and improve the energy efficiency skills of construction craftsmen. Conducting effective training is especially difficult for rural residents due to their low level of education and traditional lifestyle. Most of them are unfamiliar with the advantages of energy-efficient technologies. Thus, the training channel and approach should differ from those used in the urban context. Conducting hierarchical top-to-bottom training is practical. The central or local government first focuses on the training of village organizations and their leaders. With complete knowledge about renewable energy technologies, economic benefits, and governmental subsidies, these trained individuals can serve as frontrunners in the promotion of RBEE. Village leaders often have the trust of rural residents because they live and work collectively [2]. They can persuade rural residents to change the way they construct new houses or retrofit existing ones through training meetings or oral presentations among rural residents. Training in the area of rural energy efficiency is a prerequisite for construction craftsmen. Local governments should organize these types of training free of charge for building craftsmen so that they have the opportunity to learn about the latest innovative building materials, master green construction technology, and utilize local renewable energy sources.

5.5. Strategy 5—Providing Economic Subsidies

To enhance energy efficiency and reduce energy consumption, the government should supply economic incentives to encourage rural residents to adopt renewable energy instead of commercial energy. The government should provide economic incentives to rural residents. Financial support is an essential aspect of RBEE [8]. The cost of building an efficient rural housing is approximately 5% greater than the cost of building a traditional one [2]. Constructing energy-efficient buildings without any policy intervention is impossible for rural residents due to the externality of BEE. In cooperation with MOF, MOHURD issued a standard for subsidies provided for the use of renewable energy resources in 2009. Under this standard, rural residents can receive 60 Yuan and 15 Yuan per square meter when they apply ground source heat pumps and integrated solar thermal systems, respectively. If individual rural residents use a solar energy bathroom and solar energy housing, 60% of their incremental cost can be compensated for. The subsidy standards can be adjusted according to the costs incurred in the application of rural renewable energy. In addition, a new energy utilization system for rural buildings must be established. The system should implement energy-saving technologies suitable for rural regions, adjust energy structure, and adopt abundant renewable energy resources, such as solar energy, biomass, and biogas, to improve the livelihood quality of rural residents. The central or local government should supply rural residents with economic incentive strategies to support the utilization of renewable energy.

In the initial stage, the government should set up special funds for R&D centers. A specific percentage of grants and allowances should be allocated to boost the budget for R&D that favors green building material production and for standardized module design companies suited for local climate conditions. In addition, the government can provide preferential tax policies, including sales tax and corporate income tax, to renewable energy equipment manufacturers and green building material suppliers. Nevertheless, the policies heavily depend on financial funds. Private firms can be invited to participate in the promotion of RBEE. For instance, public-private partnerships are recommended because they can effectively address limited governmental funds. Employing the approach of energy performance contracting can also lead to a win-win between the government and private investors.

6. Conclusions

Driven by the national strategy of constructing new socialist initiatives in the countryside, the conduct of research into BEE in rural China is crucial. With the high energy consumption, low energy efficiency, and poor living comfort in rural China, the improvement of RBEE is an area

worth exploring. We analyzed the current situation and characteristics of RBEE. On the basis of the literature review, governmental reports, and semi-structured interviews, we performed a SWOT analysis to investigate the opportunities, threats, strengths, and weaknesses of RBEE.

Three opportunities, namely, "top-to-bottom policy support", "construction of new socialist initiatives in the countryside", and "appeal for enhancing RBEE", were identified. The major threats were found to be "lack of policies and standards", "unreasonable energy structure", and "lack of supervising mechanism". The typical strengths for RBEE included "poor energy efficiency consciousness", "abundant renewable energy resources", and "requirements for improving living comfort". The major weaknesses comprised "poor energy efficiency consciousness", "inadequate knowledge and information", and "low-income level of rural residents". Corresponding strategies were proposed on the basis of the analysis. These strategies involve "formulating a carrot-and-stick policy governance mechanism", "establishing technology R&D institutions in local regions", "promoting demonstration projects of RBEE", "carrying out RBEE training", and "providing economic subsidies to rural residents". These findings may expand our understanding of the current situation of RBEE in China and provide a valuable strategic plan for improving RBEE.

The process of BEE in the countryside lags far behind that in cities [32]. With its specific features discussed above, RBEE is remarkably distinct from urban BEE. Replicating experiences in the urban context for the rural setting is unreasonable. Therefore, the proposed strategies can be adopted by policymakers to promote RBEE development in the near future. In the context of new urbanization initiatives, existing residential buildings in rural China should be retrofitted to offer significant opportunities to reduce energy consumption and greenhouse gas emissions [49]. The present research mainly focused on the BEE of newly constructed rural buildings. However, the energy efficiency potentials of existing buildings in a real-world situation should not be ignored. Extant studies can offer valuable references [50–54]. Therefore, future studies should consider exploring suitable BEE strategies for existing buildings in rural China.

Acknowledgments: This work was financially supported by the National Social Science Foundation of China (grant number 14BJY060), Shandong Province Social Science Foundation of China (grant number 17CGLJ12), Jinan Social Science Foundation of China (grant number JNSK18DS12), and National Science Foundation of China (grant number 71403150). The authors would like to thank everyone who contributed to the interviews and to the review of the manuscript.

Author Contributions: Lin Zhang and Shan Guo contributed to conceive and design the study; Lin Zhang conducted semi-structured interviews and wrote the paper. Zezhou Wu analyzed governmental reports and revised the paper. Ahmed Alsaedi and Tasawar Hayat collected and consulted the relevant references.

Conflicts of Interest: The authors declare no conflict of interest.

Nomenclature List

BEE	Building energy efficiency
RBEE	Rural building energy efficiency
SWOT	Strength-weakness-opportunity-threat
MOHURD	Ministry of Housing and Urban–Rural Development
L	Literature reviews
I	Semi-structured interviews
G	Governmental reports
MOF	Ministry of Finance
GOOSC	General Office of the State Council of the People's Republic of China
MOIIT	Ministry of Industry and Information Technology
BEERCTU	Building Energy Efficiency Research Center of Tsinghua University

References

1. He, B.J.; Yang, L.; Ye, M.; Mou, B.; Zhou, Y. Overview of rural building energy efficiency in China. *Energy Policy* **2014**, *69*, 385–396. [CrossRef]

2. Evans, M.; Yu, S.; Song, B.; Deng, Q.; Liu, J.; Delgado, A. Building energy efficiency in rural China. *Energy Policy* **2014**, *64*, 243–251. [CrossRef]
3. 13th Five-Year Plan for Building Energy Saving and Green Building Development. Available online: http://www.mohurd.gov.cn/wjfb/201703/t20170314_230978.html (accessed on 1 March 2017).
4. Lu, S.; Tang, X.; Ji, L.; Tu, D. Research on Energy-Saving Optimization for the Performance Parameters of Rural-Building Shape and Envelope by TRNSYS-GenOpt in Hot Summer and Cold Winter Zone of China. *Sustainability* **2017**, *9*, 294. [CrossRef]
5. Yau, Y. Eco-labels and willingness-to-pay: A Hong Kong study. *Smart Sustain. Built Environ.* **2012**, *1*, 277–290. [CrossRef]
6. Yuan, H. A SWOT analysis of successful construction waste management. *J. Clean. Prod.* **2013**, *39*, 1–8. [CrossRef]
7. Shan, M.; Wang, P.; Li, J.; Yue, G.; Yang, X. Energy and environment in Chinese rural buildings: Situations, challenges, and intervention strategies. *Build. Environ.* **2015**, *91*, 271–282. [CrossRef]
8. He, B.-J.; Yang, L.; Griffy-Brown, C.; Mou, B.; Zhou, Y.-N.; Ye, M. The assessment of building energy efficiency in China rural society: Developing a new theoretical construct. *Technol. Soc.* **2014**, *38*, 130–138. [CrossRef]
9. Wu, Y.; Yin, S. Investigating the critical factors to improve rural buildings energy efficiency. *J. Constr. Technol.* **2014**, *16*, 70–72. (In Chinese)
10. Liu, W.; Spaargaren, G.; Mol, A.P.J.; Heerink, N.; Wang, C. Low carbon rural housing provision in China: Participation and decision making. *J. Rural Stud.* **2014**, *35*, 80–90. [CrossRef]
11. Wang, H.; Wang, L.; Su, F.; Tao, R. Rural residential properties in China: Land use patterns, efficiency and prospects for reform. *Habitat Int.* **2012**, *36*, 201–209. [CrossRef]
12. Wang, Y.; Guo, X.; Liu, H. Synthetic evaluation of new socialist countryside construction at county level in China. *China Agric. Econ. Rev.* **2011**, *3*, 383–401. [CrossRef]
13. Li, Y.; Jia, L.; Wu, W.; Yan, J.; Liu, Y. Urbanization for rural sustainability—Rethinking China's urbanization strategy. *J. Clean. Prod.* **2018**, *178*, 580–586. [CrossRef]
14. Chen, Z.M.; Chen, G.Q. An overview of energy consumption of the globalized world economy. *Energy Policy* **2011**, *39*, 5920–5928. [CrossRef]
15. Chen, Z.M.; Chen, G.Q.; Chen, B. Embodied Carbon Dioxide Emission by the Globalized Economy: A Systems Ecological Input-Output Simulation. *J. Environ. Inform.* **2015**, *21*, 35–44. [CrossRef]
16. Chen, Z.M.; Chen, G.Q.; Zhou, J.B.; Jiang, M.M.; Chen, B. Ecological input–output modeling for embodied resources and emissions in Chinese economy 2005. *Commun. Nonlinear Sci. Numer. Simul.* **2010**, *15*, 1942–1965. [CrossRef]
17. Chen, G.Q.; Guo, S.; Shao, L.; Li, J.S.; Chen, Z.M. Three-scale input–output modeling for urban economy: Carbon emission by Beijing 2007. *Commun. Nonlinear Sci. Numer. Simul.* **2013**, *18*, 2493–2506. [CrossRef]
18. Guo, S.; Chen, G.Q. Multi-scale input-output analysis for multiple responsibility entities: Carbon emission by urban economy in Beijing 2007. *J. Environ. Account. Manag.* **2013**, *1*, 43–54. [CrossRef]
19. Li, J.S.; Chen, G.Q.; Lai, T.M.; Ahmad, B.; Chen, Z.M.; Shao, L.; Ji, X. Embodied greenhouse gas emission by Macao. *Energy Policy* **2013**, *59*, 819–833. [CrossRef]
20. Han, M.Y.; Chen, G.Q.; Shao, L.; Li, J.S.; Alsaedi, A.; Ahmad, B.; Guo, S.; Jiang, M.M.; Ji, X. Embodied energy consumption of building construction engineering: Case study in E-town, Beijing. *Energy Build.* **2013**, *64*, 62–72. [CrossRef]
21. Shao, L.; Chen, G.Q.; Chen, Z.M.; Guo, S.; Han, M.Y.; Zhang, B.; Hayat, T.; Alsaedi, A.; Ahmad, B. Systems accounting for energy consumption and carbon emission by building. *Commun. Nonlinear Sci. Numer. Simul.* **2014**, *19*, 1859–1873. [CrossRef]
22. STDPC. *Report on the Development of Chinese Building Energy Conservation*; China Architecture & Building Press: Beijing, China, 2016. (In Chinese)
23. Ke, Y.; Zhao, X.; Wang, Y.; Wang, S.Q. SWOT analysis of domestic private enterprises in developing infrastructure projects in China. *J. Financ. Manag. Prop. Constr.* **2013**, *14*, 152–170. [CrossRef]
24. Chen, W.M.; Kim, H.; Yamaguchi, H. Renewable energy in eastern Asia: Renewable energy policy review and comparative SWOT analysis for promoting renewable energy in Japan, South Korea, and Taiwan. *Energy Policy* **2014**, *74*, 319–329. [CrossRef]
25. Jaber, J.O.; Elkarmi, F.; Alasis, E.; Kostas, A. Employment of renewable energy in Jordan: Current status, SWOT and problem analysis. *Renew. Sustain. Energy Rev.* **2015**, *49*, 490–499. [CrossRef]

26. Lupu, A.G.; Dumencu, A.; Atanasiu, M.V.; Panaite, C.E.; Dumitrașcu, G.; Popescu, A. SWOT analysis of the renewable energy sources in Romania—case study: Solar energy. *IOP Conf. Ser. Mater. Sci. Eng.* **2016**, *147*, 012138. [CrossRef]
27. Jiang, R.; Mao, C.; Hou, L.; Wu, C.; Tan, J. A SWOT Analysis for Promoting Off-site Construction under the Backdrop of China's New Urbanisation. *J. Clean. Prod.* **2017**, *173*, 225–234. [CrossRef]
28. Qin, Y.; Zhang, L. SWOT Analysis for PCDM Development in Building Energy Conservation in China. *Energy Procedia* **2012**, *16*, 172–177. [CrossRef]
29. Shen, L.Y.; Zhao, Z.Y.; Drew, D.S. Strengths, Weaknesses, Opportunities, and Threats for Foreign-Invested Construction Enterprises: A China Study. *J. Constr. Eng. Manag.* **2006**, *132*, 966–975. [CrossRef]
30. Yang, P.Y.; Zhao, L.Y.; Liu, Z.L. Influences of new socialist countryside construction on the energy strategy of china and the countermeasures. *Energy* **2010**, *35*, 698–702. [CrossRef]
31. Wu, Y.; Liu, X.; Qin, L. Study on status, trends and development of building energy efficiency in rural areas in Northern China. *J. Build. Sci.* **2010**, *26*, 7–14. (In Chinese)
32. Sha, K.; Wu, S. Multilevel governance for building energy conservation in rural China. *Build. Res. Inform.* **2016**, *44*, 619–629. [CrossRef]
33. Zhang, D.; Wang, J.; Lin, Y.; Si, Y.; Huang, C.; Yang, J.; Huang, B.; Li, W. Present situation and future prospect of renewable energy in China. *Renew. Sustain. Energy Rev.* **2017**, *76*, 865–871. [CrossRef]
34. Li, Q.; Shan, M.; Yang, M.; Yang, X. Development approach and emission reduction potential of energy saving in rural buildings. *J. Constr. Technol.* **2010**, *5*, 40–42. (In Chinese)
35. Zhang, L.; Yang, Z.; Chen, B.; Chen, G. Rural energy in China: Pattern and policy. *Renew. Energy* **2009**, *34*, 2813–2823. [CrossRef]
36. Ai, S.; He, Z.; Shu, W.; Wang, D. Analysis on the difficulties and Countermeasures of energy-saving retrofitting of rural buildings in Chinese hot summer and cold winter areas. *Real Estate Biwkly* **2017**, *9*, 204. (In Chinese)
37. Wimala, M.; Akmalah, E.; Sururi, M.R. Breaking through the Barriers to Green Building Movement in Indonesia: Insights from Building Occupants. *Energy Procedia* **2016**, *100*, 469–474. [CrossRef]
38. Zhang, Y.; Wang, Y. Barriers' and policies' analysis of China's building energy efficiency. *Energy Policy* **2013**, *62*, 768–773. [CrossRef]
39. Peng, C.; Jiang, Y. *Roadmap for China's Building Energy Conversation*; China Architecture & Building Press: Beijing, China, 2015.
40. Liu, L.-Q.; Liu, C.-X.; Sun, Z.-Y. A survey of China's low-carbon application practice—Opportunity goes with challenge. *Renew. Sustain. Energy Rev.* **2011**, *15*, 2895–2903. [CrossRef]
41. BEECRTU. *Research Report on the Annual Development of Chinese Building Energy Conservation*; China Architecture &Building Press: Beijing, China, 2012. (In Chinese)
42. Zhu, J.; Tao, L. Research on Environmental Legal System Innovation in Construction New rural. *J. Yunnan Univ.* **2011**, *24*, 78–82. (In Chinese)
43. BEECRTU. *Annual Development Report of Chinese Building Energy Saving*; China Architecture &Building Press: Beijing, China, 2008. (In Chinese)
44. Li, H.; Dong, L.; Duan, H. On Comprehensive Evaluation and Optimization of Renewable Energy Development in China. *Resour. Sci.* **2011**, *33*, 431–440. (In Chinese)
45. Li, C. Potential Analysis on Energy and Resources of Green Towns in Severe Cold Area. Master's Thesis, Harbin Industrial University, Harbin, China, June 2017. (In Chinese)
46. Ji, S. A Research on Chinese Migrant Workers' Employment Studys. *J. Econ. Theory Manag. Res.* **2011**, *2*, 93–99. (In Chinese)
47. Shen, L.; He, B.; Jiao, L.; Song, X.; Zhang, X. Research on the development of main policy instruments for improving building energy-efficiency. *J. Clean. Prod.* **2016**, *112*, 1789–1803. [CrossRef]
48. Jaillon, L.; Poon, C.S. Sustainable construction aspects of using prefabrication in dense urban environment: A Hong Kong case study. *Constr. Manag. Econ.* **2008**, *26*, 953–966. [CrossRef]
49. Ma, Z.; Cooper, P.; Daly, D.; Ledo, L. Existing building retrofits: Methodology and state-of-the-art. *Energy Build.* **2012**, *55*, 889–902. [CrossRef]
50. Lv, S.; Wu, Y. Target-oriented obstacle analysis by PESTEL modeling of energy efficiency retrofit for existing residential buildings in China's northern heating region. *Energy Policy* **2009**, *37*, 2098–2101.

51. Bao, L.; Zhao, J.; Zhu, N. Analysis and proposal of implementation effects of heat metering and energy efficiency retrofit of existing residential buildings in northern heating areas of China in "the 11th Five-Year Plan" period. *Energy Policy* **2012**, *45*, 521–528. [CrossRef]
52. Galatioto, A.; Ciulla, G.; Ricciu, R. An overview of energy retrofit actions feasibility on Italian historical buildings. *Energy* **2017**, *137*, 991–1000. [CrossRef]
53. Rey, E. Office building retrofitting strategies: Multicriteria approach of an architectural and technical issue. *Energy Build.* **2004**, *36*, 367–372. [CrossRef]
54. Asadi, E.; da Silva, M.G.; Antunes, C.H.; Dias, L. Multi-objective optimization for building retrofit strategies: A model and an application. *Energy Build.* **2012**, *44*, 81–87. [CrossRef]

energies

MDPI

Article

The Co-Movement and Asymmetry between Energy and Grain Prices: Evidence from the Crude Oil and Corn Markets

Zhan-Ming Chen, Liyuan Wang, Xiao-Bing Zhang * and Xinye Zheng

School of Applied Economics, Renmin University of China, Beijing 100872, China; chenzhanming@ruc.edu.cn (Z.-M.C.); wangliyuan@ruc.edu.cn (L.W.); zhengxinye@ruc.edu.cn (X.Z.)

* Correspondence: xiaobing.zhang@ruc.edu.cn

Received: 27 February 2019; Accepted: 3 April 2019; Published: 9 April 2019

Abstract: This paper investigates the co-movement and asymmetric interactions between energy and grain prices, based on the evidence from the crude oil and corn markets, the most important energy and grain markets, respectively. Time series analysis indicates that there is a consistent trend between the crude oil price and corn price with a significant positive correlation coefficient 0.7471 during the sampling period, from January 2008 to February 2016. In addition, we find that there is a long-run equilibrium relationship between the two commodities' prices. Moreover, while linear Granger causality tests suggest that there is a two-way Granger causality relationship between the price changes in the two markets, non-linear Granger causality tests suggest that there is only a one-way causality relationship from corn to oil price. However, both linear and non-linear Granger causality tests indicate the asymmetry of causality relationship between the two markets (the price change in corn market can more significantly Granger cause the change in crude oil market). Further analysis suggests that the contribution of the corn market to price discovery in a large commodity market is larger than that of the crude oil market.

Keywords: crude oil market; corn market; asymmetry; price discovery

1. Introduction

In recent years, the energy policies around the world tend to become more environment-friendly and there is an increasing focus on renewable energy. In this respect, one of the most remarkable developments in the energy sector is the rapid development of biofuels. Biofuel policy has been in place in the United States (US) since the Energy Policy Act of 1978, which was conceived by the US Congress as a response to the OPEC-induced oil shock. In 1990, with the concerns about climate change and pollution, the US Congress conceived the Clean Air Act of 1990, requiring that the gasoline must contain a minimum percentage of oxygen. Ethanol and methyl tertiary-butyl ether (MTBE) are both additives into regular gasoline, and MTBE was more popular because it was cheaper and more available and easier to transport and distribute. However, after the hidden costs and health risks of MTBE were convinced, the US Congress passed the Energy Policy Act of 2005. The new renewable fuel standards established by the Energy Policy Act of 2005 make ethanol the only available gasoline additive and the new standard became applicable in May 2006, which consequently lead to the ethanol production boom in the United States.

Along with the booming of ethanol, there are more and more corns that are used for ethanol production in the United States. As shown in Figure 1, corns used for fuel ethanol account for more than 35% of the whole production of corn in the US since 2010, competing with the traditional uses of corns (including for food and livestock feed). Meanwhile, fuel ethanol production and consumption in the US also takes off and the fuel ethanol plays an increasingly important role in the transportation

sector. The market share of the fuel ethanol consumption, which is calculated by dividing the volume of ethanol consumption by the sum of motor gasoline and ethanol consumption, has reached 9.51% by the year 2015.

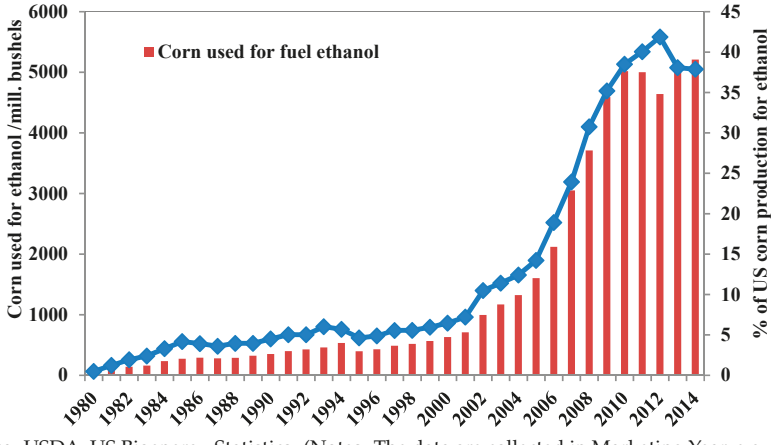

Source: USDA, US Bioenergy Statistics. (Notes: The data are collected in Marketing Year, e.g., '2014' means from September 2014 to August 2015).

Figure 1. Corn used for ethanol in the US.

Since the ethanol boom in the US in 2006, the interaction between the energy market and the agriculture market has become much stronger. Agriculture uses energy products directly in the form of gasoline, diesel and electricity as the fuel of the farm machinery. Meanwhile, the agriculture sector also uses energy-based input such as fertilizer and pesticides. Higher energy prices can make agricultural goods more expensive by raising the costs of production (including fuel, fertilizer, chemicals and other inputs) and transportation. Besides, crude oil and corn are naturally linked through the substitution possibility between gasoline and bio-ethanol. Higher oil prices would stimulate the growth of corn-based biofuels production and the expansion of the demand for corns, which can consequently boost the corn price.

Furthermore, along with the globalization, the gradual liberalization of financial markets, the rapid development of advanced communication technologies, and the financialization of commodity markets, different goods and assets have become more and more interlinked. For instance, crude oil and corn prices are both affected by the US dollar exchange rate, local military conflicts, monetary policy pursued by central banks and the increased demand for basic materials from rapidly growing emerging markets [1,2].

Giving that there is a close link between the energy sector and the agricultural sector, it would be of great significance to investigate the long- and short-run dynamic relationship between the energy and agriculture commodity markets. Due to their different attributes, the energy and agricultural products may respond differently to the same economic, political or natural shocks. The extreme weather and climate events, and natural disasters, for instance, may have more significant effects on the agriculture commodity market. For example, the severe drought in 2002–2003 in Australia, one of the world's largest wheat producers, significantly cut down the global wheat production, thereby raising the wheat price dramatically, while the effect on the crude oil price is less significant.

Understanding the relationship between the energy and agriculture commodity markets will be useful for farmers, investors and even politicians. Commodity price shocks and varying degrees of fluctuations pose serious policy challenges to the decision-makers. Sharp movements in commodity prices have serious impacts in terms of trade, real income and fiscal position of countries that depend on these commodities. Therefore, a better understanding of the recent dynamics of energy and agriculture

markets could assist decision-makers for a better macroeconomic policies and regulations of the commodity markets, which motivates this study.

In this paper, we use the crude oil market as the representation of the energy market, and the corn market as the representation of the agriculture market, due to the fact that corn is the most widely produced feed grain in the United States and is the most important feedstock in the extraction of the fuel ethanol. Meanwhile, corn is one of the most heavily-traded contracts in the agricultural commodity market. Focusing on the relationship between crude oil and corn markets, we investigate the long- and short-term interaction between crude oil and corn prices and examine whether there is (linear and non-linear) Granger causality relationships between the two commodity markets. Moreover, we calculate the two markets' respective contribution to the price discovery of large commodity markets. Our results show that there is a long-run equilibrium relationship between the crude oil and corn markets. Moreover, while linear Granger causality tests suggest that there is a two-way Granger causality relationship between the returns in the two markets, non-linear Granger causality tests suggest that there is only unilateral causality running from the corn market to the crude oil market. Nevertheless, both linear and non-linear Granger causality tests indicate the asymmetry of the causality relationship between the two markets (the change in the corn market more significantly Granger causes the change in the crude oil market). Further analysis suggests that the contribution of the corn market to the price discovery in large commodity markets is larger than that of the crude oil market.

The reminder of the paper is organized as follows. Section 2 presents a review of the literature. Section 3 provides a description of the data. Then, we present the empirical methodologies in Section 4. Section 5 analyzes the empirical results of this study, including the long-term equilibrium and short-term adjustment between the crude oil and corn prices, the linear and non-linear Granger causality between the two markets, and their respective contribution to price discovery. Finally, Section 6 gives some concluding remarks.

2. Literature Review

There is an increasing number of studies on the agriculture commodity market due to the increasing concerns on agriculture supply security in the world, especially that in the developing world. A large literature on prices of agriculture commodities has mainly focused on analyzing the co-integration relationships between spot and futures prices and the basic conclusion is that, though a co-integration relationship does exist, futures prices generally dominate spot prices in agriculture commodity markets. For instance, Garbade and Silber [3] analyzed the price movements and price discovery in spot and futures markets for seven storable commodities, including corn, wheat, oats, orange, copper, gold and silver and they found that futures prices dominate spot price changes for most of these commodities. Yang et al. [4] investigated the price discovery function for storable agriculture commodities (corn, oats, soybeans, wheat, cotton and pork bellies) and non-storable agricultural commodities (hogs, live cattle, feeder cattle) and found that although, in general, storability does not affect the future price discovery function, future contracts can be used as a price discovery tool in all of these markets. Zapato et al. [5] investigated the co-integrating relationship between the New York futures prices and the Dominican Republic spot prices and found that the World Futures Sugar (WFS) price has a predictive power for the spot price of a small sugar-producing country. Mattos and Garica [6] examined the relationship between spot and futures prices in six agricultural markets of Brazil and found that the thinly traded future contracts have some degree of long-run co-integration relationship with the spot price but the highly-traded corn contracts show almost no interrelations between the future and spot prices.

While there is a large literature on world oil market focus on identifying the driving forces and determinant factors behind the volatility of oil price, such as economic crisis, oil supply and demand, OECD commercial inventory, OPEC behaviors, US dollar exchange rate, local military conflicts, natural hazards and speculative trading activities [7–10], or on the linkage between crude oil and other financial markets [11,12], there is an increasing number of studies on the linkage and relationship between energy (mainly oil) and agriculture commodity markets. However, the results are mixed and there

has been no consensus on the food-energy nexus. Some researchers indicate that the oil price has a significant effect on the agriculture commodity price. Trujillo-Barrera et al. [13] focused on the volatility spillovers in the US from energy to agricultural markets in the period 2006–2011. They discovered significant spillovers from oil to corn and ethanol markets, which seems to be particularly strong in high volatility periods for oil markets. They also identified significant volatility spillovers from corn to ethanol markets. Using co-integration and a linear Granger causality test Avalos [14] exploits a natural experiment arising from a significant change in 2006 on the nature of ethanol policies in the US to assess the relationship between oil, corn and soybean prices. He finds that there are substantial changes in the dynamic properties of corn and soybean prices and they are more closely related to oil prices, but the predictive causality seems to run from the crops to oil prices. In contrast, some research indicates that there is no direct relationship between oil and agricultural commodity prices. Zhang et al. [15], using monthly data from March 1989 through July 2008, found that there is no long-term relationship between oil and food (corn and soybeans) prices.

The studies on the mechanism of the linkage between oil and agricultural prices mainly focus on three key channels: (i) oil as a production cost in agriculture; (ii) biofuels; and (iii) co-movement of commodity prices with macroeconomic factors and financial indicators, according to Nazlioglu et al. [16], where they provide a comprehensive review on the studies based on each linkage. For instance, in terms of oil as an input for agriculture production, Baffes [17,18] investigated the spillover effect of crude oil price changes on the prices of 35 internationally traded primary commodities and calculated the pass-through of crude oil price changes to the overall non-energy commodity index, the fertilizer index, agriculture and metals. They found that the highest pass-through of oil price changes is to the fertilizer index followed by agriculture. Considering biofuels as the channel for the linkage between oil and agriculture prices, the findings are mixed. Serra et al. [19] and Hassouneh et al. [20] examined the price linkages and transmission patterns in the US and Spain, respectively, and they both found long-run equilibrium relationships among the prices of biofuels and oil and strong links between energy and food prices. However, Zhang et al. [15] investigated both short- and long-run relationships between prices of fuel and agricultural commodities and found that there is no direct long-run price relationship between fuel and agricultural commodity prices and there is only limited, if any, direct short-run relationships. Recently, Sari et al. [21] investigated the roles of futures prices of crude oil, gasoline, ethanol, corn, soybeans and sugar in the energy–grain nexus, taking into account the own- and cross-market impacts for the lagged grain trading volume and the open interest in the energy and grain markets. They reveal that the conventional view, which states that the impacts run from oil to gasoline to ethanol to grains in the energy–grain nexus, does not hold well in the long-run because the oil price is influenced by gasoline, soybeans and soybean oil. Besides, in the short-run, there is a two-way feedback in both directions for all markets. The grain trading volume's effect across the oil and gasoline markets is more pronounced in the short-run than in the long-run. As for the third channel for the linkage between oil and agriculture prices, i.e., macroeconomic policies and financial indicators, Krichene [22] examined oil price movements between January 2000 and October 2007 and argued that the rapid increase observed in oil and other commodity prices can be attributed to the expansionary monetary policies during the early 2000s.

To sum up, it should be noted that the existing research related to energy and agriculture commodity prices has focused more on the co-movement of the two markets rather than the asymmetric interactions between the two markets or their asymmetric role in price discovery. Therefore, this study attempts to investigate both the co-movement and asymmetric interactions between energy and grain prices, based on the evidence from the crude oil and corn markets, which are the most important energy and grain markets, respectively. By employing the time-series econometric methods, this paper analyzes the co-integration and (linear and non-linear) causality relationship between the two markets and their respective contribution to price discovery. Some recent studies share similar interest with this paper. For instance, Nazlioglu [23] investigated the co-integration and (linear and non-linear) Granger causality relationship between the world oil and agricultural commodity prices (corn, soybean and

wheat) by using the weekly data spanning from 1994 to 2010. Her linear causality test indicates that the oil prices and the agricultural commodity prices do not influence each other while the non-linear causality analysis shows that there is a persistent unidirectional non-linear causality running from the oil prices to the corn and to the soybean prices. Different from Nazlioglu [23], we used daily data from January 2008 to February 2016, given that high frequency data may capture the dynamic casual linkages between different commodity markets better. Our conclusions are very different from that of Nazlioglu [23]. Moreover, we also conducted the price discovery (Permanent-Transitory (PT) and Information Share (IS) models) analysis to further investigate the contribution of different markets in price discovery of large commodity markets, which is absent in the previous studies on the co-movement and transmission among energy and food commodity prices.

3. The Data

In this paper, we used daily time series spot price data for the crude oil and corn prices from 22 January 2008 to 29 February 2016 (this choice of the study period was restricted by our access to the daily corn price from the Chicago Mercantile Exchange). The crude oil price is the Brent crude oil spot price in US dollars per barrel from the US Energy Information Administration (EIA). The corn price is the US No.2 yellow maize (corn) price in US cents per bushel from the Chicago Mercantile Exchange. It can be seen in Figure 2 that the two markets do have some consistent trends in the sample period. The correlation coefficient between the crude oil price and the corn price is 0.7471, indicating that they could have co-movement and share common information in their price dynamics. The descriptive description of the data is presented in Table 1.

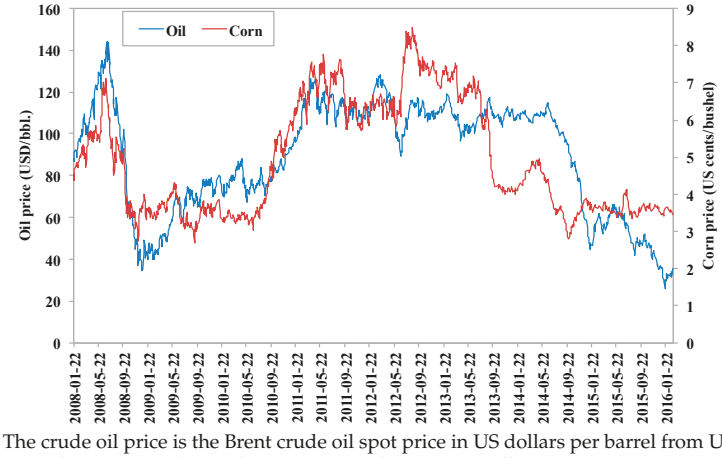

Source: The crude oil price is the Brent crude oil spot price in US dollars per barrel from US Energy Information Administration (EIA); the corn price is the US No.2 yellow maize (corn) price in US cents per bushel from the Chicago Mercantile Exchange.

Figure 2. Daily crude oil spot price and the corn spot price.

Table 1. Descriptive Statistics.

Variable	Obs	Mean	Std. Dev.	Min	Max
Crude oil price P^o	1831	89.495	26.004	26.01	143.95
Corn price P^c	1831	4.972	1.528	2.695	8.49
Ln (P^o)	1831	4.443	0.339	3.258	4.969
Ln (P^c)	1831	1.557	0.304	0.991	2.139
First-order diff. Ln (P^o)	1830	−0.000490	0.024	−0.168	0.181
First-order diff. Ln (P^c)	1830	−0.000148	0.022	−0.121	0.109

Figures 3 and 4 show the returns of the crude oil price and the corn price, respectively. Returns are calculated as the first differences of the logarithms of the prices. During the periods of 2008–2009 and 2015–2016, the crude oil market has more dramatic volatility than the other periods in the sampling period. As for the corn market, the fluctuation of return is higher in the first half of the sampling period.

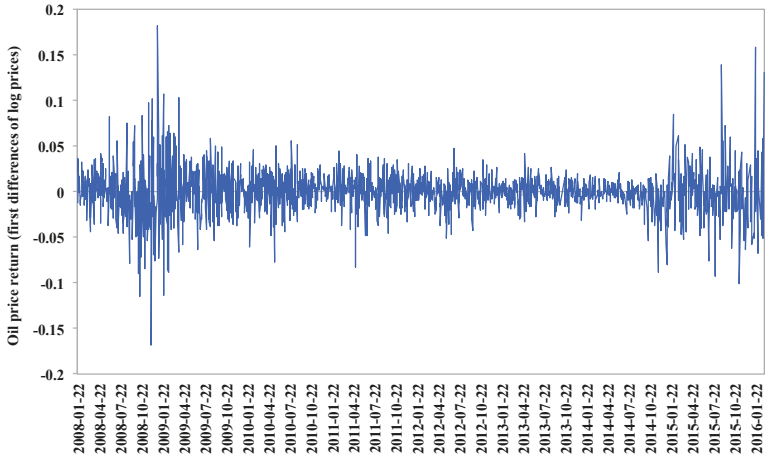

Figure 3. Returns of the crude oil price (the first differences of the logarithm of the prices).

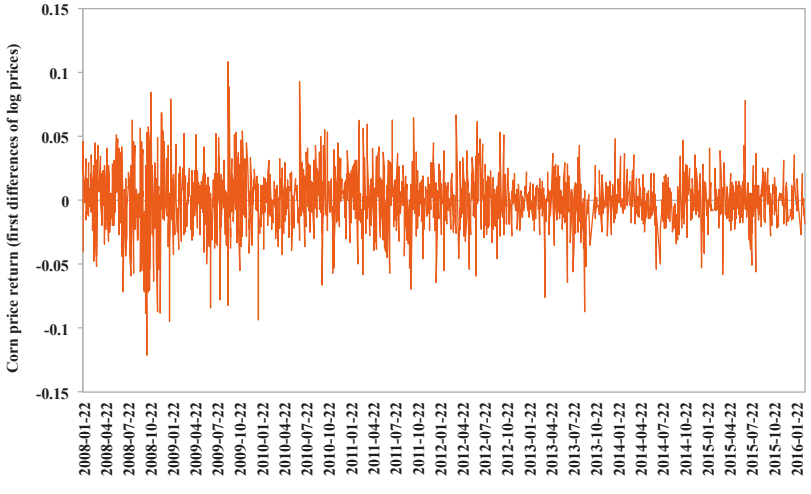

Figure 4. Returns of the corn price (the first differences of the logarithm of the prices).

We used the ADF (augmented Dickey–Fuller) test to check the stationarity of the logarithm of the prices and the returns, as displayed in Table 2. The results of the ADF test show that the logarithm of the two commodities' prices are not stationary, but the first order difference of the (log) prices is stationary, which implies that both price series are I(1), i.e., the returns of the oil and corn prices are stationary. Therefore, we used the logarithm of the prices in the Vector Error Correction (VEC) Model. In addition, the Vector Auto-Regression (VAR) Model was estimated in terms of the returns (the first differences of the logarithm of the oil and corn prices) to avoid spurious regression and inferences.

Table 2. T statistic values of ADF test for the crude oil price and the gold price.

	lnP_t^o	lnP_t^c
Level (log) price	−0.530 (0.9822)	−1.388 (0.8643)
First-order diff. (log) prices	−41.467 (0.0000)	−42.570 (0.0000).

Note: *p*-values are reported in parentheses.

4. Methodology

Given the importance of testing whether there exists a lead-and-lag price mechanism between the two commodities for the whole large commodity market forecast, in this section, we first present the methods to detect whether there is a co-integration relationship between the crude oil and corn markets, and then we test both the linear and non-linear Granger causality between the returns of crude oil and corn. Finally, we use the Permanent-Transitory (PT) model and Information Share (IS) model to find out the contribution of the crude oil price and the corn price to the common effective price of the co-integration system.

4.1. Co-Integration Test between the Crude Oil and Corn Markets

Non-stationary variables may obey a common long-run relationship, which means that there is a stationary linear combination of these variables. If the linear combination does exist, we may say that there is a co-integration relationship between these variables. To test whether there is a long-run equilibrium relationship between the two commodities, we use the two-step procedure provided by Engle and Granger [24]. The long-run equilibrium equations are:

$$\begin{aligned} LnP_t^o &= \phi_1 + \theta_1 LnP_t^c + z_{1t}, \\ LnP_t^c &= \phi_2 + \theta_2 LnP_t^o + z_{2t}, \end{aligned} \tag{1}$$

where P_t^o is the price of the crude oil, P_t^c is the price of the corn, and z_{1t} and z_{2t} are residuals, respectively. If the stationarity test indicates that the residuals are stationary, a long-run equilibrium may exist between the crude oil price and corn price.

4.2. Granger Causality Test

4.2.1. Linear Granger Causality Test

We use the stationary price returns of the commodities (logarithmic difference of original price series) to detect the lead and lag relationship between the oil and the corn prices. Specifically, we establish the VAR model:

$$\begin{aligned} r_t^o &= \pi_{10} + \sum_{i=1}^{p} \varphi_{1i} r_{t-i}^o + \sum_{j=1}^{p} \phi_{1j} r_{t-j}^c + \varepsilon_{1t}, \\ r_t^c &= \pi_{20} + \sum_{i=1}^{p} \varphi_{2i} r_{t-i}^c + \sum_{j=1}^{p} \phi_{2j} r_{t-j}^o + \varepsilon_{2t}, \end{aligned} \tag{2}$$

where $r_t^o = LnP_t^o - LnP_{t-1}^o$ denotes the price returns of the crude oil, $r_t^c = LnP_t^c - LnP_{t-1}^c$ denotes the price returns of the corn, and p is the lag length of the equation, which is chosen according to the Akaike Information Criterion (AIC) and should ensure that there is no autocorrelation in the ε_{1t} and ε_{2t}. For the first equation, we will test the null hypothesis: $\phi_{11} = \phi_{12} = \cdots = \phi_{1p} = 0$, if the null hypothesis is rejected, the change in the corn price return linearly Granger causes the change in the crude oil price return. Similarly, we test $\phi_{21} = \phi_{22} = \cdots = \phi_{2p} = 0$ to investigate whether the oil price return is the linear Granger causality of the corn price return.

4.2.2. Non-Linear Granger Causality Test

Previous studies show that financial time series usually have remarkable non-linear dynamics. However, the traditional linear Granger test can fail to identify the non-linear relationship between variables, which implies significant bias can appear when employing the linear Granger method to test the Granger causality between the variables that may potentially have a non-linear relationship. Baek and Brock [25], and Hiemstra and Jones [26] proposed a method to conduct the non-linear Granger causality test, which has been widely applied in the empirical studies in the economics and finance fields. However, Diks and Panchenko [27] showed that the non-linear Granger causality test proposed by Hiemstra and Jones [26] has the issue of over-rejection and therefore developed a non-parametric T_n test to investigate whether there is non-linear Granger causality between variables. This non-parametric test method has the advantage that it will consider the possible variations in conditional distribution based on the chosen bandwidth so as to overcome the over-rejection problem in the H-J test, thereby making the results of the test more robust and reliable. Therefore, we used the non-parametric T_n test proposed by Diks and Panchenko [27] to investigate whether there are the non-linear Granger causality relations between oil and corn prices. The basic idea of T_n test is as follows:

Let $\{X\}$ and $\{Y\}$ denote the residuals obtained from the two equations in the VAR model (2), respectively. Suppose that $X_t^{Lx} = (X_{t-Lx+1}, \cdots\cdots, X_t)$ and $Y_t^{Ly} = \left(Y_{t-L_y+1}, \cdots\cdots, Y_t\right)$, where Lx, $Ly > 0$, are the delay vectors. Let us examine the null hypothesis that the past observations of X_t^{Lx} do not contain any additional information about Y_{t+1} (beyond that in Y_t^{Ly}), i.e.,

$$H_0 : Y_{t+1} \Big| \left(X_t^{Lx}; Y_t^{Ly}\right) \sim Y_{t+1} \Big| Y_t^{Ly}. \tag{3}$$

The null hypothesis implies that the $(Lx + Ly + 1)$-dimensional vector $W_t = \left(X_t^{Lx}, Y_t^{Ly}, Z_t\right)$, (where $Z_t = Y_{t+1}$) has invariant distribution. If we ignore the time notation and let $Lx = Ly = 1$, the null hypothesis implies that the distribution of Z given that $(X, Y) = (x, y)$ is the same as that of Z given $Y = y$, which implies that H_0 can be restructured using the joint probability density function:

$$\frac{f_{X,Y,Z}(x,y,z)}{f_Y(y)} = \frac{f_{X,Y}(x,y)}{f_Y(y)} . \frac{f_{X,Z}(y,z)}{f_Y(y)}. \tag{4}$$

In other words, Equation (4) states that X and Z are independent, when $Y = y$ for each fixed value of y. Diks and Panchenko [27] show that the restated null hypothesis implies:

$$q \equiv E[f_{X,Y,Z}(X,Y,Z) f_Y(Y) - f_{X,Y}(X,Y) f_{Y,Z}(Y,Z)] = 0. \tag{5}$$

Let $\hat{f}_W(W_i)$ denote a local density estimator of a d_W-variate random vector W at W_i, i.e., $\hat{f}_W(W_i) = (2\varepsilon_n)^{-d_w}(n-1)^{-1} \sum_{j,j\neq i} I_{ij}^W$, where $I_{ij}^W = I\left(\|W_i - W_j\| < \varepsilon_n\right)$ and $I(\cdot)$ is the indicator function and ε_n is the bandwidth, which depends on the sample size n. Then, the non-parametric test statistic T_n can be constructed as Equation (6), which can be used to conduct the non-linear Granger causality test between variables:

$$T_n(\varepsilon_n) = \frac{n-1}{n(n-2)} \sum_i \left(\hat{f}_{X,Z,Y}(X_i, Z_i, Y_i)\hat{f}_Y(Y_i) - \hat{f}_{X,Y}(X_i, Y_i)\hat{f}_{Y,Z}(Y_i, Z_i)\right). \tag{6}$$

For $Lx = Ly = 1$ and if $\varepsilon_n = Cn^{-\beta}\left(C > 0, \frac{1}{4} < \beta < \frac{1}{3}\right)$, Diks and Panchenko [27] prove that the test statistic in Equation (6) satisfies:

$$\sqrt{n}\frac{(T_n(\varepsilon_n) - q)}{S_n} \xrightarrow{D} N(0,1), \tag{7}$$

where $\xrightarrow{D}$ denotes convergence in distribution and S_n is an estimator of the asymptotic variance of $T_n(\cdot)$ [27].

4.3. PT and IS Model for Price Discovery

Based on the results of the VEC model, we adapt two popular common factor models to investigate the mechanisms of price discovery: The first model is the Permanent-Transitory (PT) model by Gonzalo and Granger [28]; the second model is the Information Shares (IS) model by Hasbrouck [29]. We first used the PT model to estimate the common long-memory components of the co-integration system between the crude oil price and the corn price and the two markets' contribution to the common factor, which is a function of the coefficients of the error-correction model. Then, the IS model is employed to measure the two markets' information share, which is defined as the proportional contribution of that market's innovation to the innovation in the common efficient price.

4.3.1. Permanent-Transitory (PT) Model

As proved by Stock and Watson [30], if two time series are co-integrated, in other words, $z_t = y_t - Ax_t$ is stationary, there must exist a common factor f_t.

$$\begin{bmatrix} y_t \\ x_t \end{bmatrix} = \begin{bmatrix} A \\ 1 \end{bmatrix} f_t + \begin{bmatrix} \widetilde{y}_t \\ \widetilde{x}_t \end{bmatrix},$$

where y_t and x_t are I(1), $\widetilde{y}_t$ and $\widetilde{x}_t$ are I(0), f_t is the common effective price, and might be the unobserved factor and the driving force resulting in the co-integration relationship. Each time series Y_t can be decomposed into two components, $Y_t = f_t + \widetilde{Y}_t$, one is the permanent component f_t, and the other is the transitory component $\widetilde{Y}_t$, which can be called the noisy price of the market. The two components convey different kinds of information.

There are several reasons why we are interested in f_t. Firstly, if the model of the complete set of variables is too complex, and if we are only interested in the long-run behavior, we can use a small set of common long-run effective factors. Secondly, the estimation of the common factor allows us to decompose a variable into two components that convey different kinds of information, the permanent component (trend component) f_t and the transitory components (cyclical component) $\widetilde{Y}_t$. Finally, singling out the common factors allows us to investigate the relationship between the common factor and other variables.

Based on the Vector Error Correction Model (VECM):

$$\Delta LnP_t^o = \alpha_1\left(LnP_{t-1}^o + \beta LnP_{t-1}^c\right) + \sum_{i=1}^{q} \gamma_{1i}\Delta LnP_{t-i}^o + \sum_{i=1}^{q} \theta_{1i}\Delta LnP_{t-i}^c + \varepsilon_{1t},$$
$$\Delta LnP_t^c = \alpha_2\left(LnP_{t-1}^o + \beta LnP_{t-1}^c\right) + \sum_{i=1}^{q} \gamma_{2i}\Delta LnP_{t-i}^o + \sum_{i=1}^{q} \theta_{2i}\Delta LnP_{t-i}^c + \varepsilon_{2t},$$

where α_1 and α_2 are the error-correction coefficients. β denotes the cointegrating coefficient. ε_{1t} and ε_{2t} are serially uncorrelated innovations with zero mean.

In the equation $Y_t = f_t + \widetilde{Y}_t$, where $Y_t = \left(LnP_t^o, LnP_t^c\right)'$, and $f_t = \Gamma Y_t$, $\Gamma = (\gamma_1, \gamma_2)$, f_t can be regarded as a weighted average of the prices of the two markets. In addition, $\Gamma = (\gamma_1, \gamma_2)$ is the coefficient vector of common factor, which can be considered as the weights of crude oil price and corn price in the portfolio, and $\gamma_1 + \gamma_2 = 1$. Besides, as shown by Gozalo and Granger [28], Γ is orthogonal to the error-correction coefficient $(\alpha_1, \alpha_2)'$, in other words, $\alpha_1\gamma_1 + \alpha_2\gamma_2 = 0$. Therefore, along with the condition $\gamma_1 + \gamma_2 = 1$, γ_1 and γ_2 can be solved out from the two equations above.

4.3.2. Information Shares (IS) Model

According to Hasbrouck [29], a market's contribution to price discovery is its information share, which is defined as the proportion of the efficient price innovation variance that can be attributed to that market. Price variables can be expressed as the vector moving average (VMA) form:

$$\Delta P_t = \Psi(L)e_t,$$

where e_t is a zero-mean vector of serially uncorrelated disturbances with covariance matrix Ω,

$$\Omega = \begin{bmatrix} \sigma_1^2 & \rho\sigma_1\sigma_2 \\ \rho\sigma_1\sigma_2 & \sigma_2^2 \end{bmatrix},$$

where σ_1^2 and σ_2^2 are the variance of ε_{1t} and ε_{2t}, respectively; and ρ is the correlation coefficient between ε_{1t} and ε_{2t}. Ψ is a polynomial in the lag operator. If the prices are cointegrated of order n-1, then all the rows of $\Psi(1)$ are identical, and $\Psi(1)e_t$ constitutes the long-run impact of a disturbance on each of the price. Letting ψ denote the common row vector, the price levels can be written as:

$$P_t = P_0 + \iota\psi\left(\sum_{s=1}^{t} e_s\right) + \Psi^*(L)e_t,$$

where $\iota = (1,1)'$. Additionally, $\Psi^*(L)$ is a matrix polynomial in the lag operator. The second term $\iota\psi\left(\sum_{s=1}^{t} e_s\right)$ is the random-walk component that is common to all prices. The variance of the common factor is $\mathrm{Var}(\psi e_t) = \psi\Omega\psi'$. The information share of a market is the proportion of value $\mathrm{Var}(\psi e_t)$ that is attributable to that market. If the covariance matrix Ω is diagonal, the information shares of the crude oil market and the corn market are:

$$S_o = \frac{\psi_1^2\sigma_1^2}{\psi\Omega\psi'},$$

$$S_c = \frac{\psi_2^2\sigma_2^2}{\psi\Omega\psi'}.$$

Baillie et al. [31] investigated the relationship between the PT model and the IS model, and they discovered that $\frac{\psi_1}{\psi_2} = \frac{\gamma_1}{\gamma_2}$. Therefore, the information shares are:

$$S_o = \frac{\gamma_1^2\sigma_1^2}{\gamma_1^2\sigma_1^2 + \gamma_2^2\sigma_2^2},$$

$$S_c = \frac{\gamma_2^2\sigma_2^2}{\gamma_1^2\sigma_1^2 + \gamma_2^2\sigma_2^2}.$$

However, if the covariance matrix is not diagonal, one can use Cholesky factorization to minimize the correlation, where $\Omega = MM'$,

$$\mathrm{M} = \begin{bmatrix} m_{11} & 0 \\ m_{12} & m_{22} \end{bmatrix} = \begin{bmatrix} \sigma_1 & 0 \\ \rho\sigma_2 & \sigma_2\left(1-\rho^2\right)^{1/2} \end{bmatrix}.$$

Therefore, the information shares can be written as:

$$S_o = \frac{\left(\gamma_1 m_{11} + \gamma_2 m_{21}\right)^2}{\left(\gamma_1 m_{11} + \gamma_2 m_{21}\right)^2 + \left(\gamma_2 m_{22}\right)^2},$$

$$S_c = \frac{\left(\gamma_2 m_{22}\right)^2}{\left(\gamma_1 m_{11} + \gamma_2 m_{21}\right)^2 + \left(\gamma_2 m_{22}\right)^2},$$

and $S_o + S_c = 1$.

The factorization imposes a greater share on the first price, unless $m_{12} = 0$, therefore, we need to change the order of variables in the factorization procedure to get an upper and a lower limit of

the information share of a market price. The average of the lower bound and upper bound can be regarded as a reasonable estimation of a market's contribution to price discovery [11,31].

5. Empirical Results

In this section, empirical results are reported and discussed in three parts. The first part reports the results from the VEC model, discussing the long-run equilibrium and the short-run adjustment of the two markets. The next part is the lead and lag relationship between the two markets, i.e., the Granger causality relationship between the crude oil and corn prices. The last part reports the two markets' contribution to price discovery from the PT model and the IS model.

5.1. The Long-Run Equilibrium and the Short-Run Adjustment between the Crude Oil Market and the Corn Market

According to the results of the unit root test in Section 3 (see Table 2), we confirm that the Ln (crude oil price) and the Ln (corn price) are both I(1). Then, we have to identify whether there is a co-integration relationship between the crude oil price and the corn price. The results of the unit root test of the error term from Equation (1) are displayed in Table 3.

Table 3. Estimation results of integration Equation (1) and the ADF test results of the residuals.

Dependent Variables	ϕ	θ	F-Statistic	*T* Statistic of ADF Test for *z*
LnP_t^o	3.1901 (0.0000)	0.8043 (0.0000)	1974.48 (0.0000)	−1.699 (0.0893)
LnP_t^o	−1.3100 (0.0000)	0.6454 (0.0000)	1974.48 (0.0000)	−2.303 (0.0213)

The results show that both equations are jointly significant at the 1% level and that residuals are stationary (at the 10% level and 5% level, respectively). Therefore, we know that there is a long-run equilibrium relationship between the crude oil price and the corn price, which is likely due to the common economic factors (e.g., the US dollar index) that affect the two markets and the possible substitution of biofuel from coal and oil in some sectors (e.g., transport sector) of the world economy. This result is consistent with a number of previous studies (see e.g., Harri et al. [32] where they identified a long run equilibrium relationship between oil prices and all agricultural prices except wheat).

Based on the long-run equilibrium between the crude oil market and the corn market, we can introduce a Vector Error Correction Model (VECM) to study the short-run adjustment between the two markets. The estimation results of the VECM equations are presented in Table 4, where the optimal maximum lag is determined by the principle of minimum AIC value.

Table 4. Estimation results of the Vector Error Correction Model (VECM) equations.

	Dependent Variable: $\Delta Ln\mathbf{P_t^o}$	Dependent Variable: $\Delta Ln\mathbf{P_t^c}$
$ecm(-1)$	–0.004428 ***	0.000767
	(–2.75)	(0.51)
ΔLnP_{t-1}^o	0.006250	–0.041922 *
	(0.26)	(–1.86)
ΔLnP_{t-1}^c	0.067460 ***	0.016345
	(2.61)	(0.68)
Constant	–0.000038	–0.000222
	(–0.07)	(0.41)
χ^2	17.2294 ***	3.8113
R^2	0.0094	0.0021

(T statistic in parentheses, *** $p < 0.01$, * $p < 0.1$).

The estimations of α_1 and α_2 are –0.004428 and 0.000767, respectively. The estimation of α_1 is significant at the 1% level in the ΔLnP_t^o equation, while the estimation of the α_2 is insignificant in the ΔLnP_t^c equation. This result indicates that the long-term equilibrium between the crude oil market and

the corn market may significantly adjust the short-term price change of the two markets so that they do not deviate from the long-term equilibrium path very far. Specifically, the adjustment to the short-term price change of the crude oil is significant, while the adjustment to the short-term corn price change is not significant. That is, when there is a deviation from the long-run relationship between the corn and oil price, it seems that it is the crude oil price that will be adjusted to preserve the long-run relationship.

Besides, regarding the interactions between the two markets in terms of their price change, the results show that the change of the corn price has a strongly positive effect on the change of crude oil price, while the effect of the change of the oil price on the change of the corn price is found to be less significant. While many studies in the literature report neutrality or a weak effect of agricultural prices to oil price changes (see, e.g., Zhang et al. [15]; Zhang and Reed [33]), the positive effect of the change in agricultural price on crude oil price has also been found in previous studies (see, e.g., Nazlioglu and Soytas [34]). This might be related to the portfolio diversification strategies of global investors/speculators and the increasing investment in agricultural commodities, which leads to a higher integration between energy-finance and agricultural markets (Nazlioglu and Soytas [34]).

5.2. The Lead-And-Lag Relationship between the Crude Oil and Corn Market

We have shown that there is a long-run equilibrium relationship between the crude oil and corn market. Now let us further investigate the spillover effect between the two markets and examine the price or return lead-and-lag relationship between the two markets through Granger causality test. Since it requires the concerned time series to be stationary, we use the first differences of the logarithm of the prices (i.e., the return), which were proven to be stationary in Section 3.

5.2.1. The Linear Granger Causal Relationship

According to the principle of minimum AIC value, we chose the optimal lag order for the VAR model like Equation (1) to be 1, which implies that the VAR model is actually specified as follows:

$$r_t^o = \beta_{10} + \beta_{11} r_{t-1}^o + \gamma_{11} r_{t-1}^c + \varepsilon_{1t},$$

$$r_t^c = \beta_{20} + \beta_{21} r_{t-1}^c + \gamma_{21} r_{t-1}^o + \varepsilon_{2t}.$$

The estimation results of the VAR model are shown in Table 5. It can be seen that the return of corn has a significantly positive effect on the return of crude oil, while the return of crude oil has a negative effect on the return of corn.

Table 5. Estimation results of the Vector Auto-Regression (VAR) model.

	Dependent Variable: r_t^o	**Dependent Variable: r_t^c**
r_{t-1}^o	0.00649	−0.04196 *
	(0.27)	(−1.86)
r_{t-1}^c	0.07280 ***	0.01542
	(2.82)	(0.64)
Constant	−0.00047	−0.00015
	(−0.85)	(−0.28)
R^2	0.0048	0.0019
No. of observations	1829	1829

(T statistic in parentheses, *** $p < 0.01$, * $p < 0.1$).

In a VAR model, each random disturbance influences all the endogenous variables. In addition, random disturbances may exhibit their influence in some of the endogenous variables earlier and others later. The Granger causality test can check a VAR for this type of temporal ordering, in other words, the lead-and-lag relationship between the two markets. The results of the linear Granger causality test are reported in Table 6. It can be seen that the change in the corn price return does Granger cause the return of the crude oil at the 1% level. Additionally, the change in the crude oil

price return also Granger causes the change in the corn price return at the 10% level. This implies that the Granger causality relationship between the two markets is asymmetric: the price change in corn market can more significantly Granger cause the change in the crude oil market. While many studies in the literature find a bidirectional spillover effect between crude oil and agricultural commodity markets through similar Granger causality tests (see, e.g., Nazlioglu and Soytas [34]), there are studies which found only unidirectional volatility spillovers from corn to crude oil after the 2008–09 financial crisis (see, e.g., Lu et al [35]). Our findings somehow lie between these two branches of literature.

Table 6. Results of the linear Granger causality test.

Null Hypothesis	W Statistic	*p*-Value
$r_t^c \nRightarrow r_t^o$	7.9674	0.005
$r_t^o \nRightarrow r_t^c$	3.4581	0.063

Note: $\nRightarrow$ denotes that there is no linear Granger causality from the left market to the right market.

5.2.2. The Non-Linear Granger Causal Relationship

As mentioned above, the traditional linear Granger causality test can fail to identify the non-linear relationship between variables, which is actually common in the economics and finance fields (Zhang and Wei [11]). Therefore, here we conduct the non-linear Granger causality test based on the method proposed by Diks and Panchenko [27], as described in Section 4.2.2. Following previous studies [15], we present the results of the non-linear Granger test for different maximum lags ($Lx = Ly = 1, 2, \cdots\cdots, 8$), as shown in Table 7.

Table 7. Results of the non-linear Granger causality test.

Null Hypothesis	*Lx*=*Ly*	T_n Statistic	*p*-Value
$Y \nRightarrow X$	1	2.403	0.0081
$X \nRightarrow Y$		0.423	0.3363
$Y \nRightarrow X$	2	2.356	0.0092
$X \nRightarrow Y$		0.600	0.2743
$Y \nRightarrow X$	3	2.948	0.0016
$X \nRightarrow Y$		1.338	0.0905
$Y \nRightarrow X$	4	2.932	0.0017
$X \nRightarrow Y$		1.470	0.0707
$Y \nRightarrow X$	5	2.834	0.0023
$X \nRightarrow Y$		0.950	0.1711
$Y \nRightarrow X$	6	2.661	0.0039
$X \nRightarrow Y$		0.574	0.2830
$Y \nRightarrow X$	7	2.494	0.0063
$X \nRightarrow Y$		0.503	0.3076
$Y \nRightarrow X$	8	2.184	0.0145
$X \nRightarrow Y$		0.257	0.3985

Note: Y denotes residual series when the corn price return acts as the dependent variable in the VAR model and X denotes the residual series when the crude oil price return acts as the dependent variable in the VAR model; $\nRightarrow$ denotes that there is no non-linear Granger causality from the left market to the right market.

It can be seen that the non-linear Granger test results generally support the Granger causality relationship from the corn market to the crude oil market, while do not support the hypothesis of Granger causality from the crude oil market to the corn market. This reinforces our previous conclusion based on the linear Granger causality test that the Granger causality relationship between the two markets is asymmetric and that the price change in corn market can more significantly Granger cause the change in the crude oil market.

The finding that in the short run, impulses seem to flow from crop prices to oil prices, is consistent with Avalos [14], where he employed co-integration and a linear Granger causality test to assess the

relationship between oil, corn and soybean prices, through exploiting a natural experiment arising from a significant change in the US biofuel policy in 2006. He found that the predictive causality seems to run from the crop prices to oil prices, in reverse of the expected direction. Our results from the non-linear Granger causality test reinforce the causality direction from crop prices to oil prices.

5.3. Analysis of the Two Markets' Contribution to Price Discovery

As two of most important large commodity markets, their price movement can reflect the price trends of the whole large commodity market. By investigating their respective contribution to price discovery, it would be helpful for forecasting the price trend of the whole large commodity market.

5.3.1. Permanent-Transitory (PT) Model

As mentioned above, Stock and Watson [30] think the price vector can be divided into two components, $LnP_t = f_t + \widetilde{Y}_t$, where f_t denotes the common effective price in the two markets and $\widetilde{Y}_t$ is the transitory component. In our case, $f_t = \gamma_1 LnP_t^o + \gamma_2 LnP_t^c$, where two equations $\gamma_1 + \gamma_2 = 1$ and $\alpha_1\,\gamma_1 + \alpha_2\gamma_2 = 1$ hold. According to the estimation of the vector error correction coefficient (see Table 4), $\hat{\alpha}_1 = -0.004428$ and $\hat{\alpha}_2 = 0.000767$. Then γ_1 and γ_2 can be solved from the two equations: $\gamma_1 = 0.1476$, $\gamma_2 = 0.8524$, which means that the contribution of the crude oil market is 14.76%, and the contribution of the corn market is 85.24%, i.e., the contribution of the corn market is much larger than the crude oil price. The common effective price $f_t = \gamma_1 LnP_t^o + \gamma_2 LnP_t^c$ can then be obtained, as shown in Figure 5.

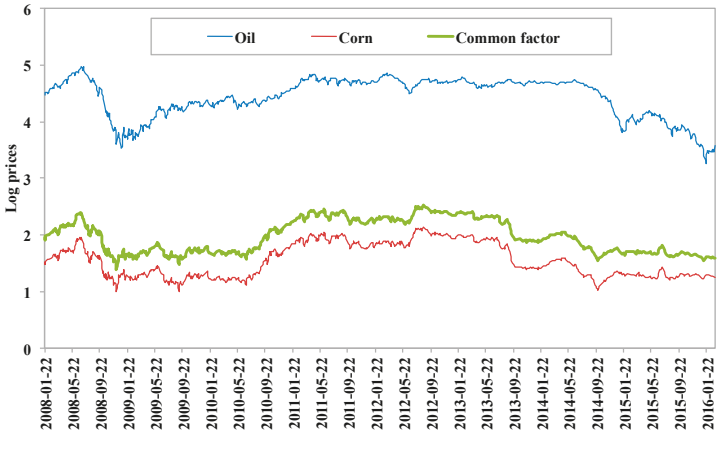

Figure 5. The crude oil price, corn price and their common effective price

5.3.2. Information Shares (IS) Model

Based on the results of the PT model, we constructed an IS model and calculated the information shares of the two markets. With the estimation of $\rho = 0.2350$, $\sigma_1 = 0.02375$, and $\sigma_2 = 0.02218$, one can then calculate the information shares with two different orders of variables (whether crude oil price or corn price works as the first variable, see details in Section 4) as follows:

Case 1 (when oil price works as the first variable):

$$\mathrm{M} = \begin{bmatrix} m_{11} & 0 \\ m_{21} & m_{22} \end{bmatrix} = \begin{bmatrix} \sigma_1 & 0 \\ \rho\sigma_2 & \sigma_2\left(1-\rho^2\right)^{1/2} \end{bmatrix}.$$

$m_{11} = \sigma_1 = 0.02375$, $m_{21} = \rho\sigma_2 = 0.0052123$, and $m_{22} = \sigma_2\left(1-\rho^2\right)^{1/2} = 0.02156$, which implies that information shares of the markets are:

$$S_o = \frac{\left(\gamma_1 m_{11} + \gamma_2 m_{21}\right)^2}{\left(\gamma_1 m_{11} + \gamma_2 m_{21}\right)^2 + \left(\gamma_2 m_{22}\right)^2} = 0.1576,$$

$$S_c = \frac{\left(\gamma_2 m_{22}\right)^2}{\left(\gamma_1 m_{11} + \gamma_2 m_{21}\right)^2 + \left(\gamma_2 m_{22}\right)^2} = 0.8424.$$

Case 2 (when corn price works as the first variable):

$$\mathrm{M} = \begin{bmatrix} m_{11} & 0 \\ m_{21} & m_{22} \end{bmatrix} = \begin{bmatrix} \sigma_2 & 0 \\ \rho\sigma_1 & \sigma_1\left(1-\rho^2\right)^{1/2} \end{bmatrix}.$$

$m_{11} = \sigma_2 = 0.02218$, $m_{21} = \rho\sigma_1 = 0.005581$, $m_{22} = \sigma_2\left(1-\rho^2\right)^{1/2} = 0.02156$, which implies:

$$S_c = \frac{\left(\gamma_2 m_{11} + \gamma_1 m_{21}\right)^2}{\left(\gamma_2 m_{11} + \gamma_1 m_{21}\right)^2 + \left(\gamma_1 m_{22}\right)^2} = 0.9711,$$

$$S_o = \frac{\left(\gamma_1 m_{22}\right)^2}{\left(\gamma_2 m_{11} + \gamma_1 m_{21}\right)^2 + \left(\gamma_1 m_{22}\right)^2} = 0.0289.$$

Following Ballie et al. [31] and Zhang and Wei [11], we take average of results in the above two (orders of variables) cases to get a reasonable estimate of contributions to price discovery.

$$\overline{S}_o = 0.0932,$$

$$\overline{S}_c = 0.9068.$$

From the results, it can be noted that the PT model and IS model have similar results. Both models suggest that the contribution of the corn market to the price discovery of the large commodity markets is larger than that of the crude oil market (85.24% versus 14.76% in the PT model; 90.68% versus 9.32% in the IS model), which implies that among the price trends of the large commodity market, the role of corn outweighs that of the crude oil. This indicates that as one of the most heavily traded contracts in the agricultural commodity market, corn has gained an important market position and wide acknowledgement of investors.

6. Conclusions

This paper investigates both the co-movement and asymmetric trends between energy and grain prices, based on the evidence from the crude oil market and corn market, which are two of most important representatives for large commodity markets. Using time-series econometric methods, we analyzed the co-integration and (linear and non-linear) causality relationship between the two markets and their respective contribution to price discovery based on daily data sampling from January 2008 to February 2016.

We find that there is a consistent trend between the crude oil price and corn price with a significant positive correlation coefficient 0.7471 during the sampling period. Additionally, co-integration analysis suggests that there is a long-run equilibrium relationship between the two commodities' prices, which is likely due to the common economic factors (e.g., the US dollar index) that affect the two markets and the possible substitution of biofuel from coal and oil in some sectors (e.g., transport sector) of the world economy.

Moreover, while linear Granger causality tests suggest that there is a two-way Granger causality relationship between the two markets, non-linear Granger causality tests suggest that there is only unilateral Granger causality running from the corn market to the oil market. However, both linear and non-linear Granger causality tests indicate the asymmetry of the causality relationship between the two markets. Specifically, the change in the corn market can more significantly Granger cause the change in the crude oil market. Interestingly, our results are very different from those in Nazlioglu [23], where she finds that the linear causality test suggests that the oil prices and the agricultural commodity prices do not influence each other but the non-linear causality analysis shows that there is a persistent unidirectional non-linear causality running from the oil prices to the corn and to the soybeans prices. Actually, our results suggest that when we analyze the main factors driving the short-term price change of crude oil, the volatility of the corn market is necessary to be considered as an important factor and can provide a supplementary reference.

Furthermore, price discovery analysis based on both the PT model and IS model suggests that the contribution of the corn market to the price discovery in large commodity markets is larger than that of crude oil market (85.24% versus 14.76% in the PT model and 90.68% versus 9.32% in the IS model), which implies that it would be helpful and important to take the main grain markets such as the corn market into account when predicting the price trend of the whole large commodity market.

This study is not without limitations. For instance, we ignored a number of factors that might affect the price dynamics of the energy and grain markets (e.g., demand shocks, climate negotiation events, and so on). A direction for further research would be to identify the common factors that have influence on both energy and grain markets and the factors that only affect one of the markets, and to investigate how the co-movement and asymmetry of the energy and grain markets can be affected by various economic, political and natural shocks (identified through structural break test) to provide a more complete story regarding the price dynamics in the two markets. For instance, further analysis with more variables incorporated, including nature disaster, OPEC behaviors, global demand change, monetary policy and financialization of commodity prices and so on, would be a valuable area to explore.

Author Contributions: All authors collectively conceived the research and carried out the analysis. L.W. and X.-B.Z. led the analysis and paper writing with contributions and guidance from Z.-M.C. and X.Z.

Funding: This research was funded by the National Natural Science Foundation of China (No. 71603267) and the Natural Science Foundation of Beijing (No. 9192012).

Acknowledgments: The authors would like to thank the two anonymous referees for their helpful comments and suggestions on the preliminary draft of this paper, according to which the content was improved. The authors also would like to thank the participants at the 2017 Annual Conference on Energy Economics and Management at Renmin University of China for their helpful discussions and comments on this paper. All errors and omissions remain the sole responsibility of the authors.

Conflicts of Interest: The authors declare no conflict of interest.

References

1. Gilbert, C.L. How to Understand High Food Prices. *J. Agric. Econ.* **2010**, *61*, 398–425.
2. Coleman, L. Explaining crude oil prices using fundamental measures. *Energy Policy* **2012**, *40*, 318–324. [CrossRef]
3. Garbade, K.; Silber, W.L. Price movements and price discovery in futures and cash markets. *Rev. Econ. Stat.* **1983**, *64*, 289–297. [CrossRef]
4. Yang, J.; Bessler, D.A.; Leathan, D. Asset storability and price discovery in commodity futures market: A new look. *J. Futures Mark.* **2001**, *21*, 279–300. [CrossRef]
5. Zapato, H.O.; Fortenberry, T.R.; Armstrong, D. Price discovery in the futures and cash market for sugar. Paper Presented at the Southern Agricultural Economics Association Annual Meeting, Mobile, AL, USA, 1–5 February 2003.

6. Mattos, F.; Garica, P. Price discovery in thinly traded markets: Cash and futures relationships in Brazilian agricultural futures markets. In Proceedings of the NCCC-134 Conference on Applied Commodity Price Analysis, Forecasting and Market Risk Management, Saint Lois, MO, USA, 19–20 April 2004.
7. Zhang, Y.J.; Fan, Y.; Tsai, H.T.; Wei, Y.M. Spillover effect of US dollar exchange rate on oil prices. *J. Policy Model.* **2008**, *30*, 973–991.
8. Kaufmann, R.K.; Ullman, B. Oil prices, speculation, and fundamentals: Interpreting causal relations among spot and futures prices. *Energy Econ.* **2009**, *31*, 550–558.
9. Zhang, Y.J. Speculative trading and WTI crude oil futures price movement: An empirical analysis. *Appl. Energy* **2013**, *107*, 394–402. [CrossRef]
10. Zhang, Y.J.; Wang, Z.Y. Investigating the price discovery and risk transfer functions in the crude oil and gasoline futures markets: Some empirical evidence. *Appl. Energy* **2013**, *104*, 220–228. [CrossRef]
11. Zhang, Y.J.; Wei, Y.M. The crude oil market and the gold market: Evidence for cointegration, causality and price discovery. *Resour. Policy* **2010**, *35*, 168–177. [CrossRef]
12. Zhang, Y.J.; Wei, Y.M. The dynamic influence of advanced stock market risk on international crude oil return: An empirical analysis. *Quant. Financ.* **2011**, *11*, 967–978. [CrossRef]
13. Trujillo-Barrera, A.; Mallory, M.; Garcia, P. Volatility spillovers in US crude oil, ethanol, and corn futures Markets. *J. Agric. Resour. Econ.* **2012**, *37*, 247–262.
14. Avalos, F. Do oil prices drive food prices? The tale of a structural break. *J. Int. Money Financ.* **2014**, *42*, 253–271. [CrossRef]
15. Zhang, Z.; Lohr, L.; Escalante, C.; Wetzstein, M. Food versus fuel: What do prices tell us? *Energy Policy* **2010**, *38*, 445–451. [CrossRef]
16. Nazlioglu, S.; Erdem, C.; Soytas, U. Volatility spillover between oil and agricultural commodity markets. *Energy Econ.* **2013**, *36*, 658–665. [CrossRef]
17. Baffes, J. Oil spills on other commodities. *Resour. Policy* **2007**, *32*, 126–134. [CrossRef]
18. Baffes, J. More on the energy/nonenergy price link. *Appl. Econ. Lett.* **2010**, *17*, 1555–1558. [CrossRef]
19. Serra, T. Volatility spillovers between food and energy markets: A semiparametric approach. *Energy Econ.* **2011**, *33*, 1155–1164. [CrossRef]
20. Hassouneh, I.; Serra, T.; Goodwin, B.K.; Gil, J.M. Non-parametric and parametric modeling of biodiesel, sunflower oil, and crude oil price relationships. *Energy Econ.* **2012**, *34*, 1507–1513. [CrossRef]
21. Sari, R.; Hammoudeh, S.; Chang, C.L.; McAleer, M. Causality between market liquidity and depth for energy and grains. *Energy Econ.* **2012**, *34*, 1683–1692. [CrossRef]
22. Krichene, N. *Crude Oil Prices: Trends and Forecast. Working Paper 08/133*; International Monetary Fund: Washington, DC, USA, 2008.
23. Nazlioglu, S. World oil and agricultural commodity prices: Evidence from nonlinear causality. *Energy Policy* **2011**, *39*, 2935–2943. [CrossRef]
24. Engle, R.F.; Granger, C.W.J. Co-integration and Error Correction: Representation, Estimation, and Testing. *Econometrica* **1987**, *55*, 251–276. [CrossRef]
25. Baek, K.G.; Brock, W.A. A Nonparametric Test for Independence of a Multivariate Time Series. *Work. Pap.* **1992**, *2*, 137–156.
26. Hiemstra, C.; Jones, J.D. Testing for Linear and Nonlinear Granger Causality in the Stock Price-Volume Relation. *J. Financ.* **1994**, *49*, 1639–1664.
27. Diks, C.G.H.; Panchenko, V. A new statistic and practical guidelines for nonparametric Grangercausality testing. *J. Econ. Dyn. Control* **2006**, *30*, 1647–1669. [CrossRef]
28. Gonzalo, J.; Granger, C. Estimation of common long-memory components in cointegrated systems. *J. Bus. Econ. Stat.* **1995**, *13*, 27–35.
29. Hasbrouck, J. One Security, Many Markets: Determining the Contributions to Price Discovery. *J. Financ.* **1995**, *50*, 1175–1199. [CrossRef]
30. Stock, J.H.; Watson, M.W. Testing for Common Trends. *J. Am. Stat. Assoc.* **1988**, *83*, 1097–1107. [CrossRef]
31. Baillie, R.T.; Booth, G.G.; Tse, Y.; Zabotina, T. Price discovery and common factor models. *J. Financ. Mark.* **2002**, *5*, 309–321. [CrossRef]
32. Harri, A.; Nalley, L.; Hudson, D. The relationship between oil, exchange rates, and commodity prices. *J. Agric. Appl. Econ.* **2009**, *41*, 501–510. [CrossRef]

33. Zhang, Q.; Reed, M. Examining the impact of the world crude oil price on China's agricultural commodity prices: The case of corn, soybean, and pork. In Proceedings of the Southern Agricultural Economics Association Annual Meetings, Dallas, TX, USA, 2–5 February 2008.
34. Nazlioglu, S.; Soytas, U. Oil price, agricultural commodity prices, and the dollar: A panel cointegration and causality analysis. *Energy Econ.* **2012**, *34*, 1098–1104. [CrossRef]
35. Lu, Y.; Yang, L.; Liu, L. Volatility Spillovers between Crude Oil and Agricultural Commodity Markets since the Financial Crisis. *Sustainability* **2019**, *11*, 396. [CrossRef]

energies

MDPI

Article

Evaluating the Impact of Fossil Fuel Vehicle Exit on the Oil Demand in China

Ziru Feng [1], Tian Cai [2], Kangli Xiang [3], Chenxi Xiang [1] and Lei Hou [4,*]

1 School of Applied Economics, Renmin University of China, Beijing 100872, China
2 School of Economics, Jilin University, Changchun 130000, China
3 Economics and Technology Research Institute of State Grid Fujian Electric Power Company Limited, Fujian 350000, China
4 Institute of World Economics and Politics, Chinese Academy of Social Sciences, Beijing 100732, China
* Correspondence: houlei@cass.org.cn

Received: 5 June 2019; Accepted: 16 July 2019; Published: 19 July 2019

Abstract: Vehicle ownership is one of the most important factors affecting fuel demand. Based on the forecast of China's vehicle ownership, this paper estimates China's fuel demand in 2035 and explores the impact of new energy vehicles replacing fossil fuel vehicles. The paper contributes to the existing literature by taking into account the heterogeneity of provinces when using the Gompertz model to forecast future vehicle ownership. On that basis, the fuel demand of each province in 2035 is calculated. The results show that: (1) The vehicle ownership rate of each province conforms to the S-shape trend with the growth of real GDP per capita. At present, most provinces are at a stage of accelerating growth. However, the time for the vehicle ownership rate of each province to reach the inflection point is quite different. (2) Without considering the replacement of new energy vehicles, China's auto fuel demand is expected to be 746.69 million tonnes (Mt) in 2035. Guangdong, Henan, and Shandong are the top three provinces with the highest fuel demand due to economic and demographic factors. The fuel demand is expected to be 76.76, 64.91, and 63.95 Mt, respectively. (3) Considering the replacement of new energy vehicles, China's fuel demand in 2035 will be 709.35, 634.68, and 560.02 Mt, respectively, under the scenarios of slow, medium, and fast substitution—and the replacement levels are 37.34, 112.01, and 186.67 Mt, respectively. Under the scenario of rapid substitution, the reduction in fuel demand will reach 52.2% of China's net oil imports in 2016. Therefore, the withdrawal of fuel vehicles will greatly reduce the oil demand and the dependence on foreign oil of China. Faced with the dual pressure of environmental crisis and energy crisis, the forecast results of this paper provide practical reference for policy makers to rationally design the future fuel vehicle exit plan and solve related environmental issues.

Keywords: vehicle ownership; Gompertz model; fuel demand

1. Introduction

China has become the world's second-largest oil consumer after the United States. In 2016, China's oil consumption was 579 Mt, accounting for 13.1% of the world's total oil consumption [1]. In the same year, the net oil import of China was 358 Mt, and its foreign oil dependency rose to 61.8% [2]. The continued rising foreign oil dependency has seriously threatened China's energy security [3]. The oil demand for road transportation is currently the largest oil consumer in China. In 2015, the proportion of oil consumption in the road transportation sector accounted for 48.4% of the total [4]. In the past three decades, with the sustained and rapid development of China's economy, vehicle ownership keeps rising, while the proportion of new energy vehicles (NEVs) is still small, which has not only increased China's oil demand, but also exacerbated related environmental problems—especially air pollution and climate change. To combat global climate change and to improve air quality, Norway,

Netherlands, India, Germany, the United Kingdom, France, and other countries have proposed and later decided to ban vehicles powered by fossil fuels, and encourage the replacement of fuel vehicles with new energy vehicles. After that, in September 2017, the Vice Minister of the Ministry of Industry and Information Technology (MIIT) of China said that MIIT has started relevant research and will make such a timeline with relevant departments, at an auto industry event in Tianjin [5]. The timeline is expected to be officially launched in 2035.

The development of NEVs is becoming a strategic choice for many countries to deal with climate change and energy security, as well as to gain advantage in international competition. Thanks to the technological advances, government subsidies, and restrictions on purchases in some cities, sales of NEVs in China continue to rise rapidly, and the substitution effect of fossil fuel vehicles by NEVs cannot be ignored any more. Therefore, it is of practical significance to quantitatively evaluate the development trend of NEVs and their impact on China's oil demand. Against the background of increasing vehicle ownership, the rising oil dependency, and the accelerating replacement of fuel vehicles with NEVs, this paper estimates China's fuel demand in 2035 based on the prediction of future vehicle ownership in China, and the impact of NEVs substitution on oil demand under three scenarios of slow, medium, and fast substitution. The results may provide practical reference for policy makers to rationally design the future fuel vehicle exit plan and solve related environmental issues.

The structure of the paper is arranged as follows: Section 2 reviews researches on the forecast of vehicle ownership and fuel demand. Section 3 introduces the empirical model, parameter estimation, and the data acquisition process of the paper. Section 4 presents the results and discussions. Section 5 conducts a robustness test of different replacement speeds. Lastly, Section 6 covers conclusions and policy implications.

2. Related Literature

Energy demand analysis and forecast have always been an important research topic. The energy demand forecasting model can be divided into the top-down model, the bottom-up model, and the hybrid model. Zhao et al. [6] gave a detailed overview of the advantages and defects of the three models, as well as their application in practice in various countries. The bottom-up model is generally based on engineering technology. It can better describe the technologies and costs used in energy production and energy consumption. It is also useful when analyzing and predicting various scenarios of future technical changes. Thus, it is more frequently used in forecasting the transportation energy demand. For example, Johansson and Schipper [7] developed a method to estimate the long-run vehicle energy demand in the United States based on the estimated results of US vehicle ownership, average fuel economy, and average mileage. After analyzing the composition of Japanese automobile market, Palencia et al. [8] measured the fuel demand of Japanese light vehicles in the long-run.

In recent years, research on China's automobile fuel demand is gradually enriched, among which the most common methods are those combining vehicle ownership forecast with different technological progress scenarios. Using the data of China's road transport sector between 1997 and 2002, He et al. [9] developed a bottom-up model to predict the fuel consumption and CO_2 emissions in 2030 under three scenarios regarding motor vehicle fuel economy improvements. Zhang et al. [10] forecast fuel demand of China in 2030 under three energy consumption decrease scenarios by establishing a Long-range Energy Alternative Planning System (LEAP) model. The scenarios are: (1) 'Business as usual'; (2) 'advanced fuel economy'; and (3) 'alternative energy replacement'. Wang et al. [11] made a scenario analysis of energy consumption and reductions in CO_2 emissions in China's transport sector in 2050 by using the Transportation Mode-Technology-Energy-CO_2 (TMOTEC) model, which is based on discrete choice method and general transport cost simulation. Wu et al. [12] used the Gompertz model to forecast China's future vehicle ownership, and then measured the fuel demand of China's road transport sector in 2050.

As China's vehicle ownership is still in a period of rapid growth and is not saturated, future vehicle ownership, which is regarded as the basis of predicting fuel demand by many researchers [12–16],

is the most important factor affecting China's fuel demand. International experience shows that vehicle ownership rate of a country increases slowly at the lowest income levels, followed by an increasing rate of growth as income rises, and then slows down as saturation is approached. That is, the relationship between vehicle ownership rate and GDP per capita can be represented by some sort of S-shape curve [12–15]. In terms of the model fitness of the S-shape curve for fuel demand forecasting, the Gompertz model is proven to be more suitable for the prediction by some researchers [17–19] because of its excellent applicability and general characteristics of the growth curve, compared with other S-shape models.

Most of the existing research focuses on fuel demand forecasting at the national level, while few studies at the regional level. Due to the vast territory of China and the large differences in provincial economic development, current vehicle ownership and its future trends between provinces are also quite different. Existing research uses the S-shape growth model to predict future vehicle ownership in China, but such a model does not fully consider provincial heterogeneity. It sets the saturation level and the growth rate of different provinces to the same parameters, and assumes that all the provinces follow the same growth trend, which has a large gap with the reality, thus not only affecting the accuracy of the prediction, but also providing less reasonable information and basis for local policy formulation. This paper takes into account provincial differences in population density, urbanization rate, and economic development, and makes a more reasonable calculation of the saturation level and variation parameters of the vehicle ownership rate in the forecasting model. Based on that, we forecast China's fuel demand in 2035 under different scenarios from the provincial level, thus making a more detailed assessment of the substitution effect of NEVs on China's oil demand.

3. Methodology

The research purpose of this paper is to evaluate the impact of fossil fuel vehicle exit on China's oil demand. For that, we predicted the fuel demand of China's 31 provinces in 2035 in two steps (Figure 1): (1) We established the Gompertz model based on the S-shape curve relationship between vehicle ownership rate and GDP per capita to forecast the vehicle ownership rate of each province, and then we took into account the population growth to predict vehicle ownership in all provinces in 2035. In particular, we took account of the provincial heterogeneity in economic development, population density, and urbanization rate when determining the saturation level of vehicle ownership in each province. (2) Based on the forecast results of vehicle ownership of each province, with which we combined the annual average vehicle miles traveled and fuel consumption rate of different types of vehicles, we measured China's fuel demand of each province in 2035 and the substitution effect of NEVs with three different substitution speeds on China's oil demand.

3.1. Vehicle Ownership Projection

Previous studies show that there is obvious positive correlation between vehicle ownership rate and GDP per capita, and the growth rate of vehicle ownership rate with GDP per capita growth is not stable, but follows an S-shape upward trend [12–15]. The internal logic is as follows: When the income level is very low, the increase in income for the residents will be preferentially spent on daily necessities. As resident income rises, together with the social transportation infrastructure improved, the demand for automobiles will rise rapidly because residents have extra money after solving the problem of food and clothing. Then, the growth of vehicle ownership rate will slow down and gradually approach saturation when resident income reaches a certain level and most residents have their traffic needs met. Finally, at an extremely high income level, residents will not have a larger number of cars, but replace the old cars with new ones when necessary.

The S-shape curves for demand forecasting can be fit using different models, such as the Bass model, the Logistic model, and the Gompertz model. All three curve models indicate that as the independent variable increases, the growth rate of the dependent variable first has an increasing growth, and then slows down, and finally approaches a saturation level. The Bass model is usually used to describe the diffusion trend of a technological innovation. The Logistic model is applicable to

describe the life cycle of a consumer product, with a curve symmetrical about the inflexion point and time as the independent variable. The Gompertz model has similar features to the Logistic model, with excellent applicability and general characteristics of the growth curve. However, its corresponding S-shape curve is asymmetrical about the inflection point, and the independent variable may not be time. Compared with the Bass model and the Logistic model, the Gompertz model is more suitable for the prediction of vehicle ownership rate. The existing research also verifies that. Based on the historical data of vehicle ownership in the United Kingdom, Muraleedharakurup et al. [17] confirmed that the Gompertz model is better than the Logistic model and the Bass model in terms of forecasting future hybrid vehicle adaptation. Similarly, Huo and Wang [18] performed regression analysis using data of vehicle sales and stocks in China. The results also showed that the Gompertz model fit best among the three models.

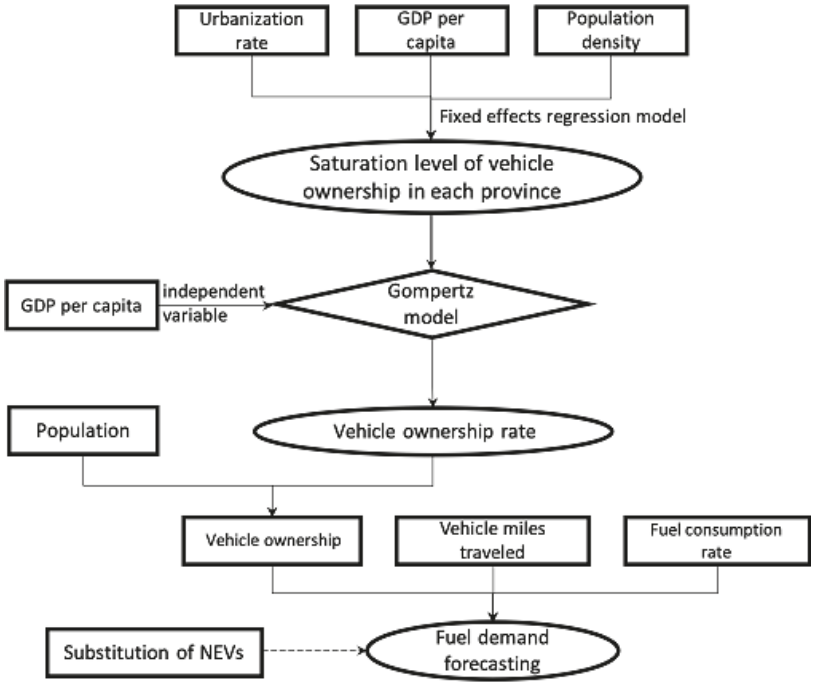

Figure 1. Fuel demand forecasting framework.

We draw on and expand the Gompertz model established by Dargay and Gately [20] to forecast the vehicle ownership of the 31 provinces of China in 2035. We assume that the relationship between vehicle ownership rate and GDP per capita can be expressed as the following:

$$Y_{it} = M_{it}e^{-a_i e^{-b_i PGDP_{it}}} \quad (1)$$

where i and t denote province and time, respectively; Y_{it} is the vehicle ownership rate (measured in vehicles per 1000 people) of province i at time t; $PGDP_{it}$ is the real GDP per capita (measured in GDP per 1000 people) of province i at time t; M_{it} is the saturation level of the vehicle ownership rate (measured in vehicles per 1000 people) of province i at time t; a_i and b_i are two parameters to be estimated that determine the shape or curvature of the function. (Let the second derivative of Equation (1) be equal to 0, and we can get the per capita GDP and the exact year of each province at the inflexion point.) This model takes into account the provincial differences both in the saturation level of vehicle ownership and in the time required to reach the saturation level in China.

Equation (1) can be mathematically transformed as:

$$ln(lnM_i - lnY_{it}) = \ln a_i - b_i PGDP_{it} \quad (2)$$

In order to predict the vehicle ownership rate of each province in 2035, we use the data of 31 provinces in the past 20 years to establish the regression model to estimate the parameters a_i and b_i . The model is as follows:

$$y_{it} = \alpha_i + \beta_i PGDP_{it} + \varepsilon_{it} \quad (3)$$

where $y_{it} = ln(lnM_i - lnY_{it})$, $\alpha_i = lna_i$, $\beta_i = -b_i$, $i = 1, 2, \ldots, 31$, $t = 1, 2, \ldots, 20$. The random error term ε_{it} satisfies the assumption of independence, zero conditional mean, and homoscedasticity. As it can be seen from Figure 3, most provinces in China have not yet reached the level of vehicle saturation, so it is necessary to set M_{it} , the saturation level of vehicle ownership rate in each province. Regarding the setting of M_{it} , there is no unified and standard method for that by now. Gu et al. [21] divided China's 31 provinces into three groups by their urbanization rate in 2007 and assigned different saturation levels to different groups in their prediction of China's vehicle ownership. Based on the saturation level of the US vehicle ownership rate, Dargay et al. [22] used the data on urbanization rates and population densities to adjust the saturation levels of different countries when predicting the vehicle ownership in 45 countries around the world. According to the domestic and foreign research results, GDP per capita, urbanization rate, and population density are important factors affecting the growth of the vehicle ownership rate in a region [23,24]. Considering the heterogeneity of different provinces in China, we estimate the saturation levels of the vehicle ownership rate in different provinces separately. For province i , the saturation level of its vehicle ownership rate at year t can be expressed as:

$$M_{it} = \delta_0 + \delta_1 PGDP_{it} + \delta_2 Urban_{it} + \delta_3 Density_{it} + e_{it} \quad (4)$$

In Equation (4), $PGDP_{it}$ represents the real GDP per 1000 people; $Urban_{it}$ indicates the urbanization rate; $Density_{it}$ is the population density. Besides, δ_0 , δ_1 , δ_2, and δ_3 are parameters of the model; e_{it} is the error term. As $PGDP$, $Urban$, and $Density$ change over time, the maximum potential value of the vehicle ownership rate in each province also changes with time. The descriptions of model parameters are shown in Table 1.

Table 1. Descriptions of model parameters.

Parameter	Description	Method	Calculation
M_{it}	Saturation level of vehicle ownership rate	Linear prediction	(1) Estimate the parameters of Equation (4) using the historical data of EU15; (2) Calculate M_{it} with the predicted GDP per capita, urbanization rate, and population density of each province in 2035.
a_i, b_i	Parameters determining the shape or curvature of the S-shape curve	Regression Analysis	Perform regression analysis between the vehicle ownership rate and the real GDP per capita using provincial data over the years.
δ_0 , δ_1 , δ_2 , δ_3	Parameters determining M_{it}	Regression Analysis	Perform regression analysis between the vehicle ownership rate and the real GDP per capita, urbanization rate, and population density using historical data of EU15 over the years.

It can be demonstrated from Equation (4) that the parameters (δ_0 , δ_1 , δ_2 , δ_3) in the above model must be obtained first to obtain the vehicle saturation level of each province in 2035. China's vehicle ownership rate has not yet reached the saturation level, and it is impossible to use China's historical data to estimate these parameters. This paper uses the historical data of EU15 to measure the

parameters in the model. This is mainly for two reasons: Firstly, countries or regions to be chosen must have already reached or approached the saturation level of vehicle ownership rate in order to meet the requirements in Equation (4). Around the world, countries and regions with a high vehicle ownership rate include countries in North America and some other developed countries in Europe. As it can be seen from Figure 2, the vehicle ownership rate in EU15 is relatively stable between 2005 and 2015. Secondly, to more accurately estimate the saturation level of China's vehicle ownership rate, it is necessary to select countries and regions with similar population distribution and geographical structure to China to minimize the error. The population density of the United States and Canada in North America is far less than China, while EU15 are more similar to China in terms of population distribution and regional structure. (In 2016, China, the United States, Canada, and EU15 had a population density of 143.1 peo./km^2, 35.3 peo./km^2, 4 peo./km^2, and 125.6 peo./km^2 respectively.) Therefore, we finally chose the historical data of EU15 to measure the parameters in Equation (4). After determining the parameters in Equation (4), the predicted real GDP per capita (2010 RMB), urbanization rate, and population density of each province in 2035 need to be estimated to obtain the saturation level of vehicle ownership rate. This paper assumes that the total population and GDP per capita of each province increases at the average annual growth rate between 2013 and 2016. The urban population grows linearly at the average number between 2013 and 2016. The land area of each province remains constant until 2035.

After determining the saturation level of the vehicle ownership rate of each province, we can estimate the parameters a_i and b_i in the Gompertz model by the regression model, using the historical data of the vehicle ownership rate and real GDP per capita (2010 RMB) of the 31 provinces from 1997 to 2016. After that, we can get the forecast results of the vehicle ownership rate of each province in 2035. On the basis of the forecast vehicle ownership rate, this paper assumes that the total population of each province increases at the average growth rate between 2013 and 2016, and obtains the forecast results of vehicle ownership in each province in 2035.

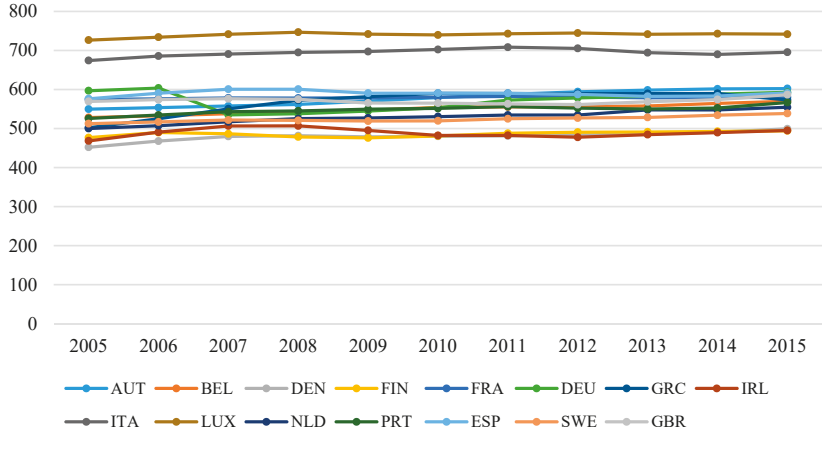

Figure 2. Annual vehicle ownership per 1000 people of EU15. Source: OICA.

In the vehicle ownership forecasting model, the data involved includes real GDP per capita of each province, the vehicle ownership rate of each province, and the saturation level of the vehicle ownership rate of each province. Among them, real GDP per capita of each province over the years comes from the China Statistical Yearbook from 1996 to 2017, deflated by the CPI, with 2010 as the base year. The vehicle ownership rate is the ratio of vehicle ownership to total population, from the China Automotive Market Yearbook and the China Statistical Yearbook over the years, respectively.

In the setting of the saturation level of the vehicle ownership rate, the data involved includes vehicle ownership, the real GDP per capita (2010 RMB), the urbanization rate, and the population

density in EU15 and in the 31 provinces of China. Among them, the data of vehicle ownership in EU15 comes from the International Organization of Motor Vehicle Manufacturers (OICA). The real GDP per capita (2010 RMB), urbanization rate, and population density are from the World Bank database. The historical data of vehicle ownership, real GDP per capita (2010 RMB), urbanization rate, and population density of the 31 provinces over the years are from the provincial statistical yearbooks.

3.2. Fuel Demand Projection

Fuel demand is determined by vehicle population, average miles traveled, and fuel consumption rates [18]. Since the average mileage and fuel economy of different types of vehicles vary greatly, we further categorize them into eight types. Fuel demand of each type can be expressed as follows:

$$FC_{it} = \sum_{j} \left(Y_{ijt} \times VMT_{ijt} \times FR_{ijt} \times FD \right) \quad (5)$$

where FC_{it} is the fuel consumption of province i in the year t ; Y_{ijt} denotes the vehicle type j ownership of province i in the year t , and $Y_{it} = \sum_j Y_{ijt}$, in million; VMT_{ijt} is the annual miles traveled by vehicle type j of province i in the year t , in kilometers; FR_{ijt} is the fuel consumption rate of vehicle type j of province i in the year t , in L/100 km; FD indicates the density of the fossil fuel, and the unit is kg/L.

The National Bureau of Statistics divides vehicles into passenger vehicles and trucks. The passenger vehicles are further divided into large passenger vehicles (LPVs), medium passenger vehicles (MPVs), small passenger vehicles (SPVs), and mini cars (MCs). Trucks are further divided into heavy-duty trucks (HDTs), medium-duty trucks (MDTs), light-duty trucks (LDTs), and mini trucks (MTs). Based on the type of fuel consumed by vehicles, each type is subdivided into petrol ones and diesel ones. Since the population of diesel vehicles in MTs and MCs, and gasoline vehicles in LPVs and HDTs is extremely small, it is feasible in our calculation to assume that all mini vehicles consume gasoline and all heavy vehicles consume diesel.

The number of each vehicle type in each province is determined both by the total vehicle population in the province and by the proportion of the vehicle type. In the past three years, the proportion of each type of automobile in China has changed little [2]. Therefore, we assume that the proportion of each vehicle type in each province remains constant from 2015 to 2035. Y is predicted by the Gompertz model; VMT and FR come from the Annual Report on Automobile Energy-saving in China (2015). The statistics show that the average annual mileage of each type of vehicle changed little in recent years [25,26]. Hence we assume that VMT for each vehicle type is constant until 2035. FR reduces by the average speed between 2004 and 2014. FD is based on National VI Standard (the fifth phase of the national gasoline and diesel national standard). Involved parameters above are summarized in Table 2.

Table 2. Model parameters: Vehicle type, mileage, and fuel economy.

	Passenger Vehicles				**Trucks**			
	LPVs	**MPVs**	**SPVs**	**MCs**	**HDTs**	**MDTs**	**LDTs**	**MTs**
Fuel Type [1]	diesel	diesel	petrol	petrol	diesel	diesel	diesel	petrol
Proportion [2]	0.01	0.01	0.83	0.02	0.03	0.01	0.08	0.00
VMT (km)	54,000	52,000	19,000	26,000	55,000	35,000	28,000	19,500
FR (L/100 km)	15.13	11.09	4.39	4.39	24.06	11.80	5.33	3.69

[1] The fuel of automobiles is divided into gasoline and diesel. Currently, most SPVs, MCs, and MTs in China consume gasoline, while LPVs and HDTs are mainly powered by diesel. Other types of vehicles are mixed with gasoline-powered and diesel-powered. Since diesel enjoys an obvious advantage in cost, fuel efficiency, and cleanliness, dieselization of trucks and large and medium passenger vehicles is increasingly obvious. Therefore, we assume that SPVs, MCs, and MTs continue consuming gasoline in 2035, while other vehicles are fueled by diesel. [2] Vehicles other than passenger vehicles and trucks account for less than 1%, so this paper ignores other vehicles when forecasting the total fuel demand.

4. Results and Analysis

4.1. Vehicle Ownership

Figure 3 shows the changes in the vehicle ownership rate with GDP per capita in different provinces of China. It does not take much to see that the trend of each province basically conforms to our assumption of the S-shape curve, and most provinces in China have not met the inflexion points where the growth begins to slow. Most provinces are still in a period of accelerated growth.

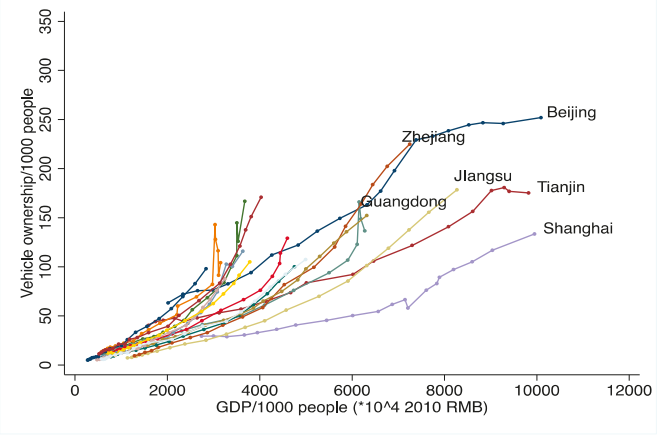

Figure 3. Vehicle ownership per 1000 people versus GDP per 1000 people in China for 1997–2016. Note: GDP data of each province is deflated by the CPI, with 2010 as the base year. All the data here comes from the China Statistical Yearbook (1998–2017).

Then, using the panel data of EU15, we establish a fixed effect model to estimate the parameters in Equation (4). The regression results are displayed in Table 3. The *t*-value is in the parentheses. R^2 is 0.846, and the model has a good fitting degree. The regression results show that GDP per capita and population density have significant positive correlations with the vehicle ownership rate. That is, the more developed the economy and the denser the population, the higher the saturation level of the vehicle ownership rate. The coefficient of urbanization rate δ_2 is significantly negative, which means that the higher the level of urbanization, the lower the saturation level of the vehicle ownership rate. That is probably because regions with higher urbanization levels are usually equipped with more developed public transportation and more improved traffic infrastructure.

Table 3. Regression results of Equation (4).

Coefficient	Result
δ_1	0.003 *** (6.92)
δ_2	−1.863 ** (−3.21)
δ_3	0.115 ** (2.85)
δ_0	584.672 *** (14.19)
R^2	0.846
N	165

Note: *t*-values are shown in the parentheses; *** $p < 0.01$, ** $p < 0.05$.

After determining the parameters of Equation (4), we can estimate the saturation level of the vehicle ownership rate M_{it} in each province. The estimation results are shown in the sixth column of Table 4. On that basis, parameters in the Gompertz model (3) is estimated from the data of the provincial vehicle ownership rate and the real GDP per capita (2010 RMB) between 1997 and 2016.

Then, we forecast the vehicle ownership rate of each province in 2035 based on the estimate results above. The regression results and forecast results are shown in Table 4 and Figure 4. Taking the population growth in to consideration, the projection results of vehicle ownership in each province in 2035 are shown in Figure 5. In particular, for the three municipalities Beijing, Shanghai, and Tianjin, the saturation level of the vehicle ownership rate is more affected by the government's control policies. The automobile purchase restriction policies of the three cities have greatly limited the growth of vehicle ownership. It could be demonstrated in Figure 3 that the vehicle ownership rate of the three cities has already entered a stage of decelerating growth in recent years. Therefore, our study assumes that the annual increase of automobiles is equal to the number of new license plates. (In fact, the purchase restriction policy is only for passenger cars. However, for the three economically developed cities, more than 90% of the increase in vehicle ownership can be accounted for by the increase of passenger cars. Therefore, the annual increase of automobiles can be approximately seen as the number of new license plates.) According to the current purchase restriction policy, the total number of new license plates in Shanghai and Tianjin is maintained at around 100,000 per year, and the number of car license plates in Beijing has dropped from 150,000 to 100,000 per year since 2018. In our forecast, it is assumed that the number of new license plates will remain at this level in the three municipalities in the future.

Table 4. Provincial projections of saturation level and vehicle ownership per 1000 people in 2035.

Province	Abbr.	$\beta_i(\times 10^{-4})$	α_i	a_i	$b_i(\times 10^{-4})$	Saturation	Inflexion	2035
Beijing	BJ	−1.15 ***	1.15 ***	3.17	1.15	765	2016	288
Tianjin	TJ	−0.88 ***	1.26 ***	3.52	0.88	803	2029	204
Hebei	HE	−3.16 ***	1.63 ***	5.12	3.16	635	2037	220
Shanxi	SX	−3.13 ***	1.53 ***	4.60	3.13	613	2051	159
Inner Mongolia	IM	−1.67 ***	1.44 ***	4.22	1.67	586	2038	204
Liaoning	LN	−1.74 ***	1.47 ***	4.36	1.74	617	2040	183
Jilin	JL	−2.10 ***	1.50 ***	4.50	2.10	600	2029	297
Heilongjiang	HL	−2.69 ***	1.61 ***	5.00	2.69	592	2057	131
Shanghai	SH	−0.79 ***	1.55 ***	4.71	0.79	1030	2026	209
Jiangsu	JS	−1.65 ***	1.67 ***	5.32	1.65	674	2019	654
Zhejiang	ZJ	−2.22 ***	1.73 ***	5.61	2.22	652	2017	612
Anhui	AH	−3.00 ***	1.69 ***	5.43	3.00	644	2026	459
Fujian	FJ	−1.93 ***	1.68 ***	5.37	1.93	627	2021	589
Jiangxi	JX	−2.92 ***	1.71 ***	5.55	2.92	619	2025	474
Shandong	SD	−2.18 ***	1.65 ***	5.22	2.18	667	2022	519
Henan	HA	−2.96 ***	1.68 ***	5.38	2.96	655	2024	512
Hubei	HB	−2.01 ***	1.60 ***	4.96	2.01	624	2023	548
Hunan	HN	−2.37 ***	1.66 ***	5.26	2.37	626	2026	459
Guangdong	GD	−1.75 ***	1.54 ***	4.66	1.75	671	2022	578
Guangxi	GX	−3.04 ***	1.69 ***	5.41	3.04	611	2026	427
Hainan	HI	−2.56 ***	1.57 ***	4.81	2.56	618	2025	455
Chongqing	CQ	−2.06 ***	1.61 ***	5.00	2.06	634	2021	621
Sichuan	SC	−3.31 ***	1.69 ***	5.42	3.31	606	2024	352
Guizhou	GZ	−3.67 ***	1.62 ***	5.03	3.67	609	2020	503
Tibet	XZ	−3.24 ***	1.43 ***	4.20	3.24	585	2021	558
Shaanxi	SN	−2.41 ***	1.55 ***	4.73	2.41	607	2026	354
Gansu	GS	−4.15 ***	1.69 ***	5.40	4.15	591	2041	173
Qinghai	QH	−2.87 ***	1.50 ***	4.46	2.87	585	2025	352
Ningxia	NX	−2.97 ***	1.52 ***	4.59	2.97	598	2022	424
Xinjiang	XJ	−2.87 ***	1.50 ***	4.50	2.87	586	2069	142
Yunnan	YN	−3.85 ***	1.54 ***	4.68	3.85	600	2024	435
China	CHN	−2.49 ***	1.60 ***	4.95	2.49	602	2023	436

Note: *** $p < 0.01$.

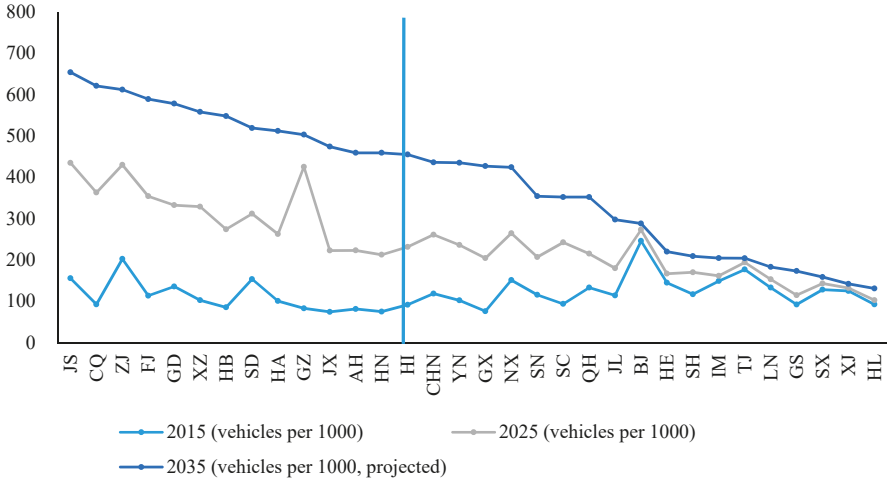

Figure 4. Provincial projections of vehicle ownership per 1000 people in 2035.

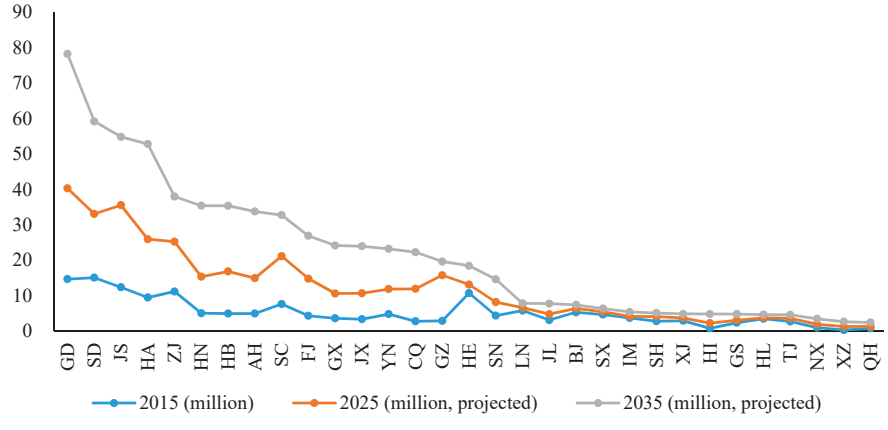

Figure 5. Provincial projections of vehicle ownership in 2035.

According to the results of regression and prediction, we can find that: (i) The two parameters a and b in the Gompertz model are positive. Combined with Equations (2)–(4), it can be concluded that with the growth of GDP per capita, its positive marginal effect on vehicle ownership rate will increase first and then decrease. That is, as GDP per capita rises, the willingness of residents to increase the proportion of their income for automobile purchase will increase firstly and then gradually decrease, but it will still be positive. Besides, the larger b is, the smaller GDP per capita, corresponding to the saturation level. (ii) Overall, the growth rate of China's vehicle ownership rate will arrive at the inflection point in 2023, which means that the growth of China's vehicle ownership rate with GDP per capita will slow down after 2023. In addition, except a few provinces such as Xinjiang, most provinces in China will meet their inflexion points between 2020 and 2029. In other words, the vehicle ownership rate in most provinces will be growing at a slower pace in 2035. (iii) The average vehicle ownership rate of China in 2035 will be 436 vehicles per thousand people, which is nearly three times the number of 118 vehicles per thousand people in 2015, with an average annual growth rate of 6.7%. At the same time, the provincial differences in the vehicle ownership rate will continue to increase in the future. In 2035, Jiangsu, Chongqing, and Zhejiang will have the highest vehicle ownership rates, with 654, 621, and 612 vehicles per thousand people, respectively. Rapid growth is inseparable from

the economic development and urban construction in these regions. While in Beijing and Shanghai, where the economy is also very developed, their vehicle ownership rates have gradually approached to saturation and grown with a narrow range due to the policy control. Heilongjiang, Xinjiang, and Shanxi, the three provinces with the lowest vehicle ownership rate, will have only 131, 142, and 159 vehicles per thousand people in 2035. The low growth in these regions is mainly affected by their geographical location and stagnant economic growth. (iv) Taking the total population into account, the total number of vehicle ownership in China will reach 667 million in 2035, which is about three times higher than the number of 163 million in 2015, with an average annual growth of 7.3%. Driven by population or economy, Guangdong, Shandong, and Jiangsu will become the three provinces with the highest vehicle ownership in China. Their vehicle ownership will reach 78.26, 59.23, and 48.84 million, respectively. While the least three provinces, Qinghai, Tibet, and Ningxia will have only 2.46, 2.68, and 3.49 million vehicles, respectively. At the same time, it can be easily found from Figure 5 that Guangdong, Shandong, and Jiangsu, which have great potential for development, will be the main driving forces for China's automobile growth in the future. Part of that is because of the restriction policy over the extremely densely populated areas, especially in Beijing and Shanghai.

4.2. Fuel Demand

On the basis of the forecast results of vehicle ownership of each province, we take into account factors including the proportion of different vehicle types, annual average mileage, fuel consumption rate, etc., and we get the forecast results of fuel consumption in each province in 2035 (Table 5). It can be seen from the forecast results that: (1) The total national automobile fuel demand is estimated to be 746.69 Mt (gasoline and diesel) in 2035, which is two times higher than the number of 230 Mt in 2015, with an average annual growth of 5.7%. (2) Guangdong, Henan, and Shandong are the three provinces with the highest demand for automobile fuel, which are 76.76, 64.91, and 63.95 Mt respectively. Compared with the previous results of vehicle ownership in each province, we can find that the ranking of vehicle ownership among the provinces is not exactly the same as the ranking of fuel demand. This can be explained by the different structure of vehicle stock in each province. Take Henan Province as an example: Henan has a lower vehicle ownership than Jiangsu and Shandong, but it has a larger number of trucks than the other two provinces. The higher fuel consumption rate of trucks increases the demand for automobile fuel in Henan Province (Figure 6). (3) Examining the percentage of gasoline and diesel demand in different provinces (Figure 7), we can come to the conclusion that more-developed regions usually have a higher demand for gasoline, while diesel often accounts for a higher proportion in less-developed regions. In economically underdeveloped regions like Tibet, Ningxia, and Xinjiang, where industry has a greater role in driving regional economic development, residents have lower demand for passenger cars because of their lower incomes. Thus, there are more trucks usually fueled by diesel in these regions. While in those relatively developed provinces, such as Zhejiang, Beijing, and Guangdong, the regional economy is more driven by the service industry. Therefore, the demand for passenger vehicles—especially cars—is much higher and the demand for gasoline is greater in these regions.

Table 5. Provincial projections of fuel consumption structure in 2035.

Province	Vehicle Ownership (million)	Fuel Demand (Mtoe)	Fuel Demand (Mt)	Diesel	Gasoline	Passenger Vehicles	Trucks
Guangdong	78.26	70.35	76.76	34.40	42.36	50.05	26.71
Henan	52.83	60.33	64.91	36.61	28.30	31.93	32.98
Shandong	59.23	58.87	63.95	31.03	32.92	36.29	27.66
Jiangsu	54.85	52.38	57.13	25.82	31.30	35.64	21.49
Anhui	33.78	45.11	48.07	31.00	17.07	19.98	28.09
Hubei	35.40	37.37	40.33	21.79	18.53	22.25	18.07
Hunan	35.42	35.50	38.44	19.66	18.78	22.61	15.83

Table 5. *Cont.*

Province	Vehicle Ownership (million)	Fuel Demand (Mtoe)	Fuel Demand (Mt)	Diesel	Gasoline	Passenger Vehicles	Trucks
Sichuan	32.79	32.21	34.98	17.00	17.98	20.54	14.44
Jiangxi	23.99	30.09	32.54	20.43	12.11	13.94	18.60
Zhejiang	38.00	30.47	33.20	11.81	21.39	23.47	9.73
Guangxi	24.19	26.99	29.02	16.51	12.51	14.53	14.49
Fujian	26.93	25.82	28.00	13.91	14.09	16.30	11.71
Chongqing	22.31	24.12	26.00	14.21	11.79	13.93	12.07
Yunnan	23.24	22.70	24.58	12.60	11.98	13.44	11.13
Hebei	18.48	21.01	22.63	12.60	10.02	10.82	11.80
Guizhou	19.66	19.95	21.53	11.56	9.97	11.73	9.80
Shaanxi	14.65	15.04	16.29	8.31	7.98	9.08	7.21
Liaoning	7.87	9.07	9.75	5.63	4.11	5.10	4.65
Jilin	7.79	8.75	9.42	5.25	4.17	4.98	4.44
Shanxi	6.39	7.25	7.81	4.30	3.51	3.86	3.95
Xinjiang	4.90	6.40	6.82	4.45	2.37	2.93	3.89
Beijing	7.44	6.19	6.81	2.58	4.23	5.33	1.48
Tibet	2.68	6.10	6.45	5.65	0.80	3.61	2.84
Heilongjiang	4.68	6.22	6.51	4.14	2.37	2.94	3.57
Inner Mongolia	5.45	5.69	6.15	3.21	2.94	3.25	2.90
Shanghai	5.13	5.38	5.82	2.99	2.83	3.66	2.15
Gansu	4.83	5.30	5.66	3.57	2.08	2.50	3.16
Ningxia	3.49	4.54	4.84	3.23	1.62	1.91	2.93
Hainan	4.86	4.56	4.93	2.43	2.49	3.18	1.75
Tianjin	4.64	4.10	4.49	1.92	2.57	2.98	1.51
Qinghai	2.46	2.67	2.87	1.64	1.22	1.46	1.41
China	666.61	690.51	746.69	390.28	356.41	414.23	332.45

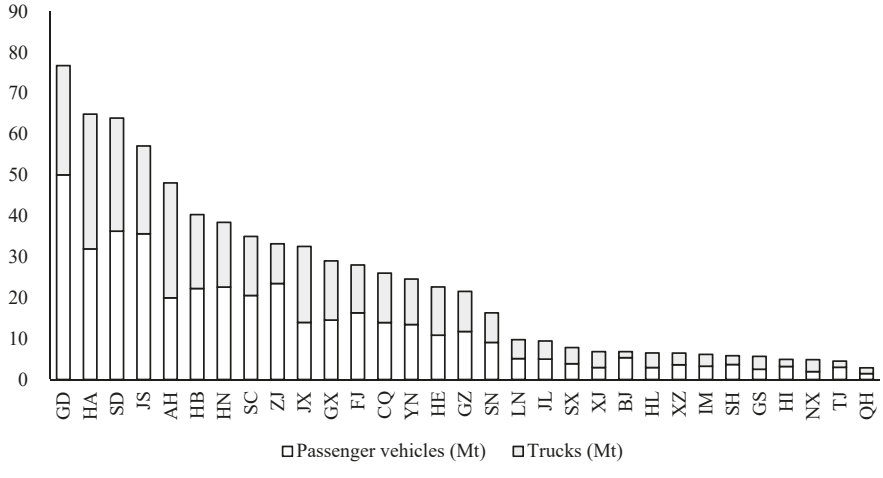

Figure 6. Provincial projections of fuel consumption in 2035.

We compare the results of this paper with other research results, as shown in Table 6. The listed studies have predicted the future vehicle ownership and fuel consumption in China. By comparing the results, we can see that our forecast results are at the middle level. In particular, compared with the study by Wu et al. [12], which also used the Gompertz model to predict the number of vehicle ownership, the prediction result of this paper is higher than theirs, which may be due to fact that Wu et al. [12] set the saturation level of vehicle ownership rate for China directly in their study, while

we set the saturation level of vehicle ownership rate in each province separately. In comparison with the study by Peng et al. [16], which also established a bottom-up model and forecast the vehicle ownership provincially, our prediction results are slightly higher. There could be two reasons: Firstly, in the setting of the saturation level of the vehicle ownership rate, Peng et al. [16] referred to the saturation level of France, and set the saturation level of the provinces unlimited to the purchase restriction policies to 376 vehicles per thousand people, while the limited provinces were uniformly set to 250 vehicles per thousand people. In our study, we comprehensively considered the provincial differences in economic status, population distribution, regional structure, and restriction policies, and then reasonably measured the saturation level of the vehicle ownership rate in each province. Secondly, Peng et al. [16] set the fuel consumption rate and the annual miles traveled by different vehicle types of each province separately when establishing the bottom-up model. The refinement of these indicators placed more emphasis on the influence of other factors, such as technological progress on fuel demand, thus leading to a lower forecast result.

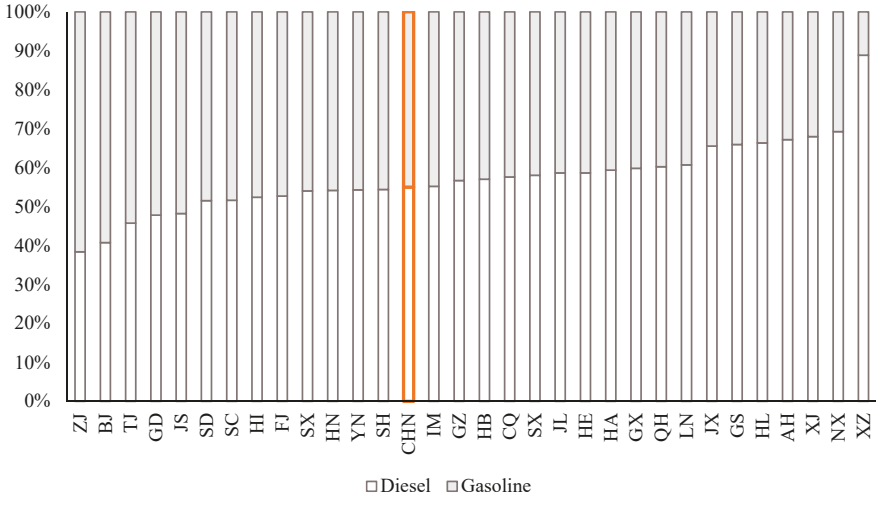

Figure 7. Provincial projections of gasoline and diesel consumption in 2035.

Table 6. Comparisons of projections of the fuel demand in China.

Source	Year Projected	Vehicle Ownership (Million)	Fuel Demand (Mtoe)	Research Level
Zhang et al. [10]	2030	867	600–992	National
Wang et al. [11]	2050	609–626	636	National
Wu et al. [12]	2050	300–463	380–586	National
Peng et al. [16]	2030	478	461–480	Provincial
Our study	2035	667	518–691	Provincial

4.3. Impact of Fossil Fuel Vehicle Exit on the Oil Demand

So far, we have not taken into account the substitution effects of NEVs, and we are going to consider that in this part. According to the statistics of the Ministry of Public Security, there were 1.53 million NEVs at the end of 2017, accounting for only 0.7% of the total number of vehicles.

However, with the continuous advancement of NEV technology, the percentage of NEVs represented by electric vehicles will continue growing before the exit timeline of fossil fuel vehicles is officially launched in China, thus making the total fuel demand lower than we predicted before [10].

Regarding the prediction of the percentage of NEVs, domestic and foreign researchers have not reached an agreement. Bloomberg [27] and ExxonMobil [28] predicted the proportion of NEVs worldwide in 2040, and their predictions were similar with 33% and 35%, respectively. As for the proportion of China's NEVs, MIIT [29] proposed the goal that NEVs should make up 10% of all the automobiles in China by 2020. What is more, according to the International Energy Agency [30], China's NEVs will account for 25% of total vehicles by 2035.

Based on the research above, this paper calculates provincial fuel demand of Chinese vehicles in 2035, considering the substitution of NEVs. The substitution speeds in different provinces may vary because of their different policy restrictions and state of supporting facilities. Taking these provincial differences into account, we made a hierarchical cluster analysis and divided the 31 provinces of China into three groups. In our study, four indicators were selected to reflect provincial differences in the two aspects we mentioned above (Table 7). For the hierarchical cluster analysis, the method of Ward [31] was selected because it outperforms other hierarchical cluster methods when outliers are absent. Some researches on regional cluster analysis also demonstrate that Ward's method gives the best interpretative solution [32,33]. To eliminate the effects of different scales, we standardized the four variables when making the cluster analysis. The dendrogram shows that the 31 provinces can be grouped into three clusters. Related information of the three groups is summarized in Table 8. It shows the mean values of the indicators in each cluster. It does not take much to see that clusters 1 and 2 are more densely populated, more urbanized, and more economically developed provinces, which means the local government is more capable of providing supporting facilities of NEVs, thus promoting the growth of NEVs. Compared with cluster 2, cluster 1 includes regions with much more dense population, with an average projected population density of 1206.4 people per square kilometer in 2035, which is two times more than that of cluster 2. More dense population will surely boost the growth of NEVs.

Therefore, in our study, we assume three different substitution speeds for the three clusters. The percentage of NEVs in 2035 will account for 25%, 15%. and 5% for clusters 1, 2, and 3, respectively. The results are shown in Table 9. Under the substitution scenario, China's automobile fuel demand in 2035 will be 652.58 Mt. The fuel demand for clusters 1, 2, and 3 will be 132.13, 183.10, and 337.35 respectively. Besides, it is also shown in Table 9 that the average fuel demand for each province in cluster 2 is much higher than two other clusters, which points out a feasible direction for future fuel demand control.

Compared to that without substitution, the fuel demand in China in 2035 can be reduced by 94.11 Mt, which is equivalent to 26.3% of China's net oil imports in 2016. This proportion will further expand as the speed of fuel vehicle exit increases. Therefore, the exit of fossil fuel vehicles will greatly reduce China's foreign oil dependency and thus ensure China's energy security.

Table 7. Indicators for cluster analysis.

Interpretation	Indicator
Policy Restrictions	Policy (D = 1 if restricted policy is implemented, and D = 0 if not)
State of supporting facilities	Population density Urban rate GDP per capita

Table 8. Summary of clusters.

Cluster	Province	N	Density (peo./km^2)	Urbanity	PerGDP (2010 RMB yuan)	Policy
1	BJ, TJ, HE, ZJ, GD, HI, GZ, SH	8	1206.4	82.59%	179,281.4	1
2	JS, FJ, SD, HB, CQ	5	531.35	83.19%	213,693.8	0
3	SX, IM, LN, JL, HL, AH, JX, HA, HN, GX, SC, XZ, SN, GS, QH, NX, XJ, YN	18	199.22	71.26%	73,064.7	0

Table 9. Fuel demand with different substitution speeds.

Scenario	Fossil Fuel Vehicle Ownership (million)	Fuel Demand (Mtoe)	Fuel Demand (Mt)	Diesel		Gasoline	Passenger Vehicles	Trucks
Baseline	666.61	690.51	746.69	390.28		356.41	414.23	332.46
CHN	578.12	603.81	652.58	344.03		308.55	358.83	293.75
Cluster 1	Total	132.35	121.21	132.13	60.23	71.90	83.42	48.71
	Mean	16.54	15.15	16.52	7.53	8.99	10.43	6.09
Cluster 2	Total Mean	168.91	168.77	183.10	90.75	92.34	105.75	77.35
		33.78	33.75	36.62	18.15	18.47	21.15	15.47
Cluster 3	Total Mean	276.86	313.83	337.35	193.04	144.30	169.66	167.69
		15.38	17.44	18.74	10.72	8.02	9.43	9.32

5. Robustness Analysis of Different Substitution Speeds

We calculated automobile fuel demand in 2035 under three scenarios with slow, medium, and fast substitution speeds. Assuming that under the three scenarios, the proportion of NEVs for provinces in Cluster 1, 2, and 3 in 2035 is (25%, 15%, 5%), (30%, 20%, 10%), (35%, 25%, 15%), respectively. The results are shown in Table 10 and Figure 8. Under the three scenarios, China's automobile fuel demand in 2035 will be 653, 615, and 576 million tons, respectively. Compared go the case without considering replacement, the total amount of gasoline and diesel can be reduced by 94, 132, and 169 million tons, respectively, which is equivalent to 118, 165, and 211 million tons of crude oil assuming 80% of the refined oil extraction ratio. The amount is about 32.9%, 46.1%, and 59.0% of China's net crude oil imports in 2016, respectively. The robustness analysis shows that China's fuel demand will decrease more under faster NEV substitution speeds, which is likely to happen when government implement more favorable policies for NEVs and stricter policies for fossil fuel vehicles.

Table 10. Fuel vehicles and fuel demand under different substitution scenarios.

Scenario			Vehicle Ownership (Million)	Fuel Demand (Mt)
Baseline			**666.61**	**747**
Slow	CHN		578.12	653
	Cluster 1—25%	Total	132.35	132
		Mean	16.54	17
	Cluster 2—15%	Total	168.91	183
		Mean	33.78	37
	Cluster 3—5%	Total	276.86	337
		Mean	15.38	19
Medium	CHN		544.78	615
	Cluster 1—30%	Total	123.52	123
		Mean	15.44	15
	Cluster 2—20%	Total	158.97	172
		Mean	31.79	34
	Cluster 3—10%	Total	262.29	320
		Mean	14.57	18
Fast	CHN		511.45	578
	Cluster 1—35%	Total	114.70	115
		Mean	14.34	14
	Cluster 2—25%	Total	149.04	162
		Mean	29.81	32
	Cluster 3—15%	Total	247.72	302
		Mean	13.76	17

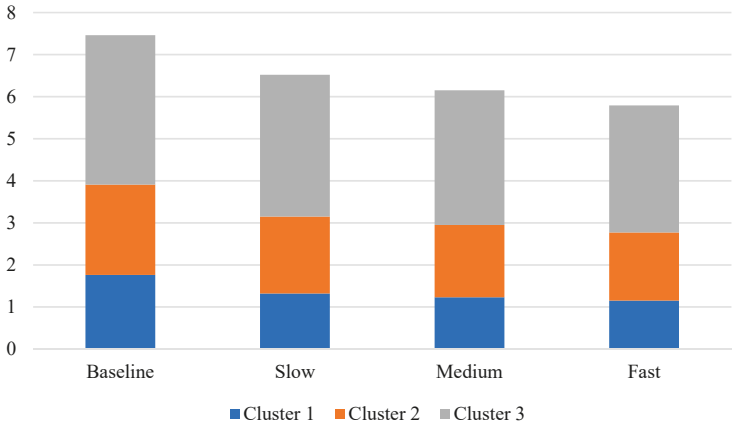

Figure 8. Fuel demand under different substitution scenarios (hundred million tons).

6. Conclusions

Vehicle ownership is one of the most important factors in determining fuel demand. As China's vehicle ownership is still in a period of rapid growth and has not reached saturation, detailed and appropriate forecast of China's vehicle ownership is necessary for the accurate prediction of oil demand in China. Our analysis shows that the relationship between the vehicle ownership rate and real GDP per capita in China conforms to the S-shape trend. Currently, most provinces are at a stage of accelerated growth. According to our results, there are gaps between the saturation levels of vehicle ownership rate among provinces, but they are acceptable compared to the time difference among provinces to reach the inflexion points. In 2035, the predicted vehicle ownership rate of each province will also be quite different, among which the top three highest vehicle ownership rates will be 654, 621, and 612 vehicles per thousand in Jiangsu, Chongqing, and Zhejiang, respectively. Besides, the total vehicle ownership of China will reach 667 million in 2035. And the top three provinces with the most vehicle ownership will be Guangdong, Shandong, and Jiangsu, with 78.26, 59.23, and 51.84 million vehicles, respectively. Without considering the impact of NEVs substitution, the total fuel demand of China's automobiles is expected to be 746.69 Mt in 2035. Guangdong, Henan, and Shandong will be the three provinces with the most demand for automobile fuel, which will be 76.76, 64.91, and 63.95 Mt respectively. Taking the substitution effects of NEVs into consideration, China's automobile fuel demand in 2035 will be 652.58 Mt, and the amount replaced by NEVs will be 94.11 Mt, which is equivalent to 26.3% of China's net oil imports in 2016.

The study contributes to the literature by using a detailed bottom-up prediction model with consideration of provincial heterogeneity in China, which helps generate more accurate forecast results. Different from previous studies which assume homogenous saturation levels of each province, we take into account the provincial differences and relate the growth pattern with provincial population density, urbanization rate, and economic development. For a country like China with vast regional disparity, this analysis can help policy makers formulate and implement more targeted and effective policies. Furthermore, the method can be applied to other countries or regions with dramatic heterogeneity.

The paper also has important policy implications. It can be inferred from our prediction results that the amount of oil saved by fossil fuel vehicle exit is huge. According to the forecast of IEA [30], China's net crude oil imports will reach the peak in 2040, with the net import of 13 million barrels, about 678 Mt per day, which is equivalent to 542 Mt of refined oil, assuming 80% of the extraction ratio. (The refined oil is produced by an industrial process plant where crude oil is transformed and refined into more useful products such as gasoline, kerosene, diesel, and other alternative fuels, such as ethanol gasoline and biodiesel, that meet the national product quality standards and have the same

use, according to Article 4 of the Refined Oil Measures (No. 23, 2006, Ministry of Commerce of the People's Republic of China.)) Therefore, the exit of fossil fuel vehicles will greatly reduce China's foreign oil dependency, thus ensuring China's energy security.

It should be pointed out that we assume the future fuel economy in China will improve at the average rate between 2004 and 2014 in our study, which makes it possible that accelerated technological progress may result in a lower actual fuel demand than our forecast. In addition, this paper does not discuss the possible future changes in people's vehicle purchase behavior. If great progress is made in the technology, price, and supporting facilities of NEVs, or if new restrictive policies of fossil fuel vehicles are introduced, such as car purchase restriction and subsidies for NEVs, the proportion of NEVs will not be negligible any more, and the growth of automobile fuel demand in the future will also be lower than our forecast results.

Based on our conclusions above, we propose the following two suggestions:

Firstly, according to the forecast results, China's automobile fuel demand will continue growing at an accelerated speed in the future if there is no control, thus exacerbating China's environmental problems and raising its dependency on foreign oil. In order to overcome such a situation, relevant policies can be introduced to address the petroleum safety problems that may arise from the excessive growth of vehicle ownership. Such policies may proceed from the perspective of promoting the adjustment of automobile stock and fuel structure, and the improvement of fuel economy.

Secondly, corresponding policies should be developed considering the provincial differences. As it has been demonstrated above, Guangdong, Henan, Shandong, and some other provinces will be the main driving forces for China's automobile fuel demand growth in the future. These provinces are usually regions with rapid economic growth and large population base. Therefore, more focus ought to be put on these regions to effectively alleviate the rapid growth of automobile fuel demand in China.

Author Contributions: Conceptualization, L.H. and Z.F.; methodology, Z.F. and T.C.; formal analysis, Z.F. and T.C.; data curation, T.C.; writing—original draft preparation, Z.F.; writing—review and editing, C.X.; supervision, K.X.; project administration, K.X.; funding acquisition, K.X.

Funding: This research was funded by the State Grid Science and Technology Research Project (Grant number SGFJJY00GHJS1900003).

Conflicts of Interest: The authors declare no conflict of interest.

References

1. BP (British Petroleum Public Limited Company). *BP Statistical Review of World Energy*; BP: London, UK, 2017.
2. National Bureau of Statistics of China. *China Statistical Yearbook (2017)*; China Statistics Press: Beijing, China, 2017.
3. Shen, L.; Xue, J.J. Development path choice and strategy framework of China's energy security. *China Popul. Resour. Environ.* **2011**, *21*, 49–54.
4. National Bureau of Statistics of China. *China Statistical Yearbook (2016)*; China Statistics Press: Beijing, China, 2016.
5. Reuters. China Studying When to Ban Sales of Traditional Fuel Cars: Xinhua. 2017. Available online: https://www.reuters.com/article/us-china-autos/china-studying-when-to-ban-sales-of-traditional-fuel-cars-xinhua-idUSKCN1BL01U (accessed on 27 March 2019).
6. Zhao, C.; Liu, G.Y.; Chen, B. Advances in theories and methods of energy forecasting and early warning. *Acta Ecol. Sin.* **2015**, *35*, 2399–2413.
7. Johansson, O.; Schipper, L. Measuring the long-run fuel demand of cars: Separate estimations of vehicle stock, mean fuel intensity, and mean annual driving distance. *J. Transp. Econ. Policy* **1997**, *31*, 277–292.
8. Palencia, J.C.; Otsuka, Y.; Araki, M.; Shiga, S. Scenario analysis of lightweight and electric-drive vehicle market penetration in the long-term and impact on the light-duty vehicle fleet. *Appl. Energy* **2017**, *204*, 1444–1462. [CrossRef]

9. He, K.; Huo, H.; Zhang, Q.; He, D.; An, F.; Wang, M.; Walsh, M.P. Oil consumption and CO_2 emissions in China's road transport: Current status, future trends, and policy implications. *Energy Policy* **2005**, *33*, 1499–1507. [CrossRef]
10. Zhang, Q.; Tian, W.; Zheng, Y.; Zhang, L. Fuel consumption from vehicles of China until 2030 in energy scenarios. *Energy Policy* **2010**, *39*, 6860–6867. [CrossRef]
11. Wang, H.; Ou, X.; Zhang, X. Mode, technology, energy consumption, and resulting CO_2 emissions in China's transport sector up to 2050. *Energy Policy* **2017**, *109*, 719–733. [CrossRef]
12. Wu, T.; Zhao, H.; Ou, X. Vehicle ownership analysis based on GDP per Capita in China: 1963–2050. *Energies* **2014**, *7*, 4877–4899. [CrossRef]
13. Dargay, J.; Gately, D. Vehicle ownership to 2015: Implications for energy use and emissions. *Energy Policy* **1997**, *25*, 1121–1127. [CrossRef]
14. Cherif, R.; Hasanov, F.; Pande, A. Riding the energy transition: Oil beyond 2040. Available online: https://www.imf.org/en/Publications/WP/Issues/2017/05/22/Riding-the-Energy-Transition-Oil-Beyond-2040-44932 (accessed on 19 July 2019).
15. Qi, F.F. *Forecasting Research on the Consumption Demand of Civilian Vehicle in China based on Panel Data Model*; University of Science and Technology of China: Hefei, China, 2010.
16. Peng, T.; Ou, X.; Yuan, Z.; Yan, X.; Zhang, X. Development and application of China provincial road transport energy demand and GHG emissions analysis model. *Appl. Energy* **2018**, *222*, 313–328. [CrossRef]
17. Muraleedharakurup, G.; Mcgordon, A.; Poxon, J.; Jennings, P. Building a better business case: The use of non-linear growth models for predicting the market for hybrid vehicles in the UK. *Ecol. Veh. Renew. Energies* **2010**. Available online: https://www.researchgate.net/publication/228998926 (accessed on 25 March 2019).
18. Huo, H.; Wang, M.; Johnson, L.; He, D. Projection of Chinese motor vehicle growth, oil demand, and CO2 emissions through 2050. *Transp. Res Record J. Transp. Res. Board* **2007**, *2038*, 69–77. [CrossRef]
19. Huo, H.; Zhang, Q.; He, K.; Yao, Z.; Wang, M. Vehicle-use intensity in China: Current status and future trend. *Energy Policy* **2007**, *43*, 6–16. [CrossRef]
20. Gately, D.; Dargay, J. Incomes effect on car and vehicle ownership. *Transp. Res. Part A Policy Pract.* **1999**, *33*, 101–138.
21. Gu, J.B.; Qi, F.F.; Wu, J.L. Forecasting on China's civil automobile-owned based on Gompertz Model. *Technol. Econ.* **2010**, *29*, 57–62.
22. Dargay, J.; Gately, D.; Sommer, M. Vehicle ownership and income growth, worldwide: 1960–2030. *Energy J.* **2007**, *28*, 143–170. [CrossRef]
23. Auffhammer, M.; Wolfram, C.D. Powering up China: Income distributions and residential electricity consumption. *Am. Econ. Rev.* **2014**, *104*, 575–580. [CrossRef]
24. Zhang, Q.; Zhao, S.C. Factors influencing private vehicle ownership in China. *Transp. Res.* **2016**, *2*, 1–5.
25. CATARC (China Automotive Technology & Research Center). *Annual Report on Automotive Energy-Saving in China (2015)*; Posts & Telecom Press: Beijing, China, 2015; pp. 15–19.
26. Huo, H.; Wang, M. Modeling future vehicle sales and stock in China. *Energy Policy* **2012**, *43*, 17–29. [CrossRef]
27. Bloomberg Forecasts EVs to be One Third of Global Vehicle Ownership by 2040. Available online: http://finance.sina.com.cn/roll/2017-07-10/doc-ifyhweua4640386.shtml (accessed on 21 March 2019).
28. ExxonMobil. *The Outlook for Energy: A View to 2040*; ExxonMobil: Irving, TX, USA, 2016.
29. Minister of MIIT: China's New Energy Automobiles Are Expected to Account for 10% of the Total. Available online: http://www.itdcw.com/news/focus/0313Y5132018.html (accessed on 6 April 2019).
30. IEA (International Energy Agency). *Oil Market Report 2017*; IEA: Paris, France, 2017.
31. Ward, J.H. Hierarchical grouping to optimize an objective function. *J. Am. Stat. Assoc.* **1963**, *58*, 236–244. [CrossRef]
32. Del Campo, C.; Monteiro, C.M.; Soares, J.O. The European regional policy and the socio-economic diversity of European regions: A multivariate analysis. *Eur. J. Oper. Res.* **2008**, *187*, 600–612. [CrossRef]
33. Yuan, Y.; Cai, W.J.; Can, W.; Wang, S.Q. Regional allocation of CO2 intensity reduction targets based on cluster analysis. *Adv. Clim. Chang. Res.* **2012**, *3*, 220–228. [CrossRef]

MDPI
St. Alban-Anlage 66
4052 Basel
Switzerland
Tel. +41 61 683 77 34
Fax +41 61 302 89 18
www.mdpi.com

Energies Editorial Office
E-mail: energies@mdpi.com
www.mdpi.com/journal/energies

MDPI
St. Alban-Anlage 66
4052 Basel
Switzerland

Tel: +41 61 683 77 34
Fax: +41 61 302 89 18

www.mdpi.com

ISBN 978-3-03921-458-7